



VENERA-D

VENUS MODELING WORKSHOP

October 5–7, 2017

PROCEEDINGS

ВЕНЕРА-Д

СОВЕЩАНИЕ ПО МОДЕЛИРОВАНИЮ ВЕНЕРЫ

5–7 октября 2017 года

СБОРНИК МАТЕРИАЛОВ

Edited by academician L. M. Zelenyi
Compiled By: L. V. Zasova, D. A. Gorino

Под редакцией академика Л. М. Зелёного
Составители: Л. В. Засова, Д. А. Горинов

VENERA-D. Venus Modeling Workshop. October 5–7 2017: Proceedings.
М.: ИКИ, 2018. 191 p.

These are the proceedings of the Modeling Workshop organized by NASA and IKI/Roscosmos which took place in the Space Research Institute (IKI), Moscow, Russia October 5–7, 2017. It was focused on the needs and limitations of current models (e.g., general circulation and interior structure), landing site selection, and the types of measurements needed to more adequately constrain parameters in the models and experiments of the planned mission “Venera-D”. This mission is devoted to the complex detailed study of the atmosphere, surface, and plasma environment of Venus to provide a major step in understanding of our sister planet. The main science objectives of the mission should address key questions about the dynamics of the atmosphere with an emphasis on the atmospheric superrotation, origin and evolution, parallel with the geological processes that have formed and modified the Venus’ surface. The report of the team of “scribes” — early career researchers who prepared the review of the conference, including reports and discussions, precedes the main part of the conference materials.

В29 ВЕНЕРА-Д. Собрание по моделированию Венеры. 5–7 октября 2017: сборник материалов.— М.: ИКИ РАН, 2018.— 191 с. : табл., ил., цв. ил.

ISBN 978-5-00015-012-2

В настоящем сборнике представлены материалы совещания, организованного НАСА и ИКИ РАН / ГК «Роскосмос», состоявшегося в Москве в Институте космических исследований с 5 по 7 октября 2017 г. Основное внимание уделялось возможностям и необходимости улучшения существующих моделей атмосферы и внутренней структуры Венеры, выбору мест посадки, а также различным экспериментам планируемой миссии «Венера-Д». Целью миссии является комплексное детальное исследование атмосферы, поверхности и плазменного окружения Венеры для более глубокого понимания ближайшей с нами планеты. Основные научные цели миссии — получение ответов на ключевые вопросы, касающиеся динамики венерианской атмосферы (суперротация, происхождение, эволюция), а также геологических процессов, ответственных за формирование и эволюцию поверхности Венеры. Отчет команды «секретарей» — молодых ученых, написавших обзор конференции, включающий доклады и дискуссии, предваряет основную часть материалов конференции.

Редактор: академик *Зеленый Л. М.*

Составители: д-р физ.-мат. наук *Засова Л. В., Горинов Д. А.*

Компьютерная верстка: *Комарова Н. Ю.*

Дизайн обложки: *Захаров А. Н.*

Серия «Механика, управление, информатика»

Подписано в печать 28.09.2018
Формат 70×100/16
Усл. печ.-л. 15.52
Тираж 150
Заказ 4172

CONTENTS

| | |
|--|-----|
| Preface | 5 |
| Scribe Meeting Report | 7 |
| General Circulation Models | |
| Brecht A. S., Bougher S. W., Parkinson C. D. The Latest on the Venus Thermospheric General Circulation Model: Capabilities and Simulations | 31 |
| Lebonnois S., Schubert G., Forget F. Behavior of Venus Planetary Boundary Layer as Predicted by the IPSL Venus GCM. | 36 |
| Rodin A. V., Mingalev I. V., Orlov K. G. Gas dynamics general circulation model of the Venus atmosphere | 39 |
| Navarro T., Schubert G., Lebonnois S. Large Stationary Gravity Waves: A Game Changer for Venus' Science. | 40 |
| Dynamics | |
| Gubenko V. N., Kirillovich I. A., Pavelyev A. G. High-Latitude Zonal Winds in the Venusian Atmosphere from Venera-15 and -16 Radio Occultation Data | 45 |
| Gorinov D., Zasova L., Khatuntsev I., Turin A. Influence of Topography at the Upper Mesosphere of Venus from Oxygen Nightglow Wind Tracking. | 51 |
| Khatuntsev I. V., Patsaeva M. V., Titov D. V., Ignatiev N. I., Turin A. V., Fedorova A. A. Cloud Level Circulation According to UV and Near-IR VMC Imaging Onboard Venus Express. | 55 |
| Chemistry and Clouds | |
| Mills F. P., Jessup K. L., Yung Y. L. Simulations of Vertical Profiles of SO and SO ₂ in Venus' Mesosphere | 59 |
| Parkinson C. D., Bougher S. W., Brecht A. S. On Understanding the Nature and Variation of the Venusian Middle Atmosphere via Observations and Numerical Modeling of Key Tracer Species | 63 |
| Port S. T., Briscoe A. C., Chevrier V. F. Experimental Results on the Stability of Galena in Venusian Conditions. | 67 |
| Krasnopolsky V. A. Modeling of Chemical Composition in the Lower and Middle Atmospheres of Venus. | 72 |
| McGouldrick K. Microphysical Modelling of the Sulfuric Acid Venus Cloud System | 74 |
| Results of Akatsuki | |
| Limaye S. S., Akatsuki Team Multispectral Day and Night Cloud Morphology of Venus from Akatsuki Cameras. | 77 |
| Lee Y. J., Horinouchi T., Yamazaki A., Imamura T., Yamada M., Watanabe S., Sato T. M., Ogohara K., Hashimoto G. L., Murakami S., Kouyama T., Takagi M., Nakajima K., Peralta J., Jessup K. L., Perez-Hoyos S., Titov D., Limaye S. Venus, Seen from the UV Imager Onboard Akatsuki. | 82 |
| Satoh T., Imamura T., Nakamura M., Akatsuki Team New Views of Venus as Obtained from Akatsuki. | 86 |
| Aerial Platforms | |
| Lebonnois S. Exploring Balloon Trajectories in a Modeled Venus Atmosphere | 91 |
| Cutts J. A., Matthies L. H., Thompson T. W. Venus Aerial Platforms and Engineering and Scientific Modeling Needs | 96 |
| Krishnamoorthy S., Komjathy A., Cutts J. A., Pauken M. T., Garcia R. F., Mimoun D., Jackson J., Kedar S., Smrekar S. E., Hall J. L. Infrasound Detection from Balloons — Perspectives From Simulations And Experiments | 100 |
| Rodin A. V., Klimchuk A. Yu., Benderov O. V., Semenov V. M., Melnikov I. V. LIDAR Spectroscopic Sounding of the Ambient Atmosphere and Cloud Layer Onboard Venus Atmospheric Platform | 102 |

Plasma

- Vaisberg O., Shuvalov S., Zelenyi L., Petrukovich A., Ermakov V.**
Solar Wind Interaction with Venus — Implication for Atmosphere and Some Lessons
from Mars 105
- Gavrik A., Kolomiets S., Gavrik Yu., Kopnina T., Lukanina L., Ilyshin Ya.**
Radio Occultation on the Venera-D Mission: A Concept of Radio Frequency Subsystem
and Radio Science Technique 111
- Collinson G., Frahm R., Glocer A., Barabash S., Futaana Y., Grebowsky J., Coates A., Mitchell D.,
Moore T., Sibeck D., Omid N., Jian L., Zhang T.**
Mysteries of Atmospheric Escape and Evolution at Venus 115

Interior and Geochemistry

- Gudkova T., Zharkov V., Lognonné Ph.**
Interior Structure Models of Venus 119
- Zharkov V., Gudkova T.**
On Parameters of the Earth-Like Model of Venus 124
- Way M. J., Del A. Genio, Amundsen D. S.**
Modeling Venus-Like Worlds through Time 128
- Lognonné Ph., Kenda B., Garcia R., Komjathy A., Makela J., Karakostas F., Drilleau M.,
Gudkova T., Banerdt W. B., Cutts J., Jackson J. M.**
Venus Seismic Interior-Atmosphere Coupling: Theory and Orbital Perspectives 132

Surface and Landing Sites

- Ernst R. E., Samson C., Bethell E., Lee J., Khawja S., Graff J. R., Davey S.**
Venera-D Landing Site Selection Based on Detailed Geological Mapping Using Magellan Radar
Images 139
- Treiman A. H., Harrington E.**
Radar Backscatter from Venus' Highlands: Confirmation of a Ferroelectric Substance, Likely
Chlorapatite 144
- D'Incecco P., Glaze L. S.**
Imdr Regio as the Landing Site of the Venera-D Mission: A Geologic Perspective 148
- Economou T. E.**
Determination of the Venus Surface Elemental and Mineralogical Composition on Venera-D
Mission 153
- Glaze L. S., Gilmore M. S., Treiman A. H.**
Scientific Rationale for Selecting Landing Sites on Venus: so Many Choices, so Few
Opportunities! 162
- Ivanov M., Eismont N., Gerasimov M., Ignatiev N., Khatuntsev I.,
Korablev O., Marov M., Zasova L., Zelenyj L., Vaisberg O.**
Estimates of the Frequency Distribution of Short-Baseline (1–3 m) Slopes for Different Terrains
on Venus Using Terrestrial Analogs 165

Technology

- Gerasimov M. V., Mikhalsky V. I., Nosov A. V.**
A Prototype of Soil Sampling System for the Venera-D 171
- Kremic T., Hunter G. W., Nero L.**
Long-Lived In-Situ Solar System Explorer (Llisse) 176
- Gromov V., Kosov A.**
The Radiometer for Thermal Sounding of Low Atmosphere and Sulfur Compound Detection 181
- Lemeshevskii S., Vorontsov V., Grafodatskiy O., Karchaev Kh., Teselkin S.**
"To Venus Together": International Project Implementation on Venus Planet Research 186
- Grafodatskiy O., Martynov A., Ustinov S., Simonov A., Teselkin S., Vorontsov V.**
"Towards Venus Together": The Preliminary Architecture of "Venera-D" Mission on the Basis
of Joint Scientific Program Proposals of Roscosmos – NASA Joint Study Group on Venus
Researches 187
- Kosov A. S. on behalf of radio-science team IKI RAN**
Venera-D: The Lander-Orbiter Radiolink 188
- Eismont N. A., Zasova L. V., Nazirov R. R., Simonov A. V.**
Venera-D Project: Scenario and Trajectory Design Problems 189
- Litvak M. L., Sanin A. B., Golovin D. V., Mitrofanov I. G., Vostrukhin A. A.**
Active gamma ray spectrometer proposed for future Venus surface missions 191

PREFACE

Venus is considered as the Earth's twin sister: both planets were formed in the inner solar system out of the same protoplanetary material. Although these 'sisters' have nearly the same size, mass, and density, unlike Earth, Venus' climate is fueled by a massive CO₂ atmosphere producing an enormous greenhouse effect (surface pressure of 90 bar and temperature of 470 °C). The atmosphere undergoes superrotation, with the upper clouds rotating at a rate 60 times faster than the surface. Shrouded in clouds of sulfuric acid, Venus' surface lacks water and has been sculpted by volcanism and deformed by faulting and folding forming belts of rifts and mountains. The lack of an intrinsic magnetic field suggests the planet's interior structure may also be different than that of the Earth. These differences indicate that the Earth and Venus had substantially different evolutionary paths. What remains unanswered is when, why and how the paths diverged. Additionally, it remains that the Earth stands as our only known and verified example of a planet with an active biosphere.

NASA and IKI/Roscosmos established in 2015 a Joint Science Definition Team (JSDT), to document the scientific goals of the Venera-D Mission and the synergy between the goals of Venera-D with those of NASA. The baseline Venera-D mission concept would consist of an orbiter and lander (Roscosmos) with advanced, modern, instrumentation. A key task of the JSDT is the identification of science gaps and the study of possible mission augmentations (experiments /elements) that could fill these gaps. A list of possible "contributed mission elements" includes aerial platform and long-lived surface stations (NASA) and a subsatellite (Roscosmos). The science objectives of the Venera-D mission should address key questions about the dynamics of the atmosphere with an emphasis on atmospheric superrotation, origin and evolution, the geological processes that have formed and modified the surface, with emphasis on the mineralogical and elemental composition of surface materials, and the chemical processes related to the interaction of the surface and the atmosphere.

As a resource to the JSDT a Venus modeling workshop took place at the NASA Glenn Research Center located in Cleveland, Ohio, USA in the month of May 2017, with the participation of the wide community of Venus scientists. It focused on understanding the limitation and needs of current models (e.g., General Circulation Models (GCMs) and interior structure models), landing site selection, and the types of measurements needed to more adequately constrain parameters in the models and experiments. This would in-turn form a basis for identifying the priorities of a new Venus mission and the types of instruments needed to achieve the goals of the mission. In October 2017 the "Venera-D Venus modelling workshop" was held at IKI (Moscow, Russia); this second workshop was devoted to informing the Venera-D mission conceptualization. Because of the strong coupling between interior, surface, atmosphere and plasmas, Venus should be considered as a system and studied simultaneously from different apparatus, such as: remote measurements from orbit and in-situ measurements in the atmosphere and on the surface. The Venera-D mission concept focuses on providing a major step in understanding our sister planet through detailed study of Venus' complex atmosphere, surface, and plasma environment. In its ongoing work, the JSDT will incorporate into its deliberations information derived from each modeling workshop. This information will be used to identify the needed high-value data/measurements that could be obtained by Venera-D that would advance the science goals defined for the Venera-D mission and those defined for future modeling work, specifically the development of new GCMs. This in turn will help the JSDT to determine the functionality and characteristics of the instruments (and mission elements) that should be included in the notional Venera-D mission concept.

The first section of the Proceedings features the workshop report, which was prepared by the "scribes" — early career scientists from Russian and American institutions, who collected and compiled all key notes, questions, discussions and answers from the event. The report was edited by the members of the JSDT at a later stage.

SCRIBE
MEETING
REPORT

EXPLANATION OF MEETING OBJECTIVES

On October 5-7, 2017 the Space Research Institute (IKI), Moscow, Russia, hosted a Venera-D Venus modelling workshop convened by Dr. Ludmila Zasova, (atmosphere) Co-Chair of the Joint Science Definition Team, and Dr. David Senske (surfaces) Co-Chair. The workshop focused on the Venera-D mission in light of the current knowledge base of the Venusian models (e.g. General Circulation Models of the atmosphere, or GCMs, as well as models of the surface and interior structure and plasma environment). The workshop discussion topics included the priorities and motivations for the landing site selection, as well as the types of measurements needed to parameterize and more adequately constrain theoretical geophysical models and the experiments needed to validate or refute results derived from these models. The intent was to form a basis for identifying the mission architecture elements required to achieve the key Venera-D science goals defined in the Roscosmos/IKI – NASA Joint Science Definition Team Phase I report such as atmosphere probes, aerial platforms or aerobots, long lived surface stations, and a lander (see the JSDT Phase I report at <https://www.lpi.usra.edu/vexag/reports/Venera-D-STDT013117.pdf>). Likewise, the workshop findings provide a basis for identifying the suite of instrumentation that would provide the highest science return from each mission element.

The workshop consisted of oral and poster presentations; the findings derived from these presentations and the ensuing presentation discussions were collated by mid-career scientists who acted as scribes for the meeting. These findings are summarized and presented in this report; while access to the individual presentations given at the workshop can be found at: <http://workshop.venera-d.cosmos.ru>.

PURPOSE AND SCOPE

The objectives of this three-day workshop were to discuss (1) the modeling of Venus' exosphere, atmosphere, surface, and interior as they relate to the Venera-D mission; including a review of the findings from the May 2017 Venus modelling workshop and (2) the science factors that would help guide the Venera-D mission architecture. The workshop participants included the JSDT, a delegation of NASA Venus scientists as well as researchers from Russia and other countries, who employ numerical, computational, or analytical methods to study Venus.

WORKSHOP STRUCTURE AND ORGANIZATION

The workshop was designed to be interactive and consisted of a combination of cross-disciplinary plenary sessions. Invited talks were given for the purpose of providing a focus for discussion on the Venera-D science optimization. The plenary briefings provided short overviews and summary information and lay a foundation for attendees to have an open dialogue on focus topics. Plenary topics included summaries of recent modeling efforts, the state of understanding regarding Venus' evolution, Venus interior and landing sites and Venera-D mission architecture elements (orbiter, lander, payload, aerial platform, etc.) in relation to its science priorities. A portion of the time was allocated to review the scribe record of the plenary discussions on Venus' exosphere and orbital environment, atmosphere, surface, and interior. Venera-D orbit recommendations were also discussed and identified.

The scientific workshop content was developed by the JSDT program committee taking into account the findings from the Venus Exploration and Analysis Group (VEXAG) modelling workshop held in May 2017.


This workshop report will be archived on the VEXAG and IKI website to enable open and future access.

The findings from this Modeling Workshop will serve as a reference to the Venera-D JSDT as they further refine the mission architecture concept and identify the trade space for possible contributed elements. The Venera-D JSDT Phase 2 report is due January 31, 2019.

LIST OF MEETING ATTENDEES

| Participant Name (Last, First) | Affiliation as of October 2017 |
|---------------------------------------|--|
| Belyaev, Denis | IKI |
| Brecht, Amanda | Ames Research Center |
| Collinson, Glyn | Goddard Space Flight Center |
| Cutts, James | JPL |
| D'Incecco, Piero | Arctic Planetary Science Institute, Germany |
| Economou, Thanasis | University of Chicago |
| Eismont, Natan | IKI |
| Ernst, Richard | Carleton University (USA), Tomsk State University (Russia) |
| Fedorova, Anna | IKI |
| Gavrik, Anatoly | Kotelnikov Institute of Radioengineering and Electronics (IRE) |
| Gerasimov, Mikhail | IKI |
| Glaze, Lori | Goddard Space Flight Center |
| Gorinov, Dmitry | IKI |
| Grandidier, Jonathan | JPL |
| Green, Jim | NASA Planetary Science Division, Director |
| Gromov, Vladimir | IKI |
| Gubenko, Vladimir | Kotelnikov Institute of Radioengineering and Electronics (IRE) |
| Gudkova, Tamara | Schmidt Institute of Physics of the Earth (IPE) |
| Guseva, Evgenia | GEOKHI |
| Hall, Jeffrey | JPL |
| Ignatiev, Nikolay | IKI |
| Immel-Walter, Rodion | Lavochkin Association |
| Ivanov, Mikhail | GEOKHI |
| Jessup, Kandis-Lea | Southwest Research Institute |
| Khatuntsev, Igor | IKI |
| Kolomiets, Sergey | Kotelnikov Institute of Radioengineering and Electronics (IRE) |
| Korablev, Oleg | IKI |
| Kosov, Alexandr | IKI |
| Krasnopolsky, Vladimir | MIPT |
| Kremic, Tibor | Glenn Research Center |
| Ksanfomality, Leonid | IKI |
| Lebonnois, Sebastien | IPSL, France |
| Lee, Yeon-Joo | ISAS/JAXA, Japan |
| Limaye, Sanjay | University of Wisconsin |
| Linkin, Vyacheslav | IKI |
| Lipatov, Alexandr | IKI |
| Lognonné, Philippe | Institut de Physique du Globe, France |
| Luginin, Mikhail | IKI |
| Martynov, Alexey | Lavochkin Association |
| McGouldrick, Kevin | University of Colorado |
| Mills, Franklin | Australian National University |
| Navarro, Thomas | University of California |
| Nikolaev, Eugene | Skolkovo Institute of Science and Technology |
| Ocampo, Adriana | NASA |

| | |
|------------------------|-------------------------------------|
| Parkinson, Christopher | University of Michigan |
| Patsaeva, Marina | IKI |
| Port, Sara | University of Arkansas |
| Rodin, Alexandr | IKI, MIPT |
| Satoh, Takehiko | ISAS/JAXA, Japan |
| Senske, David | JPL, JSDT Co-Chair |
| Treiman, Allan | Lunar and Planetary Institute |
| Ustinov, Eugene | JPL |
| Vaisberg, Oleg | IKI |
| Vorontsov, Viktor | Lavochkin Association |
| Way, Michael | Goddard Institute for Space Studies |
| Zasova, Ludmila | IKI, JSDT Co-Chair |
| Zeleny, Lev | IKI, Director |

 Indicates Venera-D Joint Science Definition Team Members

Modelling Workshop Meeting Scribes: Glyn Collinson (Scribe Content Editor), Amanda Brecht, Kevin McGouldrick, Sara Port, Thomas Navarro, Dmitry Gorinov, Mikhail Luginin, Evgenia Guseva.

SUMMARY OF ANSWERS PROVIDED AS AIDS TO THE VENERA-D CONCEPT DEVELOPMENT

Orbital Science:

- **For atmospheric observations, what is the desired orbit of the orbiting spacecraft, (note that this might be constrained due to the need of the orbiter to perform relay for the lander(s))?**
- **Orbit preference: equatorial vs polar orbit. Elliptical vs circular?**

Multiple participants from multiple disciplines advocated for an elliptical, polar (or non-equatorial) orbit, offering access to a wide range of phases (latitude, longitude, and altitude) at multiple local times.

However, the high science return possible from an equatorial orbit as it relates to the study of super-rotation (which is ranked as a high mission priority) based on zonal cloud motions and low-latitude emissions within the atmosphere was openly discussed.

Additionally, a specific concern was raised concerning communications links to, and delivery of, VAMP possibly requiring an equatorial orbit.

A common need was for long time-baseline remote-sensing observations of key atmospheric parameters, at multiple latitudes.

The lowest ultimate periapsis requested (for in-situ measurements of the atmosphere and ionosphere) was 200–300 km.

The highest apoapsis requested was >30,000 km.

A study of the long-term evolution of the orbit was suggested as an action item.

Landed Science:

- **What is the prioritized terrain types for a lander and are there constraints on the latitude of the landing site? — bearing in mind landing must be in the daylight.**

Under an initial assumption of a 7° maximum slope, regional plains were chosen as a priority target. However, a later discussion by specialists from Lavochkin Association (NPOL) suggest 15° is attainable which allows additional access to landing sites and is thus worthy of future discussion.

A landing site free of impact ejecta would be preferred.

The landing site should be on regions that are representative of the most common rock on Venus, e.g., the regional volcanic plains that contain large areas of lava flooding.

Smooth plains of impact origin were suggested as the safest to land on, but the distribution of impact ejecta at these sites needs to be accurately accounted for (see notes section for details).

NPOL specialists reported that there are minimal trajectory constraints on the latitude of the landing site.

- **List of prioritized targets vs science return**

1. Regional plains (Compromise between excellent science and minimal slopes).
2. Smooth plains (Safest landing option, but likely to include impact ejecta that complicates interpretation).
3. Tesserae (Highest possible science, but very risky landing without high-resolution surface information and precision landing).

- **How many long-lived stations are optimal? What is the best distribution?**

A single long-lived element on the main lander was discussed as the simplest and lowest risk.

The value of using two to three long-lived stations (or dropsondes) at regions of varying elevation to establish the gradient of temperature as a function of altitude was discussed.

Delivery of Long-Lived Stations in conjunction with the larger descent lander pre-determines the relative range between landing sites for a collection of long-lived stations.

Aerial Platforms:

- **For observations in the atmosphere (aerial vehicles—balloon or airship) what key measurements need to be made and what instrumentation is needed? What are the limitations?**

Numerous possible types of measurements were discussed (see executive summary below).

The two types of measurements most frequently raised at the meeting were for basic atmospheric properties (temperature, winds, etc.), and measurements of aerosols (composition, size, vertical and spatial distributions and variations in these distributions).

However, prioritization of science and instruments is currently underway.

Payload:

- **Prioritized payload in the orbiter, the lander and aerial platform.**

A broad range of potential instruments was discussed relative to the Workshop Splinter topics which were: General Circulation Models; Atmospheric Chemistry and Clouds; Aerial Platforms; Plasmas; Interior, Surface, Landing site. A summary of the potential candidates is provided in the following pages per topic; specific prioritization of the payload items was not discussed/assigned.

It is vital that sponsoring agencies (NASA/Roscosmos) make early investments in instrument development and technology for in-situ investigations, including sampling systems.

Potential Additional Elements:• **What is the best science to be performed by a sub-satellite**

1. Simultaneous measurements of upstream conditions (Sub-satellite) and ionosphere (Main Orbiter) to study the influence and impact of external driving factors on Venus.
2. Observations of airglow by both sub-satellite and main orbiter to expand both temporal coverage and vertical coverage.

EXECUTIVE SUMMARIES BY TOPIC

GENERAL CIRCULATION MODELS

Science Needs:

- Understand “transition region” (~90–110 km; region where the zonal super rotation and the sub-solar-antisolar flow merge), and the driver of zonal super rotation.
- Understand the Planetary Boundary Layer.
- Understand how the Ionosphere and Thermosphere couple: the role the ionosphere plays in super-rotation.

Measurement Requirements:

- Remote Spectroscopy.
- High precision measurement of bulk atmosphere (CO₂ and N₂) through the atmosphere.
- Accurate measurements of radiant flux through the atmosphere from ionosphere to surface.
- Near surface atmospheric properties: wind velocity, temperature, lapse rate, including CO₂ and N₂ at high precision, radiative fluxes.
- Neutral atmosphere ~60 km and up: temperature, winds, composition, wave parameters (e.g. planetary waves, gravity waves), nightglow (NO UV, O₂ IR, OH IR), dayglow, minor species (CO, O, SO_x).
- In-situ particles: thermal electron/ion temperature, ion/neutral winds.
- Observing NO UV and O₂ IR nightglow simultaneously provides 3rd dimension.
- Longer observing times (nightglow, surface wind speeds).

Possible Instruments:

- LIDAR.
- RADAR.
- One or more short to long term surface weather stations/dropsodnes; multiple long-lived stations that are co-located in latitude and longitude but residing at different near surface elevations were strongly desired.
- Imaging Spectrometers.
- Neutral/Ion mass spectrometer with winds.
- Langmuir Probe.
- Cold Ionospheric Ion Spectrometer (with density and winds).

Orbital requirements:

- High Circular/Elliptical Polar orbit/ or High Circular/Elliptical Equatorial Orbit.
- High circular polar/precession orbits required to view both poles with same resolutions and to get a more global view — this is the preferred orbit.
- Long term observations of both day and nightside atmosphere at multiple latitudes from equator to pole and multiple altitudes extending from 10 to 100 km; and ability to communicate with long term observations from aerial platform in the deep atmosphere; and from long-lived surface stations.

Lander requirements:

- Long term (~3 months or longer) meteo (wind, T, P) observations in surface boundary layer.
- High precision measurements of bulk atmosphere (CO_2 and N_2) and radiant flux during descent from highest altitude possible to surface.

Aerial Platform requirements:

- Long term (~3 months or longer) observations (w, T, P, radiant flux) at, below and above cloud top level.

ATMOSPHERIC CHEMISTRY AND CLOUDS**Science Needs:**

- Measurements of different types of emission (airglow [O , O_2], nightglow [O_2 , NO , OH]), which emerge from different altitudes; airglow measurements trace zonal transport of minor species.
- Remote sensing (orbital) determination of minor species abundances: H_2O , HDO , CO , HCl , HF , OCS , SO_2 , SO , HBr , SO_2Cl_2 ; and if possible: O_3 , SO_3 , ClO and S_x to understand sulfur and oxygen budgets, and the role of chlorine in mesospheric chemistry.
- D/H isotopic ratio might answer the question: what happened to water on Venus?
- Pressure and temperature profiles are needed for a correct retrieval of minor species. (Solar/ Radio occultation and in-situ).
- Aerosol properties can be determined with glory phenomena analysis (phase function) and aerosol extinction analysis recorded in visible and IR spectral regions. (remotely or in-situ).

Measurements:

- Nadir spectroscopic observations can give information on minor species abundances, different kinds of emission, distribution of an unknown UV absorber, upper clouds, scale height, deep atmosphere on the night side.
- Solar occultation observations will provide vertical profiles of pressure, temperature, abundances of minor species, aerosol extinction coefficients.
- Spectroscopic and LIDAR measurements may be used to determine abundances of minor species and aerosols inside the cloud layer.
- In-situ observations will give information on aerosol properties (size, phase, distribution) inside the clouds that is impossible to do with the remote sounding (this is a very high priority).

Possible Instruments:

- Orbital: High spectral resolution spectrometers.
- Orbital: Imaging spectrometers and cameras.
- Aerial: instruments to determine composition, distribution and particle properties of aerosol species: infrared spectroscopy, lidar, nephelometer, polarimeter, other particle detecting (imaging) instrumentation.
- Aerial: instruments to determine composition and distribution of UV absorber: UV, visible and infrared spectroscopy, life detection microscope.

Mission Functional Requirements:

- All of the described measurements should be made at different local times, latitudes, throughout whole mission lifetime to present diurnal, latitudinal, inter-annual variabilities.
- Orbit: Polar orbit allows access to large phase space (latitude, longitude and local time). Although it is harder to get detailed equatorial measurements of emissions and to trace local-time-driven chemistry from polar orbit; it is impossible to get continuous polar observations from an equatorial orbit.

AERIAL PLATFORMS

Science needs:

- Understand the atmospheric circulation and super-rotation.
- What is the radiative budget in the atmosphere, in particular as a function of the altitude?
- What are the physical properties of the clouds?
- What is the atmospheric composition and chemistry in the deep atmosphere?
- Can we detect and characterize seismic activity?
- Can volcanic activity be detected?
- Detect signature of surface processes (seismic activity, volcanoes) in the atmosphere.
- Measure heating and cooling rates, in the visible and infrared bands.
- Measure cloud particulates.
- Extended goal: Imaging of Tesserae.

Possible Instruments:

- Nephelometer.
- Gas Chromatograph Mass Spectrometer (For isotopic ratios, Halogens, D/H, and SO_x).
- Particulate microscope (potentially with life detection capabilities).
- Accelerometer/Thermometer/Barometer.
- Solar and Thermal Flux Radiometers.
- Active UV and IR spectrometers.
- Cloud Internal Field Radiometer (CIFR).
- Magnetometer for planetary magnetic field detection.
- *Extended goal: Surface imager [Visible imaging challenging due to visibility of the surface and temperature >100 °C, therefore other techniques should be studied].*

Options for aerial platform:

- Fixed altitude VEGA-style balloon (55 km), 120 kg payload with 7 m JPL balloon [*Easiest engineering, highest technology readiness level, but stuck near one altitude*].
- Controlled altitude with deep dives [*advocated as the best scientific return over cost ratio, but does not exist yet and would require much development due to thermal challenges*].
- VAMP aircraft [*Most science return, but has the largest impact on mission architecture, still has long lead time for development which may impact launch timeline and/or overall mission cost — proper assessment should be derived from NASA sponsored aerial platform study report, available April 2018*].

PLASMAS

Science needs:

- How are ionospheric dynamics driven by the solar wind? How are they coupled?
- What are the absolute planetary ion escape fluxes/compositions?
- What is the escape rate of Hydrogen versus Deuterium?
- Detangle the complex web of competing escape channels and processes (Upper atmosphere and ionosphere pickup, ionosphere scavenging, ionospheric clouds and streamers, Ambipolar fields, current sheets). Which ones dominate? How do they interact?
- How do solar wind ions precipitate and accumulate in the atmosphere?
- What is the influence of solar wind and radiation on cosmogenic time scales?
- What role does friction between the ionosphere and thermosphere play in driving super-rotation?

Mission requirements:

Simultaneous measurements of upstream conditions (Sub-satellite) and ionosphere (Main Orbiter) strongly desired to directly study the influence and impact of external driving factors on Venus. Oleg Vaisberg gave a comprehensive review of the best package on behalf of Lev Zeleny advocating:

- Orbit: Elliptical, polar, inclined
 - Periapsis ~200/300 km.
 - Apoapsis: 10,000–15,000 km preferred.
- Comprehensive modern particles and fields package on orbiter, reduced payload on sub-satellite.

Payload/instrument requirements (using modern package, reduced sub-satellite option, see O. Vaisberg presentation for additional details:

Main orbiter instruments:

- Ion spectrometer.
- Electron spectrometer.
- Langmuir probe.
- Magnetometer.
- Plasma waves.
- Energetic electrons detector.
- Energetic ions detector.
- UV photometer.

Sub-satellite instruments:

- Ion spectrometer.
- Electron spectrometer.
- Magnetometer.
- Energetic ions detector.

INTERIOR, SURFACE, LANDING SITES

Science needs:

- Study seismic waves on Venus.
- What is the bulk composition and mineralogy for a representative surface rock?
- Are the tesserae made of different material than the plains? Are they all composed of the same material?
- Do the surface rocks retain evidence of the past?
- Are there any remnant continents? I.e. Ishtar Terra, potential candidate for low-density (continental?) crust. Implications for water and plate tectonics.
- Is there current volcanic activity on Venus? (Spikes in SO₂ seen by both PVO and VEX).
- What chemical/physical reactions are responsible for the abrupt changes in reflectivity seen at high altitudes in radar observations?

Measurements:

- Analyze the mineralogy and chemical composition of surface and the composition beneath the surface. Go for the lava, take one drilling, take multiple samples down through it to understand weathering, and the dust on top.
- Study atmospheric composition near the surface and surface/atmospheric interactions.
- Better D/H constraints for water inventory.
- Need in-situ measurements of Xe, Kr, Ar, and isotopes to constrain geochemistry and mantle redox states.
- Improved resolution of the surface to better understand the geomorphology.
- Use acoustic waves to search for Venus quakes/seismic activity (red airglow) — these measurements may be accessed from aerial platform, orbiter or sub-satellite observations (additional study required to determine most effective/cost efficient platform).

Possible Lander Instruments:

- Elemental chemistry and mineralogy:
 - XRD: Used to determine mineralogy. Spaceflight heritage. However challenging because sample will need to be ingested.

- XRF/APXS: Currently the choice instrument for elemental chemical composition. Detects all elements above sodium (Na). Lots of spaceflight heritage. Could possibly use on aerosols on descent, measuring sulphur, etc. 0.5 kg, 0.5 W.
- CAP/LIMS—under development by IKI for chemical/isotopic analysis of gases, aerosols on descent and surface rocks on landing.
- Raman/LIBS [Remote Sensing]: Preferred instrument for mineralogical composition in laboratory, not flown in space yet, will fly on ExoMars rover and Mars 2020. Can be inside the lander and remotely sample through a window. 8–10 kg, power 20–80 W — concerns were raised by Russian colleagues about temperature control; a review of recent work/tech development was suggested by Lori Glaze.
- Neutron/Gamma spectrometer: passive observations will provide gamma and neutron spectra from the subsurface under the lander via passive and active observations in cycle, providing measurements of decay of short and long living isotopes. Passive observations (prior to operations with Pulse Neutron Generator unit) will characterize abundance of natural radioactivity elements. Active observations (during operations with PNG unit) will characterize subsurface elemental composition. Passive observations (after end of operations with PNG unit) will characterize subsurface elemental composition. 7 kg, power 5 W (passive mode) / 19 W (active mode).
- Mossbauer Spectrometer: works only on iron bearing minerals, 0.5 kg, 0.6 W, several hours accumulation time required. [*Discussion: Would only be useful on the plains, would need to be sure there would be enough time for a measurement.*]
- Mechanism to remove outer rock surface, if possible.
- Surface/Atmosphere interaction:
 - Gas Chromatograph Mass Spectrometer (tunable laser spectrometer). Technically very challenging but would be desirable for isotopic composition of rock forming elements and near surface atmospheric composition. 10.5 kg, 12 W.
- Morphology
 - Imaging: Descent, Panoramic, and Sample.
 - Higher resolution SAR (~100 m) to better constrain surface properties for science and future landings.

Funding for instrument development for Venera-D is critical, as in-situ Venus missions are very challenging. Requests were made for support from NASA in influencing the release of funds to our Russian counterparts in a timely manner so that sufficient resources are available for instrument development and the refurbishing of the required testing facilities. Near-term funding from both NASA and the Russian space agencies is essential, especially since engineers with expertise regarding in-situ Venus missions are rapidly retiring.

Landing Sites/Orbit:

- Orbiter:
 - Measurement of Acoustic Waves:
 - * Requirement: Image Venus with a slow orbital drift, implying high apoapsis (>30,000 km).
 - * 6U-12U satellite option could be piggyback on a Venus orbiter mission, left behind at high altitudes.
 - * Needs long time series images.
- Lander:
 - VEXAG Priority Sites:
 - * Tesserae
 - * Volcanic plains
 - * Young volcanic terrain
 - Slopes are a major threat to lander mission. 7° degree slope limit for Venera-D [*Discussion: Venera-9 landed at a 30 degree slope, but probably came close to failure, so wouldn't risk this today. Lavochkin suggested that 15° is attainable, which allows additional access to landing sites.*]
 - Land away from impact ejecta to go for pristine basalt.
 - Plausible Sites:
 - 1. Regional Plains:** Given the 7° slope limit, pristine lava in the region plains were advocated as a primary landing site.
 - 2. Smooth plains** (Impact related): As a backup, being easier to land, but being more contaminated by impact ejecta.

- Long-lived lander
 - Measurements: Temperature and Wind.
 - Instruments: Simple Meteorological station.
- Additional Comments:
 - Divide Venus into three latitude ranges; specify best landing sites, and science that can be done from that orbit. IKI to work with orbital engineer.
 - A Venus program with additional or multiple landers which go to other landing sites?
 - Drop a sonde from aerial platform for optical images of Tessera surface? Data can then be used for future missions.
 - Does life exist, or could it have possibly existed on Venus? How could we determine this?

NOTES FROM TALKS IN AID OF VENERA-D CONCEPT DEVELOPMENT

GENERAL CIRCULATION MODELS

Alexander Rodin: *Gas dynamics general circulation model*

- Key measurements needed are remote spectroscopy at the transition from zonal flow to sub-solar anti-solar.
- In-situ accurate measurements of local dynamics, including the various transitions for solar atmosphere interactions. Airglow/nightglow/aurora, for photochemistry.
- Instruments: LIDAR and RADAR. High resolution spectrometer at wavelengths appropriate for atmospheric molecules, his main focus is to look at emissions at different altitudes.

Orbit: Circular Polar Orbit, sufficiently high to observe global view. Circular, so spatial resolution the same at both hemispheres. *[Post presentation discussion indicates this would rule out in-situ measurements in the thermosphere and ionosphere.]*

Sebastian Lebonnois: *Behavior of Venus planetary boundary layer as predicted by the GCM*

- Interested in Atmospheric structure parameters (wind velocity, and temperature), lapse rate (change in temperature with altitude) at the surface.
- Characterize relative mixing ratios of CO₂ and N₂ at the surface to high precision.
- If we drop multiple long-lived landers, wants to see them at different surface elevation (one at surface and one on mountain). Two probes would do, but co-located, e.g. at Aphrodite terra, one high and one low. *[Discussions at the meeting suggest this is impracticable, since precision landing is not possible, and flat surfaces are required.]*
- Interested in surface wind speeds over a diurnal cycle *[JSDT clarification: current anticipated long lived lander lifetime is 3 months].*

Orbit: Highly elliptical for long term observations, Polar PVO-like.

Amanda Brecht: *The latest on the VTGCM*

- Measure temperature, winds, and composition at the cloud-tops and up.
- Measure atmospheric wave parameters (planetary Gravity Waves).
- Nightglow via remote sensing (NO UV, O₂ IR, OH IR).
- Minor species (CO, O, SO_x).
- Electron/Ion temperatures, Ion and Neutral Winds, for Ionosphere/Thermosphere coupling to investigate the role that the ionosphere plays in super-rotation.
- *[Participant Comments: Observing NO and O₂ nightglow simultaneously permits for simultaneous measurements at two altitudes.]*
- *[Participant Comments: Time series of evolution of nightglow desirable to study mesospheric circulation.]*

Orbit: Highly elliptical for long term observations, equatorial preferred, could live with polar.

Thomas Navarro: Large Stationary Gravity Waves

- Measure length of day passively by landing radar retro-reflector on the surface, and then with an orbiter measure Doppler shift. [*Ed: later discussions suggested that the reflector would have to be very large, and you may not do any better than the natural surface features, since lava flows already give very sharp edges. The other problem is that, unlike the Lunakohd or Apollo reflectors, nobody knows for sure where the Venera probes are exactly. One estimate from experiments at Earth suggested you might need a surface reflector of area 100 m².*]
- Wants to monitor stationary features (Akatsuki discovered), especially the smaller scale features, to better understand the dependence on topographical features on the surface.
- Long-lived In-situ measurements of winds, density, over a day, to understand the stability conditions in the boundary layer. Should ideally happen on the flank of an equatorial mountain. [*Participant discussion: This last requirement is extremely challenging due to slope constraints.*]

Orbit: Design elliptical orbit and field of view to monitor stationary atmospheric features, equatorial.

Dmitry Gorinov: Circulation of Venusian atmosphere at 95-100km from apparent motions of 1.27 micrometer O₂ nightglow

- We need to observe nightglow at equatorial latitudes. Reasoning for the observation: they are located altitude wise in a transition region between two main atmospheric circulation modes - the region is currently not well understood.
- We need a longer time-series of observations, for a spacecraft to look at the same location from to get a) orbit-to-orbit variations and b) more consecutive images within one orbit.
- We need equal coverage of all geographic longitudes to fill in VIRTIS data gaps.

Orbit: 24 Hour Elliptical; line of apsides — 0–45°.

AKATSUKI

Takehiko Satoh: Venus from Akatsuki

- Large (up to of order 1000 km long) bow shaped waves seen in the Venusian afternoon by LIR camera (~10 micron) at cloud top altitudes as atmosphere moves over topographic rises exceeding 3 km above mean Venus surface elevation.
- Correlation between cloud height seen by IR2 camera (~2 micron) and the wave brightness temperature revealed at the 10 micron (higher cloud height corresponds to cooler brightness temperatures; and vice versa).
- UVI camera shows evidence of 0.28 micron contrasts (diagnostic of SO₂ abundance) correlated in space and time with observed 10 micron bow shaped wave.
- Multi-wavelength observations of Venus are important to understand atmospheric dynamics.

Orbit: Equatorial for detailed study of the super-rotation mechanism.

Yeon Joo Lee: Venus seen from UV Imager Onboard Akatsuki

- Long term monitoring the ultraviolet albedo of Venus, to characterize the unknown absorber cloud top distribution, relationship to sulfur species and impact on cloud top radiant energy. Investigations of unknown absorber distribution relies on observations made from the UV into the mid-visible wavelengths.
- Remote Sensing of the aerosols at low phase angle to obtain more “glory” phenomenon observations (to characterize its behavior with wavelength and hence confirm the particle size distributions in the upper clouds).

Orbit: Equatorial/Polar; equatorial provides more detail for study of hemispheric asymmetry and long-term monitoring of low-latitude region where UV absorber is most prominent.

Sanjay Limaye: *Multispectral Day and Night Cloud Morphology of Venus from Akatsuki Cameras*

- Discussed how the cloud cover appears different at different wavelengths and on the day and night sides due to different cloud forming processes.
- Wants cloud particle physical shapes and size distribution.
- Chemical composition of cloud particles — organic, inorganic.
- Ambient environmental conditions (bulk composition and abundances of trace species, T, P, wind, up/down radiative fluxes).
- Really wants VAMP and upper cloud and balloons in lower cloud region and lower and instruments to make sustained measurements.

Orbit: Elliptical, permitting communications with VAMP.

ATMOSPHERIC CHEMISTRY AND CLOUDS

Vladimir Krasnopolsky: *Modeling of Chemical Composition in the Lower and Middle Atmospheres of Venus*

- Wants to measure HBr, SO_2Cl_2 , ~ 1 ppb. [*Participant Comment: This is probably unmeasurable with existing technologies.*]
- Like to have active infrared spectroscopy in the clouds [McGouldrick: This can provide aerosol and atmospheric composition.]
- [*McGouldrick: He would desire Iron Chloride measurements, which he has put forward as a possibility for the unknown UV absorber.*]
- Requires In-situ measurements.

Franklin Mills: *Simulations of Vertical Profiles of SO and SO₂ in Venus' Mesosphere*

- Addressed diurnal variations of SO_x . Needs detailed geographical, vertical, and temporal resolution observations of sulfur-oxide species and atmospheric species that control the sulfur oxide chemistry.
- Needs better understanding of sulfur distribution within cloud layers with local time.
- Needs more complete lab data on reaction rates for chemical pathways expected to influence sulfur-oxide chemistry cycle.

Orbit: Equatorial is best / Polar is tolerable.

Kevin McGouldrick: *Microphysical Modeling of the Sulphuric Acid Venus Cloud System*

- Seconded Sanjay: Camera to look at particle shapes (habit – crystal shape), sizes.
- Composition of aerosols and resolve what they are. Direct compositional measurements of aerosols below cloud decks. Existing measurements have been inconsistent. Advocates for long-lived platform. (In-situ measurements.)

Christopher Parkinson: *Understanding the nature and variation of the Venesian middle atmosphere via Observations and Numerical modeling of the Key Tracer Species*

- Amount of H_2O strongly regulates the amount of SO_2 that you have (and vice versa), because the SO_x and H_2O rapidly become H_2SO_4 , which thus controls cloud formation.
- Wants descent profiles of SO_x , H_2O , H_2SO_4 , in the clouds from a descent probe.
- Wants to understand the spatial variations of these aforementioned species.

Sara Port: *Metal Sulfides and their Relationship with Gaseous Sulfur on Venus*

- Interested in near surface environment ($\sim 15\text{km}$ and below): mineralogy, winds, and gas composition/mixing ratios. Will aid in better understanding the chemical compositions near the surface and weathering.
- XRD/Raman/GCMS on lander element.

AERIAL PLATFORMS

James Cutts: *Venus Ariel platforms and engineering*

- Discussed possible aerial platforms:
 - Vega style balloons at a constant altitude (55 km). 110 kg payload for 7m balloon tested at JPL. Lifetime is 10+ days (approximately two circumnavigations). 20–30 kg useful science payload.
 - Altitude controlled balloon (metal bellows), rising and falling.
 - VAMP aircraft.
 - Partially buoyant metal “balloon” to sample deep atmosphere (0–30 km).
- Altitude controlled balloon may be the sweet spot in the option space, giving a balance between cost/risk and science value, excepting the 24 limited lifetime of the vehicle. *[Discussion: The deeper you go into the atmosphere with your balloon, the more development time and cost required; proper assessment of technology development requirements to come from NASA sponsored aerial platform study, February 2018 publication.]*
- Determine atmospheric circulation.
- Measurement of heating rates and cooling rates. Radiative transfer fluxes of radiance (short-wave, long-wave).
- Measurement of cloud particles.
- We need better measurements of lower atmosphere and how it fits into the whole system, as right now is treated as a boundary layer: Deep atmosphere supercritical fluid questions, such as the kinetics and chemistry of how they interact with the surface. However, this science is limited by visibility of the surface.

Siddharth Krishnamoorthy: *Infrasound Detection from Balloons*

- Advocates use of two barometers on balloon enables spatial filtering for separating an upward traveling waves associated with earthquakes.
- Other applications include detection of volcanoes. Infrasound community that is active looking at infrasound on Earth.
- There is some concern about background noise from atmospheric turbulence.
- Limitation: At 55 km altitude, need to be within a few hundred kilometers from epicenter of volcano or earthquake. *[Post presentation discussion indicated that odds of detecting activity requires the lifetime of platform to be >> 10 days.]*
- Could make deep dives with balloons to lower altitudes, but the real challenge in low altitude (<50 km) balloons is making instruments that will function >100 °C.

Eugene Ustinov: *Cloud Internal Field Radiometer (CIFR)*

- CIFR would conduct in-situ measurements of microphysical characteristics of cloud droplets.
- Multi-spectral, multi-angle measurements of vertical distribution of the field of scattered radiation within the cloud.
- The instrument has a heritage of use, beginning from Venera-9 and -10 landers.

PLASMAS

Glyn Collinson: *Mysteries of Atmospheric Escape and Evolution at Venus*

Science needs:

- Measure 3D cold ionospheric ions (never done before), catch all escaping plasma.
- Detangle and understand the competing mechanisms of atmospheric escape and loss (a la MAVEN). Which mechanisms dominate, how do they work, how has loss evolved over time?
- Map and understand Deuterium loss / Water loss.

Instrument needs: A comprehensive particles and fields package

- Cold and Hot Ion Spectrometer: Measure all atmospheric loss.

- Electron spectrometer + Langmuir Probe: Map and measure ambipolar field, measure ionospheric structure.
- Magnetometer: Understand how plasma is being lost.
- Neutral and Ion Mass Spectrometer: Measure isotopic fractionation, understand neutral source for plasma.

Orbit: Elliptical, polar, inclined, periapsis ~200km, PVO-like would be ideal.

Oleg Vaisberg: *Lessons from MAVEN*

Science needs:

- Simultaneous measurements of upstream conditions and ionosphere to directly study the influence and impact of driving factors on Venus such as the solar wind and solar EUV.
- Absolute planetary ion escape composition and flux measurements needed.
- What are the escape channels and processes? Upper atmosphere and ionosphere pickup, ionosphere scavenging, ionospheric clouds and streamers [Ambipolar fields, current sheet.]
- How do solar wind ions precipitate and accumulate in the atmosphere?
- Understand the influence of solar wind and radiation in cosmogenic time scale.

Instrument needs:

- Ionospheric plasma (low energy ions, Langmuir probe for electrons).
- Hot plasma (ions, ion composition, super-thermal electrons).
- Magnetic field.
- Plasma waves.
- Energetic particles (ions electrons).
- Atmospheric emissions (airglow, aurora).
- Ultraviolet Photometer for solar EUV.

Orbit: Elliptical, polar, periapsis 200km to 300 km.

INTERIOR, SURFACE, LANDING SITES

Philippe Lognonné: *Venus Seismic Interior-Atmosphere Coupling*

- Wants to use ionospheric acoustic waves to search for Venusquakes and seismic waves. Needs greater than 5.3 magnitude quake to see anything, detected a ~60° distance from epicenter at altitude of 250–300 km. Analysis of the frequency of the waves propagating from the epicenter may help to constrain thickness of the Venus crust.
- Payload: Cooled IR imager.
- Requirement: Image Venus with a slow orbital drift, implying high apoapsis (>30,000 km).
- 6U-12U satellite option could be piggyback on a Venus orbiter mission, left behind at high altitudes.
- “Needs a movie”, long time series images.

Orbit: Elliptical, high apoapsis (>30,000 km).

Lori Glaze: *Scientific Rationale for Selecting Landing Sites on Venus:*

- All prior Venus descents (Venera, Vega, PVO have been “Unassisted”. Assuming similar EDL, landing site must be large and uniform for safety.

Science Needs:

- What is the bulk composition and mineralogy for a “typical” surface rock?
- Are the tesserae made of different material than the plains?
- Do all the tesserae share the same composition?
- Do the surface rocks retain evidence for earlier climate conditions?

- Are there any remnant continents? I.e. Ishtar Terra, potential candidate for low-density (continental?) crust.
- Is there current volcanic activity on Venus? (Spikes in SO₂ seen by both PVO and VEX).
- What chemical/physical reactions are responsible for the abrupt changes in reflectivity seen at high altitudes in radar observations?

Instruments:

- Elemental chemistry and mineralogy:
 - XRD [challenging due to sample ingestion].
 - Raman/LIBS [Remote Sensing].
 - Neutron/Gamma spectrometer.
- Morphology
 - Descent imaging.
 - Panoramic imaging.
 - Sample imaging.
- Surface/Atmosphere interaction (Mass spectrometer / tunable laser spectrometer).
- Mechanism to remove outer rock surface, if possible.

Landing Sites: Top priorities from VEXAG's Venus Exploration Targets Workshop

- Tesserae.
- Volcanic plains.
- Young volcanic terrain.
- No matter where we land, we will learn critical new information about Venus' origin and evolution.

Richard Ernst: *Venera-D landing site selection based on Magellan radar images*

- Suggested landing site: Alpha Regio.
 - Also suggested various other tesserae, rift zones, and coronae.
- Tesserae would be the real prize: are they felsic or mafic?
- Otherwise, land in safe plains area with lobate flows that can be integrated into larger geological picture.
- Wants to investigate whether Venusian coronae are analogous to circumferential dyke swarms on Earth. Implications for past volcanic activity on Venus.
- Advocated for better Synthetic Aperture Radar data, to better elucidate this relationship, and constrain surface properties for future landings.

Piero D'Incecco: *Imdr Regio as the landing site of the Venera-D mission: a geologic perspective (poster)*

- Could provide information about variations in composition and physics of different melts

Thasanis Economou: *Venus Surface Elemental and Mineralogical Composition*

Instruments: Described the full range of possibilities

- X-Ray Fluorescence Spectrometer/Alpha Particle X-Ray Spectrometer: *Currently the choice instrument for elemental chemical composition.* Detects all elements above sodium (Na). Lots of spaceflight heritage. Could possibly use on aerosols in descent, measuring sulphur. Etc. 0.500 kg, 0.500 W.
- Chemical Analysis Package: Gas Chromatograph Mass Spec. Challenging for VENERA-D due to the requirement for high vacuum for proper operation, and this cannot be maintained inside the lander. But would be desirable for isotopic composition of rock forming elements. 10.5 kg, 12 W.
- Active Detection of Radiation of Nuclei: active gamma ray and neutron spectrometer. Provides subsurface elemental composition, radioactivity and decay rates of short and long-lived isotopes. 7 kg, 5 W (passive) / 19 W (active).
- Mossbauer spectrometer: Works only on iron bearing minerals, 0.5 kg, 0.6 W, several hours accumulation time required. [*Post presentation discussion: Would only be useful on the plains, would need to be sure there would be enough time for a measurement.*]

- Raman spectrometer: Preferred instrument for mineralogical composition in laboratory, not flown in space yet, will fly on ExoMars rover and Mars 2020. Can be inside the lander and remotely sample through a window. 8–10 kg, power 20–80 W.
- None of the old instruments are in existence today, and even if they could exist, we would not want to use them for a new mission due to mass, power, and old technology.
- Requests that NASA fund instrument development for Venera-D. Russia's practice of funding instrument development after selection of a mission is prohibitive to establishing needed infrastructure in a timely manner.

Mikhail Ivanov: Estimates of the frequency distribution of short-baseline slopes

- Slopes are a major threat to lander mission, but the best resolution available (MAGELLAN) is ~5 km/px.
- 7° slope limit for Venera-D. [*Post presentation discussion: Venera-9 landed at a 30° slope, but probably came close to failure, so wouldn't risk this today.*]
- To model, used DTMs (digital terrain models) of Earth (Iceland) to mimic relief found on Venus.

Discussion of the possible regions of Venus for landing

- Tessera are a window into the geological past, of great scientific interest. Doesn't look like friendly terrain to land on. Three types of basic topographic features. (1) Open Valley, (2) Cellular relief, (3) Ridge flank.

In most cases, the modeled slopes are very large, 30–40°. Probability of encountering steep slopes is very high in the Tessera. Smooth and flat regions are rare to absent.

[*Lori Glaze: Different interpretation of Tessera. Based on stereo radar of Ovda Tessera, can see that the slopes there are on average less than 5 to 10°. Less than 5 % of the area is sloped greater than 5°. Mikhail Ivanov: These results unfortunately do not have high enough resolution to spot roughness that appeared in our work.*]

- Several types of plains. In all model cases, the mode of the slope distribution in shield and regional plains is higher than the 7 degrees safety limit. The slope distribution mode for dark flows of lobate plains and smooth plains is well below this limit.
 - **Smooth plains** (Impact related): extensive areas, low radar albedo, smooth deposits of fine-grained ejecta. Dark parabolas around the large impact craters. Parabolas are many hundreds of kilometers wide. Dimensions of the darkest (smoothest) spots are many tens of kilometers. Potentially represent much better areas for safe landing. Form well-mixed and representative samples of the upper crust of Venus.
 - **Regional plains:** likely represent a sample of the upper mantle of Venus, huge areas homogeneous, lava flooding with regular ridges. Relief is complicated by wrinkle ridges. Albedo is lower than in shield plains. Flat areas between the ridges are typically 20–25 km across. May provide better surfaces for safe landing. The plains themselves are thousands of km across, and thus make for a safer landing site. Backscatter radar indicates they are as smooth as parking lots.
 - **Shield plains:** represent a result of crustal melting. Fractional differentiation and crustal contamination are expected. Relief complicated by numerous volcanic constructs. Flat areas between the shields are typically 10–15 km across. May not provide sufficiently large areas for a safe landing. Not as safe as regional plains.
 - **Lobate plains:** Large and numerous lava flows; polyphase eruptions. Likely represent a result of decompressional melting of deep-seated diapirs. Complexes of smooth (dark) and rough (bright) lava flows. Dark flows are typically small and always neighboring with bright flows. Do not provide sufficiently large areas for safe landing.
- Landing site: Advocated smooth plains of impact origin.

Allan Treiman: Venus' Radar-Bright Highlands: Different Causes at low and high latitudes

- Landing site: Advocates for a landing on high-radar reflectance surface near Cleopatra impact site on Maxwell Montes. Identify what the radar bright surface is. Relatively flat and smooth. Need mineralogical and chemical analyses, surface and shallow depth. Candidate for continental

crust, low-density siliceous rock is a possible explanation for high elevations. Major implications for the role of water and possible plate tectonics.

- Tight landing ellipse required. Crater is 105 km in diameter.
- Landing ellipse is 300 km.
- Likely very steep cliffs and full of boulders.

Michael Way: Modeling Venus through Time and its Implications for the Habitable Zone

- Kasting limit. If ~0.1 % mixing ratio of H₂O, atmosphere loses an Earth ocean's worth of water in a few Gy. Doesn't think that this is how Venus lost its water, based on how these ancient models evolve.

Scientific Needs:

- Need in-situ measurements of Xe, Kr, Ar, and isotopes to constrain geochemistry and mantle redox states.
- Better D/H constraints for water inventory.
- Can present day interior and structure and topography tell us about the history of plate tectonics (stagnant lid, subduction, etc.).
- Should we consider looking for signs of life? (very speculative, but we have no idea where life began on Earth) If life did ever exist for any length of time, it could have filled every niche, including the skies and upper cloud decks. Not unreasonable, given there may have been mass exchange between Earth and Venus.
- Exoplanets will inform Venus' climatic history and possibly vice-versa.

MISSION ARCHITECTURE

Mikhail Gerasimov: A Prototype of the Soil Sampling System

- VEGA/VENERA-13 Soil Sampler mass was 26 kg.
- Half of mass of instrument is gas tank.
- Sample to be ingested is ~5 g (assuming density of basaltic rock and stated cylinder with $d = 16$ mm, $h = 36$ mm).
- Sample acquisition time is 204 seconds.
- Sample analysis time was unstated.

DISCUSSION: INTERIOR, SURFACE, LANDING SITES

CONCLUSIONS:

Landing site:

- Guiding science question: "What is a representative rock on the surface of Venus?"
- Go for the lava, take one drilling, take multiple samples down through it to understand weathering, and the dust on top.
- Landing terrain selected: **Target the Regional Plains.**
- Land away from impact ejecta to go for pristine basalt.
- Divide into three latitude ranges, specify best landing sites, and science that can be done from that orbit. IKI to work with orbital engineer.

Sample collecting discussion:

M. Gerasimov asks, how many samples will be collected. Also asks, if dust/sand/soil should be collected. Mutual opinion: analyze rock; more important than soil. Gerasimov suggests a combination of a 'vacuum cleaner' and driller. Driller withdraws samples from the depth to the surface, 'vacuum cleaner' collects it; also at first it could collect and analyze the soil on top, then drill to analyze the rock beneath.

Strawman Instruments:

- XRF.
- Fast Mossbauer Spectrometer – Thanasis Economou suggests instrument optimization since Mars instruments require hours for integration!
- Raman/LIBS, vis Mars 2020? There were concerns it may be difficult/complex to put this instrument on the lander because a window which transfers heat inside.
- CAP/LIMS under development by IKI for chemical/isotopic analysis of gases, aerosols on descent and surface rocks on landing.
- **Vital that sponsoring agencies (NASA/Roscosmos) make early investments in instrument development and technology for Venus.**

Possible Mission Enhancements:

- Enhanced scenario, a Venus program with additional or multiple landers which go to other landing sites?
- Drop a sonde from aerial platform for optical images of Tessera surface? Information can be used for a future lander on the tesserae.

DISCUSSION: MISSION ARCHITECTURE AND ORBIT***Notes concerning Landers:***

The discussion began with a 24 Hours polar orbit, and Viktor was asked about the roadmap for the mission.

Viktor Vorontsov [Paraphrased from notes]: “This was discussed. Today represented the first science input because of new instruments. Let’s follow the tasks given to us by the directors, which are to define the architecture of the lander and then the orbiter. This will depend on analysis of launch capabilities. Mass of spacecraft is on the order of a ton. Architecture will depend upon orbital maneuvers.”

Discussed specifics on the architecture of the mission with regard to the lander. He mentioned thermal diffusion on the lander as being important, since different instruments will need to be at different operating temperatures. The IKI proposal timescale is required soon and the payload and resource budgets (mass, power, data) are needed soon. Lavochkin Association assumes VAMP as part of the launched payload, but as a black box, which is very challenging.

Venera-9 lander was landed at 15° slopes. If NPOL is designing lander for 30° slopes, this enables tesserae landing sites, more appealing from the science point of view. [This new possibility requires that M. Ivanov completes new landing analysis simulations, as the one he presented on this meeting was made in assumption of 7° slopes to be safe for landing.]

They are considering 4 launch dates: 2026, 2028, 2029, 2031. The first and the last are preferable, as they provide maximal scientific payload. Overall mass of the SC is in range 5800-7000 kg. [Scientific payload mass on the order of ~2000 kg.]

NOTE: The outside dimensions, mass, and design of the lander are fixed and will not change

Key unresolved questions:

- The mission architecture and payload are currently vague, and need to be defined, before all other engineering issues can be settled. This needs to be done soon.
- Is the aerial platform optional or to be included in the Lavochkin Association (NPOL) baseline definition? Considering both cases is not easy.

It was discussed that the Aerial platform will be defined at the beginning of 2018. The deployment is dependent on the type of platform; VAMP needs a circular orbit because of its inflation requirement prior to atmospheric entry. Jim Cutts and Jeff Hall pointed out that all the other platforms can enter at the same entry speeds as the lander.

Notes concerning Atmosphere and Aerial Platforms:

Alexander Rodin: Proposed an inter-comparison between Venus Global Circulation Models, with the goal of a standard atmospheric reference model as a baseline for Venera-D. Advocated for orbital science focused on spectroscopy of non-local thermal equilibrium emissions.

Sebastian Lebonnois: Emphasized importance of measuring in-situ heating rates and solar rates on an aerial platform at altitude of 30–40 km [Note: *this is technically challenging due to the high temperatures below 50 km.*]

Lori Glaze: Advocated for a mass spectrometer to measure noble gasses (Kr, Xe, Ne) below the homopause (110 km).

Notes concerning Long Lived Landers:

Chris Parkinson: Advocated for a lander at the equator taking atmospheric composition measurements during descent using LIDAR.

Sebastian Lebonnois: Advocated for wind-measurements on the long-lived lander package, with accuracy of 1cm/s, to be made at least 50cm above the surface. Also advocated weather measurements with 0.1K and sub pascal accuracy. One set of measurements every 24 hours.

Jeff Hall: Strongly advocated the simplicity of mounting a long-lived surface element as part of the main lander, since this will take care of all Entry, Descent, and Landing. [Seconded by Sanjay.]

Notes from Orbital Discussion: Polar versus Equatorial debate

Ludmila Zasova [Polar advocate]: Significant measurements that are able to look at simultaneous day and night style behavior are best obtained from a polar orbit.

Takehiko Satoh [Equatorial advocate]: Equatorial vantage point is needed to study super-rotation, and Akatsuki did not enter its optimal orbit.

Oleg Vaisberg [Polar advocate]: To study atmospheric circulation, a wide geographical phase space (latitude, longitude, altitude) coverage is needed. A [PVO-like] polar orbit gives complete coverage of this phase space, whereas an equatorial orbit is much more limited — in particular the ability to study polar circulation is lost.

Glyn Collinson [Polar advocate]: Advocates an elliptical polar, inclined orbit, with line of apsides (latitude of perigee) near the equator (PVO like) to cover the whole thermosphere and ionosphere over the course of the mission. Asked if the long term evolution of the orbit could be examined. In terms of night-time observations and period of observation of the nightside.

Natan Eismont: The long term evolution of the orbit can be studied for altitude and changes in orbit inclination. [Sanjay Limaye: *Due to the lack of a J2 bulge, the inclination evolution is expected to be minimal, and dominated by solar pressure.*]

Enhancing Elements/Observations Discussion:

Glyn Collinson: Advocated for a comprehensive particle and fields package to understand the evolution of Venus over time, and the interaction between thermosphere and ionosphere to understand super-rotation.

Missing Orbiter instruments:

Glyn Collinson: Advocated that a EUV solar photometer (as proposed by Oleg Vaisberg) and thermospheric neutral winds instruments be added to the Venera-D orbiter instrument package.

GENERAL
CIRCULATION
MODELS

THE LATEST ON THE VENUS THERMOSPHERIC GENERAL CIRCULATION MODEL: CAPABILITIES AND SIMULATIONS

A. S. Brecht¹, S. W. Bougher², C. D. Parkinson²

¹ NASA Ames Research Center, Moffett Field, CA USA

² Climate and Space Sciences and Engineering at the University of Michigan (CLaSP), USA

Abstract

The Venus Thermospheric General Circulation Model (VTGCM) is being updated with new chemistry, heating parameterizations, and wave parameterizations. This is being accomplished in order to make comparisons with Venus Express observations as well as ground-based observations. The updates provide more constraints to the VTGCM and realistic ways to simulate atmospheric variability. Furthermore, these updates will make the VTGCM well poised to analyze and provide context to future observations such as the Russian mission, Venera-D.

Introduction

Venus has a complex and dynamic upper atmosphere. This has been observed many times by ground-based, orbiters, probes, and fly-by missions going to other planets. Two over-arching questions are generally asked when examining the Venus upper atmosphere: (1) what creates the complex structure in the atmosphere, and (2) what drives the varying dynamics. A great way to interpret and connect observations to address these questions utilizes numerical modeling; and in the case of the middle and upper atmosphere (above the cloud tops), a 3D hydrodynamic numerical model called the Venus Thermospheric General Circulation Model (VTGCM) can be utilized. The VTGCM simulates observable features that are used as “tracers” for Venus’ circulation, such as chemical species abundances and distributions, nightglow emissions, temperature, electron density. Recently, the VTGCM simulations have been compared to various ESA Venus Express (VEX) observations and also have been updated to incorporate new chemical constituents and parameterizations.

Table 1: A list of observations used as constraints to validate VTGCM simulations. Also provided are the local time of the observations and the specific mission that obtained these observations

| Model Constraint | Local Time | Mission (Instrument) |
|--|-----------------------------------|--|
| O, N(4S), CO, CO ₂ profiles (i.e. peak density and altitude (DY-NT variability)) | Day and Night (Terminator for CO) | Pioneer Venus (ONMS, OAD), Venus Express (SOIR, VIRTIS, SPICAV), Ground-based |
| Temperatures: Exosphere, 110 km (day), varying ~100 km with associated vertical velocities (night), and profiles | Day, Night, Terminator | Pioneer Venus (OIR, ORO, in situ), Venus Express (VIRTIS, SOIR), Ground-based |
| Trace species distributions (~70–100 km) | Day, Night, Terminator | Pioneer Venus (ONMS), Venus Express (SOIR, SPICAV), Akatsuki (IR1, IR2, UVI), Ground-based |
| Peak electron density and altitude (SZA variations) | Day | Pioneer Venus (ORO), Venus Express (VeRa) |
| 3 Nightglow emissions: peak intensity and alt. of layers (NO UV, O ₂ IR, and OH IR) | Night | Pioneer Venus (OUVS), Venus Express (VIRTIS, SPICAV), Akatsuki (LAC) |
| SS-AS and RSZ wind comp. (time averaged +variability) | Terminator | Ground-based |

Venus Thermospheric General Circulation Model (VTGCM)

The VTGCM is a hydrodynamic, forth-order, centered finite-difference three-dimensional code. It has 69-log pressure levels and is a 5x5 latitude vs longitude grid (e.g. Bougher et al., 1988). The vertical range is ~70 to ~250 km altitude on the dayside. The VTGCM can produce climatological averages of key features in comparison to observations (i.e. nightside temperature, O₂ IR nightglow emission) (Brecht et al., 2011) with the utilization of two Rayleigh friction (RF) terms. One RF term is symmetric about the sub-solar point with a cos(latitude) variation which provides constant deceleration to the winds (RF-sym). The second RF term is asymmetric about the sub-solar point with a cos(latitude) variation in order to simulate the retrograde super-rotation zonal wind (RSZ).

The purpose of RF is to obtain a first order approximation of the necessary wave momentum deposition to reproduce observations. Therefore, the RF provides guidelines for the implementation and adjustment of new gravity wave momentum deposition parameterizations.

Along with the key VEX features observed, there are many more observables used for constraining the VTGCM (see Table 1). The continuous evolution of the VTGCM is important, as more observations are conducted, to provide a useful tool to de-couple and diagnostically examine the Venus' middle-upper atmosphere structure and winds in all of its variability and complexity.

Recent VTGCM Simulations vs Measurement Comparisons

The VTGCM has been focused on constraining the thermal structure and tracer density profiles. As of late, detailed comparisons have been conducted with VEX SOIR and VIRTIS instruments.

SOIR

VEX SOIR terminator temperature and CO₂ density profiles (in the northern hemisphere) have been collected and compared to the VTGCM (Bougher et al., 2015), see Fig. 1. It was demonstrated that the VTGCM simulates the temperature minimum near 125 km and the stronger temperature maximum over ~130–150 km as observed and at the pressure/altitude levels at low latitudes. However, the magnitudes of the simulated and measured temperatures are different as a function of latitude. The model also produces an asymmetry between the two terminators which the SOIR observations do not show. From this work it was determined that both radiative and dynamical processes are responsible for maintaining averaged temperatures at the terminator.

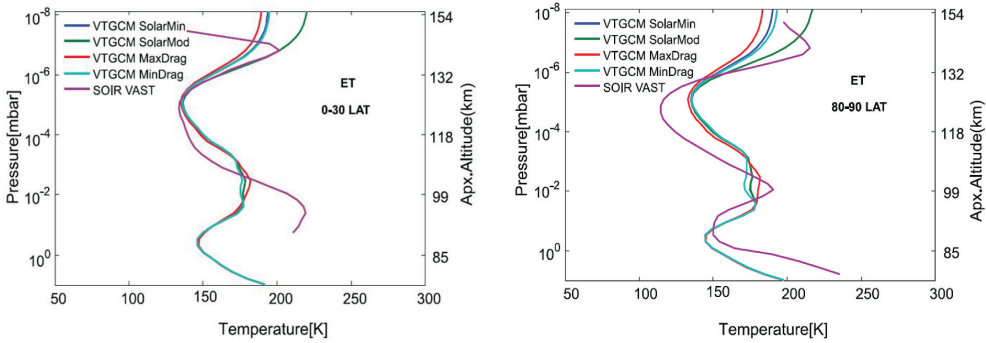


Figure 1: VEX SOIR temperature versus VTGCM simulation at the evening terminator at different latitude ranges. There are two different solar condition and two different zonal wind strengths for the VTGCM simulations. See (Bougher et al., 2015) for more details

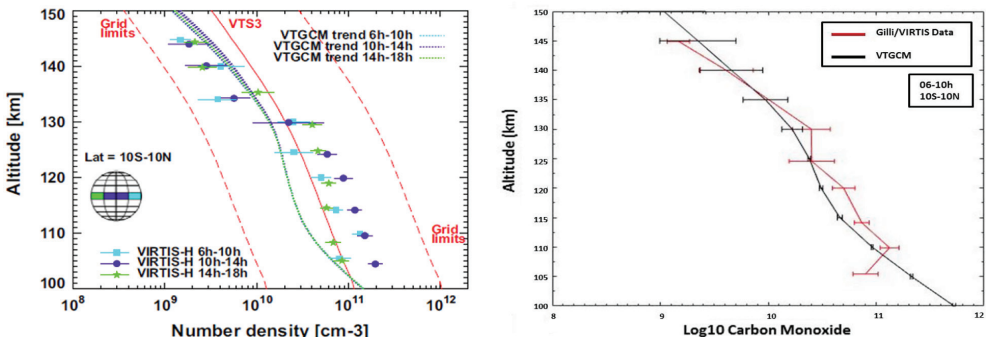


Figure 2: VEX VIRTIS carbon monoxide observations versus VTGCM simulated carbon monoxide (Gilli et al., 2015). Left plot is VTGCM simulations without aerosol heating and right plot is VTGCM simulation with aerosol heating at LT = 6–10 h and 10°S – 10°N latitude.

VIRTIS

VEX VIRTIS instrument provided temperature and CO density profiles covering mainly the northern hemisphere and dayside with an altitude range from ~100 km to 150 km. These observations were originally compared with the VTGCM simulations by (Gilli et al., 2015); see Fig. 2 (left plot).

The VTGCM reproduced the CO density profiles reasonably above ~ 125 km and below ~ 125 km the model under produced the CO density. Preliminary work has shown that by including aerosol heating in the VTGCM the CO density increases in the altitude range of ~ 90 km to ~ 130 km due to increasing scale heights, see Fig. 2 (right plot). As for the temperature profiles, the model overestimates sub-solar temperatures near the equator from ~ 100 km to 130 km altitude. However, the VTGCM is in better agreement with observations at higher latitudes (noontime meridian) and at the terminators (near the equator). The temperature discrepancy could be related to the observations having large error bars or the VTGCM is not capturing all the physics necessary to simulate the circulation.

Current VTGCM Improvements

The latest improvements to the VTGCM enable the model to address the driving forces in Venus' upper atmosphere and its' variability.

Chemistry

The SO_x chemistry has been included (e.g. SO₂ and SO) and also the necessary OH chemistry to model the OH nightglow emission (Parkinson et al., 2010, 2015). Additionally, the OH chemistry improves the O₂ chemistry, thus providing more sources and sinks for the O₂ IR nightglow emission. The inclusion of these chemical species (and nightglow emission) provides tracers of the global circulation at different altitudes in the upper atmosphere.

Heating

The VTGCM lower boundary is at ~ 70 km, which is near the cloud tops. Near this level, aerosols provide heat to the middle atmosphere. A parameterization guided by (Haus et al., 2015) has been incorporated and tested. The additional heating increases the scale heights in this altitude range (~ 75 – 90 km) and therefore augments density profiles (~ 100 – 130 km) and modifies wave propagation, as shown in Fig. 2.

Additionally, an updated simplified non-LTE formulation utilized within the LMD-MGCM and LMD-VGCM codes is in the process of being adapted into the VTGCM (González-Galindo et al., 2013; Gilli et al., 2017). The non-LTE model uses five CO₂ levels and bands, instead of two molecular levels. It calculates the full exchange between atmospheric layers, instead of using the cool-to-space approximation which was the basis of the previous thermospheric parameterization in the VTGCM (Dickinson, Ridley, 1976; Bougher et al., 1988). We expect to find VTGCM temperatures warmer over ~ 80 – 110 km (day and night) and about the same (cool to space approximation is fine) in the Venus dayside and nightside thermosphere (above ~ 110 – 120 km).

Waves

Due to observations of waves near the cloud tops, Kelvin and Rossby planetary waves have been implemented as part of the VTGCM lower boundary. But most importantly, they have been implemented with a self-consistent moving lower boundary (winds are not equal to zero and temperature is not constant). This lower boundary is taken from the Oxford Venus GCM; 5 day time averaged fields (T, U, V, Z) were provided (Lee, Richardson, 2010, 2011). The combination of the moving lower boundary and Kelvin waves produces variability which impacts the intensity and local time location of the O₂ IR nightglow emission. These variations in the nightglow emission (as much as ~ 1 – 3 MR) are of a similar magnitude as observations. Waves are important to understand because of their impact on the varying dynamics of Venus' upper atmosphere.

Furthermore, a gravity wave momentum deposition parameterization (GWMD-Y) is being implemented into the VTGCM. It is a whole atmosphere spectral non-linear parameterization (Yigit et al., 2008). It accounts for many wave dissipation processes that are important in the Venus upper atmosphere, including molecular diffusion and viscosity, plus radiative damping. The GWMD-Y parameterization is different from the Alexander and Dunkerton (1999) (AD) parameterizations because it allows gravity waves to be saturated at multiple heights and the waves are not completely removed at a single breaking level. The computed momentum deposition ("drag") and heating/cooling rates are applied to the momentum and energy conservation equations, respectively. However, the GWMD-Y parameterization does not take into account total internal reflection as does the AD parameterization.

VTGCM Connection to the Venera-D mission

The VTGCM is strongly connected to the Venera-D mission science and objectives. The spatial domain and physics within the VTGCM encompasses the goals and objectives listed in Table 2 and 3.

Furthermore, the VTGCM will greatly benefit from tighter constraints from the Venera-D mission mission regarding; wave parameters, nightglow emissions (NO UV, O₂ IR, OH IR), and minor species (CO, O, SOx) distributions to trace circulation patterns (“transition” region) and address variability. Additionally, observations are needed of the electron and ion temperatures to address the connection between the super rotating ionosphere and the neutral RSZ winds.

Table 2: Science goals and anticipate science results expressed in the Venera-D Joint Science Definition Team document (31-1-2017). The VTGCM is poised to help support these science goals and achieve these results

| Science Goals | Anticipate Science Results |
|--|--|
| Understanding atmospheric super-rotation and global circulation | Validate different processes that maintain super-rotation |
| Understand the radiative balance and driver for the super-rotation | Quantify the structure and relationship of solar thermal tides to energy deposition and their role in super-rotation |

Table 3: Objectives express in the Venera-D Joint Science Definition Team document (31-1-2017) Table 3.3-2 in which science using the VTGCM can help support. The “O” objectives relate to the orbiter and “L” objectives relate to the lander

| Venera-D Objectives |
|---|
| O2. Atmospheric dynamics and airglow |
| O4. Vertical Structure and composition of the atmosphere |
| O6. Ionosphere and atmosphere |
| O8. Atmospheric density, temperature, wind velocity, mesospheric minor constituents and CO ₂ dayglow |
| L1. Atmosphere composition during descent |
| L3. Atmospheric structure and dynamics |

Conclusions

The ability to understand Venus’ complex and dynamic upper atmosphere relies on well-equipped numerical models to fill in the gaps where observations are not available, as well as new observations to help constrain these numerical models. This balance is delicate and occurring within the context of improvements presently being made to the VTGCM and the available observations thus far. The perspective of the Venera-D mission will enhance our ability to simulate Venus’ atmosphere thus understand underlying processes driving the complex and dynamical structure of the upper atmosphere of Venus

Acknowledgements

A.S. Brecht and S.W. Bougher have been supported by NASA Grant #NNX14AB66A. C.D. Parkinson has been supported by NASA Grant #NNX15AH30G.

References

- Alexander, M. J., Dunkerton, T. J. (1999) A Spectral Parameterization of Mean-Flow Forcing due to Breaking Gravity Waves, *J. Atmospheric Sciences*, 56, 4167–4182.
- Bougher, S. W., Dickinson, R. E., Ridley, E. C., Roble, R. G. (1988) Venus Mesosphere and Thermosphere: III. Three-Dimensional General Circulation with Coupled Dynamics and Composition, *Icarus*, 73, 545–573.
- Bougher, S. W., Brecht, A. S., Schulte, R., Fischer, J., Parkinson, C. D. Mahieux, A., Wilquet, V., Vandaele, A. (2015) Upper Atmosphere Temperature Structure at the Venusian Terminators: A Comparison of SOIR and VTGCM Results, *Planetary and Space Science*, 113–114, 336–346.
- Brecht, A. S., Bougher, S. W., Gerard, J. C., Parkinson, C. D., Rafkin, S., Foster, B. (2011) Understanding the Variability of Nightside Temperatures, NO UV and O₂ IR Nightglow Emissions in the Venus Upper Atmosphere, *J. Geophysical Research*, 116, E08004.
- Dickinson, R. E., Ridley, E. C. (1976) Venus Mesosphere and Thermosphere Temperature Structure: II. Day-Night Variations, *Icarus*, 30, 163–178.
- Gilli, G., Lopez-Valverde, M. A., Peralta, J., Bougher, S., Brecht, A., Drossart, P., Piccioni, G. (2015) Carbon Monoxide and temperature in the Upper Atmosphere of Venus from VIRTIS/Venus Express non-LTE Limb Measurements, *Icarus*, 248, 478–498.

- Gilli, G., Lebonnois, S., González-Galindo, F., López-Valverde, M. A., Stolzenbach, A., Lefèvre, F., Chaufray, J.Y., Lott, F. (2017) Thermal structure of the upper atmosphere of Venus simulated by a ground-to-thermosphere GCM, *Icarus*, 281, 55–72.
- González-Galindo, F., Chaufray, J.-Y., López-Valverde, M. A., Gilli, G., Forget, F., Leblanc, F., Modolo, R., Hess, S., Yagi, M. (2013) Three-dimensional Martian ionosphere model: I. The photochemical ionosphere below 180 km, *JGR: Planets*, 118, 2105–2123.
- Haus, R., Kappel, D., Arnold, G. (2015) Radiative Heating and Cooling in the Middle and Lower Atmosphere of Venus and Responses to Atmospheric and Spectroscopic Parameter, *Planetary and Space Science*, 117, 262–294.
- Lee, C., Richardson M.I. (2010) A General Circulation Model Ensemble Study of the Atmospheric Circulation of Venus, *J. Geophysical Research*, 115, E04002.
- Lee, C., Richardson, M.I. (2011) A Discrete Ordinate, Multiple Scattering, Radiative Transfer Model of the Venus Atmosphere from 0.1 to 260 μm , *J. Atmospheric Sciences*, 68, 1323–1339.
- Parkinson, C.D., Brecht, A., Bougher, S.W., Yung, Y.L. (2010) Observations of night OH in the mesosphere of Venus, International Venus Conference, Aussois, France, 21–26 June, 2010.
- Parkinson, C.D., et al. (2015) Distribution of sulphuric acid aerosols in the clouds and upper haze of Venus using Venus Express VAST and VeRa temperature profiles, *Planetary and Space Science*, 113–114, 205–218.
- Yiğit, E., Aylward, A.D., Medvedev, A.S. (2008) Parameterization of the effects of vertically propagating gravity waves for thermosphere general circulation models: Sensitivity study, *J. Geophysical Research*, 113, D19106.

BEHAVIOR OF VENUS PLANETARY BOUNDARY LAYER AS PREDICTED BY THE IPSL VENUS GCM

S. Lebonnois¹, G. Schubert², F. Forget¹

¹ *Laboratoire de Météorologie Dynamique/IPSL, Sorbonne Universités, UPMC Univ Paris 06, ENS, PSL Research University, Ecole Polytechnique, Université Paris Saclay, CNRS, Paris, France, sebastien.lebonnois@lmd.jussieu.fr*

² *Department of Earth, Planetary, and Space Sciences, UCLA, CA, USA*

Keywords: climate model, planetary boundary layer, diurnal cycle, surface convective activity

Introduction

The deep atmosphere of Venus remains largely unexplored, because of the difficulty to get observations below the dense and planet-wide cloud cover, and with only a small number of Venera, Pioneer Venus and VeGa probes that reached the surface. However, the interaction between the surface and the atmosphere is a key player in understanding the processes driving the atmospheric structure. The exchanges of heat and angular momentum drive the temperature and wind structure in the deepest layers of Venus's atmosphere, and affect the drivers of Venus' superrotation. While waiting for additional observations, the analysis of the planetary boundary layer (PBL) is investigated here with the help of the latest simulations from the IPSL Venus Global Climate Model.

Model

The IPSL Venus Global Climate Model has been developed for roughly 10 years (Lebonnois et al., 2017). It includes a full description of the radiative transfer based on the latest modeling of the solar flux (Haus et al., 2015) and infrared net exchange rates taking into account the latest latitude-dependent cloud model (Haus et al., 2014), slightly tuned to get a vertical structure of the temperature very close to observations. The latest simulations reproduce quite well the atmospheric structure, including the cold collar and the superrotation (Garate-Lopez, Lebonnois, 2018). In the deep atmosphere, the planetary boundary layer scheme used is based on (Mellor, Yamada, 1982), a simple but efficient scheme used e.g. to study Titan's planetary boundary layer (Charnay, Lebonnois, 2012).

Characteristics of Venus Planetary Boundary Layer

The strength of the convective activity in the PBL is investigated through analysis of the sensible heat flux at the surface, the convective flux and potential temperature profiles. Surface temperatures are very stable, with diurnal variations limited to a couple of degrees.

Diurnal cycle and latitudinal behavior

The sensible heat flux is strongly driven by the solar flux received at the surface, as seen in Fig. 1. Convective activity peaks at noon (12LT), and is also correlated with latitude. At high latitudes, solar heating is compensated by infrared cooling and no convective activity is predicted.

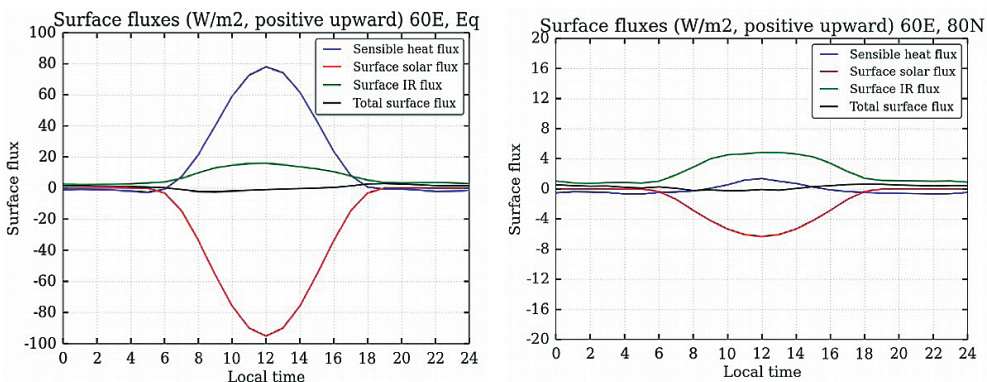


Figure 1: Diurnal cycle of the sensitive heat and radiative fluxes at the surface for 60°E longitude and (left) Equator and (right) 80°N

Role of topography

Figure 2 shows that the strength of the convection and the thickness of the noon convective layer is strongly correlated to topography, in particular in mid- to low-latitude regions. Noon surface solar flux is higher than zonal average over higher topographical features, inducing stronger convective activity.

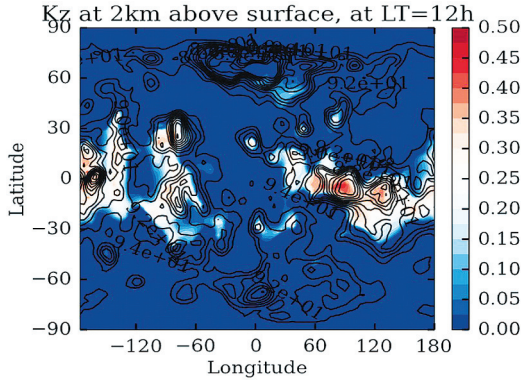


Figure 2: Map of the mixing coefficient associated to the noon convective activity at 2 km altitude above the surface, with contours indicating the topography. Every grid point is taken at noon local time

This is also clearly seen in the potential temperature profiles, as shown in Fig. 3. The deepest layer is more stable for low topography, and convective activity is usually limited to less than 2 km above surface, while it can reach up to 7 km for high topographic locations.

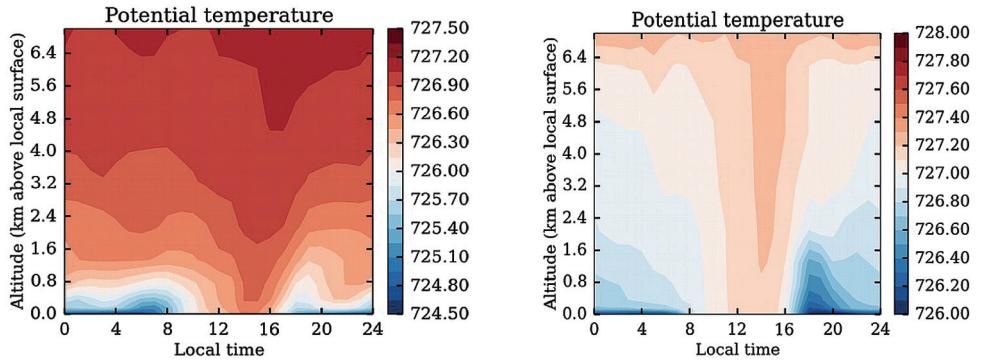


Figure 3: Diurnal cycle of the vertical profile of potential temperature, at 170°W longitude and (left) 30°N, which is a low-topography region, and (right) near equator, a high-topography region. The mixing of potential temperature seen during daytime hours is the result of convective activity

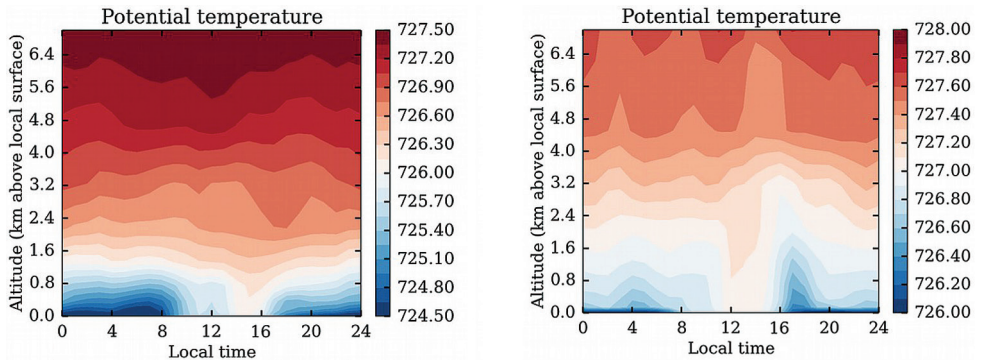


Figure 4: Same as Fig. 3, but for a simulation that takes into account the vertical gradient of the nitrogen abundance proposed by (Lebonnois, Schubert, 2017)

Impact of the possible gradient of nitrogen

As proposed in (Lebonnois, Schubert, 2017), it is possible that the deepest 7 km of the atmosphere may not be uniformly mixed, with a vertical gradient of nitrogen, from 3.5 % at 7 km to almost 0 at surface. This has an impact on the stability of the PBL, as the mean molecular mass gradient is reducing the buoyancy. When this gradient is taken into account in the GCM simulation, it affects the vertical extension of the convective layer above topographical features, as shown in Fig. 4, to be compared to Fig. 3.

References

- Charnay, B., Lebonnois, S. (2012) Two boundary layers in Titan's lower troposphere inferred from a climate model. *Nature Geoscience*, 5, 106–109.
- Garate-Lopez, I., Lebonnois, S. (2018) Latitudinal variation of clouds' structure responsible for Venus' cold collar, *Icarus*, Submitted.
- Haus, R., Kappel, D., Arnold, G. (2014) Atmospheric thermal structure and cloud features in the southern hemisphere of Venus as retrieved from VIRTIS/VEX radiation measurements, *Icarus*, 232, 232–248.
- Haus, R., Kappel, D., Arnold, G. (2015) Radiative heating and cooling in the middle and lower atmosphere of Venus and responses to atmospheric and spectroscopic parameter variations, *Planet. and Space Sci.*, 117, 262–294.
- Lebonnois, S., Schubert, G. (2017) The deep atmosphere of Venus and the possible role of density-driven separation of CO₂ and N₂, *Nature Geoscience*, 10, 473–477.
- Lebonnois, S., Sugimoto, N., Gilli, G. (2016) Wave analysis in the atmosphere of Venus below 100-km altitude, simulated by the LMD Venus GCM, *Icarus*, 278, 38–51.
- Mellor, G.L., Yamada, T. (1982) Development of a turbulent closure model for geophysical fluid problems, *Rev. Geophys. Space Phys.*, 20, 851–875.

GAS DYNAMICS GENERAL CIRCULATION MODEL OF THE VENUS ATMOSPHERE

A.V. Rodin^{1,2}, I.V. Mingalev³, K.G. Orlov³

⁰¹ *Moscow Institute of Physics and Technology*

² *Space Research Institute of the Russian Academy of Sciences*

³ *Polar Geophysical Institute of the Russian Academy of Sciences*

Keywords: atmospheric dynamics, climate model, polar vortex

We report recent developments of the general circulation model of the Venus atmosphere (VGCM) based on the full set of gas dynamics equations for compressible, viscous gas. The solution is calculated on a dense uniform mesh with the resolution 0.46° in horizontal coordinates (about 50 km at low latitudes) and 250 m in the vertical. Model domain extends from the surface to 120 km. Magellan topography is utilized as a boundary condition at the bottom. At the top of the model atmosphere, only mass conservation is assumed, without artificial sponge layer. Gas composition is suggested to be constant at all altitudes. The changes of the atmospheric composition and equation of state in the deep layers of the Venus atmosphere is neglected. The model lacks radiation block, with radiative forcing being simulated by the relaxation to a prescribed thermal profile. It is this profile, as well as relaxation time, are the parameters that control suggested heat sources and sinks.

Due to suggested thermal regime in the polar regions, the model succeeds to simulate both zonal superrotation and subsolar-antisolar circulation. The interface between these two regimes, located near 90–95 km, is subject to strong wind shear and dissipation of superrotation kinetic energy. Model simulations suggest that this altitude range may reveal complex multiscale dynamics and hence, should be subject to comprehensive studies by future missions to Venus.

The model is also capable to reproduce the structure of polar vortices with high spatial resolution. Simulation results are consistent with the hypothesis that their structure is determined by the presence of heat sources at high latitudes above the cloud layer.

LARGE STATIONARY GRAVITY WAVES: A GAME CHANGER FOR VENUS' SCIENCE

T. Navarro¹, G. Schubert¹, S. Lebonnois²

¹ Department of Earth, Planetary, and Space Sciences, University of California, Los Angeles, USA, tnavarro@epss.ucla.edu

² Laboratoire de Météorologie Dynamique, IPSL, Paris, France

Keywords: gravity wave, mountain wave, climate model

Introduction

Illustrated in figure 1, the recent discovery of a stationary planetary-scale structure in the atmosphere of Venus by the spacecraft Akatsuki (Fukuhara et al., 2017) leaves many unanswered questions: What is the nature of this wave? What is its origin? What is its role in the superrotation of the atmosphere? Etc... In this work, we tackle these issues with the use of a Global Climate Model (GCM). It appears that the implications of this study are of substantial importance for the design of future space-based measurements.

Model

The model used in this study is the Institut Pierre-Simon Laplace (IPSL) Venus GCM (Lebonnois et al., 2010). It includes a dynamical core on a longitude-latitude grid and a full parameterization of the physics with, among other things, a predicted vertical stability profile, a complete radiative transfer and a latitude-dependent cloud layer. In order to address the origin of the gravity wave seen by Akatsuki, we implement a parameterization of the effects of subgrid topographic slopes on the flow, a classic implementation for Earth GCMs (Lott, Miller, 1997).

Results

As seen in Fig. 1, the GCM is able to reproduce well the observations above Aphrodite Terra (Fig. 2) by turning on the slope parameterization. The results show a direct link of the topography on the whole Venesian atmosphere, with preferred locations above topographic heights, suggesting that the nature of this wave is a mountain wave.

Implications

Before the Akatsuki-era, such a big structure dominating the atmosphere was unthinkable. The ability to reproduce it with a model opens the possibility to better understand and study it. In the face of this discovery, there are several considerable, previously not recognized, implications for science on Venus that we will elaborate on at the workshop. We hope to see these issues tackled by Venera-D in its future design.

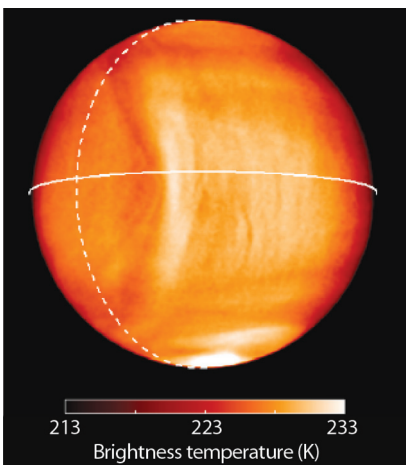


Figure 1: Temperature at 70 km simulated by the IPSL GCM, with and without slope parameterization of sub-grid topography. Topography at the GCM grid scale is shown in black contours

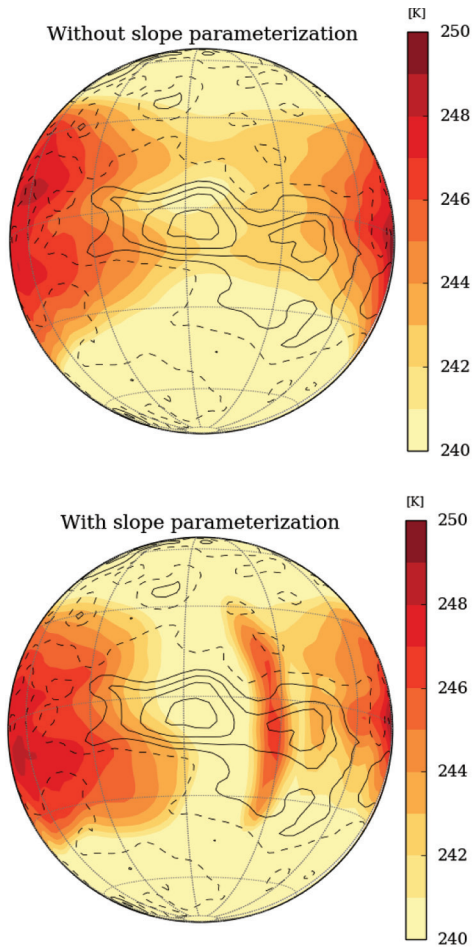


Figure 2: Brightness temperature of the Venus disk acquired by Akatsuki's Long Infrared camera on December 7th, 2015 (from (Fukuhara et al., 2017))

References:

- Fukuhara, T. et al. (2017) Large stationary gravity wave in the atmosphere of Venus, *Nature Geoscience*, 10(2), 85–88.
- Lebonnois, S. et al. (2010) Superrotation of Venus' atmosphere analyzed with a full general circulation model, *J. Geophysical Research*, 1159(6).
- Lott, F., Miller M.J. (1997) A new subgrid-scale orographic drag parametrization: Its formulation and testing, *Quarterly J. Royal Meteorological Society*, 123, 101–127.

DYNAMICS

HIGH-LATITUDE ZONAL WINDS IN THE VENUSIAN ATMOSPHERE FROM VENERA-15 AND -16 RADIO OCCULTATION DATA

V. N. Gubenko, I. A. Kirillovich, A. G. Pavelyev

Kotel'nikov Institute of Radio Engineering and Electronics of the Russian Academy of Sciences, Fryazino, Moscow region, Russia

Abstract

Vertical temperature and pressure profiles in the atmosphere of Venus obtained by the radio occultation (RO) method using the Venera-15 and -16 spacecraft measurements made from October 1983 to September 1984 are used for a wind speed analysis. The altitude and latitude profiles of a zonal wind speed in the middle atmosphere for Northern and Southern hemispheres of planet at altitudes from 50 to 80 km and in the latitude interval from 60° to 85° have been found. Zonal wind speeds were determined assuming cyclostrophic balance. The jet with a maximum wind speed ~ 100 m/s located at an altitude of ~ 60 km and latitudes $73\text{--}75^\circ\text{N}$ is shown to exist in the Northern near-polar atmosphere. Above an altitude level of 65 km in the Northern hemisphere, the polar atmosphere is warmer than the near-polar one and a wind speed usually decreases with increasing altitude at these levels. The wind speed determination results at Southern latitudes show clearly the presence of the jet with a maximum speed ~ 115 m/s located at an altitude of ~ 62 km and latitudes $70\text{--}72^\circ\text{S}$. These high-latitude jets are due to by the negative latitude-temperature gradients at altitudes below jet axes in the near-polar atmosphere.

Introduction

The available data indicate a zonal wind rotation of the Venus's atmosphere from East to West. The wind speed changes almost monotonically with altitude, reaching about 100 m/s at the level of upper cloud layer. The strong zonal winds near the cloud tops and below are essentially in cyclostrophic balance in which the equatorward horizontal component of centrifugal force on a zonally rotating atmospheric parcel is balanced by the poleward meridional pressure gradient force (Leovy, 1973; Schubert et al., 1980; Schubert, 1983; Newman et al., 1984). The cyclostrophic balance approximation and results of the temperature and pressure determination from the RO data of Pioneer Venus Orbiter were used to derive the zonal wind profiles in the atmosphere of planet (Newman et al., 1984; Limaye, 1985). The zonal wind speeds were determined at altitudes from 40 to 80 km in the latitude range from 15 to 85° under the assumption of the thermal symmetry in the Northern and Southern hemispheres (Newman et al., 1984). The authors of the work (Newman et al., 1984) have indicated that the radio occultation events used in their study had been carried out, in general, at low latitudes (below 65°S) in the Southern hemisphere, and at high latitudes ($>60^\circ\text{N}$) in the Northern one. However, they did not exclude the violation of hemispheric symmetry at high latitudes. The vertical pressure and temperature profiles from the Venus Express RO sounding (Tellmann et al., 2009) were used to derive cyclostrophic zonal winds in the mesosphere of Venus assuming hemispheric symmetry, also (Piccialli et al., 2012). In the investigation made by (Piccialli et al., 2012), the selected 116 vertical profiles had a complete latitudinal coverage in the Southern hemisphere only, but measurements in the Northern hemisphere were mainly constrained to high latitudes. In this context, it is important to derive the zonal wind speeds for the Northern and Southern hemispheres, separately. The aim of our research is to determine a zonal wind speed in the polar and near-polar regions of Venus at altitudes from 50 to 80 km from an analysis of the Venera-15 and -16 spacecraft RO data.

Processing and analysis of the original Venera-15 and -16 radio occultation data

For determining the zonal wind speed we used the cyclostrophic balance approximation and results of the RO measurements at latitudes from 60 to 87° in 17 regions of the Southern hemisphere, and in 27 regions of the Northern hemisphere of Venus. These measurements were made during the period from October 1983 to September 1984. Orbits of the Venera-15 and -16 spacecraft were such that the entries into occultation took place in the Northern hemisphere and exits in the Southern one. Some information about the Venera-15 and -16 spacecraft investigations, the dates and locations of the RO measurements in latitude, longitude, solar zenith angle can be found in the works (Yakovlev et al., 1991; Gubenko et al., 2001, 2008; Gubenko, Andreev, 2003). To find a zonal wind speed, we used the altitude profiles of temperature and pressure obtained from the

processing of radio occultation data at a decimeter radio wavelength ($\lambda = 32$ cm). The characteristic properties of the RO technique and experimental data processing are described by (Yakovlev et al., 1991; Gubenko et al., 2008). The results of the radio occultation data processing are the vertical temperature and pressure profiles, which provide the values of these parameters at various altitudes in the interval from 40 to 90 km (Yakovlev et al., 1991). In the range of pressure variations from 1098 to 5 mbar corresponding to the 50–80 km altitude interval, we marked 28 fixed “standard” pressure levels (nodes). The temperatures at these nodes were found by linear interpolation based on the RO temperature retrievals in the points nearest to the chosen levels. The number of chosen nodes allowed the retention of individual characteristics in the temperature profiles.

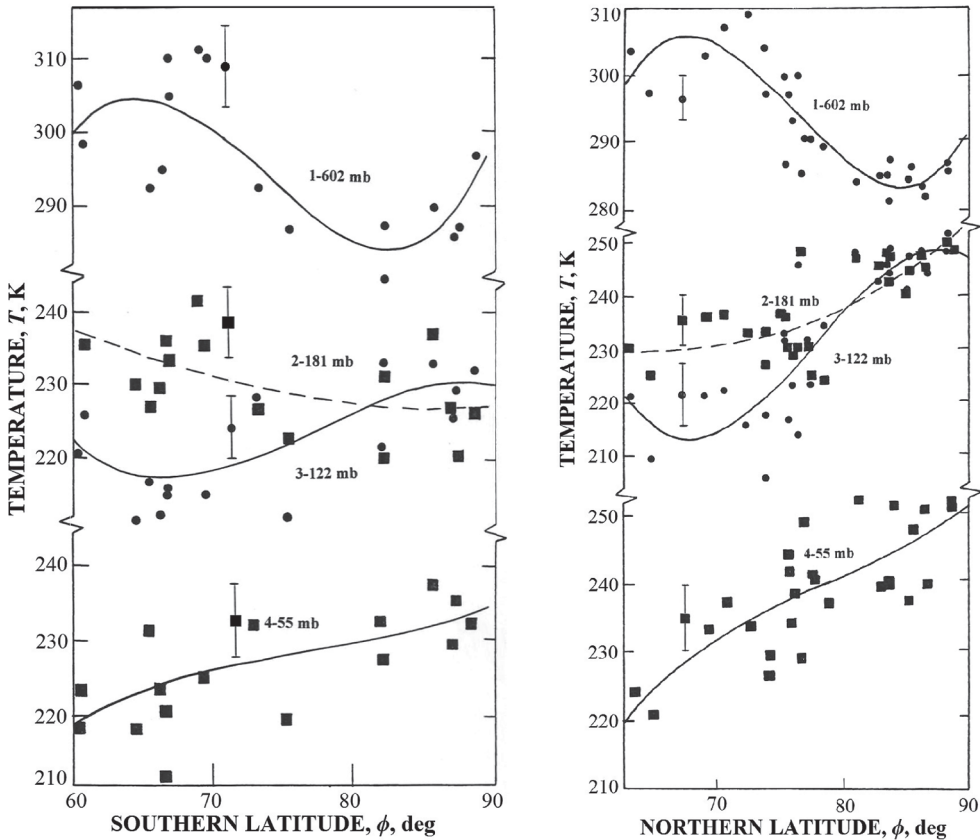


Figure 1: Profiles of temperature on latitude in the Southern (left panel) and Northern (right panel) hemispheres of Venus at four pressure levels: 1–602 mbar; 2–181 mbar; 3–122 mbar; 4–55 mbar

Fig. 1 shows examples of latitude dependence of temperature at four constant pressure levels in the Southern (left panel) and Northern (right panel) hemispheres of Venus. The temperature values obtained from the RO data at corresponding latitudes and pressures are shown by circles and squares in Fig. 1. The circles apply to the curves 1 and 3, the squares — to the curves 2 and 4. The curves describing the latitude-temperature profiles are the cubic polynomials fitted by the least squares technique to the experimental data. These least squares fits were used in order to obtain the latitude-temperature gradients. The quality of fitting is defined by the root mean square variance σ on the every “standard” pressure level (representative values of σ are drawn as error bars for each curve in Fig. 1). From fitted curves in Fig. 1 (left panel) it is seen that the temperature decreases with increasing Southern latitude at a pressure level 602 mbar in the latitude interval from 66 to 82°S. This trend is characteristic also for latitude-temperature dependence at lower pressure levels down to 180 mbar. The transitional region lies within the pressure range of 180 to 120 mbar, corresponding to altitudes from 61 to 63 km, where a change of the sign of latitude-temperature gradient occurs in the latitude interval from 66 to 82°S as shown in Fig. 1 (curves 2 and 3, left panel). Small temperature contrasts between the Southern polar and near-polar atmosphere are characteristic of the transitional region (Yakovlev et al., 1991). In the Southern hemisphere, the

temperature increases with increasing latitude at fixed pressure levels from 120 to 30 mbar, which correspond to altitudes from 63 to 70 km. For determining the zonal wind speed in the Northern hemisphere, we use the temperature and pressure data obtained from radio occultation in 27 regions at latitudes more than 60°N (Yakovlev et al., 1991). The temperature decreases with increasing latitude at a level of 602 mbar in the latitude interval from 69° to 84°N. This trend continues at lower levels down to 220 mbar. A change of sign of the latitude-temperature gradient at Northern latitudes from 69° to 84°N occurs in the pressure range from 220 to 180 mbar. A transitional atmospheric region, for which small values of the latitude-temperature gradient are characteristic, exists in this pressure range corresponding to the altitude interval from 60 to 61 km. Curve 2, corresponding to the upper boundary of this transitional region in the Northern hemisphere of Venus, illustrates this tendency. A temperature rise with increasing latitude (curves 3 and 4, right panel) is observed at pressure levels lower than 180 mbar. By comparing the latitude profiles of temperature in the Northern and Southern hemispheres, one notices that the latitude-temperature gradients are negative at pressures from 1100 to 220 mbar at high latitudes from 70 to 80°, and their values are almost the same at corresponding latitudes and pressure levels in the Northern and Southern hemispheres of Venus. This indicates hemispheric symmetry of the thermal structure in this pressure range. However, indicated symmetry no longer exists at pressures lower than 220 mbar, i.e. at altitudes higher than 60 km.

Technique of determining the zonal wind speed

It is known that the Venus's atmosphere from an altitude of ~10 km to the cloud tops in non-equator regions is in a state of approximate cyclostrophic balance, i.e. a dynamic state where the centrifugal force component directed towards the equator is balanced by the poleward meridional pressure gradient force (Schubert, 1983). Leovy (1973) first suggested that a cyclostrophic balance approximation is valid on Venus for both the upper and lower atmosphere layers. Following Schubert (1983) and Newman et al. (1984), the cyclostrophic balance equation can be written:

$$\frac{u^2}{a} \tan \varphi = -\frac{1}{\rho} \cdot \frac{\partial p}{\partial y}, \quad (1)$$

where u is the zonal wind speed; ρ is the atmosphere density; φ is latitude; y is a locally poleward pointing Cartesian coordinate; a is the radius of Venus; and p is the pressure. The validity of using Eq. (1) for the description of the middle atmospheric dynamics of Venus was proven by comparing the values of zonal wind speeds obtained on the basis of this approximation applied to the results of temperature and pressure measurements on Pioneer Venus probes (Seiff et al., 1980; Schubert et al., 1980; Seiff, 1982; Schubert, 1983) with the results of direct zonal wind measurements with the differential long-baseline interferometry experiment (Counselman et al., 1980). Taking into account the hydrostatic equation and the perfect gas law, one can find the thermal wind equation for cyclostrophic balance from Eq. (1):

$$2u \frac{\partial u}{\partial \xi} = -\frac{R}{\tan \varphi} \cdot \frac{\partial T}{\partial \varphi} \Big|_p, \quad (2)$$

where $R = 191.4 \text{ J} \cdot \text{kg}^{-1} \cdot \text{K}^{-1}$ is the gas constant of the Venus's atmosphere; $\xi = -\ln(p/p_0)$ is the log pressure coordinate; and $p_0 = 1098 \text{ mbar}$ is the pressure at a level assumed to be the lower boundary. For convenience of calculations, it is advantageous to integrate Eq. (2) normal to isobaric surfaces using a trapezoidal formula (Newman et al., 1984):

$$u_{n+1}^2 = u_n^2 - \frac{R \Delta \xi}{2 \tan \varphi} \left[\frac{\partial T}{\partial \varphi_{n+1}} + \frac{\partial T}{\partial \varphi_n} \right], \quad (3)$$

where $\Delta \xi = \xi_{n+1} - \xi_n = \ln(p_n/p_{n+1})$, indices n and $(n+1)$ correspond to adjacent pressure levels. The value of the index n increases with increasing altitude and changes from 0 to 27. The value $n = 0$ corresponds to the pressure $p_0 = 1098 \text{ mbar}$, and $n = 27$ corresponds to the pressure 5 mbar. Pressure values on any adjacent levels chosen by us meet the condition $\Delta \xi = \ln(p_n/p_{n+1}) = 0.2$. The relationship determining the zonal wind speed u on an arbitrary pressure level $(n+1)$ for given latitude φ follows from formula (3):

$$u_{n+1}^2 = u_0^2 - \frac{R \Delta \xi}{2 \tan \varphi} \left[\frac{\partial T}{\partial \varphi_0} + \frac{\partial T}{\partial \varphi_{n+1}} + 2 \sum_{i=1}^n \frac{\partial T}{\partial \varphi_i} \right]. \quad (4)$$

It is seen from expression (4) that, in addition to the latitude-temperature gradients, the latitude dependence of the zonal wind speed $u_0(\varphi)$ at the pressure level $p_0 = 1098 \text{ mbar}$ (lower boundary)

must be known in order to calculate the wind speed field. The following expression was chosen to represent the lower boundary condition $u_0(\varphi)$ for both the Northern and Southern hemispheres of Venus:

$$u_0(\varphi) = 47.29 + 3.94(|\varphi| - 60) - 0.37(|\varphi| - 60)^2 + 6.1 \cdot 10^{-3}(|\varphi| - 60)^3, \quad (5)$$

where φ is expressed in degrees and u_0 is expressed in m/s. The choice $u_0(\varphi)$ for the Northern hemisphere corresponds to the results given in Fig. 9 by (Newman et al., 1984). Since data about circulation at high latitudes of the Southern hemisphere are absent at present, the application of the same function $u_0(\varphi)$ here is based on the assumption of a circulation symmetry in the two hemispheres at the level $p_0 = 1098$ mbar. An indirect evidence for this suggestion is the thermal structure symmetry for both hemispheres at pressure levels more than 220 mbar (Yakovlev et al., 1991), as discussed above.

Zonal winds in the Southern and Northern hemispheres of Venus

The previous circulation observations of the Venus's zonal speed exhibited a strong mid-latitude jet centered between 50 and 55° latitude with a maximum speed ranging from ~110 m/s (Zasova et al., 2000) to ~140 m/s (Newman et al., 1984). The Venera-15 and -16 radio occultation data have shown strong zonal jets with a maximum speed of 100–115 m/s centered at high latitudes (>70°) of both Southern and Northern hemispheres of Venus (Gubenko et al., 1992; Vaganov et al., 1992). The Northern high-latitude jet with a speed of 95 m/s centered at 70°N and 60 km altitude have been detected in the Pioneer Venus data, also (Newman et al., 1984). The vertical profiles of the zonal wind speed in the near-polar atmosphere of the Southern (left panel) and Northern (right panel) hemisphere of Venus at three latitude levels are given in Fig. 2. The altitude dependence of the zonal wind speed in the Southern near-polar atmosphere at latitudes of 66, 68 and 70°S are shown by curves 1, 2 and 3 in Fig. 2 (left panel). A common feature of vertical profiles of the wind speed at these latitudes is a speed increase with increasing altitude from 50 to 62 km. At an altitude of ~62 km corresponding to a pressure ~149 mbar, the wind speed reaches its maximum 114 m/s at the latitude 70°S, 106 m/s at 68°S, and 94 m/s at 66°S. The altitude dependence of the zonal wind speed in the Northern near-polar atmosphere at latitudes of 74, 76 and 78°N are shown by curves 1, 2 and 3 in Fig. 2 (right panel). It is seen that the wind speed increases with increasing altitude between 50 and 60 km at these latitudes. At an altitude of ~60 km corresponding to a pressure ~220 mbar, the wind speed reaches a maximum of 102 m/s at the latitude 74°N, 100 m/s at 76°N, and 90 m/s at 78°N. As it is followed from Fig. 2, the zonal wind speed decreases quickly with increasing altitude above 60 km and actually is zero at an altitude of 75 km, which is a characteristic of the Northern high-latitude atmosphere. In the Southern hemisphere, such circulation suppression is not observed. Fig. 3 shows examples of latitude dependence of the zonal wind speed at four constant pressure levels in the Southern (left panel) and Northern (right panel) hemispheres of Venus. It is seen from Fig. 3 (left panel) that there are maxima in the wind speed at Southern latitudes from 70 to 72°S. It points to the existence of the jet with the speed maximum ~115 m/s in this latitude interval of the Southern hemisphere, the center of which is located at an altitude of ~62 km. This jet is due to a negative latitude-temperature gradient at altitudes from 50 to 62 km in the Southern near-polar atmosphere of Venus. The results shown in Fig. 3 (right panel) reveals the jet in the latitude interval from 73° to 75°N of the Northern hemisphere with the wind speed maximum ~100 m/s, which is located at an altitude of ~60 km. The high-latitude jets found at Southern and Northern latitudes are due to by the negative latitude-temperature gradients at altitudes below jet axes in the near-polar atmosphere of Venus.

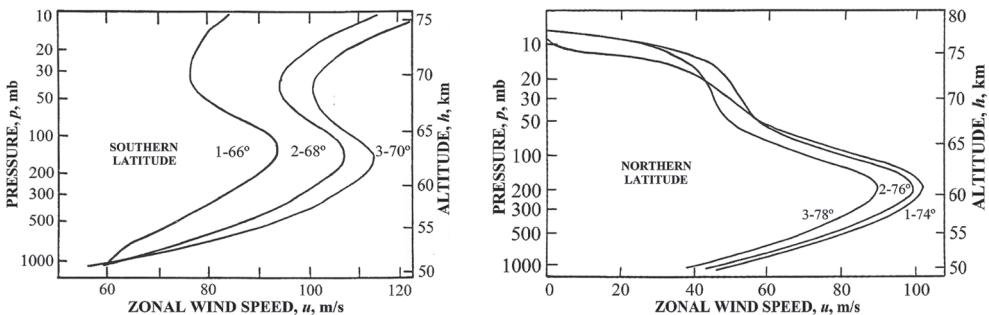


Figure 2: Vertical profiles of the zonal wind speed in the near-polar atmosphere of the Southern (left panel) and Northern (right panel) hemisphere of Venus at three latitude levels

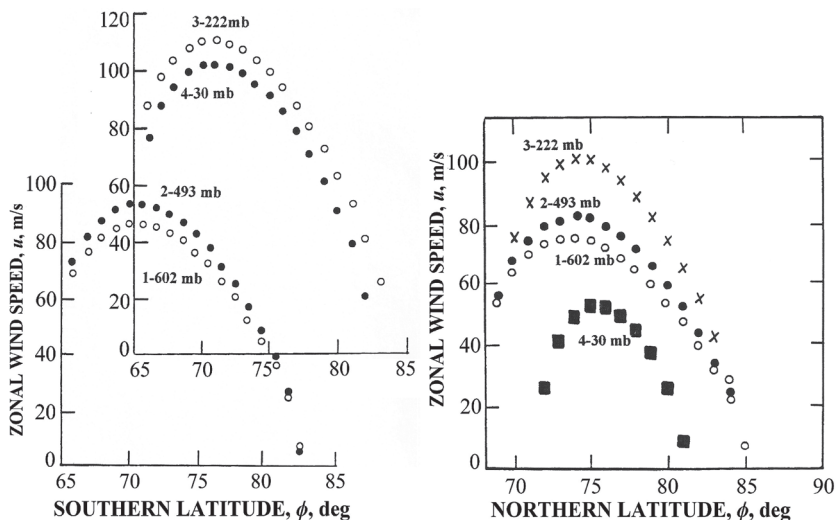


Figure 3: Latitude profiles of the zonal wind speed in the Southern (left panel) and Northern (right panel) hemispheres of Venus at four pressure levels: 1–602 mbar; 2–493 mbar; 3–222 mbar; 4–30 mbar

Conclusion

An analysis of the Pioneer Venus and Venera-15, -16 data on atmospheric circulation at high latitudes of the Northern hemisphere of Venus have provided evidence of the zonal wind speed stability at altitudes below 59 km in the time interval of 5 years between above-mentioned RO measurements. According to our results and data of (Newman et al., 1984), the high-latitude jet was observed in the Northern near-polar atmosphere, having a maximum speed of 95–100 m/s. The jet axis altitude remained practically the same (~60 km), and the jet axis latitude was confined in the interval 70°–74°N. If a small change in latitude (~4°) of the jet position is real, then this is important for understanding the dynamical processes in the Venus's atmosphere. A characteristic feature of the atmospheric state at high latitudes is the suppression of zonal circulation at altitudes >75 km in the Northern near-polar atmosphere of Venus. In the Southern hemisphere, such circulation suppression is not observed. The comparison of the wind speeds in both hemispheres indicates approximate hemispheric symmetry relative to the equatorial plane at altitudes below 59–60 km. According to our analysis of the Venera-15 and -16 data, there appears to be a violation of the hemispheric circulation symmetry at high latitudes above ~63 km.

Acknowledgements

This work was partially supported by the Program No. 28 of the RAS Presidium.

References

- Counselman III, C. C., Gourevitch, S. A., King, R. W., Lorient, G. B., Ginsberg, E. S., Prinn, R. G. (1980) Zonal and meridional circulation of the lower atmosphere of Venus determined by radio interferometry, *J. Geophys. Res.* 85, 8026–8030.
- Gubenko, V. N., Matyugov, S. S., Yakovlev, O. I., Vaganov, I. R. (1992) Zonal wind in the south polar regions of Venus from the data of the radio transillumination, *Kosmich. Issled.*, 30(3), 390–395 (in Russian).
- Gubenko, V. N., Yakovlev, O. I., Matyugov, S. S. (2001) Radio occultation measurements of the radio wave absorption and the sulfuric acid vapor content in the atmosphere of Venus. *Cosmic Res.*, 39(5), 439–445, doi: 10.1023/A:1012336911928.
- Gubenko, V. N., Andreev, V. E. (2003) Radio wave fluctuations and layered structure of the upper region of Venusian clouds from radio occultation data, *Cosmic Res.*, 41(2), 135–140, doi: 10.1023/A:1023378829327.
- Gubenko, V. N., Andreev, V. E., Pavelyev, A. G. (2008) Detection of layering in the upper cloud layer of Venus northern polar atmosphere observed from radio occultation data. *J. Geophys. Res. (Planets)*, 113, E03001, doi: 10.1029/2007JE002940.
- Leovy, C. B. (1973) Rotation of the upper atmosphere of Venus, *J. Atmos. Sci.*, 30, 1218–1220.
- Limaye, S. S. (1985) Venus atmospheric circulation: Observations and implications of the thermal structure, *Adv. Space Res.*, 5(9), 51–62.

- Newman, M., Schubert, G., Kliore, A. J., Patel, I. R. (1984) Zonal winds in the middle atmosphere of Venus from Pioneer Venus radio occultation data, *J. Atmos. Sci.*, 41(12), 1901–1913.
- Piccialli, A., Tellmann, S., Titov, D. V., Limaye, S. S., Khatuntsev, I. V., Pätzold, M., Häusler, B. (2012) Dynamical properties of the Venus mesosphere from the radio-occultation experiment VeRa onboard Venus Express, *Icarus*, 217, 669–681.
- Schubert, G., Covey, C., Del Genio, A. D., Elson, L. S., Keating, G., Seiff, A., Young, R. E., Apt, J., Counselman III, C. C., Kliore, A. J., Limaye, S. S., Revercomb, H. E., Sromovsky, L. A., Suomi, V. E., Taylor, F., Woo, R., von Zahn, U. (1980) Structure and circulation of the Venus atmosphere, *J. Geophys. Res.*, 85, 8007–8025.
- Schubert, G. (1983) General circulation and dynamical state of the Venus atmosphere. In: Hunten, D. M., Colin, L., Donahue, T. M., Moroz, V. I. (Eds.) *Venus*, University of Arizona Press, Tucson, 1183 p.
- Seiff, A., Kirk, D. B., Young, R. E., Blanchard, R. C., Findlay, J. T., Kelly, G. N., Sommer, S. C. (1980) Measurements of thermal structure and thermal contrasts in the atmosphere of Venus: Results from the four Pioneer Venus probes, *J. Geophys. Res.*, 85, 7903–7940.
- Seiff, A. (1982) Dynamical implications of observed thermal contrasts in Venus upper atmosphere, *Icarus*, 51, 574–592.
- Tellmann, S., Pätzold, M., Häusler, B., Bird, M. K., Tyler, G. L. (2009) Structure of the Venus neutral atmosphere as observed by the Radio Science experiment VeRa on Venus Express, *J. Geophys. Res. (Planets)*, 114, 19 p.
- Vaganov, I. R., Yakovlev, O. I., Matyugov, S. S., Gubenko, V. N. (1992) Wind in the northern polar atmosphere of Venus, *Kosmich. Issled.*, 30(5), 695–699 (in Russian).
- Yakovlev, O. I., Matyugov, S. S., Gubenko, V. N. (1991) Venera-15 and -16 middle atmosphere profiles from radio occultations: Polar and near-polar atmosphere of Venus, *Icarus*, 94(2), 493–510, doi: 10.1016/0019-1035(91)90243-M.
- Zasova, L. V., Linkin, V. M., Khatuntsev, I. V. (2000). Zonal wind in the middle atmosphere of Venus, *Cosmic Res.* 38, 49–65.

INFLUENCE OF TOPOGRAPHY AT THE UPPER MESOSPHERE OF VENUS FROM OXYGEN NIGHTGLOW WIND TRACKING

D. Gorinov, L. Zasova, I. Khatuntsev, A. Turin

Space Research Institute of Russian Academy of Sciences

Abstract

The $O_2(a^1\Delta_g)$ nightglow at $1.27 \mu\text{m}$ is practically the only method of studying the circulation in the 90–110 km altitude range of Venusian atmosphere. The images of the nightglow were obtained by VIRTIS-M spectrometer (Venus Express spacecraft) between 2006 and 2008. By studying patterns of the horizontal motion it is possible to detect small scale (500–2000 km) disturbances that in some cases coincide with the high elevation topographic structures directly below, or shifted several degrees in the direction of the main flow. The suspected mechanism is the emergence of the stationary gravity waves from the surface that can reach the altitudes of ~ 100 km. For future Venus missions such as Venera-D a better longitudinal coverage is suggested to further the knowledge of this phenomenon.

Introduction

The altitude range of 90–110 km in the atmosphere of Venus is not well understood in terms of dynamics due to the absence of in-situ measurements and the lack of trackers. Below, the zonal superrotation dominates from the cloud level upwards to 85–90 km which at its maximum reaches $\sim 100 \text{ m}\cdot\text{s}^{-1}$ at 65–70 km above the surface (Gierasch et al., 1997). Above (>110 km), in the thermosphere, a subsolar-to-antisolar (SS-AS) circulation cell is driven by the solar heating (Sánchez-Lavega et al., 2017). As a result, the dynamics in the transition region might be influenced by both of these mechanisms (Lellouch et al., 1997; Bougher et al., 2006). Other mechanisms, such as gravity waves (Alexander, 1992; Zhang et al.; 1996, Altieri et al., 2014; Bertaux et al., 2016; Peralta et al., 2017) and thermal tides (Zasova et al., 2007) might add up to create a complex structure of circulation.

Atomic oxygen recombines into molecular oxygen on the nightside of Venus (Connes et al., 1979; Crisp et al., 1996) and emits at $1.27 \mu\text{m}$ wavelength. The peak of its vertical distribution is found at 97.4 ± 2.5 km (Piccioni et al., 2009) and its morphology is known to remain stable for several hours (Soret et al., 2014), thus it can be used as a tracker to detect horizontal motion. This method of wind tracking requires pairs of consecutive images of the same airglow areas which are provided by the VIRTIS-M spectrometer on-board Venus Express spacecraft.

The nightglow distribution is known to manifest inconsistent behavior, as the bright areas of emission emerge in various spots on the nightside, however the mean distribution has a peak around midnight (Gérard et al., 2008) and the evening side is several hundred rayleighs brighter than the morning side.

Horizontal motion at 90–110 km and connection with the topography

The data base of VIRTIS-M contains several orbits that cover large ($50 \times 50^\circ$ and more) areas and allow for 200 and more velocity vectors to be retrieved. These orbits make it possible to study the horizontal motion at 90–110 km in details and overview how it varies from one orbit to another.

The motion behavior generally exhibits the same pattern as the mean circulation (Gorinov et al., 2018). Magnitudes and sometimes directions may vary; however, in the majority of cases the zonal component is directed from the terminators towards the 21–23 h area, with the morning flow stronger than the evening one. The morning meridional component is directed towards the south (poleward), while before midnight it is northward (equatorward) (Fig. 1). These results do not contradict the previous analysis (Hueso et al., 2008) however improve the coverage and statistical parameters since we used ~ 4 times more orbits.

Various instances of the horizontal wind distribution have been noted throughout the observations. For 30 % of all used orbits the amount of retrieved vectors made it possible to reliably map and analyze the patterns.

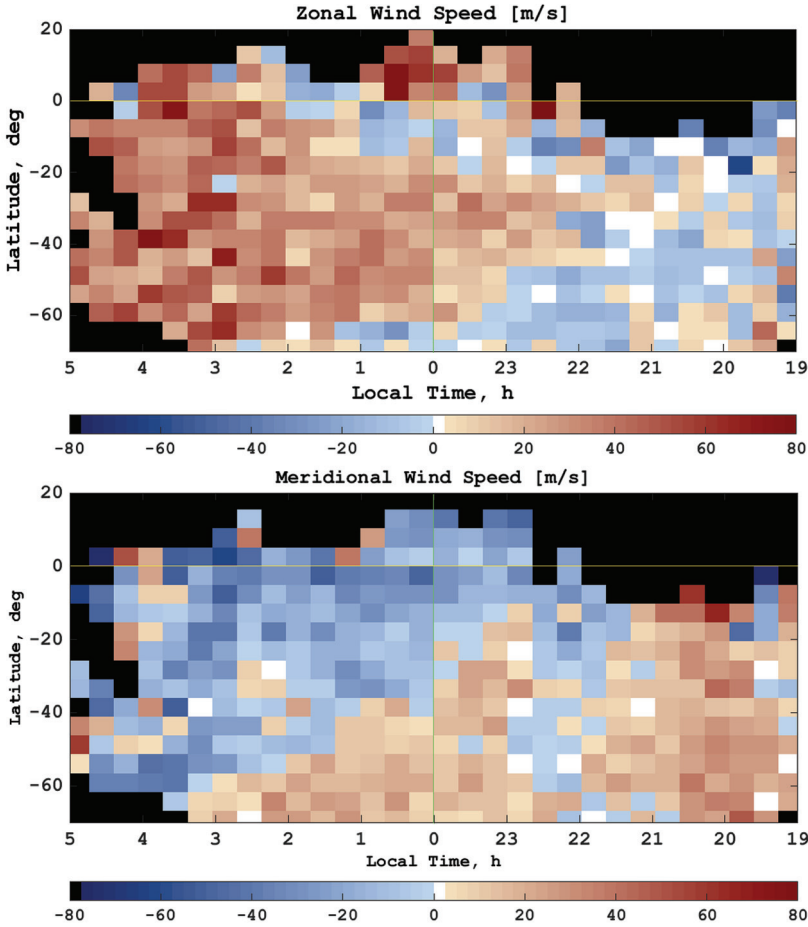


Figure 1: The zonal and the meridional components of the mean horizontal motion in the upper mesosphere of Venus from $O_2(^1\Delta_g)$ wind tracking. The "+" (red) values determine eastward direction of the zonal speed and northward direction of the meridional speed

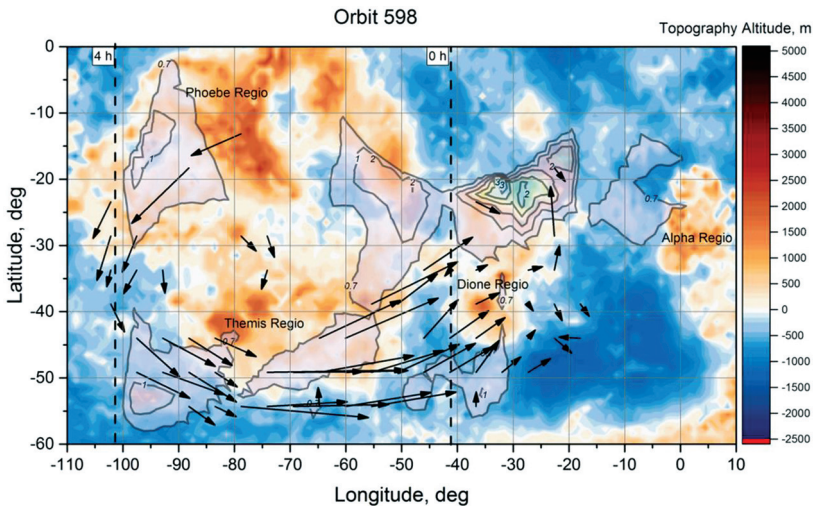


Figure 2: An example of horizontal circular motion in the upper mesosphere, retrieved from the oxygen night-glow tracking during orbit 598. The area of circular motion is located in the Southern hemisphere on the morning part of the nightside, directly above the Phoebe/Themis Regio and is approximately 4000 km in diameter

The vast majority of the VIRTIS-M nadir measurements cover a longitude range between 180° and 360°, practically excluding the area above Aphrodite Terra. The motion in some cases shows deviations from the mean circulation that are observed as curved flows, and in some cases they coincide with the highlands (Regio): directly below, or shifted up to 20 degrees in the direction of the apparent flow.

While in a majority of cases the zonal and the meridional components demonstrate a similar case to the mean distribution (see Fig. 1), others may manifest the opposite picture in terms of wind direction, which signifies the fast-changing behavior of the wind at these altitudes.

Furthermore, observed in several cases were areas of circular motion, 500–4000 km in diameter (Fig. 2). As such patterns occur above highlands (regio) on the planetary surface, we have attributed their emergence to the influence of the stationary gravity waves that may reach altitudes of ~95 km.

The theoretical basis for this hypothesis relies on the recent developments in the analyses of the gravity waves on Venus. Several studies (Bertaux et al., 2016; Fukuhara et al., 2017; Khatuntsev et al., 2017; Kouyama et al., 2017; Peralta et al., 2017) found the connection between the longitudinal distribution of parameters (albedo, wind speed) and the surface topography. Calculations in models (Mingalev et al., 2011) show the potential for the stationary gravity waves to reach altitudes of 90–95 km, where they break.

Airglow observation for future missions

Oxygen nightglow observations are extremely important to understand the circulation in the transition region, which in turn provide resources for the general circulation models. For a future mission to Venus that will include an orbiter with an instrument capable of mapping the nightside in near-IR, such as Venera-D, new strategies should be implemented to improve the legacy results of VIRTIS.

As it appears from the VIRTIS data, the influence of topography could have been better understood had the longitude range of Aphrodite Terra (20–200°) been more thoroughly covered by the images. As the areas of oxygen nightglow appear more frequently near the equator, it is crucial to select an orbit type that allows observation of the equatorial latitudes.

These improvements can allow viewing the longitudinal dependence of the nightglow intensity and velocity so that with enough data the local time bias can be avoided. As we suspect the stationary gravity waves linked to highlands be a major influential factor on the nightglow, diverse elevation in the equatorial latitudes is assumed to exhibit visible correlation with the aforementioned parameters.

In a case where the orbit of the spacecraft would not allow repeated observations of the equatorial latitudes, the Northern hemisphere is to be preferred over the Southern. The northern mid-latitudes, where the O₂(a₁Δg) 1.27 μm might still be observed, cover the prominent Beta Regio (>5000 km at peak altitude, 20–40°N latitude). Other main highlands of the Northern Hemisphere are Atla Regio at 0–20°N and Ishtar Terra at 60–80°N, thus the effects of the gravity waves from the Beta Regio should be more discernable and stronger than from the regio of the Southern hemisphere.

Conclusion

Analysis of the oxygen nightglow reveals knowledge on the dynamics in the 90–110 km altitude region, which appears to be complex and being influenced by the stationary gravity waves from the surface. The longitude coverage for VIRTIS-M was not enough to study mean correlation between the wind and the topography. To improve the results, a future orbital mission to Venus that includes an imaging infrared spectrometer should concentrate on covering all longitudes in the equatorial latitude range.

Acknowledgements

The authors are grateful to the ESA Mission and Operations teams for flawless operations of the VIRTIS instrument. D. A. Gorinov, I. V. Khatuntsev were supported by the Ministry of Education and Science of Russian Federation grant 14.W03.31.0017. L. V. Zasova, A. V. Turin were supported by the Federal Agency for Scientific Organizations (FASO Russia) grant No. 0028-2014-0004. This work was supported by the FASO project “Venera-D”.

References

- Alexander, M.J. (1992) A mechanism for the Venus thermospheric superrotation. *Geophysical Research Letters*, 19(22), 2207–2210, doi: 10.1029/93JE00538.
- Altieri, F., Migliorini, A., Zasova, L., Shakun, A., Piccioni, G., Bellucci, G. (2014) Modeling VIRTIS/VEX O₂(a1Δg) nightglow profiles affected by the propagation of gravity waves in the Venus upper mesosphere, *J. Geophysical Research*, 119(11), 2300–2316. doi: 10.1002/2013JE004585.
- Bertaux, J.-L., Khatuntsev, I. V., Hauchecorne, A., Markiewicz, W.J., Marq, E., Lebonnois, S., ..., Fedorova, A. (2016) Influence of Venus topography on the zonal wind and UV albedo at cloud top level: The role of stationary gravity waves, *J. Geophysical Research: Planets*, 121, 1087–1101. doi: 10.1002/2015JE004958.
- Bougher, S.W., Raffin, S., Drossart, P. (2006) Dynamics of the Venus upper atmosphere: Outstanding problems and new constraints expected from Venus Express, *Planetary and Space Science*, 54, 1371–1380, doi: 10.1016/j.pss.2006.04.023.
- Connes, P., Noxon, J.F., Traub, W.A., Carleton, P. (1979) O₂(1D) emission in the day and night airglow of Venus. *Astrophysical J.*, 233, L29–L32.
- Crisp, D., Meadows, V.S., Bézard, B., de Bergh, C., Maillard, J., Mills, F.P. (1996) Ground-based near-infrared observations of the Venus nightside: 1.27-mm O₂(a1Δg) airglow from the upper atmosphere, *J. Geophysical Research*, 101, 4577–4593, doi: 10.1029/95JE03136.
- Fukuhara, T., Futaguchi, M., Hashimoto, G.L., Horinouchi, T., Imamura, T., Iwagami, N., ..., Yamazaki, A. (2017) Large stationary gravity wave in the atmosphere of Venus, *Nature Geoscience*, doi: 10.1038/ngeo2873.
- Gérard, J.-C., Saglam, A., Piccioni, G., Drossart, P., Cox, C., Erard, S., ..., Sánchez-Lavega, A. (2008) Distribution of the O₂ infrared nightglow observed with VIRTIS on board Venus Express, *Geophysical Research Letters*, 35, L02207, doi: 10.1029/2007GL032021.
- Gierasch, P.J., Goody, R.M., Young, R.E., Crisp, D., Edwards, C., Kahn, R., ..., Newman, M. (1997) The general circulation of the Venus atmosphere: an assessment, In: Bucher, J.W., Hunten, D.M., Phillips, R.J. (Eds.), *Venus II — Geology, Geophysics, Atmosphere, and Solar Wind Environment*, University of Arizona Press, Tucson, 459–500.
- Hauchecorne, A. (2017) Venus: Jet-setting atmosphere, *Nature Geoscience*, 10, 622–623.
- Hueso, R., Sanchez-Lavega, A., Piccioni, G., Drossart, P., Gérard, J.C., Khatuntsev, I., ..., Migliorini, A. (2008) Morphology and Dynamics of Venus Oxygen Airglow from Venus Express/VIRTIS observations, *J. Geophysical Research*, 113, E00B02. doi: 10.1029/2008JE003081.
- Khatuntsev, I.V., Patsaeva, M.V., Titov, D.V., Ignatiev, N.I., Turin, A.V., Fedorova, A.A., Markiewicz, W.J. (2017) Winds in the middle cloud deck from the near-IR imaging by the Venus Monitoring Camera onboard Venus Express, *J. Geophysical Research: Planets*, 122. doi: 10.1002/2017JE005355.
- Kouyama, T., Imamura, T., Taguchi, M., Fukuhara, T., Sato, T.M., Yamazaki, A., ..., Nakamura, M. (2017) Topographical and local time dependence of large stationary gravity waves observed at the cloud top of Venus, *Geophysical Research Letters*, 44, doi: 10.1002/2017GL075792.
- Lellouch, E., Clancy, T., Crisp, D., Kliore, A., Titov, D., Bougher, W. (1997) Monitoring of mesospheric structure and dynamics, In: Bougher, S.W., Hunten, D.M., Phillips, R.J. (Eds.), *Venus II: Geology, Geophysics, Atmospheres, and Solar Wind Environment*, University of Arizona Press, Tucson, 295–324.
- Mingalev, I., Rodin, A., Orlov, K. (2015) Numerical simulations of the global circulation of the atmosphere of Venus: Effects of surface relief and solar radiation heating, *Solar System Research*, 49(1), 24–42.
- Peralta, J., Hueso, R., Sánchez-Lavega, A., Lee, Y.J., García-Muñoz, A., Kouyama, T., ..., Satoh, T. (2017) Stationary waves and slowly moving features in the night upper clouds of Venus, *Nature Astronomy*, 1, 0187.
- Piccioni, G., Zasova, L., Migliorini, A., Drossart, P., Shakun, A., García Muñoz, A., ..., Cardesin-Moinelo, A. (2009) Near-IR oxygen nightglow observed by VIRTIS in the Venus upper atmosphere, *J. Geophysical Research*, 114, E00B38, doi: 10.1029/2008JE003133.
- Sánchez-Lavega, A., Lebonnois, S., Imamura, T., Read, P., Luz, D. (2017) The Atmospheric Dynamics of Venus, *Space Science Reviews*, 212(3–4), 1541–1616.
- Soret, L., Gérard, J.-C., Piccioni, G., Drossart, P. (2014) Time variations of O₂(a1Δ) nightglow spots on the Venus nightside and dynamics of the upper mesosphere, *Icarus*, 237, 306–314, doi: 10.1016/j.icarus.2014.03.034.
- Zasova, L.V., Ignatiev, N.I., Khatuntsev, I.V., Linkin, V.M. (2007), Structure of the Venus atmosphere, *Planetary and Space Science*, 55, 1712–1728.
- Zhang, S., Bougher, S.W., Alexander, M.J. (1996) The impact of gravity waves on the Venus thermosphere and O₂ IR nightglow, *J. Geophysical Research*, 101(E10), 23 195–23 206. doi: 10.1029/96JE02035.

CLOUD LEVEL CIRCULATION ACCORDING TO UV AND NEAR-IR VMC IMAGING ONBOARD VENUS EXPRESS

I. V. Khatuntsev¹, M. V. Patsaeva¹, D. V. Titov²,
N. I. Ignatiev¹, A. V. Turin¹, Fedorova A. A.¹

¹ Space Research Institute of Russian Academy of Sciences, khatuntsev@iki.rssi.ru

² European Space Research and Technology Centre (ESA-ESTEC), Noordwijk, Netherlands

Keywords: dynamics, cloud level, gravity waves

Introduction

During eight years Venus Monitoring Camera (VMC) (Markiewicz et al., 2007) onboard the Venus Express orbiter has observed the upper cloud layer of Venus. The largest set of images was obtained in the UV (365 nm), visible (513 nm) and two infrared channels — 965 and 1010 nm. The UV dayside images were used to study the atmospheric circulation at the Venus cloud tops (Khatuntsev et al., 2013; Patsaeva et al., 2015). Mean zonal and meridional profiles of winds and their variability were derived from cloud tracking of UV images. In low latitudes the mean retrograde zonal wind at the cloud top (67±2 km) is about 95 m/s with a maximum of about 102 m/s at 40–50°S. Poleward from 50°S the zonal wind quickly fades out with latitude. The mean poleward meridional wind slowly increases from zero value at the equator to about 10 m/s at 50°S. Poleward from this latitude, the absolute value of the meridional component monotonically decreases to zero at the pole. The VMC observations suggest clear diurnal signature in the wind field. They also indicate a long term trend for the zonal wind speed at low latitudes to increase from 85 m/s in the beginning of the mission to 110 m/s by the middle of 2012. The trend was explained by influence of the surface topography on the zonal flow (Bertaux et al., 2016).

Results

Cloud features tracking in the IR images provided information about winds in the middle and lower cloud (49–57 km) (Khatuntsev et al., 2017). In low-to-middle latitudes (5–65°S) the velocity of the retrograde zonal wind was found to be 68–70 m/s. The meridional wind velocity slowly decreases from peak value of 5.8±1.2 m/s at 15°S to 0 at 65–70°S. The mean meridional speed has a positive sign at 5–65°S suggesting equatorward flow. This result, together with the earlier measurements of the poleward flow at the cloud tops indicate the presence of a closed Hadley cell in the altitude range 55–65 km. Following (Bertaux et al., 2016) we attribute this long-term trend to the influence from the surface topography on the dynamical process in the atmosphere via the upward propagation of gravity waves that became apparent in the VMC observations due to slow drift of the Venus Express orbit over Aphrodite Terra.

References:

- Bertaux, J.-L. et al. (2016) Influence of Venus topography on the zonal wind and UV albedo at cloud top level: The role of stationary gravity waves, *J. Geophys. Res. Planets*, 121, 1087–1101, doi: 10.1002/2015JE004958.
- Khatuntsev, I. V. et al. (2013) Cloud level winds from the Venus Express Monitoring Camera imaging, *Icarus*, 226, 140–158.
- Khatuntsev, I. V., Patsaeva, M. V., Titov, D. V., Ignatiev, N. I., Turin, A. V., Fedorova, A. A., Markiewicz, W. J. (2017) Winds in the middle cloud deck from the near-IR imaging by the Venus Monitoring Camera onboard Venus Express, *J. Geophys. Res. Planets*, 122(11), 2312–2327.
- Markiewicz, W. J. et al. (2007) Venus Monitoring Camera for Venus Express, *Planet. Space Sci.*, 55(12), 1701–1711, doi:10.1016/j.pss.2007.01.004.
- Patsaeva, M. V., et al. (2015) The relationship between mesoscale circulation and cloud morphology at the upper cloud level of Venus from VMC/Venus Express, *Planet. Space Sci.*, 113(08), 100–108, doi: 10.1016/j.pss.2015.01.013.

CHEMISTRY AND CLOUDS

SIMULATIONS OF VERTICAL PROFILES OF SO AND SO₂ IN VENUS' MESOSPHERE

F. P. Mills^{1,2}, K. L. Jessup³, Y. L. Yung⁴

¹ Australian National University, Canberra, ACT, Australia

² Space Science Institute, Boulder, Colorado, USA

³ Southwest Research Institute, Boulder, Colorado, USA

⁴ California Institute of Technology, Pasadena, California, USA

Abstract

The primary reservoir for SO₂ on Venus lies in the troposphere, but a pronounced SO₂ inversion layer has been consistently observed by multiple instruments since modern observations began in 2004. The Caltech/JPL photochemical model with simplified standard chemistry was used to calculate steady-state vertical profiles for SO₂ as a function of solar zenith angle at 58–110 km altitude. Assuming photochemistry ceases at each altitude at the solar zenith angle where the photochemical lifetime equals the zonal transport lifetime, an estimate of the actual non-steady-state vertical profile at the evening terminator has been constructed for the equatorial region. The resultant profile has a factor of two increase in the SO₂ mixing ratio from 70 to 80 km altitude. This agrees qualitatively but not quantitatively with the observations, which suggests the interaction of photochemistry and dynamics may be important for creating the observed mesospheric SO₂ inversion layer.

Introduction

Sulfur dioxide (SO₂) plays many important roles in Venus' atmosphere. It is a precursor for the sulfuric acid that condenses to form Venus' global cloud layers and is likely a precursor for the unidentified UV absorber, which, along with CO₂ near the tops of the clouds, appears to be responsible for absorbing about half of the energy deposited in Venus' atmosphere (Titov et al., 2007). Photochemically, SO₂ on Venus is analogous in many respects to O₃ in the terrestrial stratosphere (DeMore, Yung, 1982). Published simulations using standard photochemistry (Zhang et al., 2010; Krasnopolsky, 2012) indicate the mixing ratio of SO₂ should decrease roughly monotonically with increasing altitude as the source for SO₂ is the troposphere. Observations, however, have consistently found an inversion layer in the upper mesosphere (above about 85 km altitude) where the mixing ratio of SO₂ increases with increasing altitude (Sandor et al., 2010; Belyaev et al., 2012; Vandaele et al., 2017). Simulations using H₂SO₄ as the medium for transporting sulfur from the lower mesosphere to the upper mesosphere have succeeded in replicating the upper mesosphere SO₂ inversion layer (Zhang et al., 2010; 2012), but these simulations either have required assumptions that stretch significantly the boundaries of known laboratory data or their calculated H₂SO₄ abundance has significantly exceeded the observational upper limit on gaseous H₂SO₄ (Sandor et al., 2012). S₈ remains as a viable alternative medium by which sulfur can be transported from the lower mesosphere to the upper mesosphere but there are significant uncertainties in the proposed mechanism due to lack of laboratory data (Zhang et al., 2012). A new approach that shows promise as an alternative explanation for the upper mesosphere SO₂ inversion layer is outlined below.

Methods

The Caltech/JPL photochemical model (Allen et al., 1981) is used for the numerical simulations. It applies a common core of atmospheric physics to all planets, drawing planet-specific information from custom databases, and converges to a steady-state solution via a finite-difference iterative algorithm. For these simulations, the 1-d continuity equation is solved simultaneously for all species over 58–110 km altitude. Vertical transport via eddy diffusion is set based on observations, as are the lower boundary conditions for HCl, CO, and OCS. Solar fluxes are based on measurements obtained by SORCE SOLSTICE and SORCE SIM on 26 December 2010 (Harder et al., 2010; Snow et al., 2005). These are the closest match to HST observations obtained on 28 December 2010 (Jessup et al., 2015). For the solar zenith angle (SZA)-dependent simulations, the calculations are run to steady-state using the solar flux expected for a specified local time on Venus' equator.

Preliminary results and discussion

Preliminary results from the SZA-dependent simulations are shown in Fig. 1. The global-average SO₂ profile in Fig. 1 shows a much more gradual decrease in SO₂ mixing ratio with altitude due

to the inclusion of sulfur species (besides SO and SO₂) that have sufficiently long lifetimes to be transported vertically via eddy diffusion (Mills and Allen, 2007). The large difference in SO₂ values in the upper cloud region (<70 km) is due to choosing different lower boundary conditions for SO₂ in these simulations.

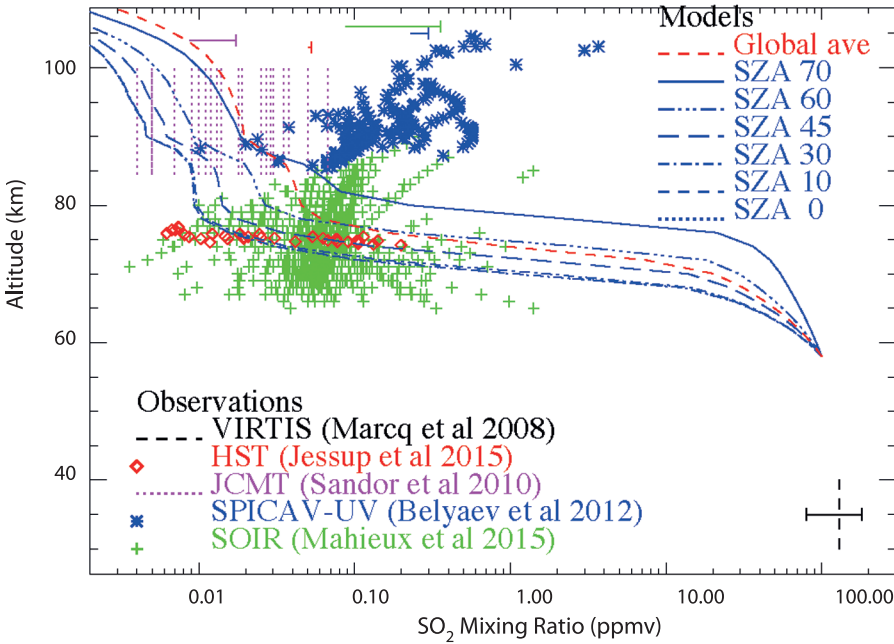


Figure 1: Observed and modeled SO₂ (after Marcq et al., 2018). The global-average result is the nominal result from (Mills, Allen, 2007). The SZA-dependent results are updated versions of the results presented in (Jessup et al., 2015)

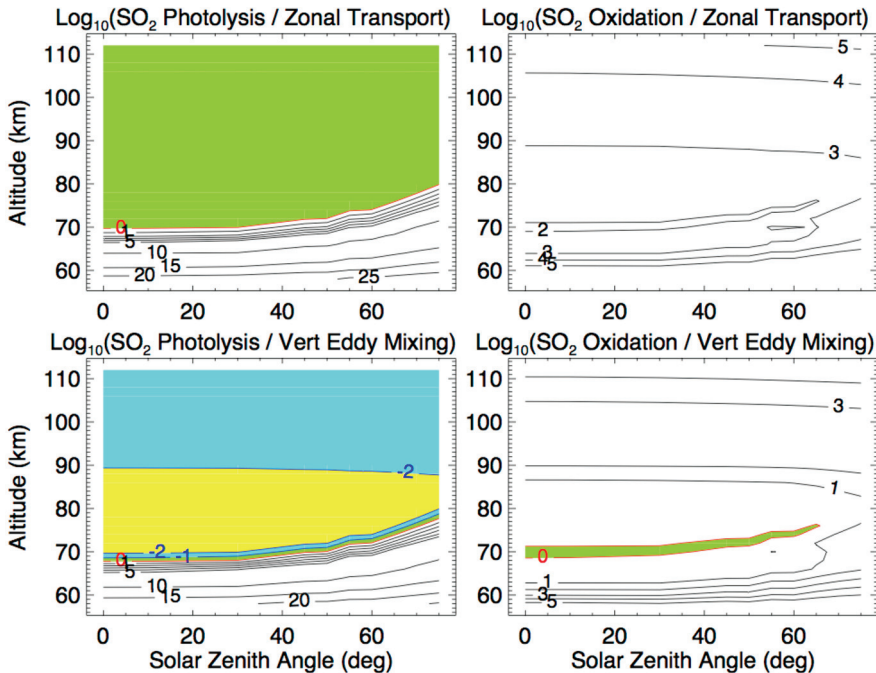


Figure 2: Relative timescales for photochemical loss of SO₂ and transport at 0–70° solar zenith angle (Updated from (Jessup et al., 2015))

The SZA-dependent SO_2 profiles illustrate the upward shift with increasing SZA of the altitude at which optical depth unity is reached for the wavelengths where SO_2 absorbs strongly (Jessup et al., 2015). These calculations represent the chemistry that would be expected if horizontal transport is neglected and the chemistry is allowed to equilibrate between vertical transport of mass and photons.

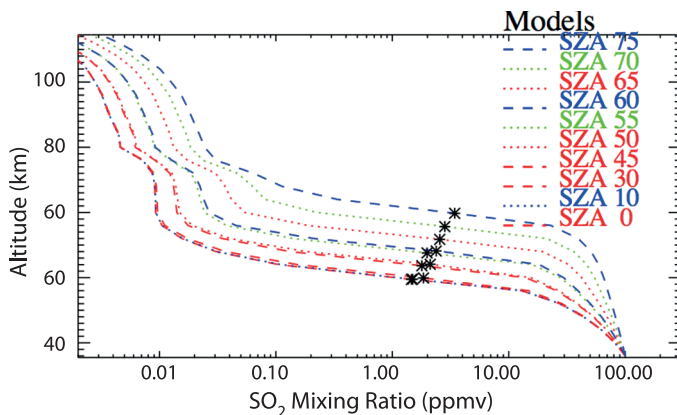


Figure 3: Estimated vertical profile for SO_2 near the equatorial evening terminator (asterisks)

Figure 2 shows the relative importance of vertical and zonal transport and photochemistry by comparing the photochemical and transport lifetimes (Jessup et al., 2015). The zonal transport lifetime was assumed to be constant with altitude in the mesosphere, while the photo-dissociation lifetime increases significantly as one goes deeper into the atmosphere. Consequently, photo-dissociation effectively stops at smaller SZAs at lower altitudes and the SO_2 mixing ratio is approximately frozen at the mixing ratio where the photo-dissociation and transport lifetimes are equal. This “quenching,” analogous to that occurring in temperature-dependent processes, results in a profile where the SO_2 mixing ratio increases by a factor of two from 70 to 80 km altitude near the terminator, Fig. 3. This agrees qualitatively, but not quantitatively, with observations. Further evidence supporting this idea comes from VTGCM simulations (Parkinson et al., 2016).

Conclusions

Simulations with a simplified standard photochemistry model suggest the combination of photochemistry and dynamics can produce a mesospheric SO_2 inversion layer that is qualitatively consistent with observations at the equatorial terminator. Further work is needed to assess the proposed mechanism at other latitudes and local solar times. Verification of the magnitude of the SO_2 inversion layer that can be produced with a full standard chemistry model is also required.

Acknowledgements

This work was partially supported by NASA grants NNX12AI32G and NNX16AN03G to Space Science Institute.

References

- Allen, M., et al. (1981) Vertical transport and photochemistry in the terrestrial mesosphere and lower thermosphere (50–120 km), *J. Geophys. Res.*, 86, 3617–3627.
- Belyaev, D. A., et al. (2012) Vertical profiling of SO_2 and SO above Venus’ clouds by SPICAV/SOIR solar occultations, *Icarus*, 217, 740–751.
- DeMore, W. B., Yung, Y. L. (1982) Catalytic processes in the atmospheres of Earth and Venus, *Science*, 217, 1209–1213.
- Harder, J. W., et al. (2010) The SORCE SIM solar spectrum: Comparison with recent observations, *Sol. Phys.*, 263, 3–24.
- Jessup, K. L., et al. (2015) Coordinated Hubble Space Telescope and Venus Express observations of Venus’ upper cloud deck, *Icarus*, 258, 309–336.
- Krasnopolsky, V. A. (2012) A photochemical model for the Venus atmosphere at 47–112 km, *Icarus*, 218, 230–246.
- Marcq, E., et al. (2018) Composition and chemistry of the neutral atmosphere of Venus, *Space Science Reviews*, 214, in press.

- Mills, F.P., Allen, M. (2007) A review of selected issues concerning the chemistry in Venus' middle atmosphere, *Plan. Space Sci.*, 55, 1729–1740.
- Parkinson, C.D., et al. (2016) Photochemical control of the distribution of Venusian water and sulphuric acid aerosols in the clouds and upper haze layer of Venus, plus new insights regarding SO₂, *International Venus Conference*, Oxford, 175–176.
- Sandor, B.J., et al. (2010) Sulfur chemistry in the Venus mesosphere from SO₂ and SO microwave spectra, *Icarus*, 208, 49–60.
- Sandor, B.J., et al. (2012) Upper limits for H₂SO₄ in the mesosphere of Venus, *Icarus*, 217, 839–844.
- Snow, M., et al. (2005) Solar-Stellar Irradiance Comparison Experiment II (Solstice II): Examination of the solar-stellar comparison technique, *Sol. Phys.*, 230, 295–324.
- Titov D.V., et al. (2007) Radiation in the atmosphere of Venus, in *Exploring Venus as a Terrestrial Planet*, American Geophysical Union, 121–138.
- Vandaele, A.C., et al. (2017) Sulfur dioxide in the Venus atmosphere: I. Vertical distribution and variability, *Icarus*, 295, 16–33.
- Zhang, X., et al. (2010) Photolysis of sulphuric acid as the source of sulphur oxides in the mesosphere of Venus, *Nature Geoscience*, 3, 834–837.
- Zhang, X., et al. (2012) Sulfur chemistry in the middle atmosphere of Venus, *Icarus*, 217, 714–739.

ON UNDERSTANDING THE NATURE AND VARIATION OF THE VENUSIAN MIDDLE ATMOSPHERE VIA OBSERVATIONS AND NUMERICAL MODELING OF KEY TRACER SPECIES

C. D. Parkinson¹, S. W. Bougher¹, A. S. Brecht²

¹ *University of Michigan, Ann Arbor, MI, USA*

² *NASA Ames Research Center, Moffett Field, CA, USA*

Abstract

The primary objective is to conduct detailed dynamical and photochemical studies of the Venus middle atmosphere (~70–110 km) to obtain a self-consistent understanding of the photochemistry, dynamics, heating, and microphysics of the Venus middle atmosphere employing existing validated models and utilizing updated photochemical schemes (Bougher et al., 2015; Brecht et al., 2011; Parkinson et al., 2015a, b). This will be achieved iteratively by:

- creating a 1-D KINETICS model atmosphere that eliminates the need for SVP H₂SO₄ photochemistry relying on recently developed chemical schemes;
- determining a reduced chemical scheme from KINETICS for use in Venus Thermospheric General Circulation Model (VTGCM) dynamical modeling using SO₂ as a tracer;
- using the Community Aerosol and Radiation Model for Atmospheres (CARMA) cloud microphysics model to better characterize Venus' spatially and temporally highly variable upper haze (UH), as populated by aerosol multiple particle size modes and in conjunction with KINETICS/VTGCM to better understand the sulfur processes in the region of interest. Data-model comparisons making use of simulated outputs from the VTGCM which will subsequently be used to examine the corresponding retrograde superrotating zonal (RSZ) and subsolar-to-antisolar (SS-AS) wind components (or residuals) required to give rise to middle atmosphere mean density and temperature distributions, and their variations.

Another objective is to address the decades long mystery of the unknown UV absorber. (Frandsen et al., 2016) identify two different (SO)₂ isomers, cis-OSSO and trans-OSSO, and find that they are good candidates to explain the enigmatic 320–400 nm near-UV absorption. We propose to use the analyses from Objectives 1 and 2 to make the connection of the variability of SO₂ to the observed light/dark clouds observed in the Venusian atmosphere. This will be done using the updated KINETICS chemical scheme utilized in the primary objective, and including a reduced KINETICS photochemical set for VTGCM+CARMA modeling. Higher abundances of SO₂ (and associated chemistry and subsequent formation of aerosols, as described by (Parkinson et al., 2015a, b)) with the relative absence of water due to a chemical bifurcation could correspond to the darker regions, while areas of depleted SO₂ and moderate to high values for H₂O could correspond to the lighter regions. In this way, photochemistry, dynamics (SO₂ tracer) and microphysics will be employed in a self-consistent way to show the direct link between the SO dimer described by (Frandsen et al., 2016) and the unknown UV absorber of (Haus et al., 2015).

Introduction

Venus' complex and dynamic upper atmosphere has been observed many times by ground-based, orbiters, probes, and fly-by missions. Numerical modeling tools are useful in interpreting these observations to address questions regarding chemistry, dynamics, and the complex structure of the middle and upper atmosphere. Several models have been employed to do this: (1) the 3-D hydrodynamic Venus Thermospheric General Circulation Model (VTGCM), (2) JPL/Caltech KINETICS, a 1-D photochemical model, and (3) CARMA, a 3-D microphysical cloud model. Recently, these numerical models have been extended to include new chemical constituents and airglow emissions, as well as new parameterizations to address waves and their impact on the varying global circulation and corresponding airglow distributions (cf. Brecht et al., this issue).

Recent Modeling vs Observational Comparisons:

The numerical models have been compared to the ESA Venus Express (VEx) observations. These studies mainly addressed the thermal structure and tracer density profiles and have been the subject of several recently published papers and ongoing research (Bougher et al., 2015; Brecht et al., 2011; Parkinson et al., 2015a, b).

Distribution of Sulphuric Acid Aerosols in the Clouds and Upper Haze of Venus Using Venus Express VAST and VeRa Temperature Profiles

Observations from Pioneer Venus and from SPICAV/SOIR aboard Venus Express (VEx) have shown the upper haze (UH) of Venus to be highly spatially and temporally variable, and populated by multiple particle size modes. Previous models of this system (e.g., (Gao et al., 2014), using a typical temperature profile representative of the atmosphere (viz., equatorial VIRA profile), did not investigate the effect of temperature on the UH particle distributions. (Parkinson et al., 2015a) show (using CARMA) that the inclusion of latitude-dependent temperature profiles from for both the morning and evening terminators of Venus helps to explain how the atmospheric aerosol distributions vary spatially. In that work, they use temperature profiles obtained by two instruments onboard VEx, VeRa and SPICAV/SOIR, to represent the latitudinal temperature dependence. They find that there are no significant differences between results for the morning and evening terminators at any latitude and that the cloud base moves downwards as the latitude increases due to decreasing temperatures. The UH is not affected much by varying the temperature profiles, however the haze does show some periodic differences, and is slightly thicker at the poles than at the equator. It was also found that the sulphuric acid “rain” seen in previous models may be restricted to the equatorial regions of Venus, such that the particle size distribution is relatively stable at higher latitudes and at the poles (cf. Fig. 1). Current work in progress show that photochemistry can drastically affect the precipitation timescale by a factor of a few greater for cases involving “water poor” conditions (see next section).

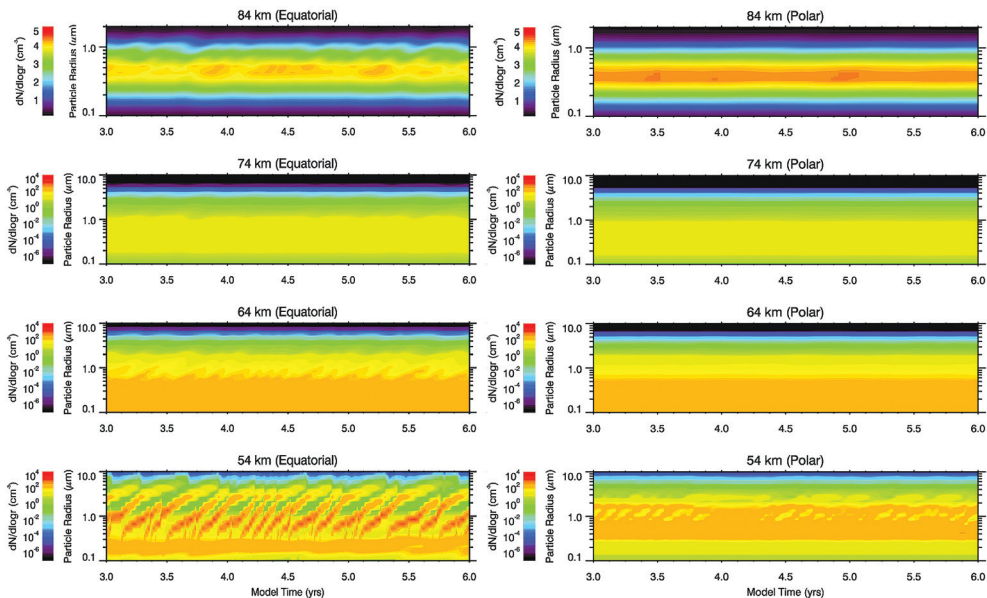


Figure 1: Time evolution of the calculated particle size distribution at 84, 74, 64, and 54 km altitude from $t = 3$ Earth years to $t = 6$ Earth years for the Equatorial MT case. Note the different number density contour and y axis scale for the 84 km plot. See (Parkinson et al., 2015a) for more details

Photochemical Control of the Distribution of Venusian Water and SO_x

(Parkinson et al., 2015b) use the JPL/Caltech 1-D photochemical model to solve the continuity diffusion equation for the atmospheric constituent abundances and total number density as a function of radial distance from the planet Venus. The photochemistry of the Venus atmosphere from 58 to 112 km is modeled using an updated and expanded chemical scheme, guided by the results of recent observations. (Parkinson et al., 2015b) model water from between 10–35 ppm at our 58 km lower boundary using an SO₂ mixing ratio of 25 ppm as our nominal reference value. They

then vary the SO₂ mixing ratio at the lower boundary between 5 and 75 ppm holding the water mixing ratio of 18 ppm at the lower boundary and find that it can control the water distribution at higher altitudes. SO₂ and H₂O can regulate each other via formation of H₂SO₄. In regions of high mixing ratios of SO₂ there exists a “runaway effect” such that SO₂ gets oxidized to SO₃, which quickly soaks up H₂O causing a major depletion of water between 70 and 100 km. In addition to explaining some of the observed variability in SO₂ and H₂O on Venus, their work can also shed light on the observations of dark and bright contrasts at the Venus cloud tops observed in the ultraviolet spectrum. The calculations produce results in agreement with the SOIR Venus Express results of 1 ppm at 70–90 km (Bertaux et al., 2007) by and using an SO₂ mixing ratio of 25 ppm SO₂ and 18 ppm water as our nominal reference values (cf. Fig. 2). Timescales for a chemical bifurcation causing a collapse of water concentrations above the cloudtops (>64 km) are relatively short and on the order of a less than a few months, decreasing with altitude to less than a few days. Ongoing studies include improved photochemical modeling of key SO_x species.

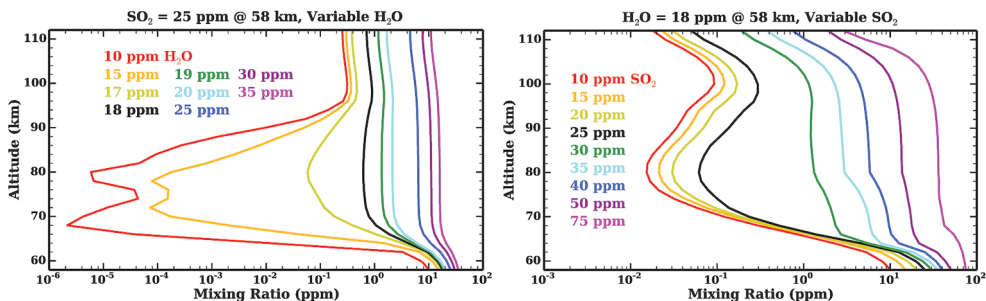


Figure 2: (a) Water profiles from a lower boundary mixing ratio sensitivity study with fixed SO₂ lower boundary of 25 ppm: H₂O varies between 10–35 ppm, (b) SO₂ profiles from a lower boundary mixing ratio sensitivity study with fixed H₂O lower boundary of 18 ppm: SO₂ varies between 5–75 ppm

Modeling of Observations of Night OH in the Venesian Mesosphere

Airglow emissions, such as NO and O₂, have been observed previously on Venus (Brecht et al., 2011). Airglow emissions provide insight into chemical and dynamical processes that control the composition and energy balance in the upper atmosphere. Venus airglow emissions have been unambiguously detected by the Visible and Infrared Thermal Imaging Spectrometer (VIRTIS) on the Venus Express (VEX) spacecraft. These emissions are attributed to the OH (2–0) and (1–0) Meinel band transitions as well (Piccioni et al., 2008). The integrated emission rates for the OH (2–0) and (1–0) bands were measured to be 100±40 and 880±90 kR respectively, both peaking at an altitude of 96±2 km near midnight local time for the considered orbit. Photochemical model calculations suggest the observed OH emission is produced primarily via the Bates-Nicolet mechanism, as on the Earth. However, the Venus background atmosphere is different than that of the Earth, and we are able to distinguish relative contributions due to different key photochemical reactions in the modeling corresponding to observed features from the VEx VIRTIS data.

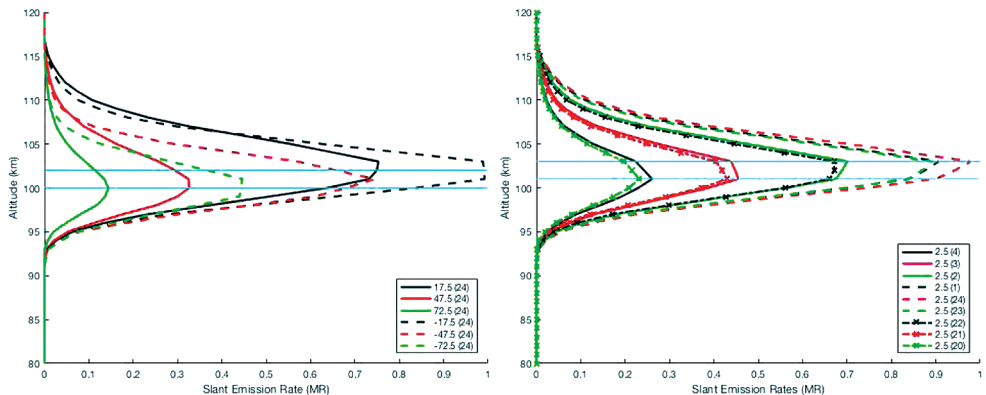


Figure 3: (a) Variation of slant path emission rates with latitude. Latitudinal differences are clearly seen between the N. hemisphere and S. hemisphere; (b) Variation of slant path emission rates with local time centered around midnight

Fig. 3 shows calculations of the OH airglow slant path intensities varying with both latitude and local time around midnight. The magnitude of this emission (both integrated vertical intensity and volume emission rate) are consistent with VEx VIRTIS slant path observations.

Improvements

The latest improvements to all of the numerical models enable the model to address the driving forces to understand the nature and variation of the Venusian middle atmosphere via observations and numerical modeling of key tracer species.

Chemistry

The SO_x chemistry has been included (e.g. SO₂ and SO) and also the necessary OH chemistry to model the OH nightglow emission. The inclusion of these chemical species (and nightglow emission) provides tracers of the global circulation at different altitudes in the upper atmosphere. These studies directly influence CO and CO₂ distributions as well as chemistry involved in modeling the unknown UV absorber.

Aerosol Heating

The VTGCM lower boundary is at ~70 km, which is near the cloud tops. Near this level, aerosols provide heat to the middle atmosphere. A parameterization guided by (Bertaux et al., 2007) has been incorporated and tested. The additional heating increases the scale heights in this altitude range (~75–90 km) and therefore augments density profiles (~100–130 km) and modifies wave propagation. These aerosol heating profiles are correlated with those used in the KINETICS and CARMA models synergistically.

Conclusion

Our work includes reference numerical modeling simulations showing the impact the latest improvements make upon the middle atmosphere and how the results compare to observations. The comparative work relating modeling and observations is very important to improving our understanding of the underlying processes driving the complex photochemical, microphysical cloud structure, and dynamical structure of the upper atmosphere of Venus.

Acknowledgements

A.S. Brecht and S.W. Bougher have been supported by NASA Grant #NNX14AB66A. C.D. Parkinson has been supported by NASA Grant #NNX15AH30G.

References

- Bertaux, J.L., et al. (2007) A warm layer in Venus' cryosphere and high-altitude measurements of HF, HCl, H₂O and HDO, *Nature*, 450, 646–649.
- Bougher, S.W., Brecht, A.S., Schulte, R., Fischer, J., Parkinson, C.D. Mahieux, A., Wilquet, V., Vandaele, A. (2015) Upper Atmosphere Temperature Structure at the Venusian Terminators: A Comparison of SOIR and VTGCM, *Results, Planetary and Space Science*, 113–114, 336–346.
- Brecht, A.S., Bougher, S.W., Gerard, J.C., Parkinson, C.D., Rafkin, S., Foster, B. (2011) Understanding the Variability of Nightside Temperatures, NO UV and O₂ IR Nightglow Emissions in the Venus Upper Atmosphere, *J. Geophysical Research*, 116, E08004.
- Frandsen, B.N., Wennberg, P., Kjaergaard, H. (2016) Identification of OSSO as a near-UV absorber in the Venusian atmosphere, *Geophys. Res. Lett.*, 43, doi: 10.1002/2016GL070916.
- Gao, P., Zhang, X., Crisp, D., Bardeen, C.G., Yung, Y.L. (2014) Bimodal distribution of sulphuric acid aerosols in the upper haze of Venus, *Icarus*, 231, 83–98.
- Haus, R., Kappel, D., Arnold, G. (2015) Radiative Heating and Cooling in the Middle and Lower Atmosphere of Venus and Responses to Atmospheric and Spectroscopic Parameter, *Planetary and Space Science*, 117, 262–294.
- Parkinson, C.D., Gao, P., Schulte, R., Bougher, S.W., Yung, Y.L., Bardeen, C.G., Wilquet, V., Vandaele, A.C., Mahieux, A., Tellmann, S., Patzold, M. (2015a) Distribution of Sulphuric Acid Aerosols in the Upper Haze of Venus Using Venus Express VAST and VeRa Temperature Profiles, *Planet. Space Sci.*, doi: 10.1016/j.pss.2015.01.023.
- Parkinson, C.D., Yung, Y.L., Esposito, L., Gao, P., Bougher, S.W., Hirtzig, M. (2015b) Photochemical Control of the Distribution of Venusian Water, *Planet. Space Sci.*, doi: 10.1016/j.pss.2015.02.015.
- Piccioni, G., Drossart, P., Zasova, L. et al. (2008) First detection of hydroxyl in the atmosphere of Venus, *Astronomy and Astrophysics*, 483, L29–L33.

EXPERIMENTAL RESULTS ON THE STABILITY OF GALENA IN VENUSIAN CONDITIONS

S. T. Port, A. C. Briscoe, V. F. Chevrier

University of Arkansas, Fayetteville, Arkansas, USA

Abstract

The mineralogy of Venus has yet to be fully characterized. Since the atmosphere is abundant in sulfur gas species the surface is expected to contain sulfur bearing minerals. Galena has been suggested as a mineral that could be found on the surface of Venus. It is a metal sulfide with a high dielectric constant and could be a source of the high radar reflective signal in the highlands. Our aim was then to study the stability of galena (PbS) in Venusian gases (CO_2 , SO_2 , COS) at Venusian temperatures. Our preliminary results show the formation of anglesite (PbSO_4) and occasionally lanarkite ($\text{PbSO}_4 \cdot \text{PbO}$) in the high temperature experiments. Upon closer inspection it was found that the initial samples showed minor contamination by anglesite resulting from fast oxidation in air. We did not however, observe any further oxidation of galena in our pressurized chamber experiments.

Introduction

Venus is considered to be Earth's twin sister, yet its surface mineralogy is still shrouded in uncertainty. With the last of only seven probes having landed in 1985, our current information on the surface mineralogy of Venus is severely lacking. Researchers have since turned to a combination of thermodynamic calculations and experimental simulations to theorize possible minerals that could be present on the surface. Since the atmosphere and surface mineralogy are interconnected in a complex chemical reaction web, carrying out simulations requires a knowledge on the composition of the atmosphere.

Venus' atmosphere is partially composed of an assortment of sulfur bearing gases. The most abundant of these is SO_2 , which is predicted to be between 130 ± 40 to 180 ± 70 ppm below 42 km (Pollack et al., 1993; Bezard et al., 1993; Marcq et al., 2008). This abundance declines at higher elevation to a few ppb (Vandaele et al., 2017). The next most abundant sulfur containing gas is COS, with an estimated abundance of anywhere from 4.4 ± 1 ppm (Pollack et al., 1993) to 2.4 ± 1 (Marcq et al., 2008). Much of the rest of the sulfur can be found bound as S_x , SO, SO_3 , H_2S , as well as H_2SO_4 droplets in the clouds (Oyama et al., 1979; Bezard et al., 1990; Marcq et al., 2008; Prinn et al., 1985; Von Zahn et al., 1983).

The large number of sulfur bearing gases in the atmosphere has led to the widely accepted theory that sulfur bearing minerals must be present and involved in the release and absorption of sulfur. Several minerals have been suggested as having a hand in the sulfur cycle, but also as a possible source for the high radar reflective signal seen on the highlands of Venus (Klose et al., 1992; Fegley et al., 1992; Hashimoto et al., 2000). Several papers published around this time proposed that a lead mineral could be the source of the reflectivity (Schaefer et al., 2004; Shepard et al., 1994; Brackett et al., 1995). Galena, a lead and sulfur bearing mineral, was discussed by both (Schaefer et al., 2004; Brackett et al., 1995) as a strong candidate due to its high dielectric constant.

Galena (PbS) is one of the most abundant lead minerals on Earth (Nowak et al., 2000; Kullerud 1969). It is found in hydrothermal vents and contact metamorphic deposits (Kullerud 1969). Both sulfur and lead have been reported to be present in eruption plumes, and galena has been found near volcanic vents on Earth (Brackett et al., 1995). Considering Venus' volcanic history, and the possibility of current volcanism, galena could form easily on the surface of Venus (Bullock, Grinspoon, 2001; Vandaele et al., 2017; Brackett et al., 1995).

Galena may also be a source and sink for SO_2 on Venus. When exposed to oxygen, galena is known to oxidize within a time frame of minutes to days (Nowak et al., 2000; Buckley et al., 1984) and release SO_2 (Zingg et al., 1978; Abdel-Rehim, 2006). The rate of oxidation only escalates when galena is heated to higher temperatures, like those observed on Venus (Hagihara, 1952; Abdel-Rehim, 2006; Shapter, 2000; Zingg et al., 1978). Based on thermodynamic models and data obtained from the Venera landers, the oxygen fugacity at the surface of Venus is believed to be around $10^{-21.7}$ to 10^{-20} bars, with more oxidizing conditions found at higher altitudes (Fegley et al., 1997). Note that

this value was calculated and thus may not represent the conditions found near the surface. This opens up the possibility that galena may convert into oxides depending on how much oxygen is currently present on Venus. However it is unknown how the chemical weathering processes present on Venus would interact with galena.

Methods

Galena was purchased as crystals from Ward's Science, and were ground using a shatterbox to approximately 250 μm . The galena powder was analyzed for any impurities then flushed with and maintained in Argon gas to prevent any further oxidation. Each experiment used one gram of galena, which was placed in a ceramic boat. The galena was then subjected to Venusian temperatures in a Lindberg tube oven. Since the temperature drastically changes with varying elevation, the conditions found at three different elevations were chosen to be simulated in our experiments. The three temperatures were 460 $^{\circ}\text{C}$ (average radius), 425 $^{\circ}\text{C}$ (4.5 km above the average radius), and 380 $^{\circ}\text{C}$ (11 km above the average radius). All experiments were also completed in one of three different gases: 100 % CO_2 , 100 ppm of SO_2 in CO_2 , and 100 ppm of COS in CO_2 . Each experiment lasted for 24 hours before being allowed to cool while exposed to gas used in the experiment. A chamber experiment was also completed in pure CO_2 at 380 $^{\circ}\text{C}$ /45 bars for 48 hours. That chamber, found at the University of Arkansas, simulates the temperatures and pressures on Venus. After the experiments were concluded, the samples were weighed and then analyzed using XRD to determine any changes in phase and mineralogy.

Results

XRD results of the galena experiments are summarized in Table 1. Closer inspection of the original sample of galena revealed trace amounts of anglesite contamination. In the pure CO_2 oven experiment heated to 380 $^{\circ}\text{C}$ the galena spectra had the highest peak match score followed by anglesite (PbSO_4). The 425 $^{\circ}\text{C}$ and 460 $^{\circ}\text{C}$ oven experiments resulted in galena having the highest score, followed by anglesite and lastly by lanarkite ($\text{PbSO}_4 \cdot \text{PbO}$). It should be noted that lanarkite was only observed in the higher temperature experiments. The spectra for the 460 $^{\circ}\text{C}$ experiment can be seen in Figure 1. In the chamber experiment completed in pure CO_2 the sample had very strong galena peaks, with very minor peaks of anglesite.

In the oven experiments completed in the CO_2/COS mix heated to 380 $^{\circ}\text{C}$, 425 $^{\circ}\text{C}$, and 460 $^{\circ}\text{C}$ galena had the highest match score followed by anglesite. Galena heated in CO_2/SO_2 at 380 $^{\circ}\text{C}$, 425 $^{\circ}\text{C}$, and 460 $^{\circ}\text{C}$ also had strong galena peaks and smaller anglesite peaks. The resulting spectra from the CO_2/SO_2 at 460 $^{\circ}\text{C}$ experiment can be seen in Fig. 1.

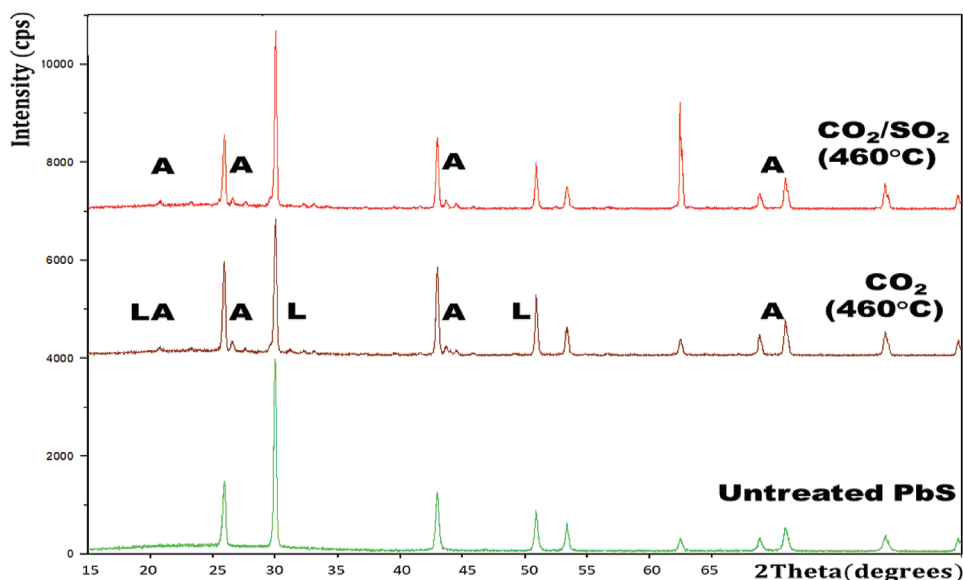


Figure 1: Galena experiments completed in the oven. The bottom spectra is pure galena. The middle spectra is galena that has been heated to 460 $^{\circ}\text{C}$ in pure CO_2 , the top spectra is galena heated to 460 $^{\circ}\text{C}$ in the CO_2/SO_2 mix. "A" highlights the formation of anglesite and "L" highlights the formation of lanarkite

Table 1: A summary of our oven experiment results

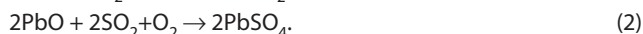
| Gas Mixture | Temperature | | |
|-----------------------------------|--|--|----------------------------------|
| | 380°C | 425°C | 460°C |
| CO ₂ | Galena Anglesite (PbSO ₄) | Galena Anglesite Lanarkite (PbSO ₄ ·PbO) | Galena Anglesite Lanarkite |
| CO ₂ /COS | Galena Anglesite | Galena Anglesite | Galena Anglesite |
| CO ₂ / SO ₂ | Galena | Galena | Galena |

Discussion

Even after only 4 hours of exposure, small peaks of anglesite were detected in the freshly ground galena. It has been documented that galena is highly reactive to air and will oxidize to anglesite in as short as a few minutes (Nowak et al., 2000) to several days (Buckley et al., 1984). Unfortunately, immediate storage of the sample in argon gas did not prevent oxidation. The XRD spectra of our samples after the oven experiments show even stronger peaks of anglesite than before the experiment. Therefore it is believed that some anglesite formed during the experiments but was also present before they even began.

In the CO₂ oven experiments we found evidence of anglesite at lower temperatures and lanarkite and anglesite at higher temperatures. Based on our results, increasing the temperature did not significantly change the abundance of anglesite, however it did increase the amount of lanarkite in the sample.

Past experiments completed by others found that anglesite forms between 170 °C and 280 °C (Hagihara 1952) or between 200 °C and 450 °C (Abdel-Rehim 2006). Anglesite forms via a two-step process (Abdel-Rehim 2006; Zingg et al., 1978):



Where SO₂ is created in (1) then used in (2). Another reaction that has been suggested is (Hagihara 1952; Ponsot et al., 1998):



At increased temperatures lanarkite will form via one of two reactions:



These reactions are expected to take place between 500 °C and 700 °C (Abdel-Rehim 2006). Other studies found the presence of lanarkite at temperatures as high as approximately 900 °C, although the exact temperature is not known because a high-powered laser was used to heat the sample (Shapter, 2000). Nonetheless, these results coincide with the results we see in our CO₂ oven experiments where anglesite formed at the lower temperature experiments and lanarkite formed at higher temperature experiments. In our experiments lanarkite formed at slightly lower temperatures than reported by (Abdel-Rehim, 2006), somewhere around 425 °C. Lanarkite has a higher lead to oxygen ratio, thus based on the results of past experiments it is likely that the energy at higher temperatures is enough to release some of the oxygen from the sample.

Based on the results of previous studies, and from reaction (1) we expected to see PbO in our sample. However our analysis of the sample could not detect any PbO. This implies that if reaction (1) is occurring, then all of the PbO is immediately being used up in reaction (2). Otherwise the path to the formation of anglesite would be via reaction (3). If PbO is not forming, then this implies that reaction (4) is the path to forming lanarkite, and not reaction (5).

When the galena was placed in the chamber for 48 hours at 380 °C/45 bar the abundance of galena and anglesite did not change when compared to before and after the experiment. Thus it appears that CO₂ at this temperature and pressure has no effect on galena. A 48 hr lowland condition experiment (460 °C/95 bars) has not yet been completed at this time and may yield different results.

The CO_2/SO_2 and CO_2/COS experiments at 425 °C and 460 °C did not exhibit lanarkite. More experiments will need to be completed to observe if these results are reproducible. One possibility is that since the sample does not oxidize uniformly, the sample we analyzed did not contain a large enough concentration of lanarkite to be detected. Another theory is that the atmospheric composition prevents lanarkite from forming by favoring the stability of anglesite.

The CO_2/COS and CO_2/SO_2 experiments had identical results at all temperatures. According to (2) SO_2 is required to form anglesite, therefore we expected more anglesite to have formed in the CO_2/SO_2 experiment. This implies that anglesite forms via reaction (3). As for the COS experiment, at low temperatures (<650 °C) COS will dissociate via (Karan et al., 2005):



A second reaction has also been postulated (Glarborg et al., 2013; Oya et al., 1994):



Because our results are purely galena and anglesite, if reaction (6) occurs then CS_2 is not expected to react with the sample. Based on our preliminary chamber experiments it appears that CO_2 does not interact with galena, or at least does not in the cooler temperature/pressure experiment. If reaction (7) occurs in the oven, based on our XRD results the products do not react, or has little effect on the sample. Another possibility is since the oven is not perfectly sealed, there is a chance that any gases formed during the experiment may have left the system immediately after formation. This would prevent any of the gases produced in reaction (7) from interacting with the mineral sample. Future experiments with the mixed gases in the chamber will need to be completed to observe if COS interacts indirectly with the sample.

Our preliminary chamber experiment exhibited that galena could be stable in the highlands of Venus. On the planet, volatile metal chalcogenides, such as galena, have been calculated to be transported from the hotter lowlands into the cooler highlands (Brackett et al., 1995). In addition, a few millimeters can accumulate on the surface after 1–10 m.y. (Brackett et al., 1995). However the oxygen fugacity on Venus is still unknown, and depending on the abundance it may result in the formation of some anglesite. Lanarkite may even be present near the hotter lowlands, assuming that not all of the lead and sulfur released from volcanism is transported to the highlands. According to (Fegley, Treiman, 1992), if Venus is oxidizing then sulfates form, if reducing, then sulfides form. They concluded that higher altitudes should have more oxidizing conditions, which would mean the production of sulfates would be favored over sulfides. If anglesite is stable in the highlands, its low dielectric constant prevents it from being the source of the radar reflective signal (Young et al., 1973; Tyler et al., 1991). A future mission will be needed to ascertain the exact oxidation state of the near surface environment and to determine if it varies by elevation.

Conclusion

Due to possible oxygen contamination in the oven, and the initial oxidation of some galena into anglesite, it is difficult to ascertain the exact effects of CO_2 , COS , and SO_2 on galena. However we can state with certainty that in CO_2 oven experiment anglesite is stable at a lower temperature regime than lanarkite. We can also state that galena oxidizes very quickly and can easily form anglesite in the presence of oxygen. Based on literature review of the reactivity and stability of CO_2 , SO_2 , and COS , we do not see an obvious reaction that could occur between the gases and galena. Despite this, there is still much we do not know about the near surface environment on Venus, therefore at this time galena should not be eliminated as a possible source and sink of sulfur gases on Venus. It can also not be eliminated as a possible source for the high radar reflective signal. In the future we will analyze the gases created in the experiments with a gas chromatograph to determine which gases are released or get consumed during the experiments. We will also study galena in the chamber in the mixed gases to observe how they interact. Future related experiments include pure lead, anglesite, and cerussite (PbCO_3) to gain more insight into the precise reactions involving lead, sulfur, carbon, and oxygen on the surface of Venus.

Acknowledgements

This work was funded by the NASA Solar System Workings grant #NNX15AL57G.

References

Abdel-Rehim, A. M. (2006) Thermal and XRD Analysis of Egyptian Galena. *J. Thermal Analysis and Calorimetry*, 86, 2, 393–401.

- Bézar, B., de Bergh, C., Crisp, D., Maillard, J. (1990) The deep atmosphere of Venus revealed by high-resolution nightside spectra, *Nature*, 345, 508–511.
- Bézar, B., de Bergh, C., Fegley, B., Maillard, J., Crisp, D., Owen, T., Pollack, J., Grinspoon, D. (1993) The abundance of sulfur dioxide below the clouds of Venus, *Geophys. Res. Lett.*, 20(15), 1587–1590.
- Brackett, R. A., Fegley, B., Arvidson, R. E. (1995) Volatile transport on Venus and implications for surface geochemistry and geology, *J. Geophys. Res.: Planets*, 100(E1), 1553–1563.
- Buckley, A. N., Woods, R. (1984) An X-Ray Photoelectron Spectroscopic Study of the Oxidation of Galena: Applications of Surface, *Science*, 17(4) 401–414.
- Bullock, M. A. Grinspoon, D. (2001) Recent Evolution of Climate on Venus, *Icarus*, 150, 19–37.
- Fegley Jr., B., Treiman, A. H., Sharp, V. L. (1992) Venus surface mineralogy: observational and theoretical constraints, In: *Proc. Lunar Planet. Sci. Conf.*, 22, 3–19.
- Fegley, B., Treiman, A. H. (1992) Chemistry of Atmosphere-Surface Interactions on Venus and Mars, In *Venus and Mars: Atmospheres, Ionospheres, and Solar Wind Interactions*, J. G. Luhmann, M. Tatrallyay, R. O. Pepin (Eds.), American Geophysical Union, 7–72.
- Fegley, B., Zolotov, M. Y., Lodders, K. (1997) The Oxidation State of the Lower Atmosphere and Surface of Venus, *Icarus*, 125, 416–439.
- Glarborg, P., Marshall, P. (2013) Oxidation of Reduced Sulfur Species: Carbonyl Sulfide, *Intern. J. Chemical Kinetics*, 45(7), 429–439.
- Hagihara, H. (1952) Surface Oxidation of Galena in Relation to its Flotation as Revealed by electron diffraction, *J. Phys. Chem.* 56, 610–615.
- Hashimoto, G. L., Abe, Y. (2000) Stabilization of Venus' climate by a chemical-albedo feedback, *Earth Planets Space*, 52, 197–202.
- Karan, K., Mehrotra, A., Behie, L. A. (2005) Thermal Decomposition of Carbonyl Sulfide at Temperature Encountered in the Front End of Modified Claus Plants, *Chem. Eng. Comm.*, 192(3), 370–385.
- Klose, K., Wood, J., Hashimoto, A. (1992) Mineral equilibria and the high radar reflectivity of Venus mountaintops, *J. Geophys. Res.: Planets*, 97(E10), 16353–16369.
- Kullerud, G. (1969) The lead-sulfur system, *Am. J. Science*, 267-A, 233–256.
- Marcq, E., Bézar, B., Drossart, P., Piccioni, G., Reess, J. M., Henry, F. (2008) A latitudinal survey of CO, OCS, H₂O, and SO₂ in the lower atmosphere of Venus: Spectroscopic studies using VIRTIS-H, *J. Geophys. Res.*, 113, E00B07.
- Nowak, P., Laajalehto, K. (2000) Oxidation of galena surface- an XPS study of the formation of sulfoxo species, *Applied Surface Science*, 157, 101–111.
- Oya, M., Shiina, H., Tsuchiya, K., Matsui, H. (1994) Thermal Decomposition of COS, *Bull. Chem. Soc. Jpn.* 67, 2311–2313.
- Oyama, V. I., Carle, G. C., Woeller, F., Pollack, J. B., Reynolds, R. T., Craig, R. A. (1980) Pioneer Venus gas chromatography of the lower atmosphere of Venus, *J. Geophys. Res.* 85(A13), 7891–7902.
- Pollack, J. B., Dalton, B., Grinspoon, D. H., Wattson, R. B., Freedman, R., Crisp, D., Allen, D. A., Bézar, B., Debergh, C., Giver, L., Ma, Q., Tipping, R. (1993) Near-infrared light from Venus' nightside: A spectroscopic analysis, *Icarus*, 103, 1–42.
- Ponsot, B., Salomon, J., Walter, Ph. (1998) RBS study of galena thermal oxidation in air with a 6-eV ¹⁶O³⁺ ion beam, *Nuclear Instruments and Methods in Physics Research B*, 136–138, 1074–1079.
- Prinn, R. G. (1985) The photochemistry of the atmosphere of Venus, In *The Photochemistry of Atmospheres*, J. S. Levine (Ed.), Academic Press, New York, 281–336.
- Schaefer, L., Fegley, B., (2004) Heavy metal frost on Venus, *Icarus*, 168(1), 215–219.
- Shapter, J. G., Brooker, M. H., Skinner, W. M. (2000) Observation of the Oxidation of Galena using Raman Spectroscopy, *Intern. J. Miner. Process*, 60, 199–211.
- Shepard, M. K., Arvidson, R. E., Brackett, R. A., Fegley, B. (1994) A ferroelectric model for the low emissivity highlands on Venus, *Geophys. Res. Lett.* 21(6), 469–472.
- Tyler G. L., Ford P. G., Campbell, D. B., Elachi C., Pettengill G. H., Simpson R. A. (1991) Magellan: Electrical and physical properties of Venus' surface, *Science*, 252, 265–270.
- Vandaele, A. C., Korabely, O., Belyaev, D., Chamberlain, S., Evdokimova, D., Encrenaz, Th., Espósito, L., Jessup, K. L., Lefevre, F., Limaye, S., Mahieux, A., Marcq, E., Mills, F. P., Montmessin, F., Parkinson, C. D., Robert, S., Roman, T., Sandor, B., Stolzenbach, A., Wilson, C., Wilquet, V. (2017) Sulfur Dioxide in the Venus Atmosphere: I. Vertical Distribution and Variability, *Icarus*, 295, 16–33.
- Von Zahn, U., Kumar, S., Niemann, H., Prinn, R. G. (1983) Composition of the atmosphere of Venus, In *Venus*, D. M. Hunten, L. Colin, T. M. Donahue, V. I. Moroz (Eds.), Univ. of Arizona Press, Tucson, 299–430.
- Young, K. F., Frederikse, H. P. R. (1973) Compilation of the Static Dielectric Constant of Inorganic Solids, *J. Phys. Ref. Data*, 2(2), 313–409.
- Zingg, D. S., Hercules, D. M. (1978) Electron Spectroscopy for Chemical Analysis Studies of Lead Sulfide Oxidation, *J. Phys. Chem.* 82(18) 1992–1995.

MODELING OF CHEMICAL COMPOSITION IN THE LOWER AND MIDDLE ATMOSPHERES OF VENUS

V. A. Krasnopolsky

Moscow Institute of Physics and Technology (PhysTech), Russia, vlad.krasn@verizon.net

Keywords: Venus, atmosphere, chemical composition, airglow, photochemistry, chemical kinetic modeling

Introduction

To respond to the current progress in the observational data on the Venus atmosphere, the following models have been developed by the author:

1. Model for excitation of the oxygen nightglow on the terrestrial planets (Krasnopolsky, 2011),
2. Photochemical model for the atmosphere at 47 to 112 km (Krasnopolsky, 2012, 2017),
3. Model for the nighttime photochemistry and nightglow at 80 to 130 km (Krasnopolsky 2013a),
4. Chemical kinetic model for the lower atmosphere up to 47 km (Krasnopolsky, 2013b),
5. Model for the $\text{H}_2\text{O}-\text{H}_2\text{SO}_4$ system in the clouds (Krasnopolsky, 2015).

The model results will be briefly presented.

Excitation of the oxygen nightglow on the terrestrial planets

The best observational data on the nightglow of the five O_2 band systems and $\text{O}(^1\text{S})$ are analyzed along with laboratory data on the excitation, excitation transfer, and quenching of the O_2 metastable states to yield the following scheme of the processes (Table 1).

Table 1: Excitation, excitation transfer, and quenching processes in the O_2 nightglow

| State | Bands | $\tau(\text{s})$ | α | α_{TE} | α_{TV} | k_{O} | k_{O_2} | k_{N_2} | k_{CO_2} |
|-----------------|--------------------|------------------|----------|----------------------|----------------------|----------------------|---------------------------------------|----------------------|----------------------|
| $A^3\Sigma_u^+$ | Hzl | 0.14 | 0.04 | 0 | 0 | $1.3 \cdot 10^{-11}$ | $4.5 \cdot 10^{-12}$ | $3 \cdot 10^{-12}$ | $8 \cdot 10^{-12}$ |
| $A'^3\Delta_u$ | Chm | 2–4 | 0.12 | 0 | 0 | $1.3 \cdot 10^{-11}$ | $3.5 \cdot 10^{-12}$ | $2.3 \cdot 10^{-12}$ | $4.5 \cdot 10^{-13}$ |
| $c^1\Sigma_u^-$ | Hzll | 5–7 | 0.03 | 0 | 0 | $8 \cdot 10^{-12}$ | $3 \cdot 10^{-14}/1.8 \cdot 10^{-11}$ | – | $1.2 \cdot 10^{-16}$ |
| $b^1\Sigma_g^+$ | 762 nm | 13 | 0.02 | 0.09 | 0.125 | $8 \cdot 10^{-14}$ | $4 \cdot 10^{-17}$ | $2.5 \cdot 10^{-15}$ | $3.4 \cdot 10^{-13}$ |
| $d^1\Delta_g$ | 1.27 μm | 4460 | 0.05 | 0.35 | 0.65 | – | 10^{-18} | $<10^{-20}$ | 10^{-20} |

Hzl, Hzll, and Chm are the Herzberg I, II, and Chamberlain bands; τ is the radiative lifetime; if two values are given, then they refer to high and low vibrational excitation on the Earth and Venus, respectively; α is the direct excitation yield; α_{TE} and α_{TV} are excitation transfer yields for Earth and Venus from the upper states including $5\Pi_g$ (see details in (Krasnopolsky, 2011)); and k_x are quenching rate coefficients in $\text{cm}^3 \cdot \text{s}^{-1}$. Two values of k_{O_2} are for $c^1\Sigma_g^+$ ($v = 0$ and $7-11$).

Photochemical model for the atmosphere at 47–112 km

New features of the model are the improved numerical accuracy, the NUV absorption based on the V14 data, the calculated (not fixed) H_2O profile, the NO and OCS chemistries based on the observed abundances, and column rates for all reactions. The model was recently updated by new results on the S_2O_2 chemistry and improved data on the H_2O , OCS, and H_2 abundances at 47 km. The calculated vertical profiles of CO, H_2O , HCl, SO_2 , SO, OCS and the O_2 dayglow at 1.27 μm generally agree with the observations. Production of CO and O, O_2 , O_3 by photolysis of CO_2 is balanced mostly by the ClCO cycle; however, the calculated O_2 exceeds the observed upper limit.

Formation of sulfuric acid peaks at 67 km and greatly reduces SO_2 and H_2O in the middle atmosphere. Abundances of SO_2 and H_2O in the middle atmosphere are very sensitive to small variations of eddy diffusion near 60 km and the $\text{SO}_2/\text{H}_2\text{O}$ ratio. Therefore the observed variations do not require volcanism.

While the production of H by photolyses of H₂O and HCl exceeds the production of Cl, odd chlorine is more abundant than odd hydrogen below 95 km because of the reaction OH + HCl → H₂O + Cl. The chlorine chemistry is very essential in the middle atmosphere. Cycles of the odd nitrogen chemistry are responsible for production of a quarter of O₂, SO₂, and Cl₂ in the atmosphere. A net effect of photochemistry in the middle atmosphere is the consumption of CO₂, SO₂, and HCl from the lower atmosphere and return of CO, H₂SO₄, and SO₂Cl₂.

Model for the nighttime chemistry and nightglow at 80–130 km

The Venus Express observations of the NO UV nightglow, the O₂ nightglow at 1.27 μm, four bands of the OH nightglow, and the nighttime ozone require a significant nighttime chemistry. This chemistry is initiated by fluxes of O, N, H, and Cl from the day side with mean hemispheric values of 3·10¹², 1.2·10⁹, 10¹⁰, and 10¹⁰ cm⁻², respectively. These fluxes are proportional to column abundances of these species above 90 km. The model includes 86 reactions of 29 species. The calculated nighttime abundances of Cl₂, ClO, and ClNO₃ exceed a ppb level at 80–90 km. A scheme for quenching of OH* by CO₂ is developed to fit the observations. Analytic relationships between the nightglow intensities, the ozone layer, and the input fluxes of atomic species are given.

Model for H₂O-H₂SO₄ system in the clouds

Coupled diffusion of H₂O and H₂SO₄ vapors is calculated in equilibrium with the liquid sulfuric acid. Variations in eddy diffusion near the lower cloud boundary stimulate variability in the cloud properties and abundances of H₂O and H₂SO₄. The preferable global-mean model fits both H₂O and H₂SO₄ observations. Concentration of sulfuric acid varies for those profiles from ~98 % near 50 km to ~80 % at 60 km and then is almost constant with 79 % at 70 km. Latitudinal variations of the H₂SO₄ production, temperature and atmospheric dynamics (simulated by eddy diffusion) induce the observed variations of H₂O and concentration of sulfuric acid.

Chemical kinetic model for the lower atmosphere at 0–47 km

Chemistry of the lower atmosphere is initiated by the fluxes of CO and H₂SO₄ from the middle atmosphere, photolysis of S₃ and S₄, and thermochemistry in the lowest scale height. The chemistry is driven by sulfur that is formed by SO+SO, produces OCS, and makes dramatic changes in abundances of OCS, CO, and S_x. The S_x + OCS mixing ratio is constant at 20 ppm, and the CO + OCS mixing ratio is constant at 35 ppm below 40 km. Free sulfur forms in the lower atmosphere with S₈ = 2.5 ppm above 40 km with condensation into sulfur aerosol near 50 km. Therefore sulfur cannot be the NUV absorber. The model predicts 3.5 ppb of SO₂Cl₂.

References

- Krasnopolsky, V. A. (2011) Excitation of the oxygen nightglow on the terrestrial planets, *Planet. Space Sci.*, 59, 754–766.
- Krasnopolsky, V. A. (2012) A photochemical model for the Venus atmosphere at 47–112 km, *Icarus*, 218, 230–246.
- Krasnopolsky, V. A. (2013a) Nighttime photochemical model and night airglow on Venus, *Planet. Space Sci.*, 85, 78–88.
- Krasnopolsky, V. A. (2013b) S₃ and S₄ abundances and improved chemical kinetic model for the lower atmosphere of Venus, *Icarus*, 225, 570–580.
- Krasnopolsky, V. A. (2015) Vertical profiles of H₂O, H₂SO₄, and sulfuric acid concentration at 45–75 km on Venus, *Icarus*, 252, 327–333.
- Krasnopolsky, V. A. (2017) Disulfur dioxide and its near-UV absorption in the photochemical model of Venus atmosphere, *Icarus*, 99, 294–299.

MICROPHYSICAL MODELLING OF THE SULFURIC ACID VENUS CLOUD SYSTEM

K. McGouldrick

Laboratory for Atmospheric and Space Physics, University of Colorado-Boulder, USA

Keywords: atmosphere, aerosols, clouds, meteorology, microphysics

Introduction

The global cloud cover at Venus is perhaps its most obvious attribute upon a first glance at the planet. Despite being analyzed by means of polarimetry, planetary emitted and reflected radiation, and in situ probes and balloons, many properties of the Venusian aerosols remain insufficiently characterized. Three modes of particles were observed by in situ probes (Knollenberg, Hunten, 1980), though internal inconsistencies in the data from various instruments have left the identity and particulars of these three modes uncertain (Toon, 1984). Analyses of the emitted near infrared radiation from Venus tend to attribute most of the observed variation to changes in the number concentrations of the third and largest mode of sulfuric acid droplets in the Venus clouds, despite that their existence and physical characteristics remain uncertain (Haus et al., 2014; Grinspoon et al., 1993). Remote observations of the upper hazes have long suggested that the primary constituent is one micron radius spherical particles of a solution of sulfuric acid and water (Hansen, Hovenier, 1974). But the frequent and persistent co-existence of an additional submicron mode of particles in the upper haze is difficult to explain if both modes are composed of sulfuric acid.

The parameter space of radiative effects of the aerosols tends to be large enough to be difficult to adequately sample by means of a purely radiative transfer analysis. Changes in the peak, width, and shape of the particle size distribution, as well as changes in the composition, and even possible phase changes all can contribute to changes in the radiative properties. Considering all of these parameters at sufficient resolution to confidently characterize the aerosol properties is almost prohibitive unless some limiting assumptions are made. By exploring the phase space of microphysical properties, we can potentially eliminate regions of the phase space of radiative effects.

Recent observations of the Venus atmosphere by the JAXA Akatsuki spacecraft have revealed a much more dynamically vibrant atmosphere than previously conceived. Contrasts exhibiting strong horizontal gradients are seen frequently in IR2 images; standing waves above surface topography are frequently seen; even mesoscale vortices can occasionally be seen. These changes suggest rapid regional variations in chemistry and microphysics that are observed as variations in radiance.

Here, I will present recent results of microphysical simulations that explore the effects of changes in microphysical properties on the structure of the Venus cloud system. In addition, I will present emitted radiances at near infrared wavelengths produced from these simulated cloud structures and compare them to those observed by Akatsuki and Venus Express. Such comparisons can be vastly improved by in situ measurements of aerosols and microphysically and radiatively significant species in the atmosphere of Venus, especially if they can be coordinated with high resolution imagery for global and regional context.

References

- Grinspoon, D.H. et al. (1993) Probing Venus's cloud structure with Galileo NIMS, *Planetary and Space Science*, 50(7), 515–542.
- Hansen, J.E., Hovenier, J.W. (1974) Interpretation of the polarization of Venus, *J. Atmospheric Sciences*, 31, 1137–1160.
- Haus, R., Kappel, D., Arnold, G. (2014) Atmospheric thermal structure and cloud features in the southern hemisphere of Venus as retrieved from VIRTIS/VEX radiation measurements, *Icarus*, 232, 232–248.
- Knollenberg, R., Hunten, D. (1980) The microphysics of the clouds of Venus: Results of the Pioneer Venus Particle Size Spectrometer Experiment, *J. Geophysical Research*, 85(A13), 8038–8058.
- Toon, O. B. et al. (1984) Large, solid particles in the clouds of Venus: Do they exist? *Icarus*, 57(2), 143–160.

RESULTS OF AKATSUKI

MULTISPECTRAL DAY AND NIGHT CLOUD MORPHOLOGY OF VENUS FROM AKATSUKI CAMERAS

S. S. Limaye¹, Akatsuki Team²

¹ University of Wisconsin, Madison, Wisconsin, USA

² Institute of Space and Astronautical Science — JAXA (ISAS/JAXA), Sagami, Japan

Abstract

The cloud cover of Venus has been of considerable interest since the contrasts in the cloud cover planet was drawn and imaged from Earth based telescopes more than a century ago in reflected blue-ultraviolet light (Danjon et al., 1913; Ross, 1928). The day and night cloud cover of Venus was mapped and imaged at thermal wavelengths (8–14 μm) many decades later (Diner et al., 1976; Murray et al., 1963) which revealed large scale global temperature variations in cloud top temperatures. But it was only in early 1980s that the near infrared windows in the carbon dioxide absorption spectrum revealed the cloud opacity differences through the detection of radiation emitted by the atmosphere below the clouds on the night side (Allen, Crawford, 1984). Since its insertion into orbit around Venus on 7 December 2015 (Nakamura et al., 2016), Akatsuki orbiter has observed Venus from ultraviolet to thermal infrared from its four cameras and provided details of the contrasts in the cloud cover on day and night side.

Introduction

Akatsuki has four imaging cameras — UVI (Yamazaki et al., 2018) with two narrow band filters in the ultraviolet, IR1 (Iwagami et al., 2011) imaging in three filters near 1 μm , IR2 (Satoh et al., 2016) observing in four filters and LIR (Fukuhara et al., 2011) between 8–12 μm . The images provide global views of both the day side and the night side cloud cover of Venus from a near equatorial vantage point in a 10.5 day orbit at 283, 365 nm, 0.900 μm , 2.02 and 8–12 μm on the day side and at 1.74, 2.26, 2.32 and 8–12 μm on the night side [Nakamura et al., 2016] (Fig. 1). The day and night side images provide information regarding different cloud levels and the 283 and 365 nm range reveals structures at the highest levels (~72 km in equatorial latitudes), while the 0.9 and 2.02 μm images probe somewhat lower (2–4 km). In contrast, the near infrared images reveal varying opacity of the upper clouds so that different amounts of radiation emitted by the lower atmosphere and the surface escapes to space. Thus, the morphologies on the day and night sides can be expected to reveal the dynamical processes that prevail in the cloud layer at a lower depth near 47 km. The calibration of the cameras and a brief overview of the images have been presented by the camera teams (Fukuhara et al., 2017; Iwagami et al., 2018; Peralta et al., 2017; Yamazaki et al., 2018). A more complete overview of the morphology has also been recently published (Limaye et al., 2018b).

Dayside Images

The day side cloud morphology in the ultraviolet collected thus far is consistent with many of the features seen from ground based images (Dollfus, 1975) previous missions (Limaye, 1984; Murray et al., 1974; Rossow et al., 1980; Titov et al., 2012), but some features have not yet been observed due to the difference in coverage and spatial resolution at different latitudes.

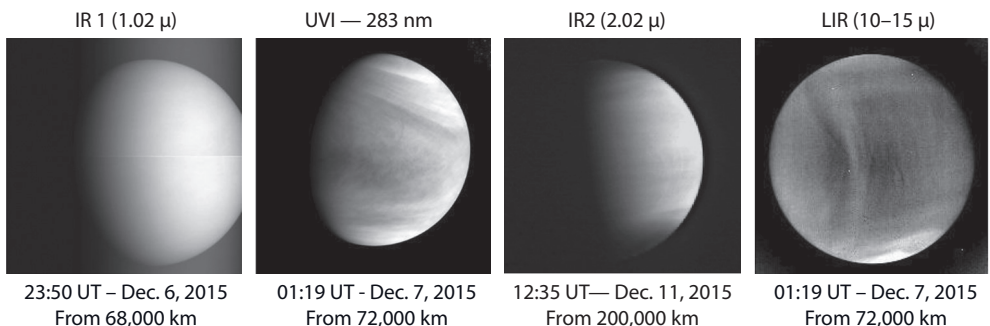
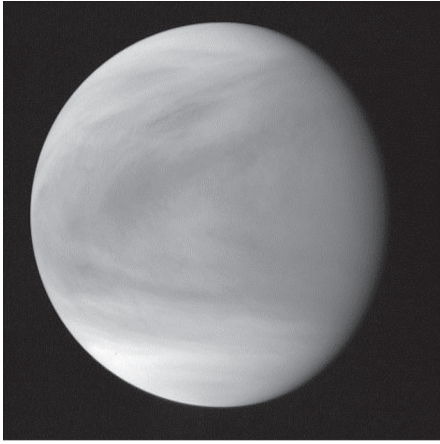
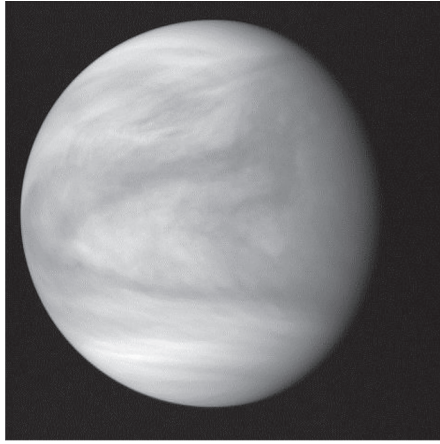


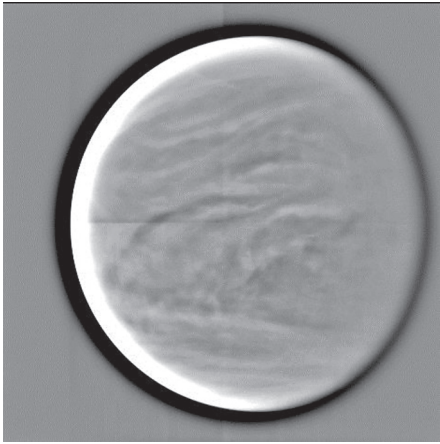
Figure 2: Akatsuki's first look at Venus after orbit insertion images from Akatsuki's cameras. IR2 camera needed to be cooled, and first images were obtained four days after orbit insertion



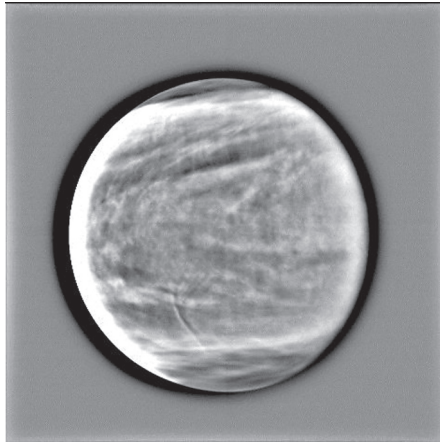
A. uvi_20160517_201339_283



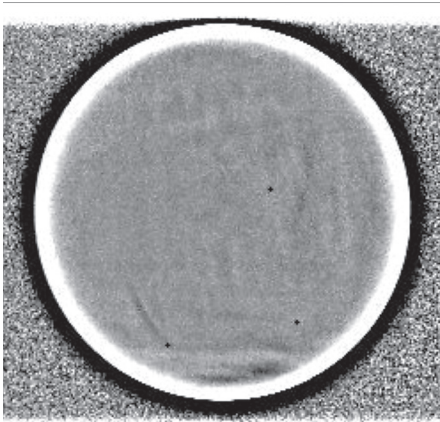
B. uvi_20160517_201715_365



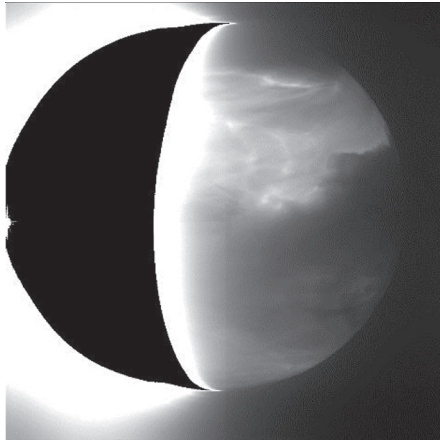
C. ir1_20160517_200207_09d



D. ir2_20160517_180823_202



E. lir_20160517_202051_pic



F. ir2_20160905_034120_232

Figure 1: A selection of images taken from Akatsuki cameras. The date, time and filter are noted below each image. Day side images (A through E) were taken on 17 May 2016 while F is a night side image (IR2 camera) taken on 5 September 2016. Images A and B are from UVI camera at 20:13:39 (283 nm) and 20:17:15 UT. Image C is taken from IR1 camera (0.9 μm) on the same day at 20:02:07 UT while image D is from IR2 camera (2.02 μm) acquired at 18:08:23 UT. Images C and D are shown in high-pass filtered versions to bring out detail. Image E is from the LIR (8–12 μm) camera taken at 20:20:51 UT. The night side image (F) is taken through 2.32 μm filter.

The two uv wavelengths (283 and 365 nm) at which Akatsuki observes Venus, show more similarity with the 270 nm polarimetry data (Limaye, 1984) in the appearance of the contrasts as compared to the two near infrared wavelengths (0.9 and 2.02 μm). The dark and bright markings at 283 nm (where SO_2 and other trace gases absorb) and 365 do not show consistent correlations, suggesting multiple processes or substances that determine the contrasts at the two wavelengths.

Figure 3 shows a three color composite created from 283 nm (Red), 365 nm (Green) and 0.9 μm (Blue) images to highlight the differences in the appearance at the three wavelengths. The polar regions appear darker due to absorption at 2.02 μm by the CO_2 above the lower polar cloud tops (Ignatiev et al., 2009). The differences along the bright limb (right edge of the planet) and the evening terminator (left side) are due to a combination of different amount of haze and perhaps even due to differences in the properties of the haze particles.

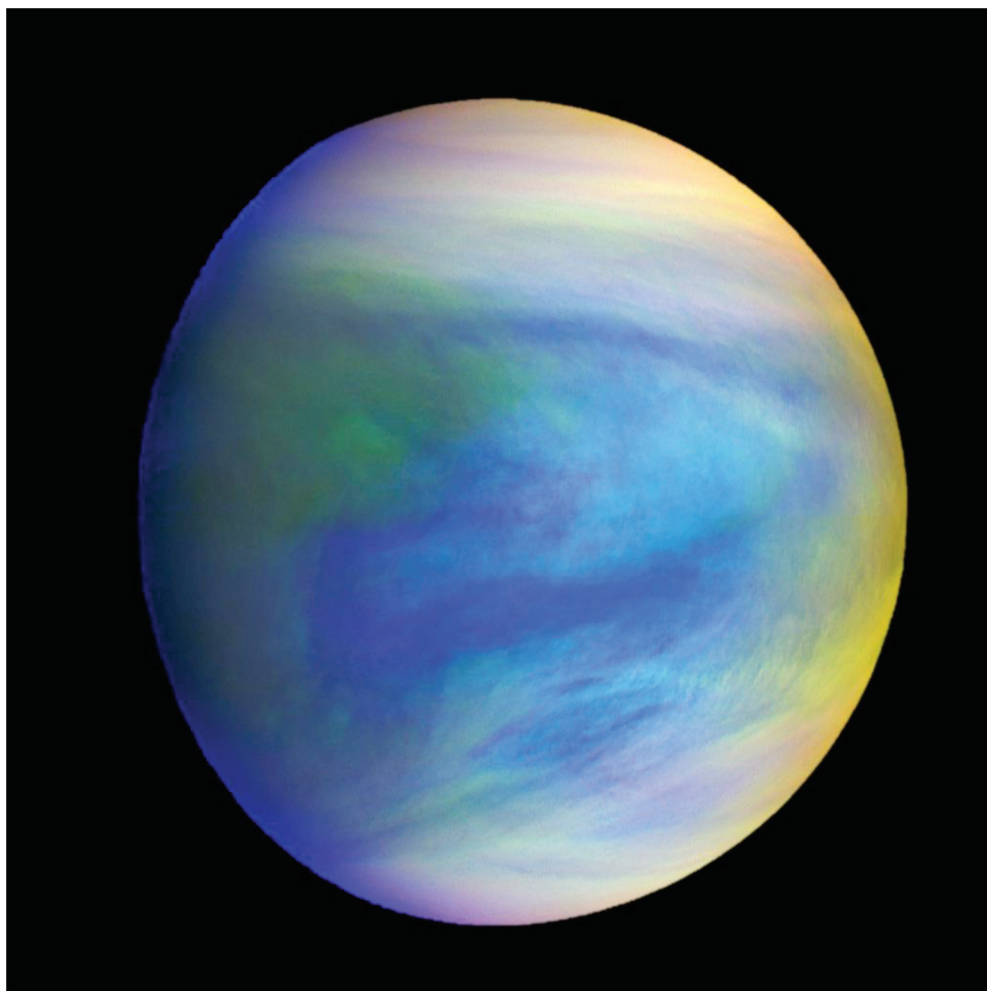


Figure 3: A color composite of 0.9 μm (IR2 camera) image shown in red, 365 nm (UVI camera) image shown in green and 0.9 μm (IR1) shown in blue taken at approximately the same time on 17 May 2016. Northern hemisphere is at the top and southern hemisphere is at the bottom with the evening terminator on the left. The color variations indicate to some degree the spatial variations in the cloud particle properties over the planet

Nightside Images in Near infrared

The nightside cloud cover was also seen briefly by the Galileo spacecraft as it flew past Venus in 1990 on its way to Jupiter, and Venus Express orbiter's VIRTIS instrument also primarily monitored the southern hemisphere (Piccioni, 2007). Akatsuki is able to see both hemispheres and shows some surprising features.

Night side features include small vortices, ribbon like structures slightly inclined toward latitude circles, and cirrus like streaky features which collectively suggest a wide range of atmospheric circulation patterns or regimes on small to global scales in the near infrared images. The longwave (thermal) infrared images have revealed the existence of standing quasi-linear or bow shaped features extending over 10,000 km from north to south that are apparently gravity waves tied to local topography, which dissipate after a few days and are generally only found at certain local times. The signature of these waves have also been detected in the 283 nm images (Fukuhara et al., 2017).

A selection of images from the four cameras is shown in Fig. 2 in which images A-E represent day-side images, while image F is a night side image from the IR2 camera. The near infrared features seen at 1.74, 2.26 and 2.32 μm tend to be somewhat similar, but there clearly are differences due to atmospheric properties.

Summary

The global cloud cover of Venus not only shrouds the surface details, its vertical extent also makes it challenging to learn about the variations over latitude and altitude over all local times difficult. On the dayside the spatial contrasts indicate presence of absorbing substances in addition to the sulfur dioxide gas. And these substance appear to absorb incident sunlight weakly from ultraviolet to long as 0.9 and 2.02 μm (where CO_2 also absorbs) as suggested by the Akatsuki images which is consistent with the variation of albedo with wavelength (Kuiper, 1969). Limaye et al. (2018a) suggest the possibility that microorganisms in the clouds of Venus may also be able to contribute to absorption of sunlight and observed contrasts in the cloud cover of Venus.

Acknowledgements

This research was supported by NASA Grant NNXAC1679G.

References

- Allen, D., Crawford J.W. (1984) Cloud structure on the dark side of Venus, *Nature*, 307, doi: 10.1038/307222a0.
- Danjon, A. et al. (1913) Vénus, *Observatoire de la Société Astronomique de France Observations et Travaux*, 2, 16–28.
- Diner, D.J. et al. (1976) Infrared imaging of Venus–8–14 micrometers, *Icarus*, 27, 191–195.
- Dollfus, A. (1975) Long-Term Variations of the Clouds, *NASA Special Publication*, 382, 140.
- Fukuhara, T. et al. (2011) LIR: Longwave Infrared Camera onboard the Venus orbiter Akatsuki, *Earth, Planets and Space*, 63(9), 1009–1018, doi: 10.5047/eps.2011.06.019.
- Fukuhara, T. et al. (2017) Large stationary gravity wave in the atmosphere of Venus, *Nature Geoscience*, 10(2), 85–88, doi: 10.1038/Ngeo2873.
- Ignatiev, N.I. et al. (2009) Altimetry of the Venus cloud tops from the Venus express observations, *J Geophys Res*, 114, doi: 10.1029/2008je003320.
- Iwagami, N. et al. (2011) Science requirements and description of the 1 μm camera onboard the Akatsuki Venus Orbiter, *Earth Planets Space*, 63(6), 487–492, doi: 10.5047/eps.2011.03.007.
- Iwagami, N. et al. (2018) Initial products of Akatsuki 1- μm camera, *Earth, Planets and Space*, 70(1), 6, doi: 10.1186/s40623-017-0773-5.
- Kuiper, G.P. (1969) Identification of the Venus cloud layers, *Communications of the Lunar and Planetary Laboratory*, 6, 229–245.
- Limaye, S.S. (1984) Morphology and movements of polarization features on Venus as seen in the Pioneer Orbiter Cloud Photopolarimeter data, *Icarus*, 57, 362–385.
- Limaye, S.S. et al. (2018a) Venus' Spectral Signatures and the Potential for Life in the Clouds, *Astrobiology*, 10(10), null, doi: 10.1089/ast.2017.1783.
- Limaye, S.S. et al. (2018b) Venus looks different from day to night across wavelengths: morphology from Akatsuki multispectral images, *Earth, Planets and Space*, 70(1), 24, doi: 10.1186/s40623-018-0789-5.
- Murray, B.C. et al. (1963) Infrared photometric mapping of Venus through the 8- to 14-micron atmospheric window, *J. Geophysical Research*, 68(16), 4813–4818, doi: 10.1029/JZ068i016p04813.
- Murray, B.C. et al. (1974) Venus: Atmospheric Motion and Structure from Mariner 10 Pictures, *Science*, 183, 1307–1315.
- Nakamura, M. et al. (2016) AKATSUKI returns to Venus, *Earth, Planets and Space*, 68(1), 75, doi: 10.1186/s40623-016-0457-6.

- Peralta, J. et al. (2017) AKATSUKI-IR2 reveals unexpected opacity disruption affecting Venus's lower clouds every 9 days, *European Planetary Science Congress*, 11.
- Piccioni, G. (2007) South-polar features on Venus similar to those near the north pole, *Nature*, 450, 637–640.
- Ross, F.E. (1928) Photographs of Venus, *The Astrophysical Journal*, 68, 57.
- Rossow, W. B. et al. (1980) Cloud morphology and motions from Pioneer Venus images, *J. Geophysical Research*, 85, 8107–8128.
- Satoh, T. et al. (2016) Development and in-flight calibration of IR2: 2- μm camera onboard Japan's Venus orbiter, Akatsuki, *Earth, Planets and Space*, 68(1), 74, doi: 10.1186/s40623-016-0451-z.
- Titov, D.V. et al. (2012) Morphology of the cloud tops as observed by the Venus Express Monitoring Camera, *Icarus*, 217, 682–701.
- Yamazaki, A. et al. (2018) Ultraviolet imager on Venus orbiter Akatsuki and its initial results. *Earth, Planets and Space*, 70(1), 23, doi: 10.1186/s40623-017-0772-6.

VENUS, SEEN FROM THE UV IMAGER ONBOARD AKATSUKI

Y. J. Lee¹, T. Horinouchi², A. Yamazaki³, T. Imamura¹, M. Yamada⁴, S. Watanabe⁵, T. M. Sato², K. Ogohara⁶, G. L. Hashimoto⁷, S. Murakami², T. Kouyama⁸, M. Takagi⁹, K. Nakajima¹⁰, J. Peralta², K. L. Jessup¹¹, S. Perez-Hoyos¹², D. Titov¹³, S. Limaye¹⁴

¹ University of Tokyo, Chiba, Japan

² Hokkaido University, Sapporo, Japan

³ Institute of Space and Astronautical Science — JAXA (ISAS/JAXA), Sagami-hara, Japan

⁴ Planetary Exploration Research Center (PERC), Narashino, Japan

⁵ Hokkaido Information University, Ebetsu, Japan

⁶ University of Shiga Prefecture, Hikone, Japan

⁷ Okayama University, Kita, Japan

⁸ National Institute of Advanced Industrial Science and Technology (AIST), Tokyo, Japan

⁹ Kyoto Sangyo Univ., Kyoto, Japan

¹⁰ Kyushu University, Fukuoka, Japan

¹¹ Southwest Research Institute (SwRI), USA

¹² University of the Basque Country / Euskal Herriko University (UPV/EHU), Bilbao, Spain

¹³ European Space Research and Technology Centre — ESA (ESTEC/ESA), Noordwijk, Netherlands

¹⁴ University of Wisconsin, Madison, USA

Abstract

UV Imager (UVI) onboard Akatsuki has been observing Venus since Dec. 2015. Two channels of UVI at 283 and 365 nm cover a broad phase angle range of Venus from 0 to 140°. We introduce results of three topics. (1) We used phase angle dependence of scattered light by cloud aerosols to understand common microphysical properties of cloud top level aerosols at the two channels. The best fit suggests that r_{eff} (effective radius) = 1.26 μm and v_{eff} (effective variance) = 0.076 for mode 2 aerosol. (2) We retrieved wind vectors at the two channels. Retrieved wind fields show similar horizontal distributions, but a few m/s faster at 283 nm than those at 365 nm. This implies a possible vertical dislocation of corresponding altitudes between the two channels, and we suspect higher altitudes at 283 nm. (3) We investigated long-term 365-nm albedo variations using four independence space-based instruments; Venus Monitoring Camera (VMC) onboard Venus Express (2006–2014), Mercury Atmospheric and Surface Composition Spectrometer (MASCS)/Mercury Surface, Space ENvironment, GEochemistry, and Ranging (MESSENGER) (2007), Hubble Space Telescope (HST) (2011), and UVI (2016–2017). Our preliminary results show that there is a clear decreasing trend from 2006 to 2011, low albedo in 2011–2014, and recovery of albedo in 2016–2017 to the level in 2008.

Introduction

UV imaging at 365 nm has been used for decades on Venus studies, owing to clear morphology at this wavelength. The dark and bright contrasts are made by an unknown UV absorber which has broad absorption from UV to visible range, while sulfuric acid cloud aerosols are scattering solar radiance effectively (Titov et al., 2012). Akatsuki's UV imager (UVI) continues this historic observation at 365 nm, targeting the unknown UV absorber. UVI has another channel at 283 nm where SO₂ band is located (Yamazaki et al., 2018). UVI's pair images show that SO₂ and the unknown UV absorber have a similarity in general morphology with dark low latitudes and bright high latitudes, as noticed in previous missions. This suggests similar transportation process of SO₂ and the unknown UV absorber. However, detail features are somehow different between 283 and 365 nm. This implies different maintenance process, or different effective altitudes between SO₂ gas and the unknown UV absorber which may allow an intrusion of haze in between. Here we introduce three recent and ongoing studies; (1) understanding cloud scattering properties using phase angle dependence of scattered solar radiance at the two channels of UVI (Lee et al., 2017), (2) investigating the strong zonal winds, so-called 'super-rotation' near the cloud top level (~70 km) at the two channels (Horinouchi et al., 2018), and (3) preliminary results of long-term UV albedo variations at 365 nm from 2006 to 2017.

Data

Study (1) used UVI data version 0.1.2, which has not completed absolute calibration at the time of analysis. Therefore, we used relative albedo compared to that at 30° phase angle. Study (2) used UVI data acquired between Dec. 2015 and Mar. 2017. This is insensitive to the absolute calibration. Study (3) used later version of UVI data with an absolute calibration correction factor using stellar data (version 20170808) (Yamazaki et al., 2018). For the study (1), we used SO₂ UV absorption cross section, refractive indices of sulfuric acid aerosols, and atmospheric structures in our radiative transfer model calculations. In the study (3) we used UV images taken by Venus Monitoring Camera (VMC) onboard Venus Express (Markiewicz et al., 2007), and UV spectra acquired by STIS/HST (Jessup et al., 2015, 2017) and MASCS/MESSENGER (Perez-Hoyos et al., 2017) to compare the albedo trend along time.

Methods

Photometric correction: We calculated UV albedo using a photometric correction for studies (1) and (3). The Lambert and Lommel-Seeliger law (LLS) was selected, and a coefficient of LLS was retrieved from the UVI's data as a function of phase angle.

Study (1): We aligned global mean albedo of each image along phase angle. We found a clear glory features at small phase angles less than 10°, and a decreasing albedo trend as phase angle increases up to around 50°. Using a radiative transfer model (LibRadtran v2.0, DISORT), we fit the observed phase angle dependence using various atmospheric conditions and microphysical properties of aerosols. The cloud top structure is assumed to have 75 % H₂SO₄ aerosols with an exponential vertical extinction structure above 60 km altitude (constant below). An assumed SO₂ abundance vertical profile was multiplied by a certain factor at all altitudes. For the unknown UV absorber, we increased imaginary index of cloud aerosols, assuming that the unknown UV absorber is combined well with the cloud aerosols, and we changed also the vertical range of the unknown UV absorber and imaginary index values as additional free parameters. Using the 70 km cloud top level and the 4 km cloud aerosols scale height, we controlled these free parameters to fit the observations; mode 1 and 2 aerosols' mean radius (r_0) and variance (σ), ratio of mode 1 and mode 2 aerosols, imaginary index of cloud aerosols, altitude range of the unknown UV absorber, a factor of SO₂ abundance.

Study (2): Horinouchi et al. used a sophisticated automated cloud-tracking method. The details are well described in (Ikegawa, Horinouchi, 2016; Horinouchi et al., 2017). Careful limb fitting had been made assuring navigation. In this study, horizontal and meridional wind speeds are retrieved over all daytime (6–16 local solar time), latitudes from 50°S to 50°N, and longitudes from 0 to 360°.

Study (3): Low latitudinal albedo (0–30°S) and high latitudinal albedo (50–70°S) are compared separately through 2006–2017. We took the stellar calibration correction factors for both of UVI and VMC, but VMC's albedo show systematically higher values than that of MASCS in 2007 and HST in 2011. Taking into account these ratios of difference, we could correct the albedo measured by VMC to the albedo levels measured by MASCS and HST, regardless on different phase angles.

Results and Discussions

Study (1): Parameters related to absorption, such as the imaginary index of mode 2 and the SO₂ factor, alter phase angle dependence effectively. However the peak location along phase angle at less than 10° (glory feature) is a unique feature mainly controlled by microphysical properties of aerosols. Fig. 1 shows the best fit, requiring mode 2 aerosol's to have r_0 (geometric mean radius) = 1.05 μm and σ (geometric mean standard deviation) = 1.31 in log-normal size distributions, which equals to r_{eff} (effective radius) = 1.26 μm and v_{eff} (effective variance) = 0.076. Exact determination of SO₂ abundance at 283 nm turns out to be difficult, as we can find various combinations to explain the observed relative albedo; at least five cases were found, ranging SO₂ abundance above the cloud top level from 80 to 400 ppbv. We also examined the vertical range of the unknown UV absorber defined with bottom and upper boundary altitudes. Best fit requires the bottom absorption layer should be below the cloud top level.

Study (2): The comparison of the two channels shows similar wind speeds ranging from 80 to 110 m/s, but winds at 283 nm can be a few m/s faster than those at 365 nm (Fig. 2). This difference may be caused by different sensing altitudes at the two channels, which implies a vertical wind shear. Horinouchi et al. (2018) suspect a higher altitude at 283 nm than that at 365 nm because SO₂ gas can create contrasts above the clouds while the unknown UV absorber should be located below the cloud top level according to Study (1).

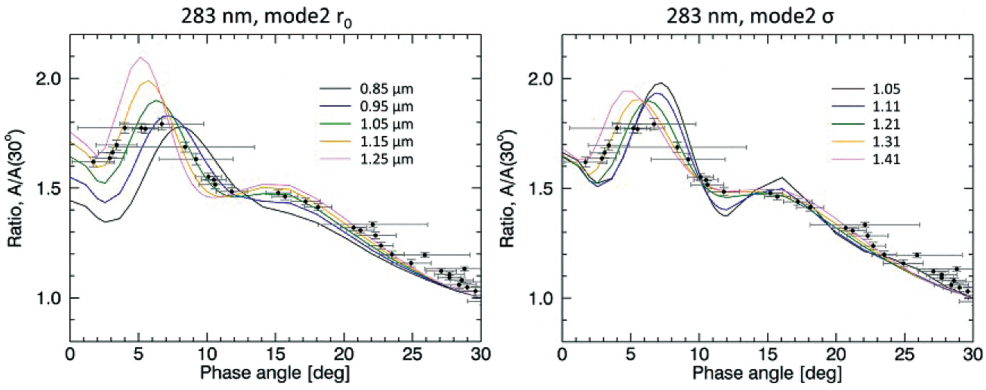


Figure 1: Observed relative global mean albedos (circles) and simulated phase curves (color). (Left) Fitting process using various r_0 for the mode 2 cloud aerosols. (Right) Same, but using various σ

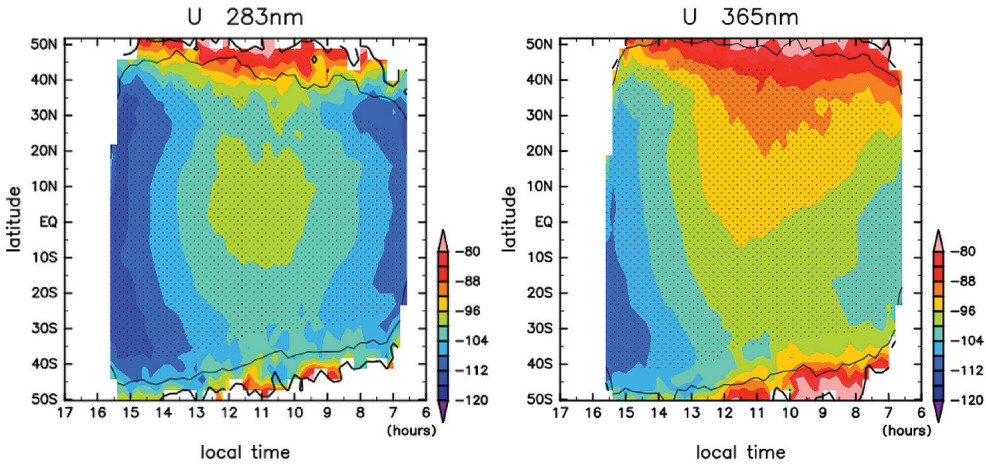


Figure 2: Mean zonal wind speeds obtained as a function of local time and latitude (Dec. 2015 – Mar. 2017). (Left) Winds at 283 nm. (Right) that at 365 nm.

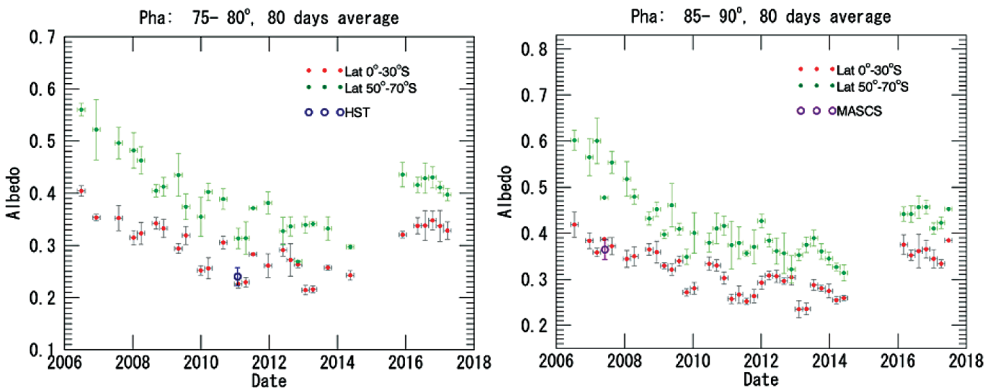


Figure 3: Long-term variations of observed UV albedo at 365 nm. VMC covers from 2006 to 2014, and UVI from Dec. 2015 to May 2017. Low and high latitudinal albedo are shown in different colors as shown in the legend. (Left) Trends at the phase angle 75–80°, and HST (open circle). (Right) That at the phase angle 85–90°, and MASCS (open circle). We show 80-days mean, which is sufficiently long to cover short-term variations

Fig. 2 also shows clear local time dependence, slow winds from morning to noon time. Horinouchi et al. find a clear hemispheric asymmetry in the latter half of data, and this is more significant at 365 than 283 nm. In addition, longitude dependence is different from (Bertaux et al., 2016), requiring further monitoring to understand the influence of surface topography relative to local time.

Study (3): Previous studies reported VMC's decreasing albedo trend from 2006 to 2011, but it was hard to exclude sensor degradation possibility (Lee et al., 2015). However, MASCS and HST data assure that the decreasing trend of UV albedo is likely (Fig. 3). The similar trends appear both at low and high latitudes, but more significant at high latitudes. The variation may be connected to the mesospheric SO₂ abundance which increased in 2007 and 2016 (Marcq et al., 2012, Encrenaz et al., 2016). This observed long-term trend of the 365-nm albedo is very important as this implies variations of solar heating rate which is caused by significant role of the unknown UV absorber in solar heating rate near the cloud top level.

Conclusions

UVI's glory analysis is powerful to understand microphysical properties of cloud top level aerosols, continuing VMC's observations. We find that the phase angle dependence of albedo holds a clue to determine the SO₂ abundance and the unknown UV absorber's vertical locations. Wind speeds are slightly different at the two-channels, implying a potential to understand vertical shear near the cloud top level. The long-term 365 nm albedo variation seems to be a real, and the range of variation is certainly surprising. UVI is the only instrument that can monitor the variation of UV albedo over month to yearlong timescales in the coming years.

References

- Bertaux, J.-L., Khatuntsev, I.V., Hauchecorne, A. et al. (2016) Influence of Venus topography on the zonal wind and UV albedo at cloud top level: The role of stationary gravity waves, *Journal of Geophysical Research: Planets*, 121, 1087–1101. doi: 10.1002/2015JE004958.
- Encrenaz, T., Greathouse, T.K., Roe, H. et al. (2016) HDO and SO₂ thermal mapping on Venus: evidence for strong SO₂ variability, *Astronomy and Astrophysics*, 585, A74.
- Horinouchi, T., Murakami, S., Kouyama, T. et al. (2017) Image velocimetry for clouds with relaxation labeling based on deformation consistency, *Measurement Science and Technology*, 28(8).
- Horinouchi, T., Kouyama, T., Lee, Y.J. et al. (2018) Mean winds at the cloud top of Venus obtained from two-wavelength UV imaging by Akatsuki, *Earth Planets Space*, 70(10), <https://doi.org/10.1186/s40623-017-0775-3>
- Ikegawa, S., Horinouchi, T. (2016) Improved automatic estimation of winds at the cloud top of Venus using superposition of cross-correlation surfaces, *Icarus*, 271, 98–119.
- Jessup, K.L. et al. (2015) Variations of sulphur dioxide at the cloud top of Venus's dynamic atmosphere, *Icarus*, 258, 309–336.
- Jessup, K.L. et al. (2017) 15th Meeting of the Venus Exploration and Analysis Group (VEXAG), 14–16 Nov 2017, Laurel, Maryland. LPI Contribution No. 2061, p. 8040.
- Lee, Y.J., Imamura, T., Schröder, S.E. et al. (2015) Long-term variations of the UV contrast on Venus observed by the Venus Monitoring Camera on board Venus Express, *Icarus*, 253, 1–15.
- Lee, Y.J., Yamazaki, A., Imamura, T. et al. (2017) Scattering properties of the Venesian clouds observed by UV imager on board Akatsuki, *Astron. J.*, 154(2), 44, <https://doi.org/10.3847/1538-3881/aa78a5>.
- Marcq, E., Bertaux, J.-L., Montmessin, F., Belyaev, D. (2013) Variations of sulphur dioxide at the cloud top of Venus's dynamic atmosphere, *Nature Geosci.*, 6, 25–28.
- Perez-Hoyos, S., Sanchez-Lavega, A., Garcia-Munoz, A., Irwin, P.G.J., Peralta, J., Holsclaw, G., McClintock, W.M., Sanz-Requena, J.F. (2017) Venus upper clouds and the UV-absorber from MESSENGER/MASCS observations, *JGR (Planets)*, 123.
- Titov, D.V. Markiewicz, W.J., Ignatiev, N.I. et al. (2012) Morphology of the cloud tops as observed by the Venus Express Monitoring Camera, *Icarus*, 217, 682–701.
- Yamazaki, A., Yamada, M., Lee Y.J. et al. (2018) Ultraviolet imager on Venus orbiter Akatsuki and its initial results, *Earth, Planets and Space*, 70(23).

NEW VIEWS OF VENUS AS OBTAINED FROM AKATSUKI

T. Satoh¹, T. Imamura², M. Nakamura¹, Akatsuki Team

¹ Institute of Space and Astronautical Science Institute of Space and Astronautical Science Agency (ISAS/JAXA), Yoshinodai, Japan, satoh@stp.isas.jaxa.jp

² Graduate School of Frontier Sciences, The University of Tokyo, Japan, t_imamura@edu.k.u-tokyo.ac.jp

Keywords: Akatsuki, atmosphere, surface, topography, multi-wavelength imaging, radio occultation

Akatsuki in Venus orbit

Akatsuki, also known as the Venus Climate Orbiter (VCO) of Japan, was launched on 21 May 2010 from Tanegashima Space Center, Kagoshima, Japan. Although the first challenge of inserting Spacecraft in Venus orbit (VOI) on 7 December 2010 failed, the second attempt (VOI-R1) on 7 December 2015 turned out to be successful (Nakamura et al., 2016). Because the main engine (500°N of thrust) was no longer operational (broken at the time of VOI), the VOI-R1 was performed with a set of 4 attitude-control engines (23°N each). In contrast to the polar orbits of Pioneer Venus or Venus Express, Akatsuki is in a near-equatorial plane and revolves westward, the same direction as the super-rotating atmosphere of Venus. The original plan was to have a orbital period of 30 hours so that the spacecraft is in pseudo-synchronization with the super rotation. However, the orbit after VOI-R1 is extremely elongated with the orbital period slightly shorter than 11 days, and the apoapsis altitude of ~0.37 million km. This orbit no longer allows pseudo-synchronization with the super rotation. Instead, Akatsuki can continuously monitor the same local time for several days and can cover full rotation of atmosphere twice in one orbital period.

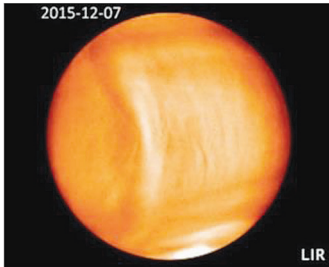


Figure 1: A huge bow-shaped feature in cloud-top temperature map as obtained with LIR (7 Dec 2015)

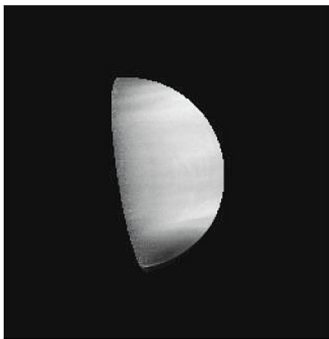


Figure 2: In this limb-darkening corrected IR2 image (2.02 um), the bow-shaped feature is hinted (11 Dec 2015)

On-board instruments

This meteorological-satellite-like concept makes Akatsuki the most unique planetary orbiter in the history (Nakamura et al., 2011). To sense the various levels of the atmosphere, to draw 3-dimensional picture of dynamics, Akatsuki is equipped with 5 on-board cameras, UVI (283 and 365 nm wavelength), IR1 (0.90, 0.97, and 1.01 um), IR2 (1.65, 1.735, 2.02, 2.26, and 2.32 um), LIR (8–12 um), and LAC (a special high-speed sensor at visible wavelengths), as well as the ultra-stable oscillator (USO) for radio-occultation measurements. Three wavelengths of IR1 as well as 3 wavelengths of IR2 (1.735, 2.26, and 2.32 um) work on Venus night-side disk by utilizing the transparency windows of CO₂ atmosphere. LIR works on both day and night as it images thermal emission from the cloud-top level. Two wavelengths of UVI, IR1 0.90 um, and IR2 2.02 um are for the day-side observations. LAC operates only when the spacecraft is in umbra to protect the detector of ultra-sensitivity.

Diurnal variation of the atmosphere revealed

The most striking discovery by Akatsuki is a huge “bow-shaped” feature as imaged with LIR right after VOI-R1. Not only its appearance (elongated in north-south direction over 10,000 km), but also its motion was so unusual. In the observation from 7th to 11th December 2015, the feature actually did not move. More precisely, it moves at a speed of the solid planetary body. The feature seems to be nailed down on Aphrodite Terra (Fukuhara et al., 2017). Surprisingly, this phenomenon repeats with a period of one Venus day: when Aphrodite Terra comes to the late afternoon sector, the bow-shaped feature appears and

develops. The feature decays when Aphrodite passes the evening terminator and disappears in the night. Such local-time modulation of atmospheric activity associated to the ground-surface topography is revealed for the first time. This feature is observed as the temperature variation by LIR, as the temporal variation of SO₂ absorption by UVI (283 nm), and as the cloud-top variation by IR2 (2.02 μm) (Satoh et al., 2018). Physical interpretation of such multi-wavelength data is in progress.

Future of Akatsuki

Two cameras, IR1 and IR2, are currently not operated as their common controller (IR-AE) has a problem. Otherwise, spacecraft itself and on-board instruments are in good health. The remaining fuel is not huge but we expect to save it to enable science observations to 2018 and beyond (hopefully to 2020 or longer).

References

- Nakamura, M. et al. (2016) AKATSUKI returns to Venus, *Earth, Planets and Space*, 68, 75, doi: 10.1186/s40623-016-0457-6.
- Nakamura, M. et al. (2011) Overview of Venus orbiter, Akatsuki, *Earth Planets Space*, 63, 443–457, doi: 10.5047/eps.2011.02.009, 2011.
- Fukuhara, T. et al. (2017) Large stationary gravity wave in the atmosphere of Venus, *Nature Geoscience*, 10, 85–88, doi: 10.1038/ngeo2873.
- Satoh, T. et al. (2018) Instrument characteristics of Akatsuki/IR2 in Venus orbit: the first year, *Earth, Planets and Space* (submitted).

AERIAL PLATFORMS

EXPLORING BALLOON TRAJECTORIES IN A MODELED VENUS ATMOSPHERE

S. Lebonnois

Dynamic Meteorology Laboratory Institut Pierre Simon Laplace (LMD/IPSL),
Sorbonne Université, CNRS, Paris, France

Abstract

Using a simulation of Venus atmospheric circulation obtained with the IPSL Venus GCM, it is possible to investigate the trajectory that an aerial platform would follow when drifting in the wind. The methodology is tested on the VeGa balloons that flew in Venus cloud layer in 1985, then the possible trajectories of such balloons are explored depending on pressure level, initial latitude and local time

Introduction

Future missions to Venus are now under preparation. One of the possible carrier that is considered to explore Venus atmosphere is an aerial platform, such as a superpressurized balloon, drifting along with the atmospheric circulation at altitudes within the cloud layer. To optimize the science return of such a mission, exploring the possible trajectories of a floating platform in the Venus atmosphere is needed. In this work, a simulation performed by the IPSL Venus GCM is used as a background atmosphere in which balloons are followed as quasi-lagrangian tracers, in the region of altitudes between $63 \text{ km}/7.2 \cdot 10^3 \text{ Pa}$ and $52 \text{ km}/5.3 \cdot 10^4 \text{ Pa}$. The density of a balloon is taken as constant, and the balloon follows the same isopycnic surface (constant density) during its flight.

It must be kept in mind that the simulation is just a model, that it does not fit perfectly all observations and therefore may not predict exactly the right circulation. Also, one given Venus day is used from the simulation. The variability of the simulated wind field from one Venus day to the other would certainly change the results depending on the chosen initial time.

The IPSL Venus GCM

This GCM is presented in detail in (Lebonnois et al., 2010, 2016). The simulation used here were computed with its most recent configuration, including latitudinal variation of the cloud structure (Garate-Lopez, Lebonnois, in revision). The circulation predicted by this model compares quite well with the observed temperature and wind features, in particular in the altitude region between 40 and 80 km, where aerial platform missions are most likely to fly. Though observations are always limited to accessible regions, depending on the observation technique and atmospheric variable, we can use the GCM simulations as reasonable extrapolations of the needed atmospheric variables everywhere.

The simulation is stored as 1000 timesteps per Venus days (i.e. every 2.8 Earth hours). Balloon motion is computed by interpolation of the wind field from the GCM grid to the position of the balloon, with 50 iterations between each simulation timestep. The initial point of the GCM simulation corresponds to midnight at the longitude 0.

VeGa balloons

Before exploring the distributions of possible trajectories, the methodology is tested in the case of the two VeGa balloons that flew in Venus atmosphere in 1985. The observed characteristics of the VeGa balloons trajectories are listed in Table 1. In the VeGa balloons data analysis (Andreev et al., 1986; Sagdeev et al., 1986), the wind speed is computed based on the Doppler shift, with the assumption that latitude is not changing, i.e. the meridional wind speed v is 0. However, this work was revised with VLBI data by (Crisp et al., 1990). They could determine the variations of latitude with time for both balloons. According to this analysis, VeGa-1 maintained its latitude during 30 h, then drifted northward with meridional wind speed increasing up to $+3 \text{ m/s}$ (for a total deviation of $+0.3^\circ$). For VeGa-2, a steady meridional wind field around 2.5 m/s made the balloon drift northward significantly ($+1.5^\circ$).

The trajectories these balloons would have in the simulation are investigated. However, since in the model, the relation between altitude, pressure and temperature is not as in the observations, three different initial pressure levels are tested (Table 1). The modeled zonal wind speed is lower

than observed, which also slightly amplifies the effect of meridional winds. The zonal wind speed and altitude are more consistent with observations for tests C, though the pressure is smaller compared to the VeGa measurements.

Table 1: Characteristics of the VeGa balloons trajectories and measured atmospheric variables (from Andreev et al., 1986; Sagdeev et al., 1986), compared to the test balloons in the GCM simulation

| | Initial latitude (grad) | Initial longitude (grad) | Flight duration (Eh) | Time of terminator crossing, LT = 6 (Eh) | Av. zonal wind speed (m/s) | Pressure (Pa) | T (K) | Altitude (km) | Initial LT (Vh) | Final LT (Vh) |
|---------|-------------------------|--------------------------|----------------------|--|----------------------------|-----------------------|---------|---------------|-----------------|---------------|
| VeGa-1 | +8.1 | 176.9 | 46 | 34 | 69±1 | (5-6)·10 ⁴ | 310-315 | 54-56 | 0.36 | 8.0 |
| VeGa-2 | -7.5 | 179.8 | 46 | 32 | 66±1 | (5-6)·10 ⁴ | 300-315 | 54-56 | 1.00 | 8.3 |
| Test A1 | +8.1 | 176.9 | - | - | 49.8 | 5.0·10 ⁴ | 294 | 52.6 | 0.36 | - |
| Test A2 | -7.5 | 179.8 | - | - | 50.1 | 5.0·10 ⁴ | 294 | 52.6 | 1.00 | - |
| Test B1 | +8.1 | 176.9 | - | - | 51.0 | 3.8·10 ⁴ | 277 | 54.3 | 0.36 | - |
| Test B2 | -7.5 | 179.8 | - | - | 54.4 | 3.8·10 ⁴ | 277 | 54.3 | 1.00 | - |
| Test C1 | +8.1 | 176.9 | - | - | 57.3 | 3.0·10 ⁴ | 270 | 55.7 | 0.36 | - |
| Test C2 | -7.5 | 179.8 | - | - | 65.6 | 3.0·10 ⁴ | 270 | 55.7 | 1.00 | - |

The variations of latitude with time are shown in Fig. 1 for the different test balloons. To estimate the day-to-day variability, 4 different Venus days were used from the simulation. During the 46 Eh of the flight, the simulated latitudes vary by a few degrees (up to ~6°), with a significant day-to-day variability. Deviations are compatible with VLBI analysis (Crisp et al., 1990) for both balloons. However, for the VeGa-2 case, northward deviations appear to be rare in the simulations.

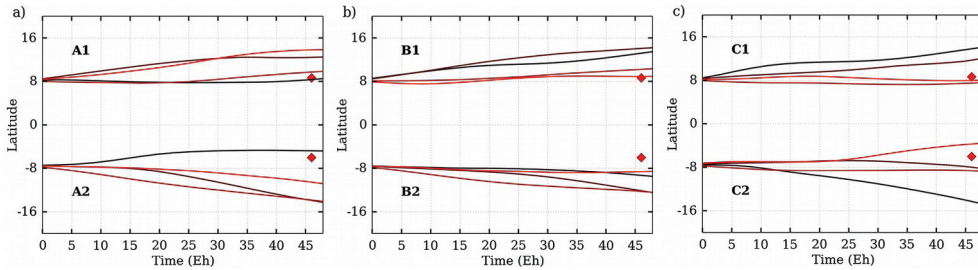


Figure 1: Variations of latitude with time of the test balloons similar to the VeGa balloons, during the 46 Eh of the VeGa balloon flights. Altitudes are: (a) 52.6 km/5.0·10⁴ Pa; (b) 54.3 km/3.8·10⁴ Pa; (c) 55.7 km/3.0·10⁴ Pa. In each panel, the different trajectories are obtained using different Venus days from the simulation. Observed deviations are plotted with red diamonds (Crisp et al., 1990)

Analysis of balloon trajectories

Protocol

To induce some variability, trajectories are sampled in a latitude range by launching balloons at 7 different latitudes within the considered range, and 14 different longitudes, corresponding to different local times, for a total of 98 balloons.

Table 2: Initial pressures used for the test balloons, and the corresponding atmospheric variables in the GCM vertical structure

| | | | | | | | |
|-------------------------------|---------------------|---------------------|---------------------|---------------------|---------------------|---------------------|---------------------|
| Pressure (Pa) | 7.2·10 ³ | 1.0·10 ⁴ | 1.4·10 ⁴ | 1.9·10 ⁴ | 2.8·10 ⁴ | 3.9·10 ⁴ | 5.3·10 ⁴ |
| Altitude (km) | 63.5 | 61.5 | 60.0 | 58.0 | 56.0 | 54.0 | 52.0 |
| Temperature (K) | 247.0 | 253.0 | 256.0 | 260.0 | 267.0 | 279.0 | 298.0 |
| Density (kg·m ⁻³) | 1.5 | 2.0 | 2.9 | 3.8 | 5.5 | 7.3 | 9.3 |

Balloons are launched at different pressure levels, corresponding to different altitudes, taking into account that the GCM uses pressure coordinates (above 1.10⁵ Pa) and that since the temperature

structure is not exactly equal to the observed temperatures, the relation between altitude and pressure is not as in e.g. the VIRA model. Levels used here are listed in Table 2. The positions of the balloons are followed during one Venus day, i.e., 117 Earth days.

Equatorial latitudes

The latitudinal excursions of the different balloons launched in the equatorial region between 10°S and 10°N after one Venus day is shown as a function of initial local time in Fig. 2.

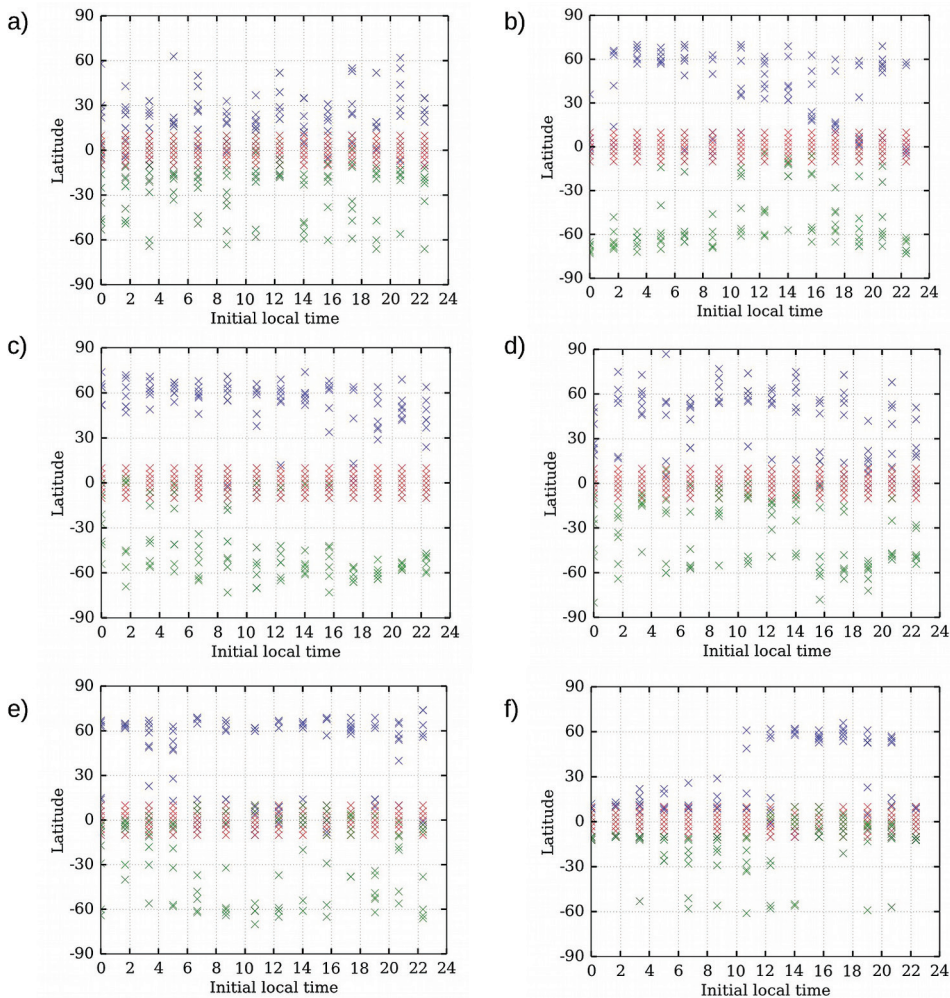


Figure 2: Maximum (blue) and minimum (green) latitudes reached over 1 Vd by balloons, depending on initial local time. The initial latitude is in red. Vertical levels are: (a) $7.2 \cdot 10^3$ Pa; (b) $1.0 \cdot 10^4$ Pa; (c) $1.4 \cdot 10^4$ Pa; (d) $1.9 \cdot 10^4$ Pa; (e) $3.9 \cdot 10^4$ Pa; (f) $5.3 \cdot 10^4$ Pa

Over 1 Vd, the different balloons often reach up to 60° of latitude in both hemispheres. For the $7.2 \cdot 10^3$ Pa level, the trajectories tend to stay below 30° . For the $5.3 \cdot 10^4$ Pa level, the trajectories with initial time between 21:00 and 9:00 local time tend to stay also below 30° . The individual trajectories in terms of latitude vs time are plotted in Fig. 3.

Latitudes 30–40

When started between 30 and 40° latitude (N or S), balloons at 1.0 and $1.4 \cdot 10^4$ Pa cover latitudes between 70°N and 70°S over 1Vd. For 2.8 , 3.9 and $5.3 \cdot 10^4$ Pa, as well as for $7.2 \cdot 10^3$ Pa, the balloons tend to remain in the hemisphere where they started, between equator and 70° . For most of the balloons, trajectories never reach polar regions. Examples of trajectories (latitude vs time) are plotted in Fig. 4.

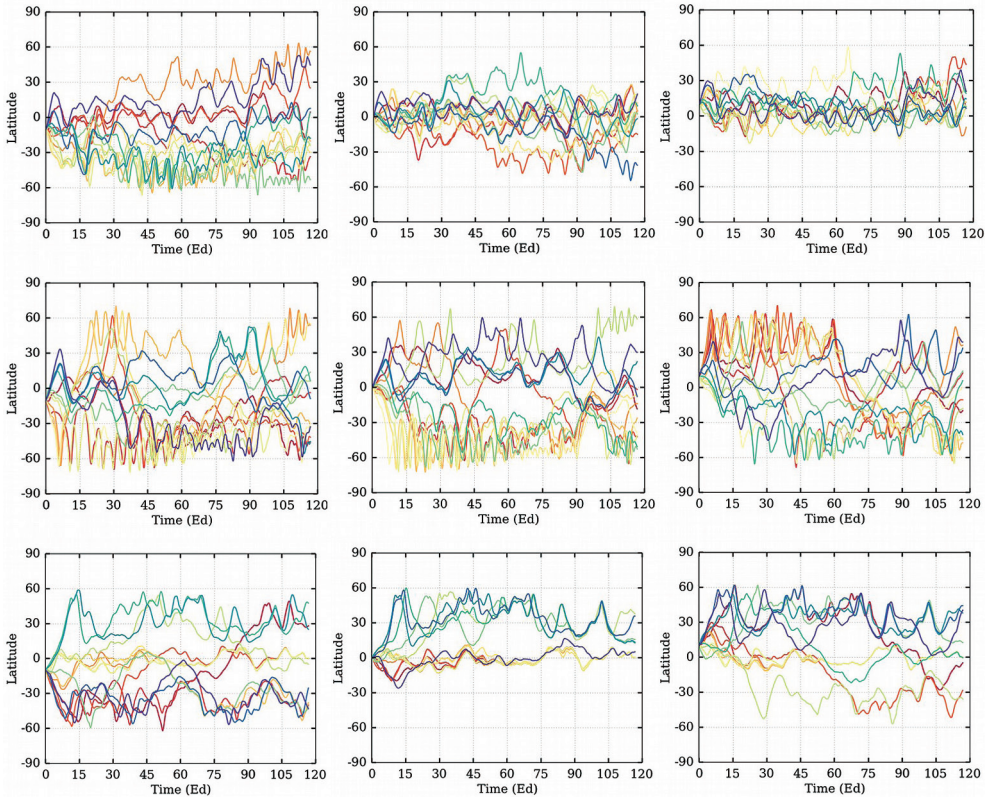


Figure 3: Trajectories (latitude vs time) for balloons at $7.2 \cdot 10^3$ Pa (upper row), $1.0 \cdot 10^4$ Pa (middle row) and $5.3 \cdot 10^4$ Pa (lower row) levels, with initial latitudes at 10°S (left column), Equator (central column) and 10°N (right column). The different colors indicate the initial local time (red is morning, orange to green is night, blue is afternoon).

Conclusions

The circulation modeled by the IPSL Venus GCM in the 40 to 80 km altitude range is in fairly good agreement with observations. Therefore, using this simulation as a background atmosphere, the possible trajectories of an aerial platform launched in the Venus cloud layer was investigated. Interdiurnal variability can affect the modeled trajectories. Also, it is difficult to predict the trajectories since the GCM simulations are not in perfect agreement with observations. However, this study shows that the latitudinal variations may be large, when considered over timescale of several tens of Earth days. They tend to be smaller for the $7.2 \cdot 10^3$ Pa and $5.3 \cdot 10^4$ Pa levels.

Controlling the latitudinal span through varying the level at which the platform flies would not be easy. However, varying the level could give precious indications on the vertical variations of the meridional wind field.

Acknowledgements

This work was granted access to the HPC resources of CINES under the allocation 2017-11167 made by GENCI.

References

- Andreev, R. A., Altunin, V. I., Kerzhanovich, V. V. et al. (1986) Mean zonal winds on Venus from the Doppler tracking of the Vega balloons, *Sov. Astron. Lett.*, 12, 17–19.
- Crisp, D., Ingersoll, A. P., Hildebrand, C. E., Preston, R. A. (1990) Vega balloon meteorological measurements, *Adv. Space Res.*, 10, 109–124.
- Garate-Lopez, I., Lebonnois, S. Latitudinal variation of clouds' structure responsible for Venus' cold collar. *Icarus*, in revision.
- Lebonnois, S., Hourdin, F., Eymet, V. et al. (2010) Superrotation of Venus' atmosphere analysed with a full General Circulation Model, *J. Geophys. Res.*, 115, E06006.

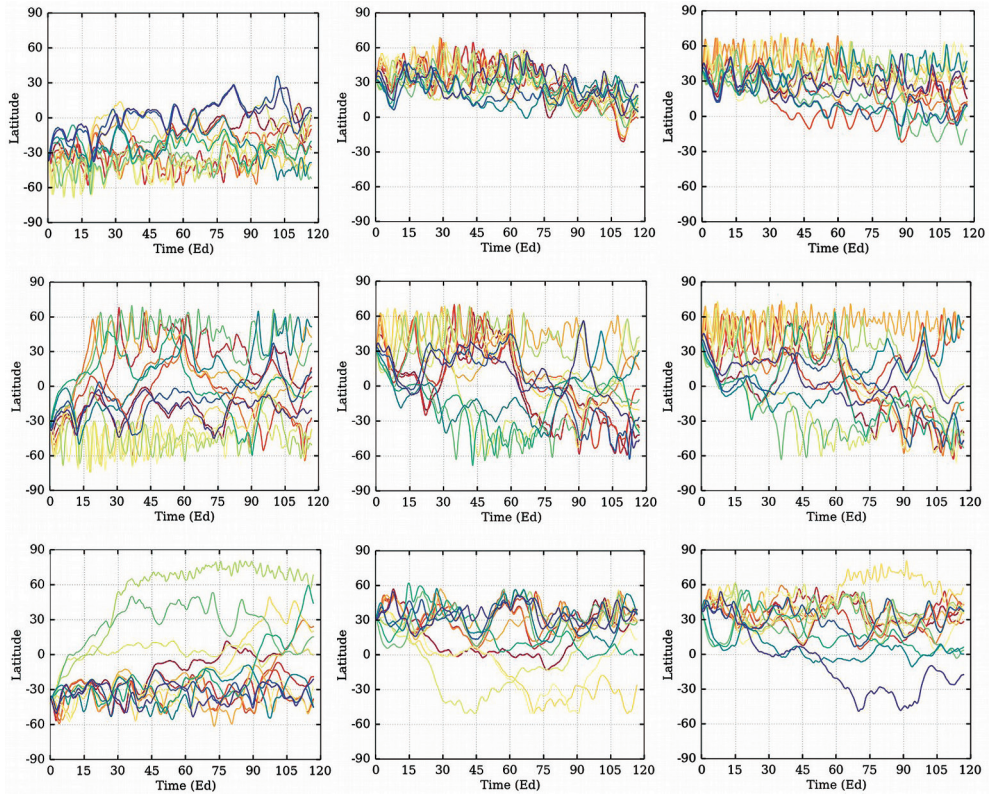


Figure 4: Same as Fig. 3, with initial latitudes at 36.5°S (left column), 32°N (central column) and 39°N (right column)

Lebonnois, S., Sugimoto, N., Gilli, G. (2016) Wave analysis in the atmosphere of Venus below 100-km altitude, simulated by the LMD Venus GCM, *Icarus*, 278, 38–51.

Sagdeev R. Z., Linkin, V. M., Kremnev, R. S. et al. (1986) The Vega balloon experiments, *Sov. Astron. Lett.*, 12, 3–5.

VENUS AERIAL PLATFORMS AND ENGINEERING AND SCIENTIFIC MODELING NEEDS

J. A. Cutts, L. H. Matthies, T. W. Thompson

Jet Propulsion Laboratory, California Institute of Technology, USA, James.A.Cutts@jpl.nasa.gov

Keywords: Venus, modeling, aerial platform, balloon, glider, altitude control, solar radiation, temperature profile, Venus mobile explorer

Introduction

NASA's Planetary Science Division is performing an assessment of the state of technology for aerial platforms for exploration of Venus. A key factor in the design of aerial platforms is knowledge of the Venus environment. Modeling the Venus environment, which is the subject of this workshop, is needed for the design of robust aerial platforms that can carry out their missions successfully. The purpose of this paper is to enumerate the kinds of models that are important for both engineering and scientific aspects of the design of an aerial platform mission. The first meeting of the NASA Aerial Platforms study team took place from May 30 to June 2, 2017 and addressed the science that can be performed by aerial platforms. A second study meeting planned for late November 2017 will be focused on technical feasibility. This paper focuses on the current status of this study.

Aerial Platforms at Venus

The first and only aerial platform missions to have been carried out at Venus were the VeGA balloons deployed by the Soviet Union in 1985 (Kremnev et al., 1986). Each of them floated in the superrotating atmosphere of Venus for approximately two days at a near constant altitude of 55 km altitude and were successfully tracked from Earth. VeGA was an important proof of concept and has led to concepts for more ambitious missions to follow.

Constant altitude balloon

One direction that has been pursued involves scaling up the VeGa concept, enabling larger payloads and missions of longer duration but still at a constant altitude. The technology needed here is still the superpressure type of balloon used for VeGa but with stronger material and greater protection against the sulfuric acid environment. These vehicles can also be used to deploy and relay data from descent probes as in the Venus Climate Mission endorsed by the Planetary Science Decadal Survey in 2011 (Hall et al., 2008).

Altitude controlled balloon

A more ambitious capability is a balloon which can change altitude in a controlled fashion, enabling atmospheric sampling over a broad range of altitudes. Concepts for implementing this over an altitude range from 70 to 30 km have been explored (de Jong, 2015).

Hybrid airship concepts

Concepts have also been devised with some degree of horizontal control. The Venus Atmospheric Maneuverable Platform (VAMP) would use a combination of flotation and lift to rise to 65 km on the dayside of Venus but sink to 50km on the night side when no solar power is available (Lee et al., 2015).

Solar powered airplane

Solar power near the cloud tops on Venus is adequate for powered flight. Heavier-than-Airplane (HTA) vehicles can remain in continuous sunlight by flying in the opposite direction to the superrotating flow (Landis et al., 2002). However, both cloud opacity and temperature will limit how deeply a solar airplane can penetrate into the cloud layers.

Deep atmosphere platforms

Concepts for buoyant vehicles that would operate near the surface of Venus have also been explored. These include concepts for lifting samples up to the more clement parts of the atmosphere for analysis since lifetimes of vehicles at the surface are limited to a few hours. A similar vehicle can also serve as the first stage in a Venus Surface Sample Return system. After arriving in low density regions of the atmosphere, the sample would be launched into orbit (Rodgers et al., 2000). This

type of vehicle has also been contemplated for a Venus Mobile Explorer mission concept studied by the Planetary Science Decadal Survey (Kerzhanovich et al., 1999).

Environmental Modeling Needs

Knowledge of the Venus environment captured in models is vital for the design of atmospheric platforms and the missions they will implement.

Atmospheric circulation models

For balloon missions, it is necessary to know where the platform will travel in order to assess the likely duration of the mission. Current expectations are that superpressure balloons deployed at 55 km will drift towards the pole, but the rate at which this occurs is uncertain. For platforms with altitude control, it will be important to know if there is any variation in this meridional component of velocity; if it were to reverse, it might enable some degree of control of latitude. For hybrid airships, the meridional component will determine how much control authority the vehicle will need to avoid drifting to pole.

Solar and thermal radiation models

Knowledge of the variation of solar radiation with depth in the cloud layer is needed for the design of many types of buoyant vehicle where heating of the envelope by the sun impacts performance. The solar flux is also a factor in the design of any long duration aerial platform mission dependent on solar power. Hybrid and HTA vehicles are most dependent on it because their need for power for propulsion will limit how deep into the cloud deck the vehicles can descend. Altitude controlled balloon missions will be much less sensitive because they do not require power for propulsion. However, it will be important to know how deep in the atmosphere it will be practical to operate a solar power system. Performance is impacted by 1) the decrease in the intensity of solar flux deeper in the clouds, 2) the selective loss of short wavelength radiation, and 3) the increase in temperature, which selectively degrades the performance of photovoltaic converters of longer wave radiation. Models (Meadows, Crisp, 1996) used in recent balloon design (Hall et al., 2008) should now be updated based on the Venus Express and Akatsuki data.

Cloud characteristics

The nature of the aerosols in the cloud layer and their size distribution will also be important to aerial platform design. Balloon missions planned to date are very conservatively designed to tolerate immersion in sulfuric acid. However, if models indicate that sulfuric acid exists only as a very finely dispersed mist, this requirement might be relaxed. There may be other implications for balloon emissivity and thermal control, the surfaces of optical instruments, and for the entry ports of gas analyzers.

Physical properties and chemistry of the deep atmosphere

As explained in a companion paper by Josette Bellan, the behavior of mixtures of gases under high pressures and temperatures can introduce counterintuitive behavior. It is possible that the anomalous lapse rates observed near the surface of Venus result from these unusual processes (Bellam, 2017).

Scientific Modeling Needs

In addition to the need for models that can ensure that the aerial vehicle can survive, generate solar power, and access the parts of the atmosphere needed to execute its mission, models will also be needed to carry out scientific experiments. There will be many different types of models needed for this purpose but we include here a discussion of some that have been the subject of recent work by the senior author and his collaborators.

Infrasound generation and propagation

Seismic disturbances on Venus couple very efficiently into the atmosphere because of the density of the Venus atmosphere. Models have been developed that characterize the propagation into the atmosphere, which indicate that Rayleigh waveforms are accurately replicated as an acoustic signal according to work by Garcia et al., (2016). However, models focusing on the epicentral waves that have been developed for the Earth still need to be adapted to Venus.

Infrasound background generation

To confirm the feasibility of detecting quake-related infrasound signatures, it is important to understand other sources of infrasound on Venus. Building on general circulation models, efforts

are underway to understand the magnitude of signals generated in the boundary layer (Schubert et al., 2016). If Venus has very high levels of seismic activity, they may prove to be a source of excitation that can be used for probing the internal structure of the planet.

Engineering Modeling Needs

Models are also required to describe how engineering systems for aerial platforms interact with the environment. Some examples of these are described below:

Entry models

Modeling of concepts with rigid entry systems is well developed for Venus, although this is in need of refinement. Modeling for concepts where the vehicles enter the atmosphere in an inflated state are required.

Balloon and airship thermal models

Solar heating of the envelopes of balloons and airships elevates the temperature of the enclosed gas, increasing its pressure and exerting stress on the envelope. Improved models integrating the environmental effects are needed to characterize these effects.

Solar power generation models

Solar power is the most practical source of power on Venus. Models are needed to optimize the design of multijunction cells to account for the changing intensity, spectral content and temperature with depth in the atmosphere.

Navigation models

Localization of the vehicles is important to the science they can accomplish. Terrain relative navigation (TRN) requires viewing the surface at high resolution and is only possible within 10 km of the surface, and even there is degraded. Models characterizing surface visibility building on the pioneering work of Moroz (Moroz, 2002) will be required.

Summary

The development of high fidelity models is vital for the further exploration of Venus and particularly for the operation and scientific utilization of aerial platforms. Environmental models are needed to characterize the environment in which the vehicles operate so that they can be designed to effectively carry out their mission. Engineering models are needed to characterize the response of the vehicles to their environment so they survive entry, diurnal changes and acquire sufficient power for operation. Finally, purely scientific models are needed so that diagnostic signatures of the phenomena under investigation can be understood.

References

- Bellam, J. (2017) Fundamental Studies of High-Pressure Turbulent Multi-Species Mixing Relevant to the Venus Atmosphere, *Venus Modeling Workshop*, Cleveland, USA, 8004.
- de Jong, M. (2015) Venus Altitude Cycling Balloon, *Venus Lab and Technology Workshop*, Langley, USA, 4030.
- Garcia, R. F., Mimoun, D., Brissaud, Q., Lebonnois, S. (2016) Infrasounds From Venus Quakes: Numerical Modeling And Balloon Observation Project, *International Venus Conference*, Oxford, UK.
- Hall J. L., Fairbrother D., Frederickson T., Kerzhanovich V.V., Said M., Sandy C., Willey C., Yavrouian A.H. (2008) Prototype design and testing of a Venus long duration, high altitude balloon, *Advances in Space Research*, 42, 1648–1655.
- Kerzhanovich, V., Balam, J., Campbell, B. et al. (1999) Venus Aerobot Multisonde Mission, *XII AIAA LTA and Balloon Technology Conference*, Norfolk, USA.
- Kremnev, R. S., Linkin, V. M., Lipatov, A. N., Pichkadze, K. M. et al. (1986) Vega Balloon System and Instrumentation, *Science*, 231, 1408–1411.
- Landis, G. A., Colozza A., LaMarre, M. C. (2002) Atmospheric Flight on Venus, *40th Aerospace Sciences Meeting and Exhibit*, NASA/TM—2002-211467.
- Lee, G., Warwick, S., Ross, F., Sokol, D. (2015) Venus Atmospheric Maneuverable Platform (VAMP) — Pathfinder Concepts, *Venus Lab and Technology Workshop*, Langley, USA, 8006.
- Meadows, V. S., Crisp, D. J. (1996) Ground-based near-infrared observations of the Venus nightside: The thermal structure and water abundance near the surface, *Geophys. Res.*, 101, 4595–4622.
- Moroz, V. I. (2002) Estimates of visibility of the surface of Venus from descent probes and balloons, *Planetary and Space Science*, 50(3), 287–297.

- Rodgers, D., Gilmore M., Sweetser T.H., Zimmerman W. (2000) Venus sample return. A hot topic, *IEEE Aerospace Conf. Proc.*, 7, 473–484, doi: 10.1109/AERO.2000.879315.
- Schubert, G., Lebonnois, S., Lefèvre, F., Solzenbach, A. (2016) Dynamics and Circulation of the Venus Atmosphere: Expected Contributions of Akatsuki Observations, *International Venus Conference*, Oxford, UK.

INFRASOUND DETECTION FROM BALLOONS — PERSPECTIVES FROM SIMULATIONS AND EXPERIMENTS

**S. Krishnamoorthy¹, A. Komjathy¹, J. A. Cutts¹, M. T. Pauken¹, R. F. Garcia²,
D. Mimoun², J. Jackson³, S. Kedar¹, S. E. Smrekar¹, J. L. Hall¹**

¹ *Jet Propulsion Laboratory, California Institute of Technology, Pasadena, CA*

² *Institut Supérieur de l'Aéronautique et de l'Espace (ISAE), Toulouse, France*

³ *Seismological Laboratory, California Institute of Technology, Pasadena, CA*

Keywords: aerial platforms, seismometers, infrasound

Introduction

The study of a planet's seismic activity is central to the understanding of its internal structure. Seismological studies of the Earth led to the discovery of the layered structure of its interior (Mohorovicic, 1909), which in turn has led to great advances in the understanding of catastrophic events such as earthquakes and volcanic eruptions. Earth's planetary twin, Venus, has shown strong evidence of recent geological activity (Ivanov, Head, 2013a, b). Seismological studies can help us understand the evolution of these geological events and aid our quest to determine why Venus is so similar to Earth in certain aspects yet so different. However, extremely high temperature and pressure conditions on the surface of Venus (National Aeronautics and Space Administration, Venus — by the numbers, <http://solarsystem.nasa.gov/planets/venus/facts>) present a significant technological challenge to performing long-duration seismic experiments. Therefore, despite visits from many spacecraft since Mariner 2 in 1962, the internal structure of Venus still remains a mystery.

Seismic experiments conducted from aerial platforms offer a unique opportunity to explore the internal structure of Venus without needing to land and survive on its surface for long durations. In particular, the dense atmosphere of Venus allows for balloons to be flown in the mid and upper atmospheric regions. These balloons may be used as vehicles for seismic experiments that can collect infrasound data as indication of seismic waves while floating in the prevailing winds. One possible way to detect and characterize quakes from a floating platform is to study the infrasonic signature produced by them in the atmosphere. Infrasonic waves are generated when seismic energy from ground motions are coupled into the atmosphere (Mutschlecner, Whitaker, 2005; Wolcott et al., 1984). The intensity of the infrasound depends heavily on the relative density of the atmosphere and the planet's crust. On Venus, where the atmospheric impedance is approximately 60 times that of Earth (Petculescu, Lueptow, 2007), the coupling of seismic energy into the atmosphere is expected to be commensurately greater.

However, the performance of seismic experiments from balloons comes with its own set of challenges – sulfuric acid in the Venusian atmosphere can degrade balloon material (Hall et al., 2011) and the remote deployment of balloons on another planet is also a technological challenge. There also exist scientific challenges – the process of infrasound generation and propagation is complex, depending on many factors such as quake location, intensity, and prevailing atmospheric conditions, to name only a few (Mutschlecner, Whitaker, 2005). Therefore, sophisticated simulations and experiments are needed to develop a scientific mission that can inform us of the internal structure of Venus.

Presentation Content

In this talk, we will review ongoing efforts to study and characterize infrasound generation, propagation, and detection from a balloon platform. JPL and its partners (California Institute of Technology and ISAE-SUPAERO, France) are in the process of developing technologies towards this goal. Since 2014, we have developed experimental concepts, infrasound sensors, and computer models to achieve the aim of performing remote seismology on Venus. We will share our experience from our efforts over the last few years and motivate a path forward towards better understanding our planetary twin.

References:

- Hall, J., Yavrouian, A. Kerzhanovich, V. et al. (2011) Technology development for a long duration, mid-cloud level Venus balloon, *Advances in Space Research*, 48(7), 1238–1247.
- Ivanov, M. A., Head, J. W. (2013a) The history of volcanism on Venus, *Planetary and Space Science*, 84, 66–92.
- Ivanov, M. A., Head, J. W. (2013b) 10.03 — Planetary Seismology, In: *Treatise on Geophysics*, 2nd ed., Elsevier, 2015, 10, 65–120.
- Mohorovicic, A. (1909) Das Beben vom 8. X. 1909, *Jahrbuch des meteorologischen Observatoriums in Zagreb (Agram) für das Jahr*, 9(4), 63 p.
- Mutschlecner, J. P., Whitaker, R. W. (2005) Infrasound from earthquakes, *J. Geophysical Research: Atmospheres*, 110(D1).
- Petculescu, A., Lueptow, R. M. (2007) Atmospheric acoustics of Titan, Mars, Venus, and Earth, *Icarus*, 186(2) 413–419.
- Wolcott, J. H., Simons, D. J., Lee, D. D., Nelson, R. A. (1984) Observations of an ionospheric perturbation arising from the Coalinga earthquake of May 2, 1983, *J. Geophysical Research: Space Physics*, 89(A8) 6835–6839.

LIDAR SPECTROSCOPIC SOUNDING OF THE AMBIENT ATMOSPHERE AND CLOUD LAYER ONBOARD VENUS ATMOSPHERIC PLATFORM

**A. V. Rodin^{1,2}, A. Yu. Klimchuk¹, O. V. Benderov¹,
V. M. Semenov^{1,3}, I. V. Melnikov¹**

¹ *Moscow Institute of Physics and Technology*

² *Space Research Institute of the Russian Academy of Sciences*

Keywords: laser spectroscopy, aerial platforms, cloud composition

Atmospheric platforms based on either balloon or unmanned aerial vehicle, are of high priority in the future missions to Venus, including planned joint Venera-D mission. Such mission elements take advantage of both in situ studies typical for landers and long-term observations characteristic for orbiting spacecraft. Among key scientific objectives of such an atmospheric platform are comprehensive studies of chemical and isotopic composition of the atmosphere within and above the main cloud deck, local and mesoscale dynamics of the interface between superrotating and non-superrotating atmospheric layers, distribution and microphysical properties of aerosol particles, measurements related to identification of still unknown UV absorber. These goals may be achieved by close-up remote measurements based on the active LIDAR sounding in the near-IR spectral range.

We propose a concept of onboard spectroscopic LIDAR for studies of the Venus atmosphere within and above the cloud layer. The instrument includes a set of semiconductor lasers with precisely controlled frequency related to spectral features of target gases (CO₂, H₂O, HDO, SO₂, OCS etc.). Laser radiation is then transmitted to the fiber-optical amplifiers which provide output power in a quasi-continuous mode of 5–10 W with the linewidth about 1MHz. This radiation is sent to the ambient atmosphere, with backscatter component being detected by an imaging array in the heterodyne mode. This allows CLADS spectroscopic studies of gas composition and Doppler measurements of the local wind systems.

PLASMA

SOLAR WIND INTERACTION WITH VENUS — IMPLICATION FOR ATMOSPHERE AND SOME LESSONS FROM MARS

O. Vaisberg, S. Shuvalov, L. Zelenyi, A. Petrukovich, V. Ermakov

Space Research Institute of Russian Academy of Sciences

Abstract

Investigations of solar wind interaction with exosphere, atmosphere and magnetosphere is a crucial part of future Venus space mission and are also important for understanding of evolution of planetary atmospheres in general. Thus there is a need to provide comprehensive suite of plasma and magnetic field instruments for Venera-D project. Addition of a small subsatellite, providing the simultaneous solar wind monitoring will improve scientific output of the mission. An example of MAVEN experimental approach is encouraging.

Introduction

It is known from Pioneer-Venus Orbiter (PVO) measurements at low altitudes that Venus does not have a global magnetic field (Acuna et al., 1998). Venusian magnetosphere is formed with the interplanetary magnetic flux tubes, piling-up at the planetary dayside and convecting to the night-side being mass-loaded by heavy planetary ions. Existence of Venus magnetosphere and the role of the solar wind in the heavy ions pick-up were established by Venera-9 and Venera-10 orbiters (launched in 1975, see e.g. (Vaisberg et al., 1976, Russell, Vaisberg, 1983). PVO (launched 1978) and Venus-Express (2005) significantly expanded our understanding of the solar wind role in formation of unique magnetosphere and ionosphere of Venus, in the planetary ions loss and mass-exchange processes (Vaisberg, Zelenyi, 1984, Zelenyi, Vaisberg, 1985, Dubinin et al., 2011, Bertucci et al., 2011, Vasko et al., 2014, Futaana et al., 2017). In particular, this interaction leads to significant contribution of minor constituents to Venusian atmosphere. The solar wind also contributes to the energetics of upper atmosphere and ionosphere, especially in the periods of catastrophic space weather events.

The Venera-D mission is expected to make a significant step forward in Venusian aeronomy and plasma studies due to progress in instrumentation and in understanding of physics of solar wind impact on planets during the last decades. The following outstanding problems will be addressed:

- energy, momentum and mass transfer from the solar wind to the upper atmosphere and ionosphere;
- influence of solar electromagnetic radiation on atmosphere;
- ionosphere dynamics caused by the solar wind, ionosphere scavenging and intrusion of plasma clouds;
- space weather at Venus — effects of flares, CMEs, CIRs;
- solar wind induced atmospheric losses (composition and flux) now and for 4.5 billion years;
- minor components in the atmosphere acquired from the solar wind for 4.5 billion years;
- mass loading in solar wind;
- structuring and dynamics of plasma and magnetic field in the magnetosphere and magnetotail, magnetosphere-ionosphere interactions.

Venus plasma science

Previous studies of Venus have been used to develop the model of magnetosphere and atmospheric ions outflow through the magnetic tail of Venus (Fig. 1) (Vaisberg, Zelenyi, 1984; Zelenyi, Vaisberg, 1985). This model includes the criterion of magnetosphere formation at a gaseous obstacle in the solar wind: $n_{sw} V_{sw} = N_0 v L$, where n_{sw} and V_{sw} are the solar wind number density and velocity, respectively, N_0 is the number density of planetary neutrals, v is the photo-ionization rate, L is characteristic scale of the gaseous obstacle. This formula can be used for calculation of the transverse size of the gaseous obstacle. Estimation of the size the Halley's plasma mantle made one year before encounter of space fleet with the comet (Vaisberg, Zelenyi, 1984; Zelenyi, Vaisberg, 1985) was accurate within 10 % with actual measurement.

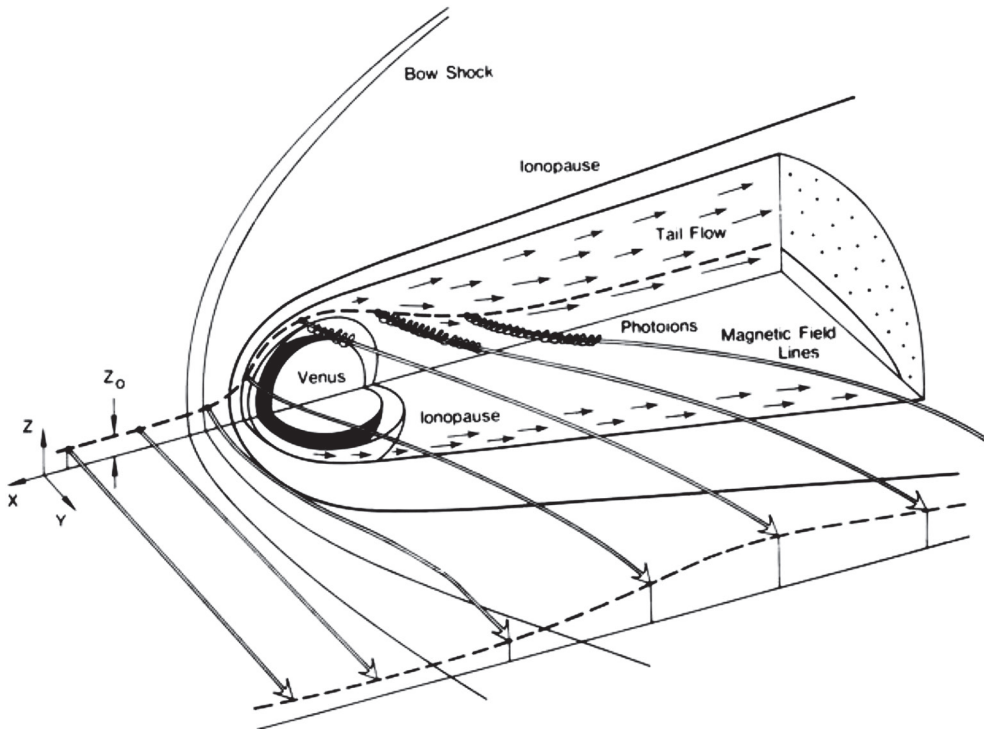


Figure 1: Semi-quantitative model of Venusian atmosphere showing the convection of the solar wind magnetic flux tubes through the bow shock and around the planet, mass-loading by atmospheric ions in the tail (Vaisberg, Zelenyi, 1984; Zelenyi; Vaisberg, 1985)

Still there is some ambiguity about the Venusian magnetic field, atmospheric losses, and the solar wind forcing. The Venus may have very small planetary magnetic field (Luhmann et al., 2015). Measurements on Venus Express in the altitude range 150 to 450 km suggest the presence of a small (few nT) but persistent radial field hemispheric bias at deep nightside, low to mid-latitude range, with more positive (outward) field in the south and the more negative (inward) fields in the north. The overall solar wind-induced atmospheric losses at Venus and Mars were estimated as $2.1 \cdot 10^{25}$ and $4.3 \cdot 10^{24}$ at solar maximum, respectively. However the efficiency (likelihood) of O^+ escape is 2–3 times higher at Mars (Curry et al., 2015). These estimates were done basing on measurements of plasma analyzers with low temporal resolution and incomplete sampling of velocity space. One of the main uncertainties here is the role of ionospheric escape (Collinson et al., 2016). Thus there is a need to perform more detailed observations of ions and neutrals of major atmospheric constituents with high-time resolution and at a variety of locations in the near-Venus environment.

As the variations of the solar wind interplanetary magnetic field play crucial role in formation of the induced magnetosphere (or, more precisely, pile-up magnetosphere) and affect mass losses, one needs to monitor the state of interplanetary medium, while the spacecraft investigates Venusian magnetosphere. With a single spacecraft, the measurements of the solar wind conditions are performed prior to or after measurements in the outer envelope of the planet, being separated a half an hour or about an hour. As solar wind and interplanetary magnetic field vary significantly, the reliability of attributing the measurements in Venus neighborhood to specific driving parameters is sometimes incorrect. The solution is to have at least one additional spacecraft that can frequently provide concurrent complementary measurements in the interplanetary medium. The importance of such 2-point or multipoint observations is widely acknowledged for terrestrial magnetosphere research and was recently demonstrated at Mars with ESA's Mars Express and NASA's MAVEN spacecraft. Besides upstream monitoring an additional spacecraft will allow a variety of two-point studies of the magnetosphere and ionosphere.

Lessons from MAVEN

Mars satellite MAVEN (Mars Atmosphere and Volatile Evolution Mission) performs measurements at Mars since October 2014. It is the first planetary orbiter that is specially designed to investigate the upper atmosphere — ionosphere and the solar wind influence on outer envelope of the planet. The comprehensive suite of instruments includes:

- Extreme Ultraviolet (EUV) Monitor, (PI Phillip Chamberlin);
- Imaging Ultraviolet Spectrograph (IUVS), (PI Nick Schneider);
- Langmuir Probe and Waves (LPW), (PI R.E. Ergun);
- Magnetometer Investigation (MAG), (PI Jack Connerney);
- Neutral Gas and Ion Mass Spectrometer (NGIMS), (PI P. Mahaffy);
- Solar Energetic Particle (SEP) (PI D. Larson);
- SupraThermal and Thermal Ion Composition (STATIC), (PI J.P. McFadden);
- SolarWind Electron Analyzer (SWEA), (PI D.L. Mitchell);
- Solar Wind Ion Analyzer (SWIA), (PI J.S. Halekas);
- The PI of MAVEN mission is Bruce Jakosky.

For the first time plasma instruments at Mars provide detailed measurements of the velocity distributions of plasma components enabling to study kinetic processes in planetary plasma.

Figure 2 shows plasma energy-time spectrograms with 4-s resolution of during MAVEN crossing of dayside magnetosphere of Mars. Protons' spectrogram overlaid by magnetic field magnitude profile enables to identify and analyze the boundaries of magnetosphere. Velocity distribution functions are also available providing investigation of ion acceleration and pick-up processes. The magnetopause separating the magnetosphere from external shocked solar wind flow is located at $\sim 18:47:00$ UT. It was shown to be a tangential discontinuity (Vaisberg et al., 2017). The boundary between magnetosphere and underlying ionosphere is not easy to identify; it was tentatively attributed to $\sim 18:41:00$ UT. The current layer seen as the change of magnetic field magnitude is accompanying this transition.

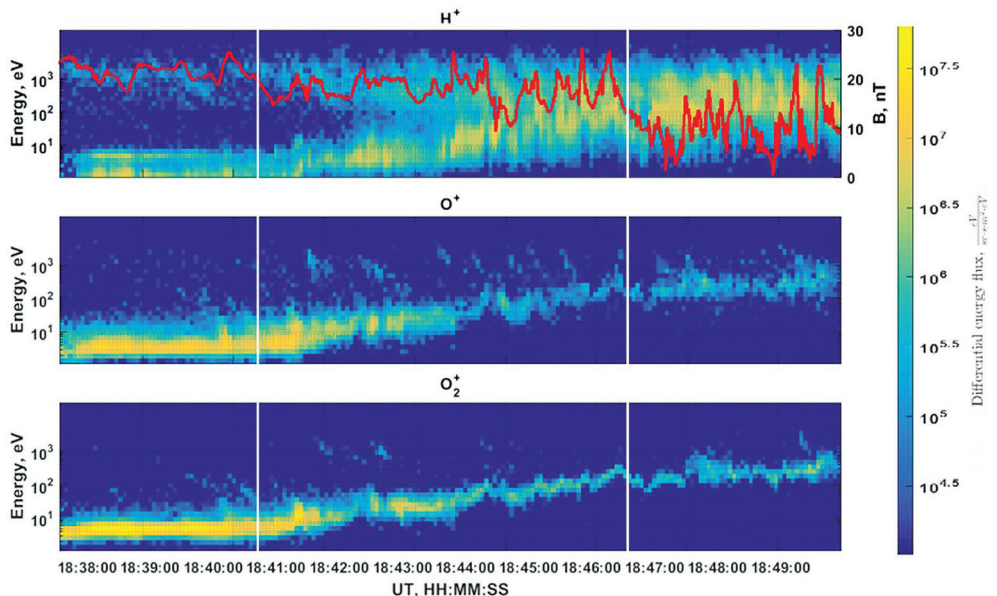


Figure 2: Energy-time spectrograms of protons, O^+ and O_2^+ ions with magnetic field magnitude curve (red line) overlaying proton diagram. White vertical lines show approximate locations of magnetopause (right) and the boundary between ionosphere and magnetosphere (left). January 4, 2015 observations

Another example of MAVEN measurements is shown in Fig. 3. This 3-min time interval shows magnetic field magnitude and components, and the energy flux-time spectrograms of the solar wind protons and planetary O^+ ions. This sample is from the case of the high-mass loading of shocked solar wind flow in the front of Martian magnetosphere. Mass loading leads to very strong turbulence

in the frequency range ~ 1 Hz. The ion spectra were measured for 4 sec that does not allow associating plasma data with different phases of waves. It makes very difficult to identify the type of turbulence that is necessary for analysis of this mass-loading process.

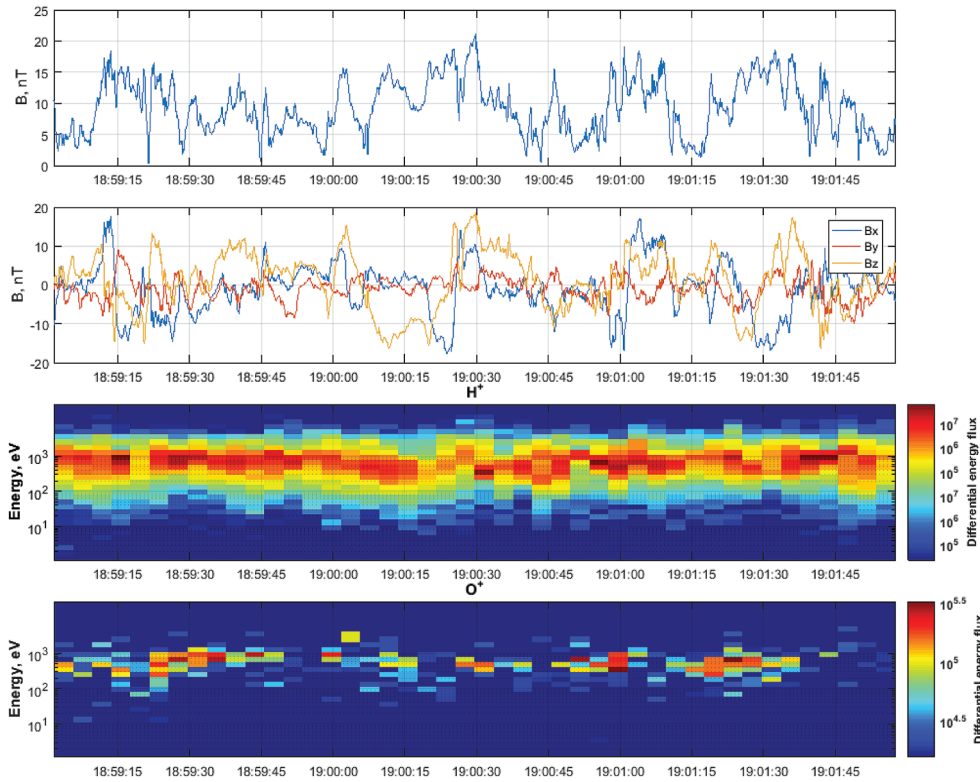


Figure 3: Case of high turbulence of mass-loaded magnetosheath plasma observed at 4 January, 2015. From up to bottom: magnetic field magnitude and components, and the energy flux-time spectrograms of the solar wind protons and planetary O^+ ions

Two examples shown confirm that MAVEN provides excellent data for studying the solar wind-Mars interaction and Martian magnetosphere. Though there are some unexpected regions, properties and events that overcome the expectations.

Considered examples indicate that it is necessary to provide more flexible regimes for instrumentation working in unknown environment. For example, instruments should have modes with highest possible temporal resolution even by making coarse phase space resolution. Another lesson from MAVEN is that the plasma instruments should cover complete possible phase space volume even at the expense of decreased phase space resolution.

Example strawman plasma payload and orbit design

In order to meet the goals of plasma experiments listed above one needs to perform the following measurements:

- Ionospheric plasma: ion and electron density, temperature, composition, solar wind flux;
- Hot plasma parameters: ion and electron velocity distributions, ion composition;
- Magnetic field;
- Plasma waves;
- Energetic particles: fluxes of ions and electrons;
- Atmospheric emissions: airglow, "aurora".

The main spacecraft should be on elliptic orbit: periapsis height 200–300 km, preferred apoapsis height 10,000–15,000 km. The subsatellite should be on the same orbit, with naturally changing distance from the main spacecraft. On a later project stage the main spacecraft may be transferred

to another (lower) orbit. The main spacecraft should contain the full plasma payload, while the subsatellite — only the reduced instrument set. Alternatively, subsatellite may contain a variant of payload, more oriented at solar wind and outer magnetosphere measurements.

Table 1: Main satellite strawman payload

| Instrument | Measurements | Range | Mass, kg | Power, W | Bit rate, kB/s |
|------------------------------|---------------------------------------|---------------|---------------|----------|----------------|
| Ion spectrometer | Hot ions parameters and composition | 5 eV–30 keV | 1.5 | 3.5 | 2–4 |
| Electron spectrometer | Hot electrons spectrum | 15 eV–5 keV | 1.2 | 2,0 | 2 |
| Langmuir probe | Ionospheric ions and electrons | 0.1–5 eV | 1.5 | 2,0 | 2 |
| Magnetometer | 3-component magnetic field | 0.1–200 nT | 4 (with boom) | 4,0 | 2–4 |
| Plasma waves | Electric and magnetic waves | 0.1 Yz–40 kHz | 1.4 | 0.3 | 2–4 |
| Energetic electrons detector | Energetic electrons spectrum | 10–200 keV | 1.5 | 2 | 1 |
| Energetic ions detector | Energetic ions energy and composition | 20–400 keV | 3.5 | 3.5 | 1 |
| UV photometer | Ly α flux | 101.6 nm | 0.5 | 0.5 | 1 |
| Total | – | – | 14.1 | 17.8 | ~16 |

Table 2: Subsattellite strawman payload

| Instrument | Measurements | Range | Mass, kg | Power, W | Bit rate, kB/s |
|-------------------------|---------------------------------------|--------------|---------------|----------|----------------|
| Ion spectrometer | Hot ions parameters and composition | 30 eV–30 keV | 1.5 | 1.5 | 0.5 |
| Solar wind spectrometer | – | 0.5–5 keV | 1.5 | 2.0 | 0.2 |
| Electron spectrometer | Hot electrons spectrum | 15 eV–5 keV | 1.2 | 1.5 | 0.2 |
| Magnetometer | 3-component magnetic field | 0.1–200 nT | 2 (with boom) | 1.5 | 0.5 |
| Energetic ions detector | Energetic ions energy and composition | 20–400 keV | 2.5 | 1.5 | 0.2 |
| Total | – | – | 7.2 | 6,0 | 1.4 |

Conclusion

Comprehensive magnetic field and plasma experiments will greatly improve the scientific program of Venera-D related with atmosphere evolution, solar wind driving, ionospheric and magnetospheric dynamics. Addition of a small subsatellite will substantially enhance reliability of solar wind driving investigations. There is a need to achieve higher temporal resolution and complete phase space coverage of plasma measurements compared to current planetary spacecraft.

References

Acuña, M.H., Connerney, J.E.P., Wasilewski, P., Lin, R.P., Anderson, K.A., Carlson, C.W., McFadden, J., Curtis, D.W., Mitchell, D., Reme, H., Mazelle, C., Sauvaud, J.A., d’Uston, C., Cros, A., Medale, J.L., Bauer, S.J., Cloutier, P., Mayhew, M., Winterhalter, D., Ness, N.F. (1998) Magnetic Field and Plasma Observations at Mars: Initial Results of the Mars Global Surveyor Mission, *Science*, 279(5357), 1676–1680.

Bertucci, C., Duru, F., Edberg, N., Fraenz, M., Martinecz, C., Szego, K., Vaisberg, O. (2011) The induced magnetospheres of Mars, Venus, and Titan, Results of an Europlanet-RI ISSI Workshop, *Space Science Reviews*, 162(1), 113–171.

Collinson, G.A. et al. (2016) The electric wind of Venus: A global and persistent “polar wind”-like ambipolar electric field sufficient for the direct escape of heavy ionospheric ions, *Geophys. Res. Lett.*, 43, doi: 10.1002/2016GL068327.

Curry, Sh.M., Luhmann, J., Ma, Y., Liemohn, M., Dong, Ch., Hara, T. (2015) Comparative pick-up ion distributions at Mars and Venus: Consequences for atmospheric deposition and escape, *Planetary and Space Science*, 119, 36–42.

Dubinin, E., Fraenz M., Fedorov A., Lundin R., Edberg N., Duru F., Vaisberg O. (2011) Ion Energization and Escape on Mars and Venus, Results of an Europlanet-RI, ISSI Workshop, *Space Science Reviews*, 162(1), 173–211.

- Luhmann, J. G., Ma, Y. J., Villarrea, M. N., Wei, H. Y., Zhang, T. L. (2015) The Venus–solar wind interaction: Is it purely ionospheric?, *Planet. and Space Sci.*, 119, 36–42.
- Russell, C. T., Vaisberg, O. L. (1983) The Interaction of the Solar Wind with Venus, In: *Venus*, D. M. Hunten, L. Colin, T. M. Donahue, V. I. Moroz (Eds.), Univ. of Arizona Press, 873–94.
- Vaisberg, O. L., Romanov, S. A., Smirnov, V. N., Karpinsky, I. P., Khazanov, B. I., Polenov, B. V., Bogdanov, A. V., Antonov, N. M. (1976) Ion Flux Parameters in the Solar Wind-Venus Interaction Region, In: *Physics of Solar Planetary Environment*, D. J. Williams (Ed.), AGU, Boulder, 904–917.
- Vaisberg, O. L., Zelenyi, L. M. (1984) Formation of the Plasma Mantle in Venusian Magnetosphere, *Icarus*, 58, 412–430.
- Vaisberg, O. L., Ermakov, V. N., Shuvalov, S. D., Zelenyi, L. M., Znobishchev, A. S., Dubinin, E. M. (2017) Analysis of dayside magnetosphere of Mars: High mass loading case as observed on MAVEN spacecraft, *Planetary and Space Science*, 147, 28–37.
- Vasko, I. Y., Zelenyi, L. M., Artemyev, A. V., Petrukovich, A. A., Malova, H. V., Zhang, T. L., Fedorov, A. O., Popov, V. Y., Barabash, S., Nakamura, R. (2014) The structure of the Venusian current sheet, *Planetary and Space Science*, 96, 81–89.
- Zelenyi, L. M., Vaisberg, O. L. (1985) Venusian Interaction with the Solar Wind Plasma Flow as a Limiting Case of the Cometary Type Interaction, In: *Advances of Space Plasma Physics*, B. Buti (Ed.), Singapore, World Scientific, 59–76.

RADIO OCCULTATION ON THE VENERA-D MISSION: A CONCEPT OF RADIO FREQUENCY SUBSYSTEM AND RADIO SCIENCE TECHNIQUE

A. Gavrik¹, S. Kolomiets¹, Yu. Gavrik¹, T. Kopnina¹, L. Lukanina¹, Ya. Ilyshin²

¹ *Kotel'nikov Institute of Radio Engineering and Electronics, Fryazino branch, Russia*

² *Lomonosov Moscow State University, Moscow, Russia*

Abstract

In the present paper a basic concept of tools, measurement technique and a new mathematical model underlying data processing are briefly outlined envisioning their possible realization on the Venera-D mission. It is noted that the occultation experiments made with optimally matched parameters of radio-frequency subsystem may pave the way to new and important findings.

Introduction

Structural characteristics of the ionosphere and atmosphere of Venus have been thoroughly investigated by means of the occultation technique and extensively described in the literature (Brace, Kliore, 1991; Hinson, Jenkins, 1995; Armand et al., 2010; Tellmann et al., 2012; Imamura et al., 2017). These results cover a wide range of altitudes and solar activity. It is important to say that, although a great deal has been learned about the Venusian ionosphere our understanding still remains rather shallow in most aspects. Venus, like Earth, is a very complex world and in order to make the next step towards its adequate understanding it is still necessary to focus on new findings from upcoming missions.

In the Venera-D mission (Senske, Zasova, 2017) our interest should be focused on smaller-scale features of the ionosphere and atmosphere and on finer processes that could impact their overall structure, including the study of their global variations. Interaction between the lower ionosphere and the upper atmosphere of Venus as well as wave processes both in the atmosphere and ionosphere — as the least investigated areas — are the most attractive point of interest now. And the experience of previous missions indicates that given a sufficient energy potential of radio links, it should be possible to reveal the nature of the lowest ionospheric layers (Gavrik et al., 2009) and collect reliable data about their variability, including through a comparison of occultation measurements and the data gathered from the instruments mounted on the Venera-D orbiter.

At the same time exploratory missions like PVO, VEX, Magellan or the Soviet Venera mission could not unravel a number of competing small-scale processes that may contribute to the great changeability of ionospheric structures. But the experience of all these missions sent to Venus now allows us to select really optimal conditions of occultation experiments as well as presenting a solid ground for our hope in the absence of hidden obstacles on that path. The idea that it is necessary to increase the information potential of the occultation experiment in order to observe new features and gain deeper insight into the ionosphere is obvious. But it's not the only one. A novel radio science model of the refracted signal formation applicable to high potential occultation put into the foundation of the experiment along with classical approaches, will allow us to obtain more reliable data on the atmosphere, night-side ionosphere and at lower altitudes of the day-side ionosphere (Gavrik et al., 2013). To summarize, occultation experiments together with the equipment on board the orbiter may be seen as one of the cheapest and safest ways to get new and important findings in the projected new and important mission to Venus.

Radio Occultation Objectives

Radio-science investigations in the Venera-D mission should be carried out with coherently related sinusoidal signals at wavelengths of X (3.6 cm) and S (13.7 cm) bands and high-potential radio links. They fall into three broad categories of experimentation and observation. First, the study of the planetary atmosphere and ionosphere. Second, investigations of the so-called 'bistatic scattering' properties, or in other words, scattering of electromagnetic waves on the propagation paths from a spacecraft via the planetary surface to an Earth receiving station. Third, measurements of the solar wind and corona properties. The following experiments can be contemplated:

1. Measurements of electron concentration profiles at altitudes from ~70 km to ~1000 km and profiles of temperature, density and pressure at altitudes from ~40 km to ~100 km. All of them can be measured as a function of latitude, local time, sunspot number and season.
2. Studying the nature of layered structures in the atmosphere and ionosphere of Venus and their relations to known or observable wave processes as well as the solar wind intensity and sunspot number.
3. Detect new and unravel the competing processes in the ionosphere, thermosphere and atmosphere on the day-side and night-side of the planet.
4. Mapping Venus surface scattering properties, its dielectric constant and density estimates, spotting areas with anomalies of 'bistatic scattering' properties.
5. Studying different scales of solar plasma inhomogeneities and their dynamics at different proximity points.
6. Verification of the mathematical models used in the wave propagation tasks adapted to space applications.

Radio Frequency Subsystems and Measurement Techniques

Experience of the previous missions indicates that the dynamic range of the radio links used should be not less than 45 dB each and be balanced. The latter is no less important for reliable interpretations. It requires that the difference in the power transmitted at X- and S-band should not be so dramatic and the potentials of both links should be high enough to prevent the noise of one of them dominating the final result. Otherwise the interpretations based on the expectedly more efficient dual-frequency technique could be even worse than interpretations utilizing just one frequency with a larger dynamic range.

Ground-based subsystems

Radio science measurements in the Venera-D mission imply the use of ground-based antennas of 70 and 64 m in diameter and receivers with hydrogen maser frequency standards. They must be assembled in a scheme implying both a wide band and narrow band (with a phase-locked loop) signal registration at X- and S-band. The latter is a precision measurement tool, while the wide band registration will allow us to expect a reliable and interpretable signal despite a high dynamic of its phase, if and when it happens, or when the probe just egresses the planetary limb and the signal power is expected to be quite low for the normal operation of the phase-locked loop subsystem.

Space-based subsystems

To accomplish all the investigations listed above there should be a 30 W X-band transmitter and not less than 40 W S-band transmitter on board. Both of them are expected to be well-stabilized, well-shielded, thermally controlled and radiation-hardened so as to provide required stability within the range of time intervals from 0.1 to 600 s, which are equal to typical periods of signal discretization in different occultation measurements. Given that short-term frequency deviations could be directly projected on to the fine structure of the planetary medium, the heterodynes on board should have a value of frequency deviation not greater than $(1-4)10^{-13}$ within the range of time intervals of up to 10 s.

Backward and direct occultation with interferometric reception

All three categories of experimentation and observation may be carried out both with direct (with transmitters on board) and backward (with transmitters on Earth) techniques, that allow us to make the information scope of the experiments wider. As for solar plasma, the use of direct occultation with a short period of signal discretization and synchronous reception by two stations (interferometric reception) looks even more important as it could give us new and more precise knowledge of the size of inhomogeneities and their speed. The latter is planned to be estimated by means of what might be called a backward 'inverse' Doppler technique.

A Novel Radio Science Model and Data Processing Technique

Using the data of the Venera-15 and 16 missions and specially-designed precision data processing techniques it has finally been experimentally confirmed that within the geometrical optics application range a change in energy flux density of the signals scattered on the medium with spherical symmetry is directly proportional to the value of the gradient of a wave vector deviation angle. It means that signal power fluctuations in atmospheric and ionospheric occultation experiments must be directly correlated to the speed of frequency changes because these media can be seen as spherically symmetrical due to the impact of the gravity field (Gavrik et al., 2013). At the same

time pure stochastic fluctuations of power (noise) and frequency are not correlated. Given the fact that this is a new way of signal representation, the door is opened to a novel data processing technique which is expected to allow us to gain deeper insight into the ionosphere and investigate the processes of interaction between the atmosphere and ionosphere more reliably, including propagation of density fluctuations from the atmosphere to the lower ionosphere (Gavrik et al., 2013).

The effect underlying such an investigation can be detected in a spherically layered medium in the absence of the diffraction and extinction of electromagnetic waves if the layers are dense enough and if the level of instrument noise is low. That is why the data of the Venera-15 and 16 missions, where the deep-space probes operated with higher transmitted power and at lower frequencies than in most other missions, was crucially required to prove the concept of a novel data processing technique. The most intriguing result obtained with this data is that the investigation of fine structures of the Venusian ionosphere at extremely low altitudes of about 80–120 km above the planetary surface level where the concentration of electrons is still extremely low became possible (Gavrik et al., 2013). The idea of such a technique comes from a comparison of two diagrams with values of signal power (X -axis) along altitudes (Y -axis), while one of them stands for experimentally observed variations and fluctuations of signal power (W_0) in the atmosphere and ionosphere and the other stands for a “prediction” of the same parameter (W_1) calculated on the basis of the signal frequency using the relations discussed. It must be emphasized that this kind of prediction applies to the ionosphere only, and so the difference allows us to investigate the upper atmosphere efficiently.

Typical stratified periodical variations of W_0 and W_1 are presented in Fig. 1. They depend on the medium refractive index and a part of them are supposedly the result of wave-like interactions between the atmosphere and ionosphere of Venus. One can see a good match between diagrams within a range of altitudes from 80 to 180 km. But fluctuations above 180 km bear a pure stochastic nature, which indicates that this interval of altitudes does not contain detectable layers with steady deviations of the refractive index. As follows from Fig. 1 the atmospheric extinction grows faster below 80 km and there are no detectable ionized layers. Thus the data of Venera-15 and -16 indicates that layers constantly exist not only in the Earth’s lower ionosphere, but also in the day-side ionosphere of Venus. A deeper investigation of the nature of such perturbations will be possible in the Venera-D mission through a comparison of data of different experiments. The proposed approach will allow us to study a fine structure of the interaction between the atmosphere and ionosphere using variations in the power and frequency of two coherent signals. As a result, new knowledge of the propagation of density perturbations from the atmosphere into the ionosphere can be gained, including the propagation of wave-type atmospheric perturbations.

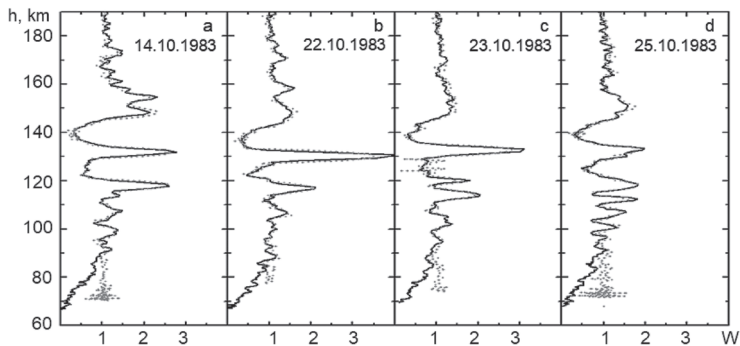


Figure 1: Comparison of profiles of $W_0(h)$ — experimentally observed variations of signal power at 32 cm wavelength due to the refraction in the atmosphere and ionosphere at h — altitude above the surface level (solid line, arbitrary units) with $W_1(h)$ — a “prediction” of $W_0(h)$ calculated on the basis of signal frequency for the ionosphere only (dots). The data were obtained in 4 sessions (a, b, c, d) of the Venera-15 mission

Conclusion

The data gathered during the period of intensive investigation of Venus made it possible for us not only to study the structure of its ionosphere and atmosphere but also to form and test new approaches to signal processing and interpretation of occultation experiments. Given the fact that there is more than five years’ time period before the carrier-rocket launch when both space- and ground-based radio-frequency systems could be re-engineered, the Venera-D mission presents

a unique opportunity of using all the positive technical solutions of all the previous missions and escape those that were not very efficient. On top of that, a discussion on the L-band use — that was beyond the scope of this paper — looks quite advisable and practical during the proposed radio systems re-engineering as it is a long-mastered and well-studied band in Venusian investigations with even higher sensitivity to ionized medium than the suggested S-band.

Taking into account advances in the field of radio-electronic components and engineering, all the ideas discussed in this paper are about small-sized devices operating together with other instruments mounted on the Venera-D orbiter. At the same time optimized and balanced radio-frequency systems allow us to use new approaches to signal processing and interpretation of occultation experiments more efficiently which is no doubt the shortest and safest way to acquiring fundamentally new data on the atmosphere and ionosphere of the planet.

Acknowledgements

The work is partially supported by the RAS Presidium Program No. 1.7P.

References

- Armand, N. A., Gulyaev, Yu. V., Gavrik, A. L. et al. (2010) Results of solar wind and planetary ionosphere research using radiophysical methods, *Physics-Usppekhi*, 53(5), 517–523.
- Brace, L. H., Kliore, A. J. (1991) The structure of the Venus ionosphere, *Space Sci. Reviews*, 55, 81–163.
- Gavrik, A. L., Pavelyev, A. G., Gavrik, Yu. A. (2009) Detection of ionospheric layers in the Daytime Ionosphere of Venus at Altitudes of 80–120 km from VENERA-15 and -16 Two-Frequency Radio-Occultation Results., *Geomagnetism and Aeronomy*, 49(8), 1223–1225.
- Gavrik, A. L., Gavrik, Yu. A., Kopnina, T. F., Kuleshov, E. A. (2013) Oscillations Detected near the Lower Boundary of the Venus Ionosphere from the Radio Occultation Measurements of the Venera-15 and Venera-16 Satellites, *J. Communications Technology and Electronics*, 58(10), 985–995.
- Hinson, D. P. Jenkins, J. M. (1995) Magellan radio occultation measurements of atmospheric waves on Venus, *Icarus*, 114(2), 310–327.
- Imamura T., Ando H., Tellmann S. et al. (2017) Initial performance of the radio occultation experiment in the Venus orbiter mission Akatsuki, *Earth, Planets and Space*, 69, 137.
- Senske, D., Zasova, L. et al. (2017) Venera-D: Expanding our horizon of terrestrial planet climate and geology through the comprehensive exploration of Venus: Venera-D Final Report, https://solar-system.nasa.gov/docs/Venera-D_Final_Report_170213.pdf.
- Tellmann, S., Häusler, B., Hinson, D. P. et al. (2012) Small-scale temperature fluctuations seen by the VeRa Radio Science Experiment on Venus Express, *Icarus*, 221, 471–480.

MYSTERIES OF ATMOSPHERIC ESCAPE AND EVOLUTION AT VENUS

G. Collinson^{1,2}, R. Frahm³, A. Glocer¹, S. Barabash⁴, Y. Futaana⁴, J. Grebowsky¹, A. Coates⁵, D. Mitchell⁶, T. Moore¹, D. Sibeck¹, N. Omidi⁷, L. Jian¹, T. Zhang⁸

¹ NASA Goddard Space Flight Center, Greenbelt, MD, USA

² The Catholic University of America, Washington, DC, USA

³ Southwest Research Institute, San Antonio, TX, USA

⁴ Institutet för rymdfysik, Kiruna, Sweden

⁵ Mullard Space Science Laboratory, University College London, UK

⁶ Space Science Laboratory, University of California, Berkeley, CA, USA

⁷ Solana Scientific, Solana Beach, CA, USA

⁸ Austrian Academy of Sciences, Space Research Institute, Graz, Austria

Keywords: evolution, atmosphere, water history, particle, fields, orbiter

Introduction

Orbiter-based in-situ particle and fields measurements are a crucial tool for the exploration and understanding of Venus. Unlike landers and aerial platforms, orbiters offer long duration observations covering the entire planet, and particle and fields instrument packages thus flew on Mariner, Venera, Pioneer Venus Orbiter, and most recently Venus Express. However, despite large existing datasets, many mysteries remain that are crucial to understanding the evolution of the atmosphere and water on Venus that can only be solved with particle and fields instruments, but cannot be answered due to limitations in past sensors on these missions. We outline some of these key questions, and advocate that a particles and fields package should be included as part of Venera-D's core science instruments, and even a single spacecraft armed with such a package could make significant advances in our understanding of Earth's closest analogue.

INTERIOR
AND GEOCHEMISTRY

INTERIOR STRUCTURE MODELS OF VENUS

T. Gudkova¹, V. Zharkov¹, Ph. Lognonné²

¹ Schmidt Institute Physics of the Earth RAS, Moscow, Russia

² Université Paris Diderot – Sorbonne Paris Cit., Institut de Physique du Globe de Paris, Paris, France

Abstract

We perform calculation of interior structure models of Venus satisfying all available observational data. The models are required to satisfy the mean density as derived from the total radius R , the mass M and the Love number k_2 . The core radius is most likely larger than 3000 km. The present limits of the moment of inertia cannot constrain the parameters of the crust.

Introduction

Contrary the Earth, the interior structure of Venus is poorly known, as no seismic data have been obtained from which to constrain its internal structure. Available interior models of the planet are based the observations of gravity field and topography: the mass, the mean radius, the value for the mean moment of inertia (though its moment of inertia is practically unknown, presently estimated to the second digit only, the I/MR^2 is in the limits of 0.331 and 0.341) and the Love number k_2 . The mean moment of inertia could be determined from the quadrupole moments of the gravitational field and the precession rate of the spin axis, but the latter is unknown. The lack of an intrinsic magnetic field and the value of Love number $k_2 = 0.295 \pm 0.066$ (which derived from the solar tidal on Venus) obtained in (Konopliv and Yoder, 1996) from Doppler radio tracking of Magellan and Pioneer Venus spacecraft data, indicate that the core is partially or entirely liquid, but there is a little to constrain the core radius.

Interior models

Venus is compositionally similar to Earth. Our current knowledge on Venus interior is mostly theoretical and derived from compositions of the Earth. The most conservative model of its deep interior is a transportation of the Earth's structure scaled to Venus' radius and mass. A number of models have been constructed based on Parametric Earth Model (Dziewonski et al., 1975) as a starting point (Zharkov et al., 1981; Yoder, 1995). For construction of a model of Venus it is reasonable to use the equation $p(\rho)$ for the Earth as the initial equation of state. The convenience of such a choice, furthermore, that it is automatically takes into account the influence of temperature on the equation of state, since the temperature distribution on both planets is evidently similar for depths greater than ~ 200 km. In these models mantle composition is varied by changing the molar fraction of Fe relative to Mg ($f_{Fe} = Mg/(Mg+Fe)$) using the properties of forsterite (Mg_2SiO_4) and fayalite (Fe_2SiO_4) as analogs. The core density is varied from an earth-like model by introducing a constant difference $\delta\rho_c$.

Parametrical Venus model (PVM), in which the density distribution $\rho(x)$ and the compressional $V_p(x)$ and shear $V_s(x)$ velocities are given by piecewise-continuous analytical functions of dimensionless radius $x = r/R$ was constructed in (Zharkov, Zaslurskii, 1982) (Table 1). The continuous segments of the distributions are described by polynomials in x , not larger than the third degree. Compressional $V_p(x)$ and shear $V_s(x)$ velocities are obtained from PEM-C model of the Earth.

Table 1: Parametrical Venus model (PVM) (Zharkov, Zaslurskii, 1982)

| $l, \text{ km}$ | $\rho, 10^3 \text{ kg/m}^3$ | $V_p, \text{ km/s}$ | $V_s, \text{ km/s}$ |
|-----------------|--|-----------------------------------|------------------------|
| 70–470 | $7,374 - 4,146x$ | $27,17 - 19,74x$ | $14,4 - 10,4x$ |
| 471–746 | $10,101 - 6,871x$ | $19,32 - 10,59x$ | $13,54 - 9,21x$ |
| 747–2843 | $6,77 - 2,467x - 0,266x^2$ | $14,84 - 0,074x - 5,011x^2$ | $6,83+2,65x - 3,95x^2$ |
| 2843–6050 | $11,742 - 0,17x - 5,402x^2 - 3,642x^3$ | $9,88+0,66x - 9,125x^2 - 0,74x^3$ | |

$\rho_{crust} = 2800 \text{ kg/m}^3; x = r/R; R = 6050 \text{ km}$

In this study we present a set of interior structure models of Venus. To construct interior structure model of a planet it is common to use the equation of hydrostatic equilibrium, the equation for mass of a sphere of radius $M(r)$, and obtained density profile should to satisfy the moment of inertia.

Unfortunately, as mentioned above, its moment of inertia is poorly known. The equation of state $\rho = \rho(p)$ for materials of which the Venus is composed should be added to this set of equations.

As a starting point we take parametric simple model of Venus PVM (Zharkov, Zasurskiy, 1982), listed in Table 1. We have varied the radius of the core R_{core} , the thickness and density of the crust (d_{crust} and ρ_{crust}), the mantle density (Table 2). The mantle density is varied by introducing the coefficient A : $\rho(p) = \rho(p)A$, where $\rho(p)$ is the equation of state for PVM model. The curves $\rho(p)$ are produced by a shift along the p axis. Specifically, this shift Δp was varied within limits of about 6 percent of p . When it is negative (A is less than unity), the models could be interpreted as possessing a deficit of iron in the silicates of the mantle. A reduction of density by 1 % corresponds to a reduction of 1.4 % in the content of iron in the silicates of the mantle (Zharkov, 1992).

Table 2. Trial interior structure models of Venus (covering a wide range of mantle compositions and core size)

| Model | d_{crust} | ρ_{crust} | A | I/MR^2 | I_{core}/MR^2 | k_2 |
|----------------------|-------------|----------------|-------|----------|-----------------|--------|
| $R_{core} = 2800$ km | | | | | | |
| 1 | 70 | 2.8 | 1.057 | 0.3440 | 0.0173 | 0.2123 |
| $R_{core} = 2900$ km | | | | | | |
| 2 | 70 | 2.8 | 1.045 | 0.3417 | 0.020 | 0.2224 |
| $R_{core} = 3000$ km | | | | | | |
| 3 | 70 | 2.8 | 1.033 | 0.3397 | 0.024 | 0.2340 |
| $R_{core} = 3200$ km | | | | | | |
| 4 | 16 54 | 2.67 2.9 | 1. | 0.3345 | 0.0325 | 0.2552 |
| $R_{core} = 3211$ km | | | | | | |
| 5 | 100 | 2.60 | 1.01 | 0.3347 | 0.033 | 0.2607 |
| 6 | 70 | 2.60 | 1.00 | 0.3331 | 0.033 | 0.2538 |
| 7 | 50 | 2.60 | 1.00 | 0.3339 | 0.033 | 0.2560 |
| 8 | 30 | 2.60 | 1.00 | 0.3347 | 0.033 | 0.2582 |
| 9 | 10 | 2.60 | 1.00 | 0.3355 | 0.033 | 0.2604 |
| 10 | 100 | 2.80 | 1.01 | 0.3359 | 0.033 | 0.2642 |
| 11 | 70 | 2.80 | 1.00 | 0.3340 | 0.033 | 0.2563 |
| 12 | 50 | 2.80 | 1.00 | 0.3346 | 0.033 | 0.2578 |
| 13 | 30 | 2.80 | 1.00 | 0.3351 | 0.033 | 0.2592 |
| 14 | 10 | 2.80 | 1.00 | 0.3357 | 0.033 | 0.2608 |
| 15 | 100 | 2.95 | 1.01 | 0.3369 | 0.033 | 0.2667 |
| 16 | 70 | 2.95 | 1.00 | 0.3346 | 0.033 | 0.2581 |
| 17 | 50 | 2.95 | 1.00 | 0.3350 | 0.033 | 0.2591 |
| 18 | 30 | 2.95 | 1.00 | 0.3354 | 0.033 | 0.2600 |
| 19 | 10 | 2.95 | 1.00 | 0.3357 | 0.033 | 0.2610 |
| $R_{core} = 3300$ km | | | | | | |
| 20 | 70 | 2.8 | 0.985 | 0.3316 | 0.0375 | 0.2667 |
| $R_{core} = 3400$ km | | | | | | |
| 21 | 70 | 2.8 | 0.966 | 0.3287 | 0.043 | 0.2771 |
| $R_{core} = 3500$ km | | | | | | |
| 22 | 70 | 2.8 | 0.946 | 0.3259 | 0.049 | 0.2891 |

The thickness of the venusian crust is under debate. Till recently, it assumed that the crust of Venus is thick, about 60–70 km. It was well founded, as the gabbro-eclogite transition should occur at this depth, and eclogite sinks because of its high density.

Estimates of venusian mean crustal thickness, obtained from the thermal history and the interpretation of the gravity and topography data, range from 15 km to 35 km (Breuer, Moore, 2007; Wicczorek, 2007). Jiménez-Díaz et al. (2015) present a crustal thickness model, in which the majority of venusian crust is 20–25 km thick, with thicker crust under the highlands. In the paper (Yang et al., 2016) it was concluded that the global crustal thickness calculated from isostatic components of the topography and gravity is in the range of 12–65 km from a mean crustal thickness

of 25 km, and is much more consistent with the Venusian dynamic evolution. Nevertheless, in the paper (Dumoulin et al., 2017), the authors take 60 km thick crust. Rock samples of various landers give the current estimate of venusian crustal composition and density of 2700–2900 kg·m⁻³ (Grimm, Hess, 1997), which corresponds to basaltic rocks.

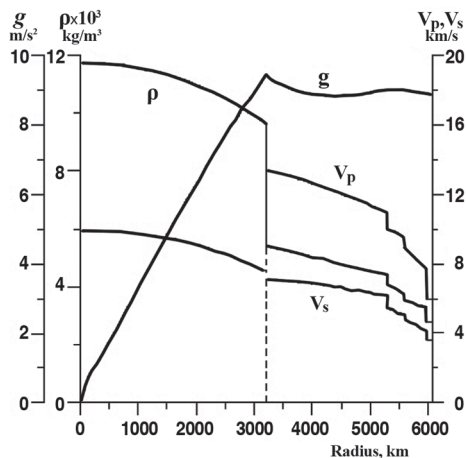


Figure 1: Distributions of density ρ , gravity g and compressional V_p and shear V_s velocities as a function of radius of Venus

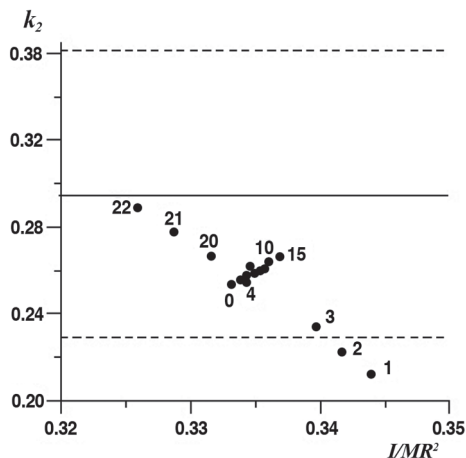


Figure 2: Model estimates of the elastic Love number k_2 versus the moment of inertia for a set of interior structure models of Venus, listed in Table 2. The Love number k_2 (solid line) and the scatter of the Love number (dashed lines) are shown

Based on foresaids, we adopt the average crustal density in the range of 2600–2950 kg·m⁻³ and vary the thickness of the crust from 10 km to 100 km, in our research.

As seen from the Table 2, the thickness of the crust strong influences the model value of the moment of inertia. Figure 1 displays the distribution of density, gravity and seismic velocities along the radius for the model V4. The model has two-layer crust (16 km and 54 km thick layers with the density 2670 and 2900 kg·m⁻³, respectively), a silicate mantle and a core (the radius is 3200 km). For each model, listed in Table 2, the Love number k_2 is calculated. Fig. 2 shows the Love number k_2 versus the moment of inertia for a wide range of crust and mantle composition, and the core size. It is seen that k_2 is most strongly correlated with the core radius.

Seismic activity

At the moment seismic activity of Venus may be only theoretically estimated. By analogy with the terrestrial geological structures, it is assumed, that mountains on Venus are of volcanic origin. It is also assumed, that complex relief points out the tectonic activity of the planet. It is possible that volcanic activity on Venus takes place at the present moment. Venus is assumed to be a seismically active planet (Stofan et al., 1993; Knapmeyer et al., 2006). Prediction suggests that 100 quakes of surface wave magnitude greater than 5 could be released. The events of magnitude 6 will occur 5 times less frequently (the maximum magnitude is 6.5).

Future experiments

There are a number of key questions about the structure of planetary mantle and a core (the radius and geophysical state of the core), which could be considered through long-lasting surface-based measurements and a multidisciplinary approach. But the temperature conditions at the surface of this planet hardly make possible long-term ground-based measurements.

Technical conditions for seismic experiments on the surface of Venus are very specific. Due to very high temperature and pressure on the surface (the surface temperature 733 K and the surface pressure 92 bar), none of the instruments worked there more than two hours. For Venus, a remote detection in the atmosphere might provide the opportunity to perform seismic measurements. That is why the detection of atmospheric signals associated with quakes might be an interesting alternative to observation performed by seismometers.

The physical mechanism producing the atmospheric infrasonic waves from seismic surface waves and their propagation is as follows: Such sources as atmospheric explosions or shallow quakes lead to a strong vertical displacements of the surface, which generate pressure waves. These pressure waves propagate in the atmosphere with sonic speed and their amplitudes are getting several orders higher while they reach the ionosphere. In particular, the surface Rayleigh waves arising after a quake, produce surface displacements, which generate spread up acoustic waves (Garsia et al., 2005; Lognonné, Johnston, 2007).

New orbital missions dedicated to more precise geodetic measurements than Magellan mission would provide a more accurate value of the mean moment of inertia ratio and thus, more insight on the interiors (Mocquet et al., 2011). The proposed VERITAS mission would generate an improved accuracy of the gravitational field of 3 mGal, with a spatial resolution of 145 m (Smrekar et al., 2016).

Conclusions

For Venus there are fewer constraints than unknowns. We have presented Earth-like interior structure models of Venus covering a wide range of density and thickness of the crust, mantle composition and core size. A lot of models fit the observations; data points within uncertainty. It is shown that k_2 is most strongly correlated with the core radius, which it is most likely larger than 3000 km. The thickness of the crust strongly influences the model value of the moment of inertia. The determination of the moment of inertia could better constrain the parameters of the crust. In this study, we have considered only elastic models of Venus. As shown in (Dumoulin et al., 2017) unelasticity of the mantle should be incorporated in the models, that leads to the increase of the model value of the Love number.

Acknowledgements

This work is partly financially supported by the Programme of Presidium RAS 28.

References

- Breuer, D., Moore, W. B. (2007) Dynamics and thermal history of the terrestrial planets, the Moon and Io, In: Spohn, T. (Ed.) *Treatise on geophysics. Planets and Moons*, 10, 299–348.
- Dumoulin, C., Tobie, G., Verhoeven, O., Rambaux, N. (2017) Tidal constraints on the interior of Venus, *J. Geophys. Res. Planets*, 122(6), 1338–1352, doi: 10.1002/2016JE005249.
- Dziewonski, A. M., Hales, A. L., Lapwood, E. R. (1975) Parametrically simple Earth models consistent with geophysical data, *Phys. Earth Planet. Inter.*, 10, 12–48.
- Garsia, R., Crespon, F., Ducic, V., Lognonné, P. (2005) Three-dimensional ionospheric tomography of postseismic perturbations produced by the Denali earthquake from GPS data, *Gephys. J. Int.*, 163, 1049–1064.
- Grimm, R. E., Hess, P. C. (1997) The crust of Venus, In: *Venus II*, Univ. of Arizona Press, Tucson.
- Jiménez-Díaz, A., Ruiz, J., Kirby, J. F., Romeo, I., Tejero, R., Capote, R. (2015) Lithospheric structure of Venus from gravity and topography, *Icarus*, 260, 215–231.
- Knappmeyer, M., Oberst, J., Hauber, E., Wahlsch, M., Deuchier, C., Wagner, R. (2006) Implications of the Martian surface fault distribution and lithospheric cooling for seismicity. A working model, *J. Geophys. Res.* 111, E11006, doi: 10.1029/2006JE002708.
- Konopliv, A. S., Yoder, C. F. (1996) Venusian k_2 tidal Love number from Magellan and PVO tracking data, *Geophys. Res. Lett.*, 23, 1857–1860.
- Lognonné, P., Johnston, C. (2007) Planetary seismology, *Treatise on Geophysics*, 10, 69–122.
- Mocquet, A., Rosenblatt, P., Dehant, V., Verhoeven, O. (2011) The deep interior of Venus, Mars, and the Earth: A brief review and the need for planetary surface-based measurements, *Planet. Space Sci.*, 59, 1048–1061.
- Smrekar, S. E., Hensley, S., Dyar, M. D., Helbert, J. (2016) VERITAS (Venus Emissivity, radio Science, InSAR, topography and Spectroscopy): a proposed discovery mission, *Lunar and Planetary Science Conference*, 47, 2439.
- Stofan, E., Saunders R., Senske D., Nock K., Tralli D. (1993) Venus Interior Structure on Venus, *Proc. Workshop on Advanced Technologies for Planetary Instruments*, Lunar and Plan. Sci. Inst., Houston, Tex.
- Wieczorek, M. A. (2007) Gravity and topography of the terrestrial planets, In: Spohn, T. (Ed.) *Treatise on geophysics. Planets and Moons*. Elsevier, Amsterdam, 10, 105–206.
- Yang, A., Huang, J., Wei, D. (2016) Separation of dynamic and isostatic components of the Venusian gravity and topography and determination of the crustal thickness of venus, *Planet. Space Sci.*, 129, 24–31.

- Yoder, C. F. (1995) Venusian spin dynamics, In: *Venus II*. 1087–1124.
- Zharkov, V. N., Kozlovskaya, S. V., Zasurskii, I. Ya. (1981) Interior structure and comparative analysis of the terrestrial planets, *Adv. Space. Res.*, 1, 117–129.
- Zharkov, V. N., Zasurskii, I. Ya. (1982) Physical model of Venus, *Astron. Vestnik*, 16, 18–28 (in Russian).
- Zharkov, V. N., (1992) Model of the interior structure: earth-like models, In: Barsukov V. L., Basilevsky A. T., Volkov V. P., Zharkov V. N. (Eds.) *Venus geology, geochemistry and geophysics research results from the USSR*, the University of Arizona Press, 233–240.

ON PARAMETERS OF THE EARTH-LIKE MODEL OF VENUS

V. Zharkov, T. Gudkova

Schmidt Institute Physics of the Earth Russian Academy of Sciences

Abstract

A short review on the history of the construction of the interior structure earth-like model of Venus is given. Analysis of available observational data is performed. By using Venusian gravity field data the parameters and the precession constant of the Earth-like model of Venus are estimated.

Introduction

Venus belongs to the planets of the Earth group, which also includes Mercury, Earth, Mars, and the Moon. All the planets of the earth-like group, including Venus and Earth, are relatively small. As a result, in the process of their formation they were unable to retain the hydrogen-helium component which is the most common in space. Moreover, all these planets have a deficit of water, methane, and ammonia — low-boiling compounds which are rather common in space. The main components of the planets of the earth-like group are silicates, iron, and compounds between iron and sulfur.

According to modern theories, the planets, satellites, and comets were formed as a result of the evolution of a protoplanetary cloud, which at an early stage of its existence was a gas/dust cloud. In constructing the model of a planet, it is important to have an idea as to the chemical composition of protoplanetary cloud contain indications as to the possibility of chemical fractionation of iron, sulfur, and radioactive sources as a function of the temperature conditions of condensation at various distances from the Sun (Grossman, Larimer, 1974; Lewis, 1972). One of the main problems in constructing models of the earth-like planets is their comparative analysis and the production of quantitative estimates of the concentration of dust component in the original gas/dust cloud, as well as confirming the conclusions of the space-chemical schemes of condensation of this cloud.

By its mechanical parameters — mass M , mean radius R , and mean density ρ_0 — Venus is reminiscence of Earth. Thus it is perfectly natural that the first modern model of Venus, by Harold Jeffreys (1937), was based on the first modern model of Earth (Bullen, 1936). At that time, which now appears to us infinitely remote, the value of the mass $M = 4.91 \cdot 10^{24}$ kg was exaggerated by 1 % and the mean radius $R = 6150$ km was known with a good precision. In the two-layer model of the planet, the density in the mantle varied from 3290 to 5440 $\text{kg} \cdot \text{m}^{-3}$, and that in the core from 9600 to 11,100 $\text{kg} \cdot \text{m}^{-3}$; at the mantle-core boundary, the pressure P was 1.23 Mbar, while at the center of Venus it was 2.4 Mbar; the mass of the core was $1.06 \cdot 10^{24}$ kg, and its radius was 2910 km. Comparing these figures with the parameters of the model of Venus, derived in (Zharkov, 1983), we may conclude that the mechanical model of the planet in (Jeffreys, 1937) (the distribution of density $\rho(l)$, pressure $p(l)$, and gravity along the depth $g(l)$) was closely related.

After the work of Jeffreys (1937), in the classical monograph of Urey (1952), the conceptual basis was considerably expanded, and has been used everywhere since then to construct models of planets, including those of the Earth group. Harold Urey emphasized the importance of cosmochemical data and cosmogonic concepts. It became customary to compare the composition of Venus not only with that of the Earth, but also with that of the meteorites. Interest grew in the problem of the distribution of the concentration of iron and the other main elements of the Earth group. A survey of the works carried out in the 1950's and 1960's is given in the books (Levin, 1970; Bullen, 1975). The basic conclusion of these works is that the interior structure of Venus is similar to that of Earth.

In the 1970's and 1980's, an increased interest has been again noted in the investigation of the internal structure of Venus (Ringwood, Anderson, 1977; Kalinin, Sergeyeva, 1979; Zharkov, Zasurskiy, 1982). In the works of Ringwood and Anderson (1977) and Kalinin, Sergeyeva (1979) it was shown that an Earth-like model of Venus should have an average density about 2 % larger than the observed average density. In the work (Kozlovskaya, 1982), a large number of mechanical models of Venus were considered in order to identify discrepancies in its composition compared with the average chemical composition of Earth. The conclusions of this work and works devoted to the

construction of a physical model of Venus (Zharkov, Zaslurskiy, 1982; Zharkov et al., 1981) were described in (Zharkov, 1983). In the work of Anderson (1980) a new interpretation was proposed for the average density of Venus, which is reduced from that of the Earth. Previously this fact had been interpreted as an indication of a difference in the bulk content of iron (Kovach, Anderson, 1965), sulfur (Lewis, 1972), or in the degree of oxidation of the mantle (Ringwood, Anderson, 1977). However, if we assume that Venus has a very thick outer basalt shell, and the corresponding basalt fraction of Earth by subduction into the mantle is present in the eclogite phase (Anderson, 1979), then the depressed average density of Venus is more likely produced by tectonic, rather than cosmochemical factors.

Since the time of the first publications of Jeffreys (1937) and Urey (1952), geophysics has greatly changed its aspect (Zharkov, Trubitsyn, 1978, 1980; Schubert, 1979; Phillips, Ivins, 1979; Stacey, 1977; Zharkov, 1983). Now, we are interested not only in a mechanical model of the planet (the distribution of $\rho(l)$, $p(l)$ and $g(l)$ in its interior), but also not to a lesser extent in a physical model that gives the distribution of many physical parameters such as the heat capacity, the coefficient of thermal expansion, adiabatic temperatures, the coefficient of heat conduction, effective viscosity, and etc. Because of the development of works on the hydrodynamics of the planetary interiors, the problem of determining the distribution of the temperature in their interiors has undergone significant changes (Toksöz et al., 1978; Zharkov, 1983; Steinberger et al., 2010; Armann, Tackley, 2012).

The tectonic regime of Venus and the other terrestrial planets differs from the plate-tectonic regime. Consequently, the Moon and, apparently, Mercury, Venus, and Mars should have significantly thicker crust layers than the Earth. The thickness of the lunar crust is ~ 50 km. The thickness of the crust in the other terrestrial planets is probably within the same limits (at present this is a mere supposition, which it is highly interesting to check out). A displacement of the center of the geometrical figure of a planet with respect to its center of mass may be interpreted as an indication of considerable regional variations in the thickness of the crust. On Venus the distance between these centers is 0.339 ± 0.088 km, which is much less than the corresponding differences for Earth (2.1 km, Balmino et al., 1973), the Moon (2.0 km, Bills, Ferrari, 1977) and Mars (2.5 km, Bills, Ferrari, 1978). Consequently, the variation of thickness of the Venusian crust is less than that of the other Earth-type planets. This fact may be regarded as an indication that the outer layers of Venus are closer to spherical symmetry than those of Earth.

Analysis of observational data

Observational data for Venus are summarized in the Table, where, for comparison, analogous parameters for Earth are given. The Table lists the mass M , the first coefficients for expansion of the gravitational potential into spherical functions (Konopliv et al., 1999), the period of rotation τ , the equatorial R_e and mean R radii, the mean density ρ_v , the nondimensional moment of inertia I/MR^2 .

The value of a small parameter of the theory of figure q , the dynamic flattening (the flattening of the outer equipotential surface of the gravitational potential of the planet) α , and the geometrical flattening e , given by

$$q = \frac{\omega^2 R_e}{GM} = \frac{4\pi^2 R_e^3}{GM\tau^2}, \quad \alpha = \frac{3}{2}J_2 + \frac{1}{2}q, \quad e = \frac{R_e - R_p}{R_e}, \quad (1)$$

where ω is the angular speed of rotation, G is the gravitational constant, and R_p is the polar radius.

For planets close to hydrostatic equilibrium, the mean radius R to a first approximation is expressed by R_e , in the formula $R = (1 - \alpha/3)R_e$. As is known (Zharkov, Trubitsyn, 1978; Zharkov, 1983), for an equilibrium planet the values of q and J_2 are of the same order of smallness. Referring to the Table 1, we find out that, for Venus, J_2 is 72 times larger than q . Consequently, we may assert that Venus is the most nonequibrated planetary body in the solar system. This fact is evidently not random, since the rotation of Venus in the past was greatly retarded by tidal friction. If we take the ratio of J_2/q for an effectively equilibrated Venus about 0.3 (i.e., the same as for the Earth, see the Table), then it is possible to determine the dynamic flattening for equilibrated Venus $\alpha_0 = 1.5J_2 + 0.5q_0 \sim 3.17J_2 \sim 13.9 \cdot 10^{-6}$. The corresponding equatorial radius R_e for Venus is shown in the Table. Thus, we see that, for Venus, R_e should practically coincide with R . The usual method of determining the moment of inertia of a planet close to a hydrostatic equilibrium from given J_2 and q is based on the formula of Radau-Darwin (Zharkov, Trubitsyn, 1978)

$$\frac{I}{MR^2} = \frac{2}{3} \left\{ 1 - \frac{2}{5} \left[5 \left(1 - \frac{3}{2} \cdot \frac{J_2}{\alpha_0} \right) - 1 \right]^{1/2} \right\}. \quad (2)$$

Table 1: Observational data and parameters of the figures of the Venus and Earth

| Parameters | Venus | Earth |
|---|--------------------------|----------------------|
| Mass M , 10^{24} kg | 4.869 | 5.974 |
| J_2 , 10^{-6} | 4.40 | 1082.64 |
| C_{22} , 10^{-6} | 0.8578 | 1.565 |
| S_{22} , 10^{-6} | -0.0955 | -0.894 |
| Period of rotation τ , days | 243.16 | 1.00 |
| Equatorial radius R_e , km | 6051.53* | 6376 |
| Mean radius R , km | 6051.5 | 6371 |
| Mean density ρ_0 , $\text{kg}\cdot\text{m}^{-3}$ | 5250 | 5514 |
| Mean moment of inertia I/MR^2 | 0.334* | 0.33076 |
| | 0.326** | |
| Small parameter of the theory of figure q | $6.1 \cdot 10^{-8}$ | $3.47 \cdot 10^{-3}$ |
| J_2/q | 72 | 0.31 |
| f , 10^{-6} | 3.45 | 7.2 |
| Precession constant H | $\sim 2 \cdot 10^{-5}$ * | 0.00327 |

* Values calculated theoretically for the interior structure model, see the text

** Value calculated with the help of formula (2), see the text

The scale of disequilibrium of Venus prevents us from finding out their moments of inertia in this manner. The constant of precession

$$h = \frac{C - A}{C}, \quad (3)$$

where C and $A \approx B$ are the polar and equatorial moments of inertia, which are also unknown for Venus and it is not clear whether H can be determined in the foreseeable future. As seen from the Table the model value of H is very small. Hence, apparently, it is not possible to obtain the moment of inertia of Venus from such observations in the near future. The young Venus, at an early epoch — when its rotation was not yet retarded by tidal friction — rotated much more quickly with a period of ~ 10 hr (Zharkov, Trubitsyn, 1978). Thus, the small parameter of the theory of figure, inversely proportional to the square of the rotation period ($q \sim \tau^{-2}$), was much larger (roughly 4 orders of magnitude) for the young planet, than the present value. The observed value of J_2 for Venus approximately 70 times greater than q , which may be regarded as certain relict value of this quantity, pertaining to the early and much larger values of q , when the rotation of the planet was not yet retarded by tidal friction to the present extent. Since the shells of Venus had been able to cool considerably and become excessively rigid (or excessively viscous), the planetary figure ‘froze’, as it was, at a certain remote epoch and therefore does not conform to the present angular speed of rotation of the planet. If we solve the formula of Radau-Darwin with respect to the period of rotation, we have

$$\tau_{J_2} = \left\{ \frac{\pi}{\rho_0 G J_2} \left[\frac{5}{6.25(1-1.5I)^2 + 1} - 1 \right] \right\}^{1/2}, \quad (4)$$

then we are able to estimate τ_{J_2} for the epoch when the corresponding equilibrium figure of the planet was ‘fixed’, as well as the value of J_2 , which has been retained to the present day. Assuming for the moment of inertia of Venus $I^* = 0.334$ (the value obtained from interior structure model calculations) or $I^{**} = 0.326$ (the value obtained with the help of formula (2)) (see the Table), we can find a certain paleoperiod of rotation of Venus, $\tau_0 = \tau_{J_2} \approx 15.7$ days. The obtained result suggests that Venus rotated more rapidly in the past. The rotation period of the young Venus was probably even less and equal to ~ 10 hr, although the disequilibrium of the planet, corresponding to such a rapid rotation, was apparently lost from the ‘memory’ of Venus due the ‘ductility’ of its mantle and core long ago.

Conclusion

Since the interior of the planets of the Earth group deviate from the state of hydrostatic equilibrium, the difference between their major moments of inertia with respect to the axes in the equa-

torial plane, is not equal to zero. This difference can be calculated from the formula (Zharkov, Trubitsyn, 1978)

$$f = \frac{B - A}{MR^2} = 4\sqrt{C_{22}^2 + S_{22}^2}. \quad (5)$$

The parameters are shown in the Table. We see that the value f for Venus is small and it is smaller than for Earth. This indicates that the density distribution in both planets is close to the axisymmetrical, with good accuracy. Moreover, this fact strengthens the idea that the large nonequilibrium value of J_2 for the planet represents a relict value which corresponds to more rapid rotation of Venus in a certain earlier epoch, as we have mentioned above.

Acknowledgements

This work is partly financially supported by the Programme of Presidium RAS 28.

References

- Anderson, D. (1979) The upper mantle transition region: eclogite? *Geophys. Res. Lett.*, 5, 433–436.
- Anderson, D. (1980) Tectonic and composition of Venus, *Geophys. Res. Lett.*, 7, 101–102.
- Armann, M., Tackley, P. (2012) Simulating the thermochemical magmatic and tectonic evolution of Venus's mantle and lithosphere: Two-dimensional models, *J. Geophys. Res. Planets*, 117, E12003, doi: 10.1029/2012JE004231.
- Balmino, G., Lambeck, K., Kaula, W. (1973) A spectral harmonic analysis of the Earth's topography, *J. Geophys. Res.*, 78, 21–22.
- Bills, B., Ferrari, A. (1977) A harmonic analysis of lunar topography, *Icarus*, 2, 244–259.
- Bills, B., Ferrari, A. (1978) Mars topography and geophysical implications, *J. Geophys. Res.* 83, 3497–3508.
- Bullen, K. E. (1936) The variation of density and the ellipticities of strata of equal density within the Earth, *Month. Not. Roy. Astron. Soc.*, Geophys. Suppl. 3, 395–401.
- Bullen, K. E. (1975) *The Earth's Density*, London, Chapman and Hall, New York : distributed by Halstead Press, 420.
- Jeffreys, H. (1937) The density distribution of the inner planets, *Month. Not. Roy. Astron. Soc.*, Geophys. Suppl. 4(1), 62–71.
- Grossman, L., Larimer, J. (1974) Early chemical history of the Solar System, *Rev. Geophys. Space Phys.* 12, 71–101.
- Kalinin, V., Sergeeva, N. (1979) On interior structure of Mars and Venus, *Phys. Earth*, 10, 3–15.
- Konopliv, A. S., Banerdt, W. B., Sjogren, W. L. (1999) Venus gravity: a 180th degree and order model, *Icarus*, 139(1), 3–18.
- Kovach, R., Anderson, D. (1965). The interiors of the terrestrial planets, *J. Geophys. Res.*, 70, 2873–2882.
- Kozloskaya, S. V. (1982) The internal constitution of Venus and the total iron content in the terrestrial planets, *Astron. Vestnik*, 16, 3–17.
- Levin, B. (1970) Internal constitution of terrestrial planets, In: A Dollfus (Ed.), *Surfaces and Interiors of Planets and Satellites*, London, Academic Press, 462–510.
- Lewis, J. (1972) Metal/silicate fractionation in the Solar System, *Earth Planet. Sci. Lett.*, 15, 286–290.
- Phillips, R., Ivins, E. (1979) Geophysical observations pertaining to solid-state convection in the terrestrial planets, *Phys. Earth. Int.*, 19, 107–148.
- Ringwood, A., Anderson, D. (1977) Earth and Venus: a comparative study, *Icarus*, 30, 243–253.
- Schubert, G. (1979) Subsolidus convection in the mantles of terrestrial planets, *Annu. Rev. Earth Planet. Sci.*, 7, 289–342.
- Stacey, F. (1977) *Physics of the Earth*, New York, Wiley, 414.
- Steinberger, B., Werner, S., Torsvik, T. (2010) Deep versus shallow origin of gravity anomalies, topography and volcanism on Earth, Venus and Mars, *Icarus*, 207, 564–577.
- Toksöz, M., Hsui, A., Johnston, D. (1978) Thermal evolutions of the terrestrial planets, Moon and Planets, 18, 281–320.
- Urey, H. (1952) *The planets: their origin and development*, New Haven, Yale Univ. Press.
- Zharkov, V. (1983) Models of the internal structure of Venus, *The moon and the Planets*, 29, 139–175.
- Zharkov, V., Trubitsyn, V. (1978) *Physics of planetary interiors*, Astronomy and Astrophysics Series, Tucson: Pachart.
- Zharkov, V., Trubitsyn, V. (1980) *Physics of planetary interiors*, Moscow, Nauka, 448 (in Russian).
- Zharkov, V. N., Kozlovskaya, S. V., Zasurskii, I. Ya. (1981) Interior structure and comparative analysis of the terrestrial planets, *Adv. Space Res.* 1, 117–129.
- Zharkov, V. N., Zasurskii, I. Ya. (1982) Physical model of Venus, *Astron. Vestnik*, 16, 18–28 (in Russian).

MODELING VENUS-LIKE WORLDS THROUGH TIME

M. J. Way^{1,2}, A. Del Genio¹, D. S. Amundsen^{1,3}

¹ NASA Goddard Institute for Space Studies, New York, NY, USA

² Department of Physics and Astronomy, Uppsala University, Uppsala, Sweden

³ Department of Applied Physics & Applied Mathematics, Columbia University, NY, USA

Abstract

We explore the atmospheric and surface history of a hypothetical paleo-Venus climate using a 3-D General Circulation Model. We constrain our model with the in-situ and remote sensing Venus data available today. Given that Venus and Earth are believed to be similar geochemically some aspects of Earth's history are also utilized. We demonstrate that it is possible for ancient Venus and Venus-like exoplanetary worlds to exist within the liquid water habitable zone with insulations up to nearly 2 times that of modern Earth.

Introduction

In a recent paper Way et al. (2016) (hereafter Paper I) demonstrated that the climatic history of Venus may have allowed for surface liquid water to exist for several billion years. Paper I utilized ROCKED-3D a planetary three-dimensional (3-D) General Circulation Model (Way et al., 2017). A number of assumptions were made in Paper I including: the use of a solar spectrum at 2.9Gya and 0.715Gya epochs, orbital parameters that remained unchanged from those of today, roughly modern Earth atmospheric gas constituents (no aerosols or anthropogenic gases were included, only 1 bar N₂, 400 ppm CO₂, and 1 ppm CH₄) and pressures (1013 mb), a shallow ocean whose volume was consistent with Deuterium to Hydrogen ratio (D/H) observations, and topographies consistent with those of modern Venus and a single simulation using modern Earth with a shallow 310 m deep fully coupled dynamic ocean. Except for one simulation that used a faster rotation rate (16 times the length of modern Earth's sidereal day) all of the simulations were able to maintain surface liquid water. In the meantime, we have inserted a more accurate radiation scheme called SOCRATES (Edwards, Slingo, 1996) that allows us to explore insulations up to 1.9 times that received by modern Earth. We have also explored a variety of boundary conditions involving different dynamic ocean depths as well as orbital configurations that include a tidally locked world as may have existed or may exist for similar exoplanetary worlds. In most of these additional cases we find that the planet is able to maintain liquid surface water while keeping the stratosphere relatively dry, hence avoiding the possibility of a moist greenhouse.

Methods

We utilized ROCKE-3D (Way et al., 2017) for the simulations in this study. ROCKE-3D is a 3-D GCM whose parent model ModelE2 (Schmidt et al., 2014) is used for Earth Climate studies. ROCKE-3D is an extension of ModelE2 that allows one to explore non-Earth specific worlds with differing atmospheric constituents, pressures, orbital parameters, gravities, incident stellar flux and other parameters that may be different on terrestrial worlds within our solar system and exoplanetary worlds outside. The choice of which model boundary conditions to assume for a paleo-Venus type world are constrained by what little data we have from ground, space and in-situ observations. The Venus topography used herein is taken from Magellan satellite data as described in Paper I. The value of the lower bound on the D/H ratio (Donahue, Russell, 1997) is such that it is possible to make a Dune-like land planet with as little as 10m water equivalent layer. We called 4 such simulations "Land Planets" (L1, L2, L1M and L2M, where $M = \text{Modern Solar Spectrum/insolation}$). In these simulations water is deposited as lakes at model start at the lowest elevation grid points. These are then allowed to expand, contract or form elsewhere as the model evolves and the competition between precipitation, evaporation and run-off take place (see Way, Wang, 2017). At the same time given the uncertainties in the history of the topography of Venus it is perhaps equally possible that it could have been a shallow aquaplanet in its early history. Hence our aquaplanet simulations utilize a shallow aquaplanet configuration of depth 158 m (A1, A2, A1M and A2M). The choice of 158 meters depth (specifically it is the lower boundary of one of our dynamic ocean levels) was a compromise between the 310 meter depth we have used for the 4 simulations with the same land/sea mask as used in Paper I (V1, V2, V1M and V2M), and the 100 meter depth typically used in $Q_{flux} = 0$ exoplanet simulations. We also explore the possibility that ancient Venus may have ex-

perienced a tidally locked, synchronously rotating phase. Previous work by Dobrovolskis, Ingersoll (1980), and Correia, Laskar (2003) and more recent work by Barnes (2017) have explored the possibility that a thinner 1-bar type atmosphere would not cause the same tidal torquing effects as the present day ~90-bar atmosphere that is theorized to explain Venus' retrograde rotation. However, see Leconte et al. (2015) for an opposing viewpoint. Thus, we explore what the climate of ancient Venus may have been like if it were tidally locked at one epoch of its history. This may be particularly relevant to exoplanetary studies since according to Barnes (2017) it is possible that any planet around a G-star including and interior to the orbit of Earth may eventually reach a tidally locked state. This type of system has rarely been explored and only for a subset of hypothetical worlds (e.g. Yang et al., 2014).

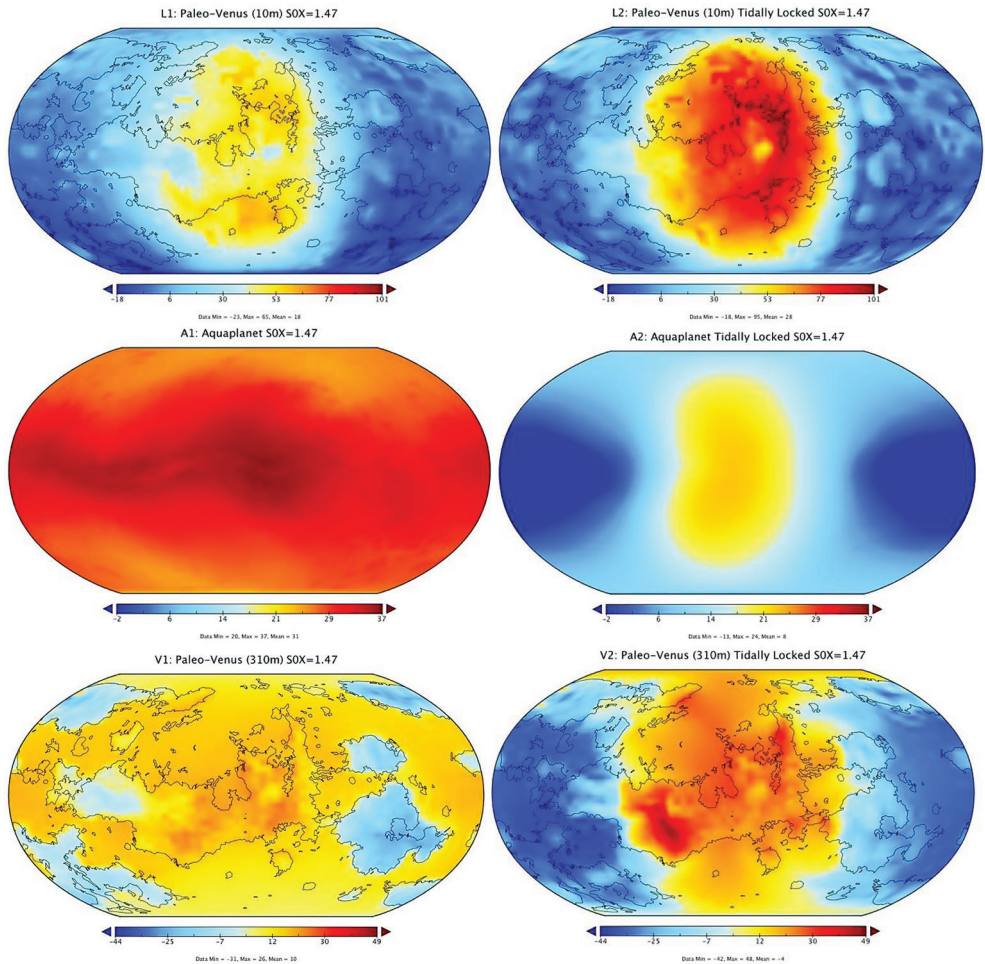


Figure 1: Surface temperature plots for the simulations listed in Table 1. Each set of 2 images have unique minimum and maximum scales. Non-tidally locked are averaged over 1/6th of a diurnal cycle, tidally locked are averaged over 100 orbits. The substellar point is located at the center of each image

Discussion

For the first 6 entries in Table 1 Fig. 1 shows images of the surface temperature averaged over 1/6 of a diurnal cycle for each non-tidally locked run and over 100 orbits for the tidally locked ones (there is too much variability on timescales comparable to those used for the non-TL runs). In Fig. 2 we show the mean surface temperature versus two different insolation (what Venus received 2.9Gya and today) for each simulation in a combined plot. These demonstrate the importance of the expanded Hadley cell (due to slow rotation rates) and the subsequent large cloud cover at the substellar point and play the same role here as in the simulations of Paper I. With the exception of the high insolation land planet simulation (L2M) and the high insolation Aquaplanet (A1M) the

planet is able to maintain liquid water across a large fraction of the surface and a dry stratosphere. For the two exceptions the situation is more complex. They are both warmer than most of the other simulations, and their stratospheres contain too much water (Fig. 2, right). L2M will lose what little water it has relatively quickly, while A1M will take perhaps a few billion years. At the same time several other of the high insolation runs are close to the limit and they may also lose their oceans over slightly longer timescales.

Table 1: Experiments and resulting temperatures: Temperature values for non-tidally locked worlds are from 1/6 of a diurnal cycle, whereas the tidally locked numbers come from a 100 orbit average

| Experiment | Land/Ocean | Spin Rate | Stellar Spectrum | Insolation | Temp. mean | Temp. max | Temp. min |
|----------------|-------------|----------------|------------------|------------|------------|-----------|-----------|
| L1 (001L) | Venus 10 m | Present Day | 2.9Gya | 1.47 | +20 | +70 | -18 |
| L2 (001L_TL) | « | Tidally Locked | « | « | +28 | +95 | -18 |
| A1 (001M) | Aquaplanet | Present Day | « | « | +31 | +37 | -21 |
| A2 (001M2_TL) | « | Tidally Locked | « | « | +8 | +24 | -13 |
| V1 (001J) | Venus 310 m | Present Day | « | « | +9 | +33 | -34 |
| V2 (001J_TL) | « | Tidally Locked | « | « | -4 | +49 | -44 |
| L1M (001Lc) | Venus 10 m | Present Day | Modern | 1.9 | +26 | +71 | -4 |
| L2M (001Lc_TL) | « | Tidally Locked | « | « | +33 | +87 | -6 |
| A1M | Aquaplanet | Present Day | « | « | +38 | +43 | +32 |
| A2M | « | Tidally Locked | « | « | +16 | +37 | -1 |
| V1M (001N2) | Venus 310 m | Present Day | « | « | +16 | +34 | -20 |
| V2M (001N2_TL) | « | Tidally Locked | « | « | +13 | +49 | -18 |

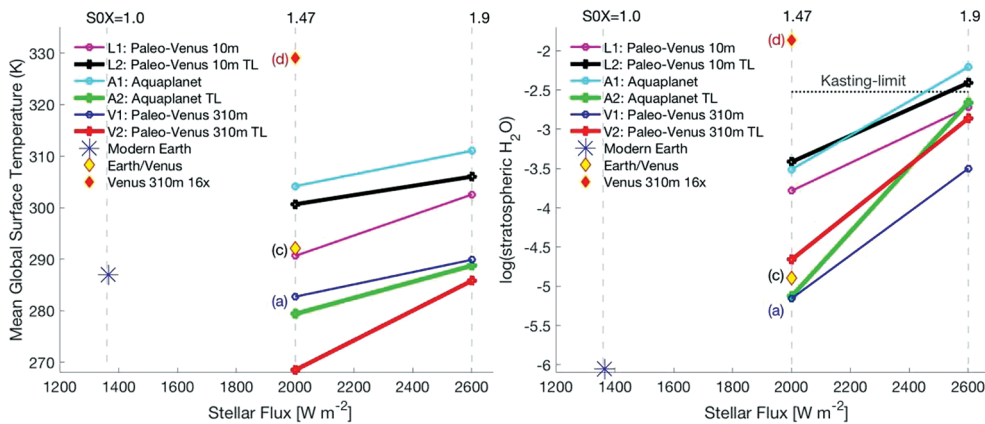


Figure 2: Left: Plots of mean global surface temperature versus insolation for simulations listed in Table 1. Points identified with (a), (c), and (d) are the same as those in Table 1/Figure 2 of Paper I. Earth/Venus refers to a simulation using Earth topography with a 310m deep bathtub ocean but with modern Venus orbital parameters and a solar spectrum from 2.9Gya ($SOX = 1.47$, where $SOX = 1$ is what Earth receives today as $1361 W/m^2$). Venus 310 m 16x uses modern Venus topography and orbital parameters with a solar spectrum from 2.9Gya, but with a sidereal day length 16 times longer than that of modern day Earth. Right: Similar to (A), but we plot $\log(\text{stratospheric water vapor content})$ versus insolation. Values above -2.5 (labeled "Kasting-limit") signify that this world could lose 1 Earth Ocean over a time period of ~ 4 billion years entering a moist greenhouse state (See Kasting, 1988).

If one looks more closely at the temperature values presented it is clear that the land planets are the hottest of all of the simulations. The explanation for this is that in order to create the large convective cloud structure at the substellar point as described in Paper I it is necessary to have a lot of available moisture. In the land planet cases there is limited moisture available, hence it is not possible to form such a large contiguous cloud structure at the substellar point. This causes more radiation to reach the surface and raise the surface temperature relative to the other non-land planet simulations.

Conclusions

Using a new suite of simulations we demonstrate that there are several ways in which Venus and Venus-like exoplanets could host liquid water on their surfaces for insolutions from 1.47 to 1.9 times modern Earth's insolation. This may imply that the reason Venus lost its surface liquid water is not because of a moist greenhouse, or runaway greenhouse effect due to its close proximity to our sun as is commonly theorized. It could be that the resurfacing events over the last 1 billion years released too much CO₂ during that time, increasing the surface temperature and pushing the planet down the moist or runaway greenhouse pathway independent of the insolation received. In addition, these point to the fact that scientists should remain open minded when considering planets found in the Venus-Zone of nearby G-dwarf stars. They may prove more interesting than we ever imagined.

Acknowledgements

The results reported herein benefited from participation in NASA's Nexus for Exoplanet System Science research coordination network sponsored by NASA's Science Mission Directorate. Resources supporting this work were provided by the NASA High-End Computing (HEC) Program through the NASA Center for Climate Simulation (NCCS) at Goddard Space Flight Center.

Thanks goes to Mareike Godolt for reminding MJW at a seminar in 2017 in Berlin that Jun Yang had previously explored insolutions up to 1.9 times modern Earth in their 2013 study.

This research has made use of NASA's Astrophysics Data System Bibliographic Services.

References

- Barnes, R. (2017) Tidal locking of habitable exoplanets, *Celestial Mechanics Dynamical Astronomy*, 129, 4, 509
- Edwards, J. M., Slingo, A. (1996) *Quar. J. Royal. Met. Soc.* 122, 689.
- Dobrovolskis, A. R., Ingersoll A. P. (1980) Atmospheric Tides and the Rotation of Venus, *Icarus*, 41, 1.
- Donahue, T. M., Russell C. T. (1997) The Venus atmosphere and ionosphere and their interaction with the solar wind, An overview, In: *Venus II Geology, Geophysics, Atmosphere, and Solar Wind Environment*, S.W. Baugher, D.M. Hunten, R.J. Phillips (Eds.), Univ. of Ariz. Press, Tucson, 3–31.
- Kane, S. R., Barclay, T., Gelino, D. M. (2013) A Potential Super-Venus in the Kepler-69 System, *Astrophysical J. Letters*, 770, 2, L20.
- Kasting, J. F. (1988) Runaway and moist greenhouse atmospheres and the evolution of earth and Venus, *Icarus*, 74, 472.
- Schmidt, G. A., Kelley, M., Nazarenko, L., et al. (2014) Configuration and assessment of the GISS ModelE2 contributions to the CMIP5 archive, *J. Advances in Modeling Earth Systems*, 6, 141.
- Way, M. J., et al. (2016) Was Venus the first habitable world of our solar system? *Geophys. Res. Lett.*, 43(16), 8376–838.
- Way, M. J., et al. (2017) Resolving Orbital and Climate Keys of Earth and Extraterrestrial Environments with Dynamics (ROCKE-3D) 1.0: A General Circulation Model for Simulating the Climates of Rocky Planets, *Astrophysical J. Supplement*, 231, 1.
- Way, M. J., Wang, J. (2017) Venus Topography and Boundary Conditions in 3D General Circulation Modeling, to appear: In: *Planetary Cartography and GISS: Concepts, tools, methods*, Springer, arXiv:1711.10528.
- Yang, J., Liu, Y., Hu, Y., Abbot, D. S. (2014) Water Trapping on Tidally Locked Terrestrial Planets Requires Special Conditions, *Astrophysical J. Letters*, 796, L22.

VENUS SEISMIC INTERIOR-ATMOSPHERE COUPLING: THEORY AND ORBITAL PERSPECTIVES

Ph. Lognonné¹, B. Kenda¹, R. Garcia², A. Komjathy³, J. Makela⁴, F. Karakostas¹, M. Drilleau¹, T. Gudkova⁵, W. B. Banerdt³, J. Cutts³, J. M. Jackson⁶

¹ Institut de Physique du Globe de Paris-Sorbonne Paris Cité, France, lognonne@ipgp.fr

² Institut Supérieure de l'Aéronautique et de l'Espace, Toulouse, France

³ Jet Propulsion Laboratory, Caltech, Pasadena, CA, USA

⁴ University of Illinois, USA

⁵ Institute of Physics of the Earth, Moscow, Russia

⁶ California Institute of Technology, Pasadena, CA, USA

Keywords: orbital seismology, planet interior, modeling

Due to the much larger density of the atmosphere, Venus atmospheric coupling is extremely strong compared to Earth. Venus appears to be a planet where seismic waves can not only lead to large atmospheric signals, as on Earth, but where in return the atmosphere significantly affects the propagation properties of surface waves in the solid planet.

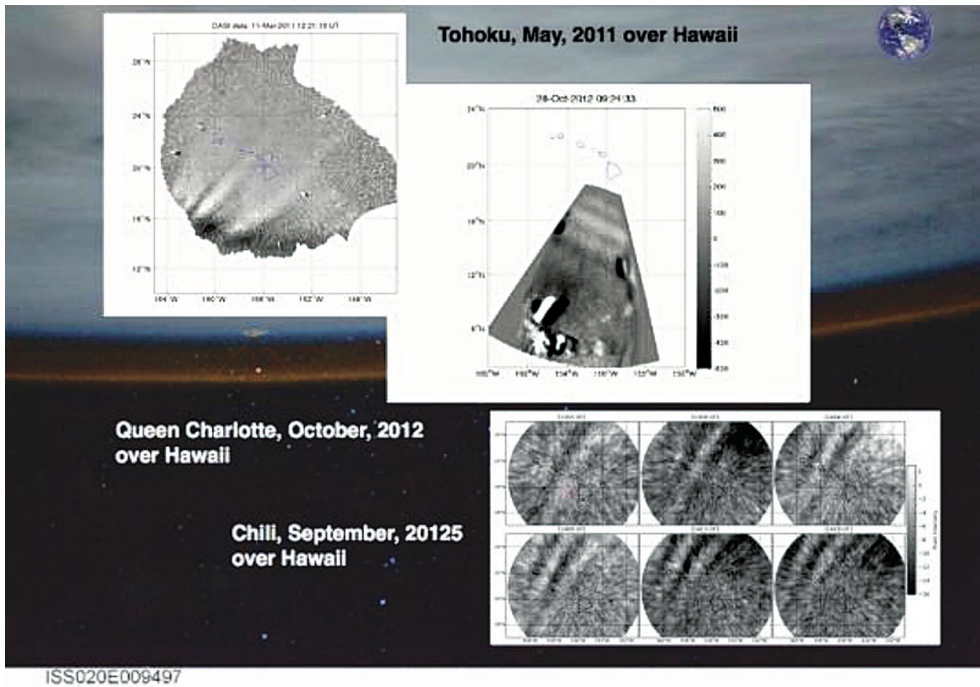


Figure 1: Example of tsunami wave observations (for three tsunamis, see on Figure) on Earth made through the 630 nm airglow. This airglow has a rather small intensity (less than 200 Rayleigh) compared to the Venus 1.27 mm, where intensity is counted in Mega Rayleigh. This $5 \cdot 10^3$ larger intensity will allow the reduction of the acquisition time of each airglow image to seconds, compared to the 300 s necessary for tsunami airglow observations, enabling the monitoring of Rayleigh wave airglow, the latter being impossible on Earth due to the too low intensity and photon noise

Detecting seismic waves in the atmosphere or, through amplification by the atmospheric scale height, in the ionosphere has therefore been proposed in the early 2000s (Garcia et al., 2005; Lognonné, 2005; Lognonné, Johnson, 2007; Lognonné et al., 2003) and this concept has been further developed more recently (Lognonné, Johnson, 2015; Stevenson et al., 2015). At the same time, breakthrough airglow observations of tsunamis in the ionosphere have been performed by an air-

glow imager (Grawe, Makela, 2017; Makela et al., 2011), demonstrating that remote sensing and full-waveform imaging of telluric waves is possible.

We present here the prospects for orbital seismology through airglow monitoring, focusing on the 1.27 μm (visible, on the night-side) airglow. Significant advantages of observing nightglow on Venus are that it is much brighter on Venus than on Earth (Krasnopolsky, 2011) and that airglow lifetime (~ 4000 s) is significantly longer than the period of seismic waves (10 to 30 s) required to be detected to provide information about the interior of the planet (Lognonné et al., 2016). This makes it very attractive for directly detecting surface waves on Venus through global imaging.

Three types of seismic signals are considered as potential targets for such airglow orbital remote sensing. The first are the acoustically generated signals above the epicenter, which occur when the seismic wave reaches the ionospheric height. This is mostly a direct P wave (Garcia et al., 2005) which allows the detection of a quake and therefore constrains the seismic activity of the planet. The two other types of signals are associated with surface waves, specifically Rayleigh waves. They might be either excited continuously, due to the global activity of the Venus atmosphere (Kobayashi, Nishida, 1998) or might be excited by quakes. These waves might be detected globally and will give access to the crustal and lithospheric structure, through the measurement of their group velocity. Structure sensitivity will be down to depths of 300–400 km for the quakes and possibly deeper for the continuously excited modes (or hum).

We modeled Rayleigh normal modes and acoustic normal modes by using an internal Venus model based on PREM, assuming the same velocities and density profile as on Earth, as a function of pressure. The atmospheric model used was the Venus-GRAM model. In contrast to previous modeling (Lognonné, Johnson, 2007), Rayleigh normal modes have been computed by adding to these models the viscosity and molecular relaxation (Bass, Chambers, 2001) computed from the atmospheric pressure and temperature of the Venus-GRAM model. Results are summarized in Fig. 2.

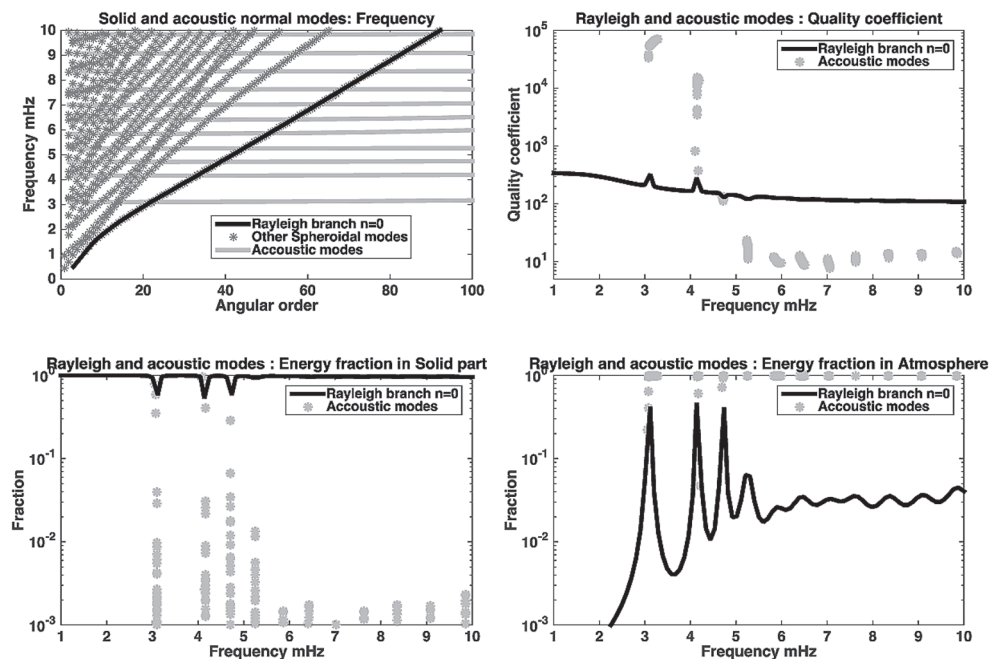


Figure 2: *Top left:* Dispersion curve of fundamental Rayleigh modes (black line), acoustic branches (light grey) and other spheroidal solid planet normal modes (dark grey). *Top right:* Quality coefficient of both the Rayleigh modes (black line) and the acoustic modes (light grey circles). The bottom right shows large resonances, with near equipartition of the energy of the resonance modes between atmosphere and solid planet

To obtain realistic fluctuations in the airglow intensity we used normal mode summation to compute the ion wind. We used a 3D statistical model of the background VER based on more than two years of Venus Express observations (Soret et al., 2012). Seismograms up to 50 mHz (20 s) were

computed for a quake at 20-km depth on Venus occurring at various epicentral distances. Such quakes may be considered as representative of a quake triggered by lithospheric cooling in the thin brittle layer of Venus. These seismograms included the Rayleigh fundamental modes and the first five overtones of spheroidal surface waves.

Further analysis (Lognonné, 2016) indicates that for a shallow quake, peak-to-peak variations larger than 3000 Rayleigh are expected at up to 60° of epicentral distance for magnitude $M_w = 6.5$. In Fig. 3 we display these airglow fluctuations for a $M_w = 5.8$ quake calculated on the night-side of Venus.

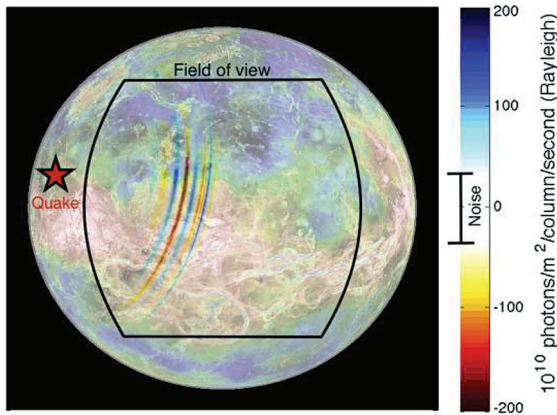


Figure 3: Modeled airglow fluctuations due to 20 s seismic waves generated by a $M_w = 5.8$ quake. The star is quake location and the colors indicate airglow fluctuations above the conservative ± 30 Rayleigh detection noise estimate using 0.3° planetary resolution

We conclude the presentation by discussing the impacts of this modeling on the design of a successful orbital seismic experiment. The first key requirement is the orbit of the mission, as the seismic monitoring requires long (\sim hr) monitoring of the same location in the ionosphere, in order to perform the high pass filtering needed for the rejection of the ionospheric background. In addition, a global view of the planet is optimum, as it maximizes the size of the monitored areas. This rejects low altitude Venus orbits, but is compatible with highly elliptical orbits. The best orbits for seismic monitoring are therefore either those available during aerobraking phases or high altitude, long period (~ 12 hr) orbits. The second key requirement is the sensitivity of the airglow imager. Because of the brightness of the airglow, this one appears affordable with the existing technology of cooled airglow IR imagers. These are light enough to be compatible with a nanosat or minisat platform which could either be a piggyback passenger on an orbital mission to Venus or designed as a low-cost dedicated mission.

References

- Bass, H. E., Chambers, J. P. (2001) Absorption of sound in the Martian atmosphere, *J. Acoust. Soc. Am.*, 109, 3069–3071.
- Garcia, R., Lognonné, P., Bonnin, X. (2005) Detecting atmospheric perturbations produced by Venus quakes, *Geophys. Res. Lett.*, 32(16), L16205, doi: 10.1029/2005GL023558.
- Grawe, M. A., Makela, J. J. (2017) Observation of tsunami-generated ionospheric signatures over Hawaii caused by the 16 September 2015 Illapel earthquake, *J. Geophys. Res. Space Physics*, 122(1), 1128–1136.
- Kobayashi, N., Nishida, K. (1998) Continuous excitation of planetary free oscillations by atmospheric disturbances, *Nature*, 395(6700), 357–360.
- Krasnopolsky, V. A. (2011) Excitation of the oxygen nightglow on the terrestrial planets, *Planet. Space Sci.* 59(8), 754–766.
- Lognonné, P. (2005) Planetary Seismology, *Annual Review of Earth and Planetary Sciences*, 33, 571–604.
- Lognonné, P., Johnson, C. L. (2007) Planetary Seismology, In: *Treatise in Geophysics, 10, Planets and Moons*, ed. G. Schubert, ch. 4, 69–122.
- Lognonné, P., Johnson, C. L. (2015) Planetary seismology, In: *Treatise on Geophysics*, ed. G. Schubert, 10, 65–120.

- Lognonné, P., Garcia, R., Romanowicz, B., Banerdt, B. (2003) A new concept for seismology on Venus using orbiting radar instead of lander, *AGU Fall Meeting 2003*, P31B-1055.
- Lognonné, P., Karakostas, F., Rolland L., Nishikawa, Y. (2016) Modeling of atmospheric-coupled Rayleigh waves on planets with atmosphere: From Earth observation to Mars and Venus perspectives, *J. Acoust. Soc. Am.* 140(2), 1447, doi: 10.1121/1.4960788.
- Makela, J.J., Lognonné, P., Hébert, H. et al. (2011) Imaging and modeling the ionospheric airglow response over Hawaii to the tsunami generated by the Tohoku earthquake of 11 March 2011, *Geophys. Res. Lett.*, 38(24).
- Soret, L., Gérard J.-C. M.C., Montmessin, F., Bertaux, J.-L. et al. (2012) Atomic oxygen on the Venus nightside: Global distribution deduced from airglow mapping, *Icarus*, 217(2), 849–855.
- Stevenson, D., Cutts, J. A., Mimoun, D., Tsai, V. C. (2015) *Probing the Interior Structure of Venus*, Technical Report.

SURFACE
AND LANDING
SITES

VENERA-D LANDING SITE SELECTION BASED ON DETAILED GEOLOGICAL MAPPING USING MAGELLAN RADAR IMAGES

R. E. Ernst^{1,2}, C. Samson^{1,3}, E. Bethell¹, J. Lee¹, S. Khawja¹, J. R. Graff¹, S. Davey¹

¹ Department of Earth Sciences, Carleton University, Ottawa, Canada

² Faculty of Geology and Geography, Tomsk State University, Tomsk, Russia

³ Department of Construction Engineering, École de Technologie Supérieure, Montréal, Canada

Abstract

Planning of both the orbital and lander/rover components of the Venera-D mission can take advantage of existing detailed surface geology mapping. Here we highlight research by our group on key classes of geological features mapped using the full resolution Magellan images (75 m/pixel): volcanic centres and associated radiating graben-fissure systems; coronae and their circumferential systems; plains, flow fields and identification of sources; giant rift (chasmata) systems and comparison to terrestrial rifts; and tessera terrains and crustal plateaus. Based on both scientific criteria and favorable logistics, we suggest a landing site in the Alpha Regio quadrangle (V-32).

Introduction

Subsequent to the pioneering Venera missions (1961–1984), the Magellan mission (1989–1994) provided radar mapping of more than 98 % of the surface of Venus. Since then, more recent missions have focused primarily on atmospheric studies (e.g. Venus Express, Akatsuki), and the Magellan dataset remains the main source of information available for researching the geology of Venus. There is a strong need for a new surface geology mission which will be satisfied through the planned Venera-D mission.

Scientists from the Ottawa-Carleton Geoscience Centre Venus Working Group (based at Carleton University, Ottawa, Canada), in collaboration with other Canadian and international colleagues, are engaged in detailed geological mapping of Magellan synthetic aperture radar (SAR) images at the highest resolution available (75 m/pixel). This research effort has implications for both components of the planned Venera-D mission: (1) the orbital component that will provide surface imaging at much higher resolution, and (2) the lander/rover component that will analyze the composition of rocks and soils in situ.

Orbital Mission: Need for Higher Resolution Images of the Surface of Venus

Extensional Lineaments

Our detailed geological mapping has focused on extensional lineaments, which include rift faults and graben-fissure systems (hypothesized to overlie dyke swarms) (Grosfils, Head 1994). Our long-term objective is to produce a global dyke swarm map of Venus. In addition, we have interpreted the tectono-magmatic history of several areas via cross-cutting relationships between interacting lineament systems. Understanding of extensional lineaments on Venus would greatly benefit from higher resolution imaging. At the resolution of the presently available Magellan SAR images, cross-cutting relationships are often ambiguous, making relative ages difficult to interpret.

Volcanic Centres and Associated Radiating Graben-Fissure Systems

There are hundreds of volcanic centres on Venus, with diameters ranging from less than 30 km to over 1,000 km, often associated with radiating graben-fissure systems. Our research group is mapping these systems in detail and have so far covered approximately 15 % of Venus' surface (Fig. 1) (e.g. Ernst et al., 2003; Studd et al., 2010; Davey, 2012; Davey et al., 2013). At least 5 times as many systems are present than were previously identified from reconnaissance-scale mapping. The relative age of distinct volcanoes can be determined through the cross-cutting relationships of their associated radiating graben-fissure systems, which can extend far beyond the edifice itself (up to 2,000 km away). This powerful relative regional dating tool will be enhanced by the use of higher resolution SAR images.

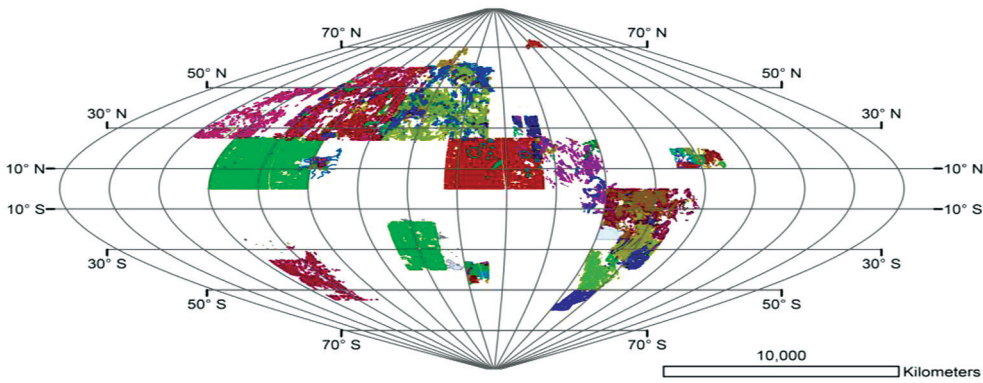


Figure 1: Mapping of graben-fissure systems by the Ottawa-Carleton Geoscience Centre Venus Working Group, completed using Magellan SAR images at the highest resolution available (75 m/pixel). In sinusoidal projection with a central meridian of -45°E

Coronae and Their Circumferential Systems

There are hundreds of coronae on Venus, large tectono-magmatic features consisting of a quasi-circular graben-fissure system and associated topography (typically a central uplift or depression, and circular rim or moat) (Stofan et al., 1992). In some instances, they are linked to a giant radiating graben-fissure system and extensive volcanism on the scale of that associated with large igneous provinces on Earth. Our recent findings suggest that coronae are analogous to giant circumferential dyke swarms on Earth (a newly recognized class of dyke swarms), and that circumferential graben-fissure systems associated with the annuli of coronae on Venus are underlain by dyke swarms (Buchan, Ernst, 2016; Bethell et al., 2016). SAR images with improved resolution would clarify cross-cutting relationships between circumferential and radiating systems, and allow us to further constrain the relative timing of the multiple events related to corona formation.

Plains, Flow Fields and Identification of Sources

Large volcanic flow fields (or ‘fluctūs’) cover surfaces larger than $50,000\text{ km}^2$, contributing to approximately 11 % of the planet’s plains material. A large majority of the documented flow fields are located within major extensional zones and are commonly associated with coronae, large volcanic shields or fracture/fissure systems (Lancaster et al., 1995; Magee, Head, 2001). Our team is currently doing detailed mapping of two fluctūs located within the Stanton (V-38) quadrangle (immediately south of Atla Regio), to distinguish individual flow units and identifying their source vents. Features observed within both the Ningyo and Henwen Fluctus include well-preserved canali and distributary delta-like systems. In addition, we are determining stratigraphic histories of fluctus emplacement through cross-cutting relationships with graben-fissure systems.

Giant Rift Systems

Large rift systems (or ‘chasmata’) are present on Venus, especially in the Beta-Atla-Themis region which features two particularly large rift systems, Parga Chasma and Hecate Chasma, which are 10,000 and 8,000 km long, respectively. From detailed geological mapping of a 1,500 km section we have proposed a model in which the discontinuous morphology of Parga Chasma is caused by local triple-junction rifting focused on individual magmatic centres distributed along the overall NW-SE rift system and we have drawn analogies with terrestrial rift systems (Graff, 2015; Graff et al., 2018). Higher resolution images would enable a more definitive interpretation of cross-cutting relationships between graben-fissure systems and rift faults, which is critical to developing a more detailed chronology of events and an improved understanding of rifting processes.

Tessera Terrain and Crustal Plateaus

Tessera, also known as complex ridge terrain, occupies approximately 8 % of Venus’ surface, forming continent-like units (crustal plateaus) embayed by adjacent volcanic plains (Bindschadler, Head, 1991). This unit consists of at least two sets of intersecting ridges and grooves, and is a result of tectonic deformation of a precursor terrain (Basilevsky, Head, 1998). However, the nature of that precursor terrain, as well as the causes and mechanisms of deformation are still under debate (Hansen, Willis, 1996). Detailed mapping of selected tesserae by our group is seeking to identify distinct domains corresponding to different deformation styles. The boundaries between these domains can then be analyzed for spatial and temporal relationships.

Lander/Rover Mission: Geological Data to Inform Landing Site Selection

Landing Site Considerations

The pre-Magellan Venera and VEGA landers relied on limited data, and thus landed on mostly unknown terrains, now thought to be volcanic plains material. In situ analyses indicated basaltic compositions (thought to be widespread on Venus), but also more unusual alkaline compositions (Kargel et al., 1993). Our detailed geological mapping can inform the selection of landing site targets of high scientific interest. Plains areas are the most practical targets from an engineering point of view (smoother topography and therefore enhanced rover terrainability). They would also allow the characterization of the geochemistry of Venusian basalt, an important science objective. Cutting the plains are canali, which are narrow (1–2 km wide) sinuous lava channels that can be traced for up to 7,000 km. A rover could test whether their compositions are carbonatite, komatiite, or sulphur-rich. Also of interest are the highly deformed tessera terrains of currently unknown composition. While typically considered to be basaltic, recent evidence suggests that a more felsic composition is also possible (Gilmore et al., 2015).

The Alpha Regio (V-32) Quadrangle as a Landing Site Target

The Alpha Regio quadrangle is located near the Venusian equator, and extends from 0 to 30°E longitude and 0 to 25°S latitude. This quadrangle is currently being mapped and characterized in detail at a scale of 1:2,500,000 as part of a Ph.D. dissertation by Erin Bethell, a member of the Ottawa-Carleton Geoscience Centre Venus Working Group. It was chosen for its numerous and diverse array of structures and terrains. The area is also adjacent to the Kaiwan Fluctus (V-44) quadrangle, a portion of which was previously mapped by Bethell (2015). The majority of the Alpha Regio quadrangle is located within the relatively low-lying and radar-dark regional plains, with the notable exception of a portion of the highlands in the southwest. Multiple previous studies have focused on features contained within the quadrangle, including, but not limited to: deformation styles and emissivity of the Alpha Regio tessera terrain (Gilmore, Head, 2000; Gilmore et al., 2015), geophysical modeling of coronae (Janes et al., 1992), wrinkle ridge kinematics (McGill, 1993), and regional stress orientations inferred by mapping of radiating dyke swarms (Bethell et al., 2017).

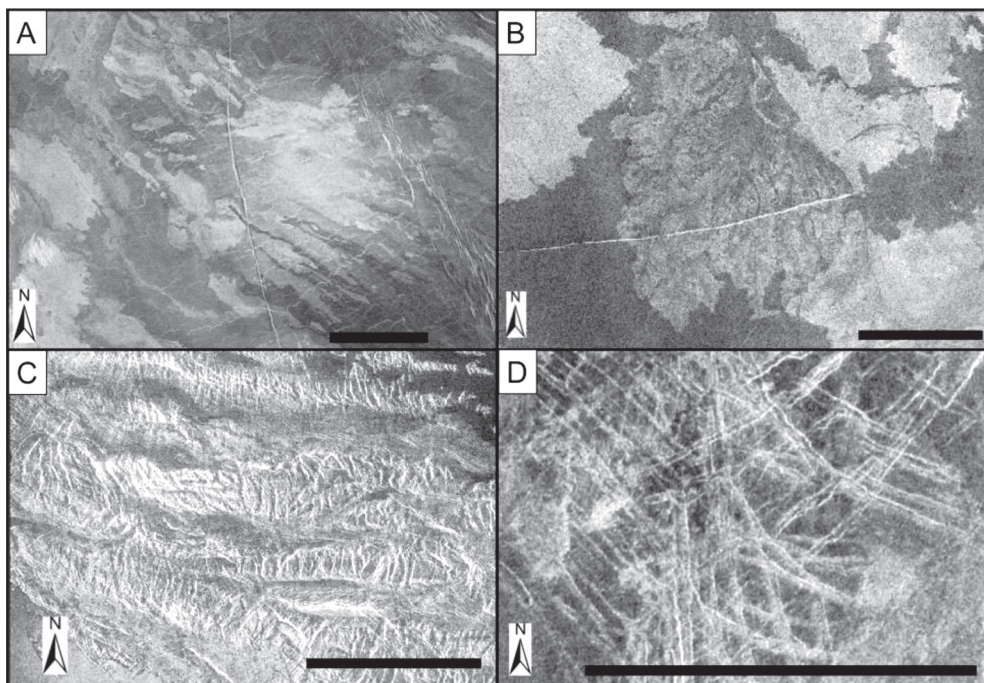


Figure 2: Selected left-looking SAR images from various study areas. Scale bars on all images are 50 km. A) Layered lobate plains between Dewi-Ratih chasma and Alpha Regio in the Alpha Regio quadrangle (central coordinates: 1.43°E, 16.56°S); B) A delta-like flow field feature within the Henwen Fluctus (central coordinates: 180.28°E, 20.11°S); C) Shear zones within Salus Tessera (central coordinates: 44.99°E, 1.23°N); D) Intersecting graben-fissure systems near X mukane corona (central coordinates: 270.32°E, 29.25°S).

The quadrangle contains the three target geological units for landing sites previously proposed by Basilevsky et al. (2007): (1) true and transitional tessera terrain, including the extensive Alpha Regio highlands, Minu-Anni tessera, as well as numerous smaller tessera inliers; (2) multiple shield plains regions that are associated with tens to hundreds of individual volcanic edifices; (3) lobate plains emanating from individual volcanic edifices and coronae. Major features of geological interest include several coronae: Kuan Yin, Atargatis, Thouris, Cybele, and Fatua (as well as structures associated with Heng-o and Thermuthis), Dewi-Ratih Chasma, and a broad regional system of wrinkle ridges. In addition, landing site selections should be free of contamination by impact ejecta (Basilevsky et al., 2007). The Alpha Regio quadrangle has many areas that are likely 'pristine', that is, not covered by the ejecta that is frequently found downwind of impact craters, as identified by the modeling of ejecta parabolas by Basilevsky et al. (2004).

Conclusions

Regional and thematic mapping using the 75 m/pixel Magellan SAR data has revealed a number of classes of magmatic and tectonic features which have been the focus of more detailed mapping by our research group: volcanism (central volcanoes, flow fields and plains), enigmatic circular features known as coronae, plumbing systems of radiating and circumferential dyke swarms, major rift systems, and tessera 'basement' terrains. The proposed Venera-D mission can be designed to address frontier questions in each of these areas. More specifically, we suggest that the Alpha Regio quadrangle contains a variety of possible landing site opportunities due to its context as a well-understood area of Venus, but also due to its proximity to the equator, relatively low elevation, abundance of geologically interesting features, and the presence of the three target geological units identified by Basilevsky et al. (2007).

Acknowledgements

This research was supported by a Discovery Grant from the Natural Sciences and Engineering Research Council of Canada (NSERC) awarded to Richard Ernst. In addition, Richard Ernst has been partially supported by Russian Government Grant No. 14.Y26.31.0012.

References

- Basilevsky, A. T., Head, J. W. (1998) The Geologic History of Venus: A Stratigraphic View, *J. Geophysical Research: Planets*, 103(E4), 8531–8544.
- Basilevsky, A. T., Head, J. W., Abdрахимов, A. M. (2004) Impact Crater Air Fall Deposits on the Surface of Venus: Areal Distribution, Estimated Thickness, Recognition in Surface Panoramas, and Implications for Provenance of Sampled Surface Materials. *J. Geophysical Research*, 109, E12003.
- Basilevsky, A. T., Ivanov, M. A., Head, J. W., Aittola, M., Raitala, J. (2007) Landing on Venus: Past and Future, *Planetary and Space Science*, 55, 2097–2112.
- Bethell, E. (2015) *Graben-Fissure Systems in the Kaiwan Fluctus Area of Venus*, B.Sc. thesis, Department of Earth Sciences, Carleton University, Ottawa, Canada.
- Bethell, E., Ernst, R. E., Samson, C., Buchan, K. (2016) Circumferential Graben-Fissure Systems of Venusian Coronae as Possible Analogues of Giant Circumferential Dyke Swarms on Earth, *Lunar and Planetary Science Conference 47*, 1471.
- Bethell, E., Ernst, R. E., Samson, C., Buchan, K. L. (2017) Detailed Mapping of Graben-Fissure Systems Associated with Fatua Corona, Venus: Implications for Magmatism and the Regional Stress Field. *Lunar and Planetary Science Conference 48*, 2177.
- Bindschadler, D. L., Head, J. W. (1991) Tessera Terrain, Venus: Characterization and Models for Origin and Evolution, *J. Geophysical Research: Solid Earth*, 96(B4), 5889–5907.
- Buchan, K. L., Ernst, R. E. (2016) Giant Circumferential Dyke Swarms on Earth as Possible Analogues of Coronae on Venus, *Lunar and Planetary Science Conference 47*, 1183.
- Davey, S. (2012) *Mapping graben-fissure systems and pit crater chains on Venus*, M.Sc. thesis, Department of Earth Sciences, Carleton University, Ottawa, Canada.
- Davey, S., Ernst, R., Samson, C., Grosfils, E. B. (2013) Hierarchical Clustering of Pit Crater Chains on Venus, *Canadian J. Earth Sciences*, 50(1), 109–126.
- Ernst, R. E., Desnoyers, D. W., Head, J. W., Grosfils, E. B. (2003) Graben-Fissure Systems in Guinevere Planitia and Beta Regio (264o-312oE, 24o-60oN), Venus, and Implications for Regional Stratigraphy and Mantle Plumes, *Icarus*, 164, 282–316.
- Gilmore, M. S., Head, J. W. (2000) Sequential Deformation of Plains at the Margins of Alpha Regio, Venus: Implications for Tessera Formation, *Meteoritics and Planetary Science*, 35, 667–687.
- Gilmore, M. S., Mueller, N., Helbert, J. (2015) VIRTIS Emissivity of Alpha Regio, Venus, with Implications for Tessera Composition, *Icarus*, 254, 350–361.

- Graff, J. R. (2016) *A History of Tectono-Magmatism Along the Parga Chasma Rift System on Venus*, M.Sc. thesis, Department of Earth Sciences, Carleton University, Ottawa, Canada.
- Graff, J. R., Ernst, R. E., Samson, C. (2018) Evidence for Triple-Junction Rifting Focused on Local Magmatic Centres along Parga Chasma, Venus, *Icarus*, 306, 122–138.
- Grosfils, E. B., Head, J. W. (1994) Emplacement of a Radiating Dike Swarm in Western Vinmara Planitia, Venus: Interpretation of the Regional Stress Field Orientation and Subsurface Magmatic Configuration, *Earth, Moon, and Planets*, 166(2), 153–171.
- Hansen, V. L., Willis, J. A. (1996) Structural Analysis of a Sampling of Tesserae: Implications for Venus Geodynamics, *Icarus*, 123(2), 296–312.
- Janes, D. M., Squyres, S. W., Bindschadler, D. L., Baer, G., Schubert, G., Sharpton, V. L., Stofan, E. R. (1992) Geophysical Models for the Formation and Evolution of Coronae on Venus, *J. Geophysical Research*, 97, 16 055–16 067.
- Kargel, J. S., Komatsu, G., Baker, V. R., Strom, R. G. (1993) The Volcanology of Venera and VEGA Landing Sites and the Geochemistry of Venus, *Icarus*, 103, 253–275.
- Lancaster, M. G., Guest, J. E., Magee, K. P. (1995) Great Lava Flow Fields on Venus, *Icarus*, 118(1), 69–86.
- Magee, K. P., Head, J. W. (2001) Large Flow Fields on Venus: Implications for Plumes, Rift Associations, and Resurfacing, In: Ernst R. E., Buchan K. L. (Eds.) *Mantle plumes: their identification through time*, 352, 81–101.
- McGill, G. E. (1993) Wrinkle Ridges, Stress Domains, and Kinematics of Venustian Plains, *Geophysical Research Letters*, 20, 2407–2410.
- Stofan, E. R., Sharpton, V. L., Schubert, G., Baer, G., Bindschadler, D. L., Janes, D. M., Squyres, S. W. (1992) Global Distribution and Characteristics of Coronae and Related Features on Venus: Implications for Origin and Relation to Mantle Processes, *J. Geophysical Research*, 97, 13 347–13 378.
- Studd, D., Ernst, R. E., Samson, C. (2011) Radiating Graben-Fissure Systems in the Ulfrun Regio Area, Venus, *Icarus*, 215, 279–291.

RADAR BACKSCATTER FROM VENUS' HIGHLANDS: CONFIRMATION OF A FERROELECTRIC SUBSTANCE, LIKELY CHLORAPATITE

A. H. Treiman¹, E. Harrington²

¹ Lunar and Planetary Institute / USRA, Houston, Texas, USA

² University of Western Ontario, London, Ontario, Canada

Abstract

Near-equatorial highlands on Venus, like Ovda Regio, show an unusual pattern of radar returns: increasing backscatter up to a critical elevation, and very low backscatter above. This pattern is also apparent, though inverted, in radar emissivity. Using Magellan stereo altimetry, we show that the critical elevation is 4.2 km above the datum, confirm that the radar backscatter pattern is consistent with presence of a ferroelectric substance, and suggest that substance to be chlorapatite. Several interesting problems remain unsolved.

Introduction

The earliest radar images of Venus showed strong variations in radar backscatter (Campbell et al., 1976) and emissivity; in most cases, backscatter increases and emissivity decreases with increasing elevation (Klose et al., 1992; Arvidson et al., 1994). The mineralogic causes of these changes have been controversial. Proposed explanations, in terms of mineralogy include either semiconductor or ferroelectric substances (Shepard et al., 1994; Fegley et al., 1997; Wood, 1997). In the absence of new relevant data from Venus' surface and a dearth of additional orbital or earth-based remote sensing (Simpson et al., 2009), we re-investigated the problem of backscatter variations with Magellan SAR data, using elevations from stereo altimetry (Treiman et al., 2016). For the Ovda Regio highlands, radar backscatter is consistent with presence of a ferroelectric substance.

Data and Methods

Radar backscatter values are from the Magellan SAR left-look FMIDR images of the Ovda Regio, converted from DN values (Ford, 1993). Elevation values are from the stereo altimetry dataset of Herrick et al. (2012), which is registered to Magellan radar altimetry. These datasets were imported into ArcGIS[®], and target regions were selected for detailed study (Treiman et al., 2016). These regions were mapped in detail (e.g., Fig. 1a), and graphs of radar backscatter versus elevation (and thus temperature) were generated (Fig. 1b).

Results

For Ovda Regio (Fig. 1), radar backscatter increases upward in elevation, with a sharp peak at ~4.2 km. Above that elevation, radar backscatter declines precipitously to values more characteristic of Venus' lowlands (Fig. 1b). This change in radar backscatter is nearly exactly inverse to changes in Magellan radar emissivity with elevation (Klose et al., 1992; Arvidson et al., 1994), although the spatial resolution of emissivity is much lower than of backscatter. The width of elevation peak in radar backscatter coefficient (Fig. 1b) is ~0.2 km, which is of the same order as the elevation uncertainty in the stereo elevations, ~0.1 km (Herrick et al., 2012). Thus, the backscatter data are consistent with a single sharp peak, and the pattern of backscatter with elevation is consistent with the presence of a ferroelectric substance (Shepard et al., 1994; Arvidson et al., 1994; Treiman et al., 2016). The ferroelectric substance must be the same across Ovda, present in approximately the same proportions in all areas examined, and have a Curie temperature of ~700 K (Fig. 1b).

Ferroelectricity

Ferroelectric substances maintain an electrical polarity (or domains within them do), and their polarity can be reversed by an applied electric field (Jona, Shirane, 1962). The ferroelectric property of a substance declines with increasing temperature (from thermal perturbations in atom positions); at some temperature, the ferroelectric property disappears and the material becomes para-electric, i.e. dielectric or 'normal.' The transition temperature is called the Curie temperature, in analogy with the transition in magnetic substances from ferromagnetic to paramagnetic. As temperature approaches the Curie point, the substance's dielectric constant (i.e., relative permittivity) approaches infinity; above the Curie point, the dielectric constant declines rapidly to 'normal' values.

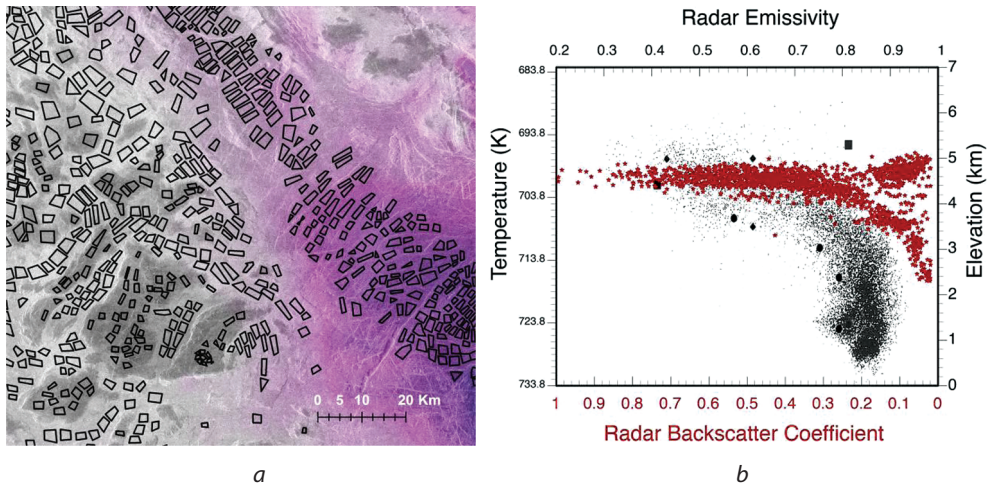


Figure 1: (a) SAR backscatter image of a portion of Ovda Regio (ctr. -7.0° , 89.5°) showing how backscatter (tone) varies with elevation (violet; darker is lower elevation) and areas plotted on Fig. 1b (black boxes). Note sharp transition from high to very low backscatter at higher elevation, attributable to the effects of a ferroelectric material (Arvidson et al., 1994; Treiman et al., 2016). (b) Radar properties of Ovda Regio. Red symbols and legend are Magellan SAR backscatter and elevation by stereogrammetry, see Fig. 1a (Treiman et al., 2016). Black symbols are Magellan emissivity for all of Ovda: small dots are elevation by Magellan altimetry; large symbols are elevation by SAR stereogrammetry (Arvidson et al., 1994)

Venus' Ferroelectric Substance

Although many synthetic ferroelectric substances are known because of potential applications (Jona, Shirane, 1962; Shepard et al., 1992; Arvidson et al., 1994; Scott et al., 2013), very few known minerals are ferroelectric. For Venus, one must stipulate further that a ferroelectric mineral is relatively common, as the ferroelectric signature seen of Ovda (Fig. 1) is present across most near-equatorial high elevations like Alpha Regio and Tepev Montes (Treiman et al., 2016). The Tepev Montes are basalt shield volcanos (Campbell and Rogers, 1994), so the ferroelectric substance must be possible in basaltic compositions.

The only mineral that satisfies these criteria is chlorapatite, $\text{Ca}_5(\text{PO}_4)_3\text{Cl}$. Chlorapatite is ferroelectric at room temperature (Rausch, 1976; Bauer, Klee, 1993), because its Cl atoms are too large to fit on symmetric positions (Hughes, Rakovan, 2002; Hughes et al., 2014); F and OH are smaller, so they can fit onto symmetric positions and neither fluorapatite nor hydroxylapatite is ferroelectric. The Curie temperature of chlorapatite is not precisely known, but is above 675 K and reasonably near 700 K (Rausch, 1976; Hitmi et al., 1984). Fluorapatite is present in nearly all igneous rocks (basaltic and felsic), and could reasonably form over time by chemical reaction with Cl in the Venus atmosphere (Treiman et al., 2016).

Temporal Constraints

Several high mountains in near-equatorial Venus do not show the characteristic radar backscatter pattern of a ferroelectric substance (Fig. 1) — these include the volcanos Maat Mons (to 10.2 km), Sapas Mons (to ~ 4.5 km), Ozza Mons (to 7.5 km). These volcanos are inferred to have erupted basalts, and so might be expected to show the ferroelectric radar pattern like Tepev Montes (to ~ 6 km). A likely explanation of difference between Tepev and the other volcanos is that the latter are young, and that their igneous fluorapatite has not had time to be converted to chlorapatite. This distinction could act as a time marker, when the rate of reaction (fluorapatite \rightarrow chlorapatite) is calibrated.

Conclusions

From these data, the radar response patterns of Ovda Regio and other near-equatorial highlands are consistent with the presence of a ferroelectric mineral, which is likely to be chlorapatite, and which forms by relatively slow chemical reaction between rock and Venus' atmosphere (Treiman et al., 2016). This hypothesis is testable, both to the ferroelectric character and Curie point of chlorapatite (Rausch, 1976) and the rate of chlorapatite formation. The radar response pattern could be caused by other ferroelectric substances (Shepard et al., 1994; Arvidson et al., 1994), al-

though none of the suggested compounds are common minerals, and all would require significant concentrations of rare elements. Alternatively, thin films of some non-ferroelectric minerals (e.g., hydroxylapatite and magnetite) can become ferroelectric, because of lattice strain induced by epitaxy and grain boundaries (Bauer, Klee, 1993; Lang et al., 2013; Lin et al., 2017). Such thin films might be reasonable products of grain boundary reactions at the Venus surface.

These results raise (at least) three significant problems. (1) Why is Maxwell different? Maxwell Montes are the tallest mountains on Venus, but do not show radar backscatter pattern typical of Ovda and many other highlands (Klose et al., 1992; Treiman et al., 2016). Instead, Maxwell shows the well-known 'snow line' — upwards of ~4 km elevation, there is a sharp increase in SAR backscatter. This pattern is completely unlike that expected of a ferroelectric substance. Could the rocks of Maxwell contain no chlorapatite? And what substance is responsible for the increase in backscatter? (2) The basalt shield volcanoes of Tepev Montes show the same ferroelectric backscatter pattern as do tesserae like Ovda and Alpha (Treiman et al., 2016). Does this imply that Ovda and other tesserae are made of basaltic rock, despite inferences that tesserae may be of more felsic rock (Ivanov, 2001; Shellnutt, 2013)? (3) Atop Ovda Regio is the famous Festoon Flow, which has a surface morphology consistent with a viscous rhyolite (Schenk and Moore, 1992; Arvidson et al., 1994). The flow has high radar backscatter (Arvidson et al., 1994; Campbell et al., 1999) and appears to be at a higher elevation than an adjacent region of very low radar backscatter; this seems inconsistent with the presence of a ferroelectric substance. It could be that the Festoon Flow is very rough, is very young, or is made of a substance that cannot produce chlorapatite. This is more than passingly odd, and clearly deserves further investigation.

Acknowledgements

This work was begun as a LPI Summer Internship by the second author, mentored by the first author. The LPI is operated by USRA under a Cooperative Agreement with NASA.

References

- Arvidson, R. E., Brackett, R., Shepard, M., Izenberg, N., Fegley, B., Plaut, J. (1994) Microwave signatures and surface properties of Ovda Regio and surroundings, Venus, *Icarus*, 112, 171–186.
- Basilevsky, A. T., et al. (2012) Geologic interpretation of the near-infrared images of the surface taken by the Venus Monitoring Camera, Venus Express, *Icarus*, 217, 434–450.
- Bauer, M., Klee, W. (1993) Induced ferroelectricity in chlorapatite. *Zeitschrift für Kristallographie-Crystalline Materials*, 206, 15–24.
- Brackett, R. A., Fegley, B., Arvidson, R. E. (1995) Volatile transport on Venus and implications for surface geochemistry and geology, *J. Geophysical Research: Planets*, 100, 1553–1563.
- Campbell, B. A., Rogers, P. G. (1994) Bell Regio, Venus: Integration of remote sensing data and terrestrial analogs for geologic analysis, *J. Geophysical Research: Planets*, 99, 21 153–21 171.
- Campbell, B. A., Campbell, D. B., DeVries, C. H. (1999) Surface processes in the Venus highlands: Results from analysis of Magellan and Arecibo data, *J. Geophysical Research: Planets*, 104, 1897–1916.
- Campbell, D., Dye, R., Pettengill, G. (1976) New radar image of Venus, *Science*, 193, 1123–1124.
- Fegley, B., Klingelhöfer, G., Lodders, K., Widemann, T. (1997) Geochemistry of surface-atmosphere interactions on Venus, In: *Venus II: Geology, Geophysics, Atmosphere, and Solar Wind Environment*, 1, 591–636.
- Ford, J. (1993) Magellan: The Mission and the System, In: J. P. Ford, et al., (Eds.), *Guide to Magellan Image Interpretation*, Jet Propulsion Lab, Pasadena CA, 1–18.
- Herrick, R. R., Stahlke, D. L., Sharpton, V. L. (2012) Fine-scale Venusian topography from Magellan stereo data, *EOS, Trans. American Geophysical Union*, 93, 125–126.
- Hitmi, N., Lacabanne, C., Young, R. (1984) TSC study of electric dipole relaxations in chlorapatite, *J. Physical Chemistry*, 45, 701–708.
- Hughes, J. M., Nekvasil, H., Ustunisik, G., Lindsley, D. H., Coraror, A. E., Vaughn, J., Phillips, B. L., McCubbin, F. M., Woerner, W. R. (2014) Solid solution in the fluorapatite-chlorapatite binary system: High-precision crystal structure refinements of synthetic F-Cl apatite. *American Mineralogist*, 99, 369–376.
- Hughes, J. M., Rakovan, J. (2002) The crystal structure of apatite, $\text{Ca}_5(\text{PO}_4)_3(\text{F},\text{OH},\text{Cl})$, *Reviews in Mineralogy and Geochemistry*, 48, 1–12.
- Ivanov, M., 2001. Morphology of the tesserae terrain on Venus: Implications for the composition of tesserae material, *Solar System Research*, 35, 1–17.
- Jona, F., Shirane, G. (1962) *Ferroelectric crystals*, Oxford, New York, Paris, Pergamon Press, Preis geb, 84.

- Klose, K., Wood, J., Hashimoto, A. (1992) Mineral equilibria and the high radar reflectivity of Venus mountaintops, *J. Geophysical Research: Planets*, 97, 16 353–16 369.
- Lang, S., et al. (2013) Ferroelectric polarization in nanocrystalline hydroxyapatite thin films on silicon, *Scientific Reports*, 3(2215).
- Lin, B.-T., Lu, Y.-W., Shieh, J., Chen, M.-J. (2017) Induction of ferroelectricity in nanoscale ZrO₂ thin films on Pt electrode without post-annealing, *J. European Ceramic Society*, 37, 1135–1139.
- Rausch, E. O. (1976) *Dielectric Properties of Chlorapatite*, Georgia Institute of Technology, 268.
- Schaefer, L., Fegley, B. (2004) Heavy metal frost on Venus, *Icarus*, 168, 215–219.
- Schenk, P., Moore, H.J. (1992) An unusual thick lava flow in Ovda Regio, Venus, *Lunar and Planetary Science Conference 23*, 1217–1218.
- Scott, J.F. (2013) Prospects for Ferroelectrics: 2012–2022, *ISRN Materials Science*, 2013, 187 313, 24.
- Shellnutt, J.G. (2013) Petrological modeling of basaltic rocks from Venus: A case for the presence of silicic rocks, *J. Geophysical Research: Planets*, 118, 1350–1364.
- Shepard, M.K., Arvidson, R.E., Brackett, R.A., Fegley, B. (1994) A ferroelectric model for the low emissivity highlands on Venus, *Geophysical Research Letters*, 21, 469–472.
- Simpson, R. A., Tyler, G. L., Häusler, B., Mattei, R., Pätzold, M. (2009) Venus Express bistatic radar: High-elevation anomalous reflectivity, *J. Geophysical Research: Planets*, 114, E00B41.
- Tian, H., Verbeeck, J., Brück, S., Paul, M., Kufer, D., Sing, M., Claessen, R., Tendeloo, G.V. (2014) Interface-induced modulation of charge and polarization in thin film Fe₃O₄, *Advanced Materials*, 26, 461–465.
- Treiman, A.H., Harrington, E., Sharpton, V. (2016) Venus' radar-bright highlands: Different signatures and materials on Ovda Regio and on Maxwell Montes, *Icarus*, 280, 172–182.
- Wood, J.A. (1997) Rock weathering on the surface of Venus, In: *Venus II: Geology, Geophysics, Atmosphere, and Solar Wind Environment*, University of Arizona Press, Tucson AZ, 637–665.

IMDR REGIO AS THE LANDING SITE OF THE VENERA-D MISSION: A GEOLOGIC PERSPECTIVE

P. D’Incecco¹, L. S. Glaze²

¹ Arctic Planetary Science Institute, Berlin, Germany

² Goddard Space Flight Center, Greenbelt, Maryland, USA

Abstract

Over the last 25 years, discussion of Venus’ geologic history has been characterized by a major debate regarding whether the planet experienced catastrophic or equilibrium volcanic resurfacing. Some have suggested that the random global distribution, combined with relatively fresh expressions, of Venus’ impact craters is consistent with a global rejuvenation of the crust about 300–600 Myr ago through a short-lived (“catastrophic”) resurfacing event. In contrast, the number and non-random distribution of volcanoes on Venus is more consistent with a steadier (“equilibrium”) resurfacing process. Preliminary observations based on the NASA Magellan and ESA Venus Express datasets suggest a possibly young geologic age of formation for Imdr Regio, a volcano-dominated large topographic rise. However, this area still remains poorly studied. Imdr Regio offers a great opportunity to improve our understanding of the recent, or possibly even present, style of resurfacing on Venus. Finding evidence that geologically recent volcanic activity occurred over a localized area would have important implications for the rheological structure of the interior of Venus. For these reasons, Imdr Regio is a potential landing site for the future Venera-D mission. In preparation for consideration of Imdr Regio as a landing site, we are currently planning an extensive geologic study of Imdr Regio. As part of this effort, candidate landing regions within Imdr Regio will be identified. During the Venera-D mission, remote observations from orbit would be combined with in-situ measurements of the surface chemical composition and volatile content to answer key questions about Imdr’s volcanic history.

Introduction

Previous studies of Imdr Regio (Fig. 1) provided hints pointing toward its relatively young geologic age. Compared to other volcanic rises of Venus, Imdr Regio exhibits the smallest amount of associated volcanic deposits, with an approximate volume of $48 \cdot 10^6 \text{ km}^3$ (Smrekar et al., 1997). Wrinkle ridge patterns predate the formation of the topographic swell and have been uplifted by about 200 m (Smrekar et al., 1997). The density of wrinkle ridges at Imdr is also relatively small compared with the neighboring areas (Bilotti, Suppe, 1999). One possible interpretation is that the wrinkle ridges within Imdr Regio have been partially covered by subsequent lava flows. More recently, the VIRTIS instrument of the Venus Express mission observed high $1 \mu\text{m}$ emissivity anomalies which indicate chemically unweathered lavas at the summit and on the eastern flank of Idunn Mons (Fig. 2) (Smrekar et al., 2010; D’Incecco et al., 2016), the major volcanic structure (200 km diameter) of Imdr Regio. The emissivity anomalies observed by VIRTIS have been interpreted as possibly due to geologically recent volcanic activity (Smrekar et al., 2010; D’Incecco et al., 2016).

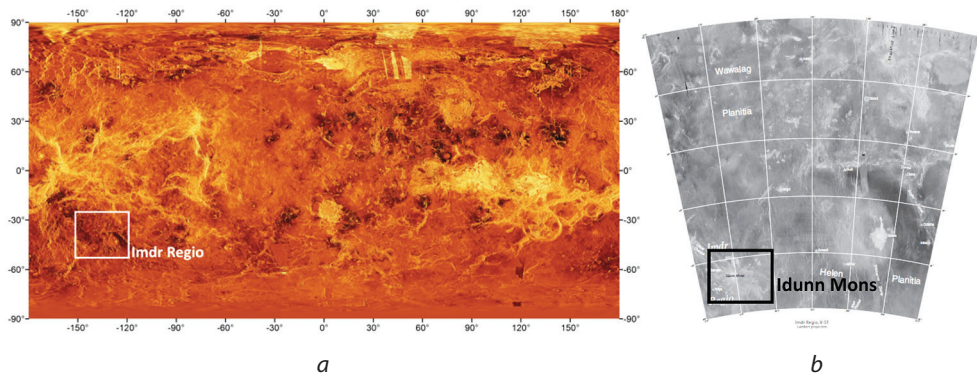


Figure 1: Magellan radar brightness mosaic of the Venus surface in cylindrical projection indicating location of Imdr Regio (25–50°S/210–240°E) (a); V-51 (Imdr Regio) quadrangle (b)

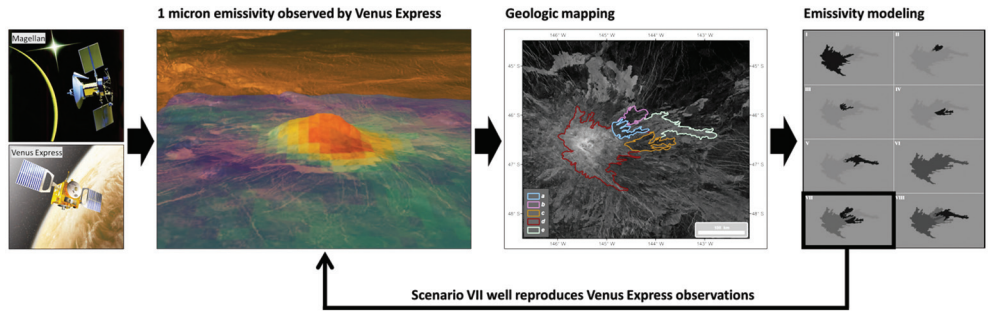


Figure 2: Schematic representation of the steps required to perform the Emissivity Modelling over the Eastern flank of Idunn Mons (46°S; 146°W)

The smaller volume of volcanic deposits, the lower density of wrinkle ridges and the 1 μm emissivity anomalies observed by the VIRTIS instrument on Idunn Mons all suggest that the topographic rise of Imdr Regio might currently be in an early stage of evolution with ongoing volcanic activity.

Geologic mapping of the V-51 (Imdr Regio) quadrangle of Venus

Following the guidelines provided by previous work (i.e., Tanaka et al., 1993; Wilhelms, 1990), the V-51 quadrangle will be mapped at the V-MAP scale resolution of 1:5,000,000. Given the latitude of the study area, the Lambert Conformal Conic projection will be used. Cycle 1 and Cycle 2 Magellan SAR images will be used as a basemap for the mapping. Using GIS software, the V-51 quadrangle will be divided into three main layers: a) all visible tectonic features (i.e., wrinkle ridges, grabens), b) geomorphologic units, and c) impact craters.

The tectonic map will provide information on the interaction between global and local scale stress fields, which contributed to the deformation of the study area until the present. Moreover, the map of all visible tectonic features will help during the determination of the relative age of units defined through geomorphologic mapping.

Geomorphologic mapping of the visible surface units will be conducted based on two main parameters: the variations in radar brightness and the cross-cutting relations between surface deposits. However, in some cases it is possible that units falling into the same geomorphologic class display different radar brightness, for example due to differing stages of chemical weathering or due to local topography which can greatly affect the radar brightness at the latitudes of Imdr Regio. For this reason, when interpreting geomorphology, both SAR left- and right-look images will be used. Additionally, where needed, information from other datasets like SAR rms slope, topography, radiothermal emissivity and reflectivity may also be used.

All visible impact craters in the study area will also be mapped. Mapping the impact craters will cover a double function. First (along with tectonic lineaments), impact craters can favor the time-correlation between the different geomorphologic units. In addition, the size-frequency distribution of the impact craters in the V-51 quadrangle can be calculated and compared with other quadrangles of Venus and with the global average.

The geologic map of the V-51 quadrangle — as for the other quadrangles of Venus — will be accompanied by: a) the description of map units (DOMU), b) the correlation chart and c) discussion of the geologic history of the study area. If necessary, additional information will be provided, such as cross sections or other maps of the study areas (at lower resolution).

Geologically supervised study of the radiothermal properties of the lava flows at Idunn Mons

Datasets Fusion Techniques as the key methodology

Datasets Fusion Techniques (DFTs) were first developed by (D’Incecco et al., 2015, 2016a, b) and used on Mercury and Venus, for the geologically supervised spectral analysis of impact and volcanic deposits, respectively. The main concept behind these techniques consists of overlapping two or more datasets, from the same or different space missions, to achieve a more complete understanding of the study area.

The DFT procedure can be divided into two main steps: 1) importing into GIS software part of or the complete datasets which are going to be overlapped, 2) performing GIS intersections between the datasets on the specific portion of the surface of interest.

During step 1, the study area to import is selected — usually a square or rectangular portion (Fig. 3a, b). When importing data directly from a database, SQL spatial queries are used. Datasets can have either raster or shapefile formats, but intersections between shapefiles are preferred for two reasons: a) facilitating the data processing and b) for better visualizing the data in the tables. Hence, if necessary, raster datasets are converted to shapefile format (points or polygons) before step 2.

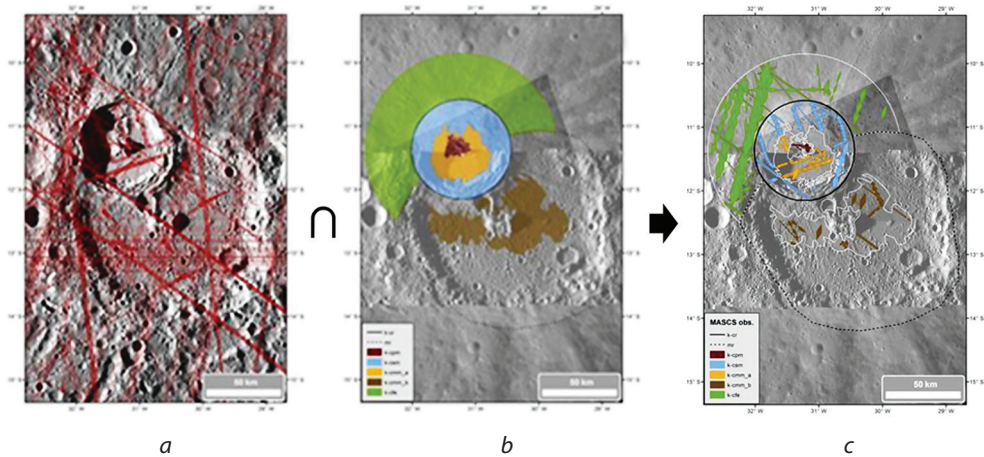


Figure 3: The images display the application of DFTs to the 62.4 km diameter Kuiper crater (11.3°S, 31.3°W) on Mercury: a) all available spectral observations are visualized as red polygons over the map representing the study area; b) the morphologic units are mapped as polygonal shapefiles on the study area; c) the spatial join between the polygons of Fig. 3a, b results in all the spectral observations completely contained within the boundaries of the mapped geologic units

During step 2, spatial intersections (joins) between the datasets are performed (Fig. 3c). Those intersections can be performed on either a local or global scale. In the most extreme case, with one single query, we simultaneously selected hundreds of thousands of spectral observations in the form of quadrilateral multipolygons that were completely contained within hundreds of impact units in the form of complex multipolygons with irregular shape, globally distributed over the surface of Mercury.

Dielectric permittivity (ϵ) as the diagnostic parameter

The dielectric permittivity (ϵ) is a key parameter for this study, as it provides important information about relative age (surface weathering), density and composition of surface deposits (Bondarenko et al., 2003; Pettengill et al., 1992). Although there are no direct estimates of the dielectric permittivity (ϵ), this parameter directly influences three types of radiophysical data: a) radar brightness, b) radiothermal emissivity and c) Fresnel reflectivity, all obtained at a wavelength of 12.6 cm by the Magellan Radar System (RDRS) with its different operational modes (Pettengill et al., 1992).

Bondarenko et al. (2003) analyzed the spectral properties of volcanic units on Venus through a qualitative survey of sharp emissivity contrasts. Although the qualitative nature of their approach does not allow using their study for statistical assessments, these authors found a recurrent correlation between radar brightness, radiothermal emissivity and dielectric permittivity (ϵ) on the volcanic deposits they analyzed. They observed that if area A is characterized by lower radiothermal emissivity and higher radar brightness compared to area B then, regardless of the roughness contrasts, area A will have higher dielectric permittivity (ϵ) than area B (Table 1). Correlating this observation with the stratigraphic position of the analyzed units, Bondarenko et al. (2003) found that older deposits are usually characterized by lower dielectric permittivity (ϵ).

Building on the qualitative approach from Bondarenko et al. (2003), the dielectric permittivity (ϵ) of the volcanic deposits of Idunn Mons and other large volcanoes on Venus will be derived using the

capabilities of DFTs for extracting the radiophysical data from the morphologically mapped lava flows. The results of this analysis will then be compared with the independent stratigraphic reconstruction of the volcanic deposits for each large volcano.

Table 1: Qualitative assessment of possible contrast between radiothermal emissivity and radar brightness (radar cross section) between two areas, A and B, due to contrast in surface roughness and dielectric permittivity (ϵ), from (Bondarenko et al., 2003).

| ξ | $\epsilon_A \approx \epsilon_B$ | $\epsilon_A > \epsilon_B$ | $\epsilon_A < \epsilon_B$ |
|-----------------------|---|---|---|
| $\xi_A \approx \xi_B$ | $E_A \approx E_B \quad \sigma_A \approx \sigma_B$ | ● $E_A < E_B \quad \sigma_A > \sigma_B$ | $E_A > E_B \quad \sigma_A < \sigma_B$ |
| $\xi_A > \xi_B$ | $E_A > E_B \quad \sigma_A > \sigma_B$ | ● $E_A < E_B \quad \sigma_A > \sigma_B$ $E_A \approx E_B \quad \sigma_A > \sigma_B$ $E_A > E_B \quad \sigma_A > \sigma_B$ | $E_A > E_B \quad \sigma_A < \sigma_B$ $E_A > E_B \quad \sigma_A \approx \sigma_B$ $E_A > E_B \quad \sigma_A > \sigma_B$ |
| $\xi_A < \xi_B$ | $E_A < E_B \quad \sigma_A < \sigma_B$ | $E_A < E_B \quad \sigma_A < \sigma_B$ $E_A < E_B \quad \sigma_A \approx \sigma_B$ ● $E_A < E_B \quad \sigma_A > \sigma_B$ | $E_A < E_B \quad \sigma_A < \sigma_B$ $E_A \approx E_B \quad \sigma_A < \sigma_B$ $E_A > E_B \quad \sigma_A < \sigma_B$ |

Emissivity, E; radar cross section, σ ; roughness, ξ ; dielectric permittivity, ϵ .
If we observe $E_A < E_B \quad \sigma_A > \sigma_B$, then regardless of ξ , we can be sure that $\epsilon_A > \epsilon_B$

Conclusions

Preliminary analyses of Imdr Regio and its major volcanic structure, Idunn Mons, show that this region might be geologically younger than the surrounding regions and that it is a scientifically compelling candidate target for future missions to Venus, such as the Venera-D mission.

The geologic mapping of the V-51 quadrangle will reconstruct the regional stratigraphic history of this area, which will be directly compared with the planetary average. The geologically supervised spectral study of Idunn Mons will constrain the eruptive style and the volatile content of the lava flows at this recently active volcano. This analysis will provide important clues about the presence (or absence) of an asthenosphere on Venus, that is the key to resolving the debate between catastrophic and equilibrium resurfacing.

The results of this study will also provide information necessary to assess the viability of Imdr Regio as a candidate landing site for the Venera-D Mission. Possible landing sites within Imdr Regio will be proposed following three main criteria: a) The scientific interest for an in-situ chemical investigation, b) The ability to safely land, and c) The suitability of the surface conditions, to increase the survival time of the lander.

References

Bilotti, F., Suppe, J. (1999) The Global Distribution of Wrinkle Ridges on Venus, *Icarus*, 139(1), 137–157, <http://dx.doi.org/10.1006/icar.1999.6092/>.
 Bondarenko, N.V., Kreslavsky, M.A., Raitala, J. (2003) Correlation of dielectric permittivity of volcanic units on Venus with age, *J. Geophys. Res.*, 108(E2), 5013, doi: 10.1029/2002JE001929.
 D’Incecco, P., Helbert, J., D’Amore, M., Maturilli, A., Head, J.W., Klima, R.L., Izenberg, N.R., McClintock, W.E., Hiesinger, H., Ferrari, S. (2015) Shallow crustal composition of Mercury as revealed by spectral properties and geological units of two impact craters, *Planet. Space Sci.*, 119, 250–263, doi: 10.1016/j.pss.2015.10.007.
 D’Incecco, P., Helbert, J., D’Amore, M., Ferrari, S., Head, J.W., Maturilli, A., Hiesinger, H. (2016a) A geologically supervised spectral analysis of 121 globally distributed impact craters as a tool for identifying vertical and horizontal heterogeneities in the composition of the shallow crust of Mercury, *Planet. Space Sci.*, <http://dx.doi.org/10.1016/j.pss.2016.08.004> (available 31.08.2016).

- D'Incecco, P., Mueller, N., Helbert, J., D'Amore, M. (2016b) Idunn Mons on Venus: location and extent of recently active lava flows, *Planetary and Space Science J.*, <http://dx.doi.org/10.1016/j.pss.2016.12.002> (available 21.12.2016).
- Pettengill, G. H., Ford, P. G., Wilt, R. J. (1992) Venus surface radiothermal emission as observed by Magellan, *J. Geophys. Res.*, 97(E8), 13091–13102, doi: 10.1029/92JE01356.
- Smrekar, S.E, Kiefer, W.S., Stofan, E. R. (1997) Large volcanic rises on Venus, In: *Venus II: Geology, geophysics, atmosphere and solar wind environment*, S.W. Bougher, D.M. Hunten, R. J. Phillips (Eds.), Tucson, Univ. of Ariz. Press, 845–878.
- Smrekar, S. E. et al. (2010) Recent hot-spot volcanism from VIRTIS Emissivity data, *Science*, 328(5978), 605–608.
- Tanaka, K. L., Schaber, G. G., Chapman, M. G., Stofan, E. R., Campbell, D. B., Davis, P. A., Guest, J. E., McGill, G. E., Rogers, P. G., Saunders, R. S., Zimbelman, J. R. (1993) The Venus geologic mappers' handbook, USGS OFR, 93–516.
- Wilhelms, D.E. (1990) Geologic mapping, In: Greeley R., Batson R. M. *Planetary Mapping*, New York, Cambridge University Press, 208–260.

DETERMINATION OF THE VENUS SURFACE ELEMENTAL AND MINERALOGICAL COMPOSITION ON VENERA-D MISSION

T. E. Economou

Enrico Fermi Institute, University of Chicago, USA

Abstract

The determination of the elemental and mineralogical composition of surface material should be one of the most important scientific goals of any lander on the surface of Venus. A detailed knowledge of these parameters is absolutely necessary to understand the origin and the development of Venus as compared to Earth and other terrestrial planets. Also very important is to understand the interaction between the surface and the atmosphere of the planet Venus. This may give us a clue of the processes that contributed to today's Venus climatic conditions.

Introduction

Although Venus is a rocky planet similar to the Earth in size and mass, its surface and atmosphere differ significantly from our planet. Shrouded by a thick atmosphere, the rocky surface lies beneath the thick layers of clouds and remained hidden until it was probed by Pioneer Venus Orbiter radar in 1978 that showed that, unlike Mars and Mercury which are both scarred by craters, Venus has a relatively smooth surface. Venus likely also has a mantle and a core. The mantle is probably rocky and the core is somewhat liquid. Venus has a much weaker magnetic field than Earth, supposedly because of its slow rotation — 243 Earth's days — and the core may not spin fast enough to create a magnetic field, the way the core of Earth and other planets do. The core may also be completely solid, or may not even exist at all. How well do we know the surface of Venus? Apparently not very well.

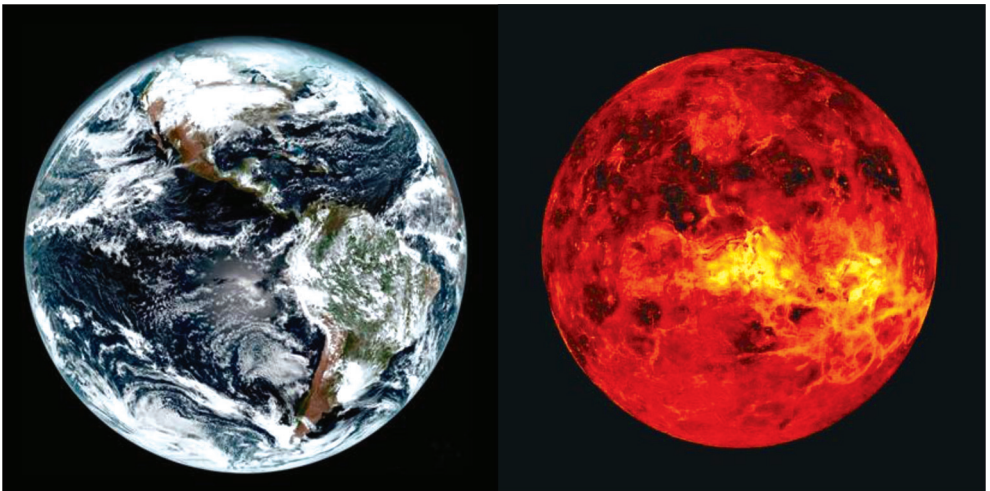


Figure 1: Although Earth and Venus are similar planets in their size, weight and age, they are completely different in their climatic conditions

The purpose of this paper is to summarize briefly the present status of surface elemental and mineralogical composition and show how we obtained it and then look ahead what science needs to be done on a new Venera-D mission to Venus and also point what new hardware can achieve it.

Whatever we know so far about Venus surface chemistry, it comes from the Soviet VENERA and VEGA space missions in 1970's and 1980's. At that time several VENERA and VEGA missions launched by the Soviet Union landed and successfully operated on the surface of Venus for more than an hour and provided us with the first crude elemental analysis (Surkov et al., 1984; 1986; 1987). These missions were incredibly successful despite the fact that the environmental condition on the surface of Venus are very vigorous with surface temperature reaching 462 °C and the

pressure almost 500 atmospheres, a 100 fold more than the pressure on Earth. Table 1 lists the individual measurements accomplished by Venera-8...-15 and Vega-1, -2. It was the Venera-8 that provided the first information on the radiogenic elements K, Th and U and the Venera-13 that provided the first surface elemental composition by XRF technique. Due to the technology limitation at that time, and also due to the short mission operation on the surface, the knowledge of the surface composition is not complete or accurate enough that we would like. But that was more than half a century ago.

Since then, many new analytical techniques have been developed and successfully applied on various space missions that provided much more accurate and more detailed compositional results (Economou et al., 1976; Rieder et al., 1997, 2004; Klingelhöfer et al., 2003). However, none of these instrumentations developed mainly for missions to the Moon, other planets, comets or asteroids have yet demonstrated that they can operate under the environmental conditions on the surface of Venus.

Table 1. List of the Soviet VENERA and VEGA missions in 1970s and 1980s that provided the first composition information about surface of Venus.

- Venera-8** Atm/surface probe Landed on 22 Jul. 1972 on the day side near the terminator at 10°S, 335°E. Measured the abundance of naturally occurring radiogenic elements K–U–Th. Operated for 50 min on the surface.
- Venera-9** Orbiter/lander. Landed on 22 Oct 1975 on the day side at 32°N, 291°E, First image from the surface, K–U–Th gamma ray analysis on the surface. Operated for 53 min on the surface. Maybe lost contact with the orbiter out of range.
- Venera-10** Orbiter/lander. Same design and science as Venera-9. Landed on 25 Oct. 1975 at 16°N, 291°E. Measured K–U–Th gamma ray surface composition.
- Venera-13** Orbiter/lander. Landed on the day side at 7.5°S, 303.0°E on 1 Mar. 1982. Conducted XRF analysis of the surface material.
- Venera-14** Orbiter/lander. Same design and science as Venera-13. Landed on the day side at 13.4°S, 310.2°E on 5 Mar 1982. Conducted XRF analysis of the surface material.
- Vega-1** flyby/lander. Lander on the night side of the planet at 8.1°N, 176.7°E. The lander conducted K–U–Th gamma ray surface composition with a GRS (XRF analysis failed) on the surface.
- Vega-2** Flyby/lander. Same design and science as Vega-1. Landed at 7.2°S, 179.4°E on 15 Jun. 1985 and conducted successfully XRF analysis and Measured K–U–Th gamma ray surface composition.

Description of some of the analytical techniques considered to be used on Venera-D mission to Venus

1. The Gamma Ray Spectrometer (GRS)

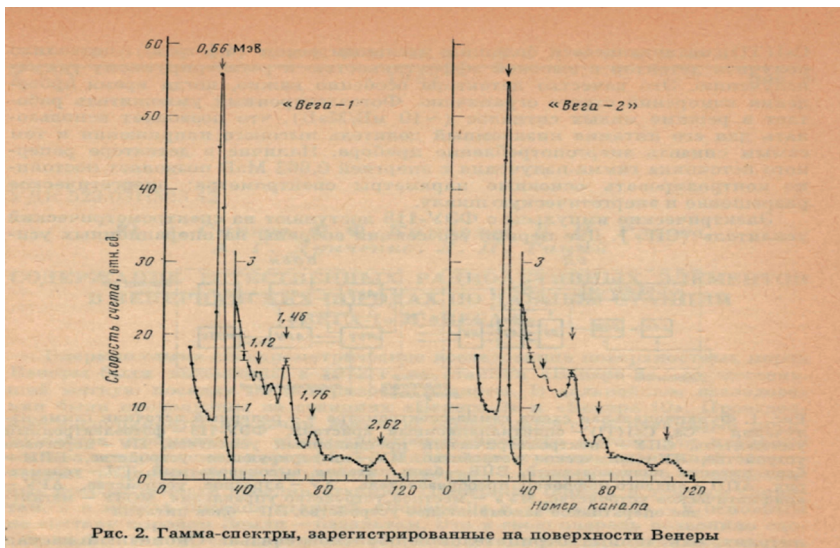


Рис. 2. Гамма-спектры, зарегистрированные на поверхности Венеры

Figure 2: The gamma ray spectra obtained by VEGA 2 mission

The GRS is used to measure the bulk elemental composition of planetary bodies as well the abundance of radiogenic elements K, Th and U in bulk samples. Venera-8, Venera-9, Venera-10 and Vega-1, -2 landers used a passive Gamma Ray Spectrometer (GRS) (Surkov et al., 1984; 1986; 1987) to obtain the radiogenic elements K, Th and U in the Venusian surface.

From the abundances of these elements, it is possible to deduce the general character of the rocks (basalt, granite, etc.) and by the analogy the approximate chemical composition. Fig. 2 shows the energy spectra obtained by Vega-1, -2 from which the abundances for these elements were calculated. These results are shown in Table 2.

Table 2: Abundances of K, U and Th as was determined by GRS on Venera-8...-10 and Vega-1, -2

| Содержание урана, тория и калия в породах Венеры | | | |
|--|---------------|------------------------|-------------------------|
| Станция | Содержание, % | | |
| | калий | уран, 10 ⁻⁴ | торий, 10 ⁻⁴ |
| «Вега-1» (1984) | 0,45±0,22 | 0,64±0,47 | 1,5±1,2 |
| «Вега-2» (1984) | 0,40±0,20 | 0,68±0,38 | 2,0±1,0 |
| «Венера-8» (1972) | 4,0±1,2 | 2,2±0,7 | 6,5±0,2 |
| «Венера-9» (1975) | 0,47±0,08 | 0,60±0,16 | 3,65±0,42 |
| «Венера-10» (1975) | 0,30±0,16 | 0,46±0,26 | 0,70±0,34 |

On Venera-D the GRS can detect the presence of naturally existing radioactive elements in Venusian soil (K, U, Th) by similar technique as was successfully used on past Venera-8, -9, -10 and Vega-1, -2 missions but with more modern sensors.

A new active gamma ray instrument, AGNESA, (GRS + Pulse Neutron Generator) has been developed at IKI that could be considered for Venus landing mission to evaluate the bulk soil composition using remote measurements. This instrument is quite advanced and has been selected for future Moon lander (Litvak, 2017). Same preliminary test results are shown in Table 3 which compares its results with the true elemental composition.

Table 3: Element composition of the simulant of martian regolith used in the ground tests (bold values correspond to a probable Venus composition)

| Element | Abundance (%) | Determined by GRS(%) |
|---------|---------------|-------------------------|
| H | 0.0 | 0.062 |
| C | - | 0.499 |
| O | 43.886 | 37.729 |
| Na | 1.912 | 8.372 |
| Mg | 5.112 | 2.369 (6.9) |
| Al | 4.968 | 5.033 (8.47) |
| Si | 20.274 | 26.707 (24.32) |
| P | 0.537 | 0.004 |
| S | 3.777 | 0.005 (1.9) |
| Cl | 1.000 | 0.721 (0.3) |
| K | 0.384 | 0.204 (0.48) |
| Ca | 4.306 | 5.552 (5.35) |
| Ti | 0.578 | 0.007 (0.12) |
| Cr | 0.200 | 0.013 |
| Mn | 0.231 | 0.064 (0.1) |
| Fe | 12.748 | 12.490 (6.2) |
| Ni | 0.049 | 0.038 |
| Cu | - | 0.040 |

| Element | Abundance (%) | Determined by GRS(%) |
|---------|---------------|----------------------|
| Zn | 0.027 | 0.004 |
| Br | 0.017 | – |
| As | – | 0.010 |
| Sr | – | 0.063 |
| Zr | – | 0.004 |
| Ba | – | 0.009 |

GRS specifications:

- Used CsI ($\varnothing 6.3 \times 100$ cm) sensor and electronic box — all inside the lander — no need of deployment or bring sample inside the lander.
- Energy range:..... 0.3–3.0 MeV
- Energy resolution: 12 % at CsI line
- Weight:..... 7.5 kg
- Power:..... 12.5 Watt
- Spectral size: 128 channel

For VENERA-D the GRS can be used in two modes:

- Passive mode, where only the radiogenic elements K, Th and U will be determined,
- Active mode, when neutrons from a pulsed neutron source are reacting with different elements in the surface samples to produce γ -ray lines from which the bulk sample composition can be determined.

The GRS sequence could be as follows: For the first 30 min it can operate in passive mode to obtain the radioactive elements K, Th, U and then switch to active mode to obtain the bulk elemental composition using the pulsed neutron source.

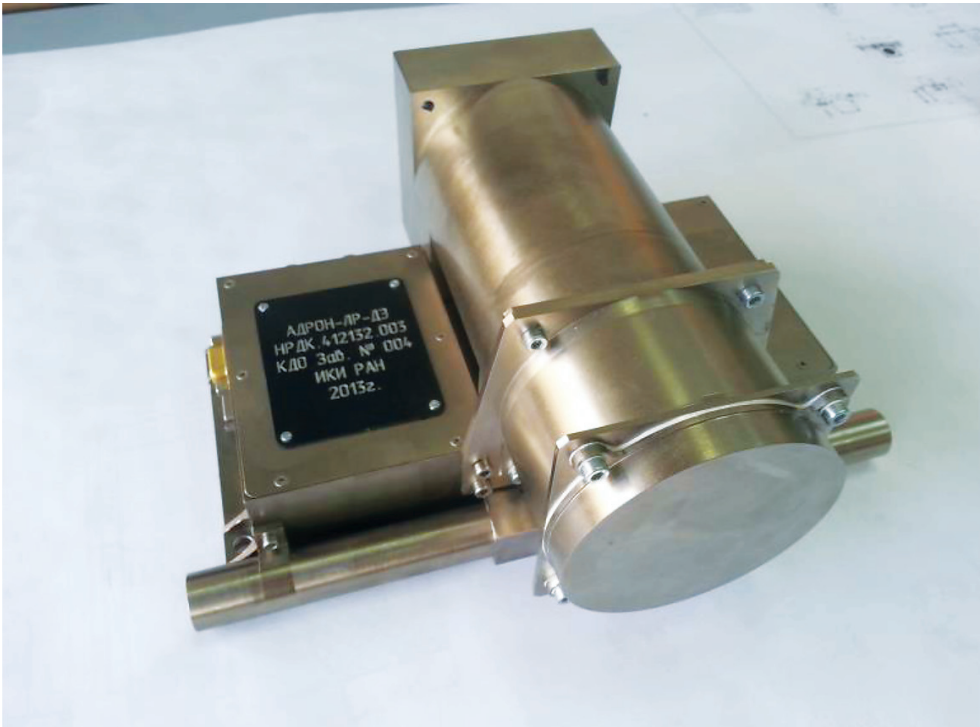


Figure 3: Photo of AGNES active GRS instrument developed at IKI for obtaining remotely the bulk composition of Venus surface

2. The X-Ray Fluorescence Spectrometer (XRF)

The XRF is a useful technique for determining the bulk elemental composition of planetary bodies and it was used by both US and Soviet lunar and martian mission in the past. It is a technique that uses an x-ray beam from a radioactive source to excite the characteristic elements in a sample and the appropriate electronics to record the generated x-ray spectra from which the composition information are computed. Venera-13 and -14 as well as Vega-1, -2 used an XRF instrument that used Fe⁵⁵ and Pu²³⁸ excitation sources and proportional counters to obtain compositional information from the surface of Venus. Fig. 4a depicts the principle of operation on the XRF technique and Fig. 4b shows the x-ray energy spectrum obtained from such an instrument on Vega-2. The compositional results obtained from these spectra are listed in Table 4.

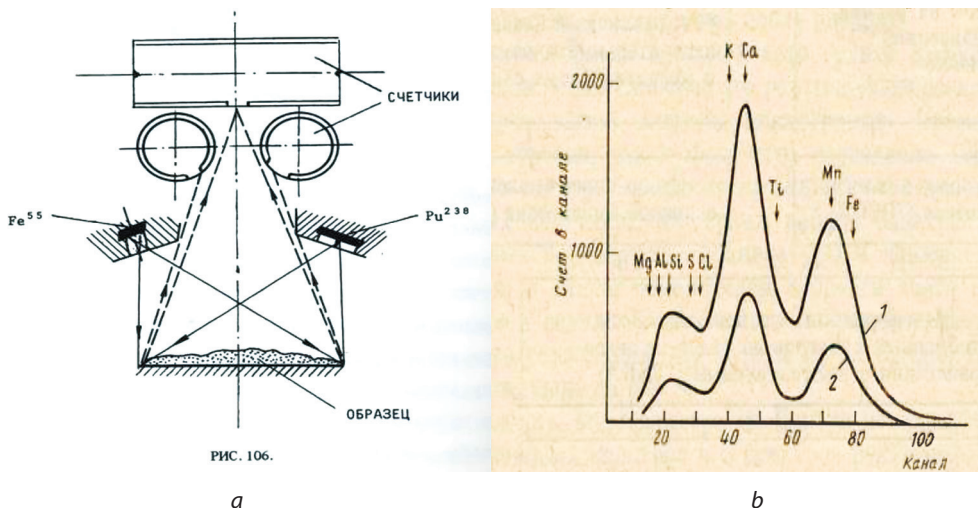


Figure 4: Diagram of XRF spectrometer used on Venera-14, -15 missions in 1970's (a); X-ray spectrum from Vega-2 (b)

Table 4. The elemental composition of surface of Venus at Venera-13, -14 and Vega-2. (For reference last column lists results of Luna-20 sample analysis)

петрохимического сопоставления $A-S$ диаграмм, где $A=Al_2O_3+CaO+Na_2O+K_2O$, а $S=SiO_2-(FeO+MgO+MnO+TiO_2)$ [5]; для «Венеры-13 и -14» из петрохимического сопоставления зависимостей $[K_2O/(K_2O+Na_2O)] - [(\sum FeO)/(\sum FeO+MgO)]$ для земных пород [2].

Определение концентрации S в исследуемом образце потребовало проведения дополнительных методических работ. Были измерены образцы (содержащие окислы основных породообразующих элементов в концентрациях, определенных в результате рассмотренного выше анализа), в кото-

| Элемент (окисел) | «Венера-13» | «Венера-14» | «Вера-2» | АНТ «Луна-20» |
|--------------------------------|-------------|-------------|-----------|---------------|
| MgO | 11,4±6,2 | 8,1±3,3 | 11,5±3,7 | 13,4 |
| Al ₂ O ₃ | 15,8±3,0 | 17,9±2,6 | 16±1,8 | 19,1 |
| SiO ₂ | 45,1±3,0 | 48,7±3,6 | 45,6±3,2 | 44,2 |
| K ₂ O | 4,0±0,63 | 0,2±0,07 | 0,1±0,08 | 0,47 |
| CaO | 7,1±0,96 | 10,3±1,2 | 7,5±0,7 | 13,3 |
| TiO ₂ | 1,59±0,45 | 1,25±0,41 | 0,2±0,1 | 0,52 |
| MnO | 0,2±0,1 | 0,16±0,08 | 0,14±0,12 | 0,12 |
| FeO | 9,3±2,2 | 8,8±1,8 | 7,74±1,08 | 6,91 |
| SO ₂ | 1,62±1,0 | 0,83±0,77 | 4,7±1,5 | 0,08 |
| Cl | <0,3 | <0,4 | <0,3 | |
| Na ₂ O * | 2,0±0,5 | 2,5±0,4 | 2,0 | 0,55 |
| | 98,1 | 98,7 | 95,8 | |

* Оценено теоретически.

The XRF was used in the past on the Moon on board of Lunokhod 1, -2, on Venus by Venera-13, -14 and Vega-1, -2 and on Mars by Viking-1, -2 and by the British Beagle 2 mission, although this mission failed during the Mars landing.

3. The Alpha Particle X-ray Spectrometer (APXS)

The (APXS), which is similar to the XRF, is now the choice instrument for the elemental chemical composition of planetary bodies. It has quite a lot of space heritage: A first version that included only the alpha and proton modes was developed in Chicago and it was used successfully on Surveyor 5, 6 and 7 missions in 1960s.

An improved version that added the x-ray mode of the APXS, (Economou et al., 1976), was used for the first time on the Soviet Phobos-1, -2 in 1988 (as a contribution by the University of Chicago and Max Planck Institute in Mainz, Germany).The APXS was also on board the Russian Mars-96 and US Pathfinder in 1996, ESA's Rosetta mission in 2002, MER missions (Spirit and Opportunity) in 2003 and Curiosity in 2012 with excellent performance and complete success on every mission. The APXS uses Cm-244 radioactive source for the excitation and the latest technology sensors and electronics for its operation. The latest version of the APXS is a very compact instrument with an excellent energy resolution of almost 140 eV FWHM at 5.9 keV. Fig. 5a shows a typical x-ray spectrum obtained Spirit and Opportunity on MER mission from which very accurate elemental abundances can be derived as shown on Table Fig. 5b is a photo of the APXS and the description of some of its components.

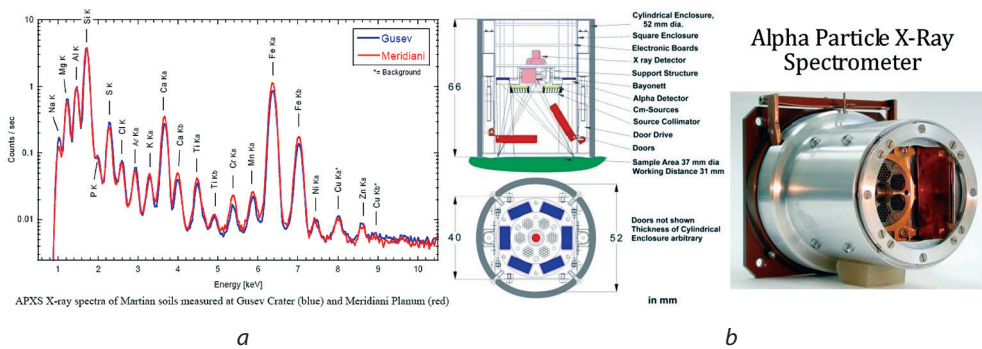


Figure 5: An X-ray spectrum from Spirit and Opportunity Mars mission (a); A photograph of the APXS for MER mission (b)

APXS Specifications:

- Uses ~50mCi of Cm-244 for excitation
- X-ray Sensor: Si PIN or Si drift detectors
- Weight:..... ~500 g
- Power:..... ~500 mW
- Energy resolution: 140 eV (FWHM) at 5.9 keV
- Detects all elements above Na, down to 10 ppm for some trace elements.

Table 5: Accuracy for the principal chemical elements and their associated errors as it was achieved by the APXS (Economou et al., 1976). The table on the right side gives examples of the detection sensitivity of the APXS for the minor and trace elements

| Table 5. Expected accuracies (at 90 % confidence limit) for principal chemical elements | | | Examples of expected sensitivities for minor elements evaluated for a basaltic matrix | | |
|---|----------|--------|---|----------|--------|
| Element | Weight % | Atom % | Element | Weight % | Atom % |
| C | ±0.2 | ±0.4 | N | 0.2 | 0.3 |
| O | ±0.7 | ±1.0 | F | 0.05 | 0.06 |
| Na | ±0.2 | ±0.2 | P | 0.2 | 0.14 |
| Mg | ±0.8 | ±0.7 | S | 0.1 | 0.07 |
| Al | ±0.4 | ~0.3 | Cl | 0.1 | 0.06 |

| Table 5. Expected accuracies (at 90 % confidence limit) for principal chemical elements | | | Examples of expected sensitivities for minor elements evaluated for a basaltic matrix | | |
|---|----------|--------|---|----------|---------|
| Element | Weight % | Atom % | Element | Weight % | Atom % |
| Si | ±1.2 | ±0.9 | K | 0.07 | 0.04 |
| K | ±0.2 | ±0.1 | V | 0.03 | 0.013 |
| Ca | ±0.2 | ±0.1 | Cr | 0.02 | 0.008 |
| Ti | ±0.15 | ±0.07 | Mn | 0.03 | 0.012 |
| Fe | ±0.4 | ±0.2 | Ni | 0.02 | 0.008 |
| | | | Cu | 0.02 | 0.007 |
| | | | Zn | 0.02 | 0.007 |
| | | | Rb | 0.001 | 0.0003 |
| | | | Sr | 0.001 | 0.0003 |
| | | | Y | 0.0005 | 0.0001 |
| | | | Zr | 0.0005 | 0.0001 |
| | | | Ba | 0.001 | 0.00017 |
| | | | La | 0.001 | 0.00016 |
| | | | Ce | 0.0008 | 0.00013 |
| | | | Nd | 0.0008 | 0.00012 |
| | | | Sm | 0.0005 | 0.00007 |
| | | | Pb | 0.005 | 0.0005 |
| | | | Th | 0.005 | 0.0005 |
| | | | U | 0.005 | 0.0005 |

Table 6: Elementary composition of Adirondack sample as was derived by Spirit APXS

| Sample Name: "A034_Adirontak_RATed" | | APXS Preliminary Analysis | | | | |
|-------------------------------------|------------------------------|---------------------------|-------|--|-------|-------|
| Spacecraft: | MLK2 | Elements | wt% | Oxides | wt% | mol% |
| Sol #: | 34 | Na ^{Na} | 2.10 | Na ₂ O | 2.85 | 2.30 |
| Measurement Start (LST): | 22:56:43 | Mg | 7.40 | MgO | 12.30 | 19.60 |
| Measurement Duration: | 10:21:44 | Al | 6.00 | Al ₂ O ₃ | 11.30 | 7.40 |
| LJA1_file #: | 2A129461188-LUK032/N1438NUM1 | Si | 20.60 | SiO ₂ | 44.10 | 47.10 |
| LBL_file #: | 2A129461188-EDR0227M1438NUM1 | P | 0.26 | P ₂ O ₅ | 0.60 | 0.27 |
| Time created: | 2004-02-07 21:33:36 | S | 0.40 | SO ₂ | 1.00 | 0.80 |
| | | Cl | 0.15 | Cl | 0.15 | 0.30 |
| | | K | 0.03 | K ₂ O | 0.03 | 0.02 |
| | | Ca | 5.10 | CaO | 7.10 | 8.10 |
| | | Ti | 0.25 | TiO ₂ | 0.41 | 0.33 |
| | | Cr | 0.44 | Cr ₂ O ₃ | 0.60 | 0.25 |
| | | Mn | 0.28 | MnO | 0.36 | 0.32 |
| | | Fe | 13.20 | (FeO) ⁽¹⁾ | 11.90 | 10.60 |
| | | Ni (ppm) | 120 | (Fe ₂ O ₃) ⁽²⁾ | 5.70 | 2.30 |
| | | Zn (ppm) | 60 | Γ _{FeO} T | 10.00 | |
| | | Rr (ppm) | ND | Σ Oxides ⁽³⁾ | 99.7 | 100.0 |

| Ratios: | | | |
|---------|-------|-------|------------------------|
| | Mg/Si | Al/Si | FeO/MgO ⁽⁴⁾ |
| | 0.30 | 0.29 | 1.40 |

Notes:

(1) sample matrix (for matrix correction and geometric yield) by closure, assuming all Fe as Fe₂O₃, and matrix free of H₂O, CO₂, etc.

(2) calculated with Fe²⁺/Fe_{tot} from MB (default assumption: Fe²⁺/Fe_{tot}=0.1).

(3) Na too low (by ~30 %) due to faulty algorithm. Will be corrected asap.

(4) assumes all Fe as FeO

4. Mineralogy Determination with Mössbauer and Raman Spectrometers

Mössbauer Spectrometer (MS) was used on MER Mars missions Spirit and Opportunity to obtain mineralogical information from martian surface samples (Klingelhofer et al., 2003). The MS is using Co-57 radioactive source and Si-drifted X-ray detectors. The MS has sufficient space heritage since it was also on board of Phobos Grunt mission, but the mission failed shortly after the launch. The MS, however has some limitation since it can provide information only on the iron bearing minerals. The MS shown on Fig. 6 performed well during the first half of the MER mission but due to short half-life of its Co-57 radioactive sources (270 days) it stopped being used after that. For a short mission to Venus, however, this will not be a problem.

The performance of MS is very good for iron bearing minerals, as it can be shown from Fig. 6 spectrum showing the presence of olivine, magnetite and pyroxene.

Most of the electronics of the MS is similar to the APXS electronics and probably, to save weight and power, these two instruments could be easily combined into one instrument for Venera-D mission.

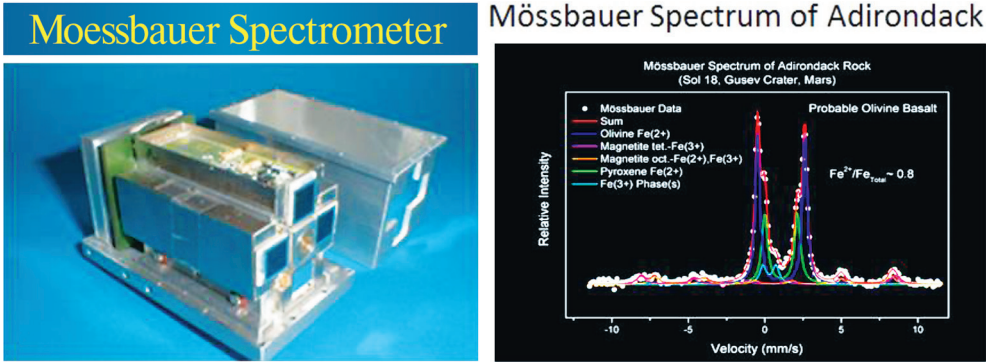


Figure 6: Photo of MS and sample spectrum of martian rock Adirondack obtained by Mars MER mission Spirit rover

More complete mineralogical information can be obtained by the Raman Spectrometer which is currently being developed for future Mars missions in the US by NASA. Raman spectrometer is a versatile technique for qualitative as well as quantitative mineralogical analyses. Samples are illuminated with a monochromatic laser beam which interacts with the molecules in the analyzed sample and the scattered light which has different frequencies is detected in the form of spectra that carry information about vibrational modes of the molecules. An example of Raman spectra is shown in Fig. 7. From these spectra accurate mineralogical information can be obtained. The CCD sensors require a significant cooling for proper operation.

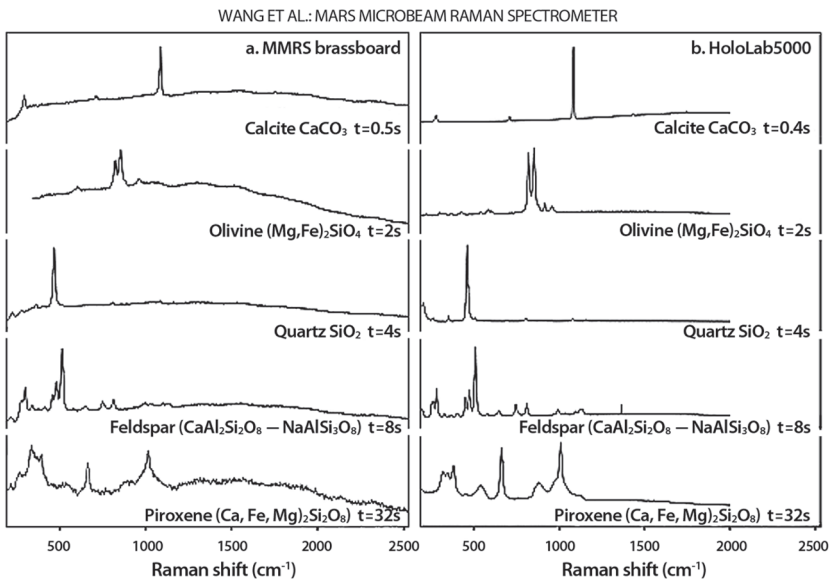


Figure 7: A typical Raman spectrum from a prototype Raman spectrometer developed by Washington University for future Mars mission (Wang et al., 2003)

The Raman Spectrometer can be placed inside the lander and analyze remotely samples outside the lander through a special window.

The very preliminary Raman spectrometer specifications:

- Weight:..... 8–10 kg
- Power:..... 20–80 W

Potentially, the Raman Spectrometer could be a US contribution on a future VENERA-D mission to Venus.

Conclusions

Some other potential instruments for the surface composition on the VENERA-D mission are the Gas Chromatograph/Mass Spectrometer (GCMS) and the Chemical Package instrument that have been developed recently at IKI. These instruments have been described elsewhere.

In the opinion of the author, in general, none of the above described instruments have demonstrated yet that they can perform properly under the severe environmental condition on the surface of Venus. They all have been tailored for either Mars or other atmosphereless bodies. Many details associated with cooling requirements, power restriction, short accumulation times, parallel running, data transmitting and many others have not been addressed yet. To have a successful mission to Venus, it will be necessary in the near future both agencies, NASA and Roscosmos, to engage in a program specifically tailored for development a Venus mission enabling instruments that can deliver the right science from the surface of Venus.

References

- Economou, T.E., Turkevich A.L. (1976) An Alpha Particle Instrument with Alpha, Proton and X-ray Modes for Planetary Chemical Analyses, *Nuclear Instruments and Methods*, 134, 391.
- Klingelhöfer, G., Morris, R.V., Bernhardt, B., Rodionov, D. (2003) Athena Mimos II Mossbauer spectrometer investigation, *J. Geophys. Res.*, 108(E12), doi: 10.1029/2003JE002138.
- Litvak, M. (2017) Active gamma ray spectrometer proposed for future Venus surface missions, *Moscow Venus Modeling Workshop*, Institute of Space Research, Moscow.
- Rieder, R., Wänke H., Economou T., Turkevich A. (1997) Determination of the Chemical Composition of Martian Soil and Rocks: The Alpha-Proton-X-Ray Spectrometer, *J. Geophys. Res.* 4027-4044.
- Rieder, R., Gellert R., Economou T., Klingelhöfer G., Lugmair G.W., Ming D.W., Squyres S.W., d'Uston C., Wänke H., Yen A., Zipfel J. (2004) Chemistry of Rocks and Soils at Meridiani Planum from the Alpha Particle X-Ray Spectrometer, *Science*, 306, 1746–1749.
- Surkov, Yu.A., Barsukov V.L., Moskalyova V.P., Kharyukova A.D., Kemurdzhian A.L. (1984) New data on the composition, structure, and properties of Venus rock obtained by Venera 13 and 14, Proc. Lunar Planet. Sci. Conf. 14th, Part 2, *J. Geophys. Res.*, 896, B393–B402.
- Surkov, Yu.A., Moskalyova V.P., Kharyukova A.D., Dudin A.D., Smirnov G.G., Zaitseva S.E. (1986) Venus rock composition at the VEGA 2 landing site, Proc. Lunar Planet. Sci. Conf. 17, Part 1, *J. Geophys. Res.*, 91, E215–E21.
- Surkov, Yu.A., Kirnozov, F.F., Glazov, V.N., Dunchenko, A.G., Tacii, L.P. (1987) Determination of natural radioactive elements in Venusian samples from VEGA 1 and VEGA 2 stations, *Kosmicheskie Issledovania*, 25(5).
- Wang, A., Haskin, L.A., Lane A.L. et al. (2003) Development of the Mars microbeam Raman spectrometer (MMRS), *J. Geophys. Res.*, 108(E1), 5-1–5-18, doi: 10.1029/2002JE001902.

SCIENTIFIC RATIONALE FOR SELECTING LANDING SITES ON VENUS: SO MANY CHOICES, SO FEW OPPORTUNITIES!

L. S. Glaze¹, M. S. Gilmore², A. H. Treiman³

¹ NASA Goddard Space Flight Center, Ocenter, USA, mgilmore@wesleyan.edu

³ Lunar and Planetary Institute, USA, treiman@lpi.usra.edu

Keywords: lander, regional plains, tessera, young volcanic deposits, basaltic, felsic

Introduction

One of the highest priority investigations for Venus science, as identified by the Venus Exploration Analysis Group (VEXAG) is to directly sample the elemental chemistry and mineralogy of a key geologic unit on the surface of Venus (Goals..., 2016). Further emphasis of the high priority for understanding surface chemistry is reinforced by the National Academy of Sciences Planetary Decadal Survey (Visions and Voyages) (Visions..., 2010), where the Venus In Situ Explorer (VISE) is listed as one of five targets for a New Frontiers mission within the current decade. While landers can achieve this science, flight opportunities are scarce and many scientific factors need to be considered when evaluating potential landing sites.

Criteria for site selection

Despite the clearly stated need for surface chemistry and mineralogy, neither the Decadal Survey nor VEXAG provide specific scientific guidance for sample site selection. However, because so little is known about Venus' surface chemistry and mineralogy (even after Venera and VEGA), several categories of landing sites can be justified within the context of (Goals..., 2016) and (Visions..., 2010). Specifically, new landing sites should address either "typical" planet-scale geochemistry questions (i.e., about the basaltic(?) plains units), or specific critical problems in Venus' present or past. Among these specific problems are the chemistry and mineralogy of: the tesserae, Maxwell Montes (possibly Venus' sole "continent"), potentially active volcanoes, and surface-atmosphere chemical reactions.

Furthermore, when considering possible landing sites, it is also important to ensure that exposed material at the site is representative of the targeted geologic unit. Not every site within a particular region is suitable as their surfaces may be affected by exogenous material, such as air fall deposits generated from distant impact craters. Impact ejecta on Venus are typically characterized by a parabola-shaped sedimentary mantling deposit (Campbell et al., 1992). These parabolas may obfuscate the original surface composition with up to 10 cm of material excavated from other geologic units (Campbell et al., 2015). Similarly, one must avoid surfaces with anomalous radar backscatter due to surface-atmosphere interactions (Pettengill et al., 1992).

"Typical" Surface

For a single geochemical lander, perhaps the most general science return would come from landing at a site where results could be extrapolated to the whole (or significant portions of) Venus. Such sites might include regional plains units (representing ~40 % of Venus' surface). Venus' regional plains are inferred to be basaltic from both Venera and Vega chemical analyses (Weitz, Basilevsky, 1993) and SAR geomorphology (e.g., (Guest et al., 1992)), but different sites have distinct chemistries (Filberto, Treiman, 2017) and (to some extent) different surface morphologies. The regional plains basalts represent significant outpourings of lava from the Venusian interior, and their compositions could (in theory) be interpreted to constrain Venus' geothermal gradient(s), its processes of magma genesis, and also the composition(s) of its upper mantle. With proper instrumentation (still in development), it might be possible to determine the basalts' eruption ages and thus test hypotheses of catastrophic versus gradual resurfacing.

Tesserae

Tessera terrain is a heavily tectonized unit comprising 8 % of the Venus surface (Ivanov, Head, 1996) that are stratigraphically older than the regional plains (Ivanov, Head, 2011). Although tesserae make up a relatively small fraction of the surface, they may hold significant clues to the first 80 % of Venus' evolutionary history that are not preserved in the young (<1 Ga) regional plains

(McKinnon et al., 1997). Relatively low 1 μm thermal emission for tessera units compared to the global average (Basilevsky et al., 2012; Gilmore et al., 2015; Mueller et al., 2008) are consistent with a more felsic composition (Gilmore et al., 2015; Mueller et al., 2008), which may require significant water and plate recycling for formation (Campbell, Taylor, 1983).

Consideration of impact ejecta deposits is particularly important in the tessera, where structural features may collect material of non-tessera composition (Campbell et al., 2015). Large portions of Tellus, Alpha and parts of Ovda tessera are free of parabola deposits presumably composed of basaltic material from plains craters (Gilmore, 2016).

Potentially Active Volcanoes:

The state of Venus' current volcanic and tectonic activity is of considerable interest because Venus is so similar to Earth in size and mass, and the interior heat must be lost through some mechanism. Although there have been tantalizing hints of possible active volcanism (Marcq et al., 2012; Shalygan et al., 2015), definitive evidence has yet to be identified. VIRTIS 1 μm thermal emission data have been used to identify surfaces that may be covered in young volcanic deposits (Smrekar et al., 2010) and may be good landing site candidates to resolve these questions.

Maxwell Montes

The Maxwell Montes highlands, part of Ishtar Terra, stands kilometers above the regional plains. It could be an Earth-style continent, standing so tall because it is composed of low-density silicic rock; if so, it could be proof that Venus once had an ocean of water (Campbell, Taylor, 1983). Most of Maxwell is extremely rough, but the floor and ejecta blanket of Cleopatra Crater are smoother, and a lander there would sample an average composition for Maxwell (Herrick, 2014).

Surface-Atmosphere Interactions

Understanding surface-atmosphere interactions would provide crucial constraints on the history of Venus' atmosphere and climate, and link to observations of exoplanets. General interactions could be studied at most typical sites, especially at younger volcanic, e.g. (Smrekar et al., 2010). Within Venus' highlands, two distinct sorts of atmosphere-surface interactions yield high radar backscatter (Treiman et al., 2016). Measurement of the mineralogy of these materials may yield insight into the composition of the surface, atmosphere, and redox state at the time of deposition.

Discussion and Conclusion

There are a range of scientifically justifiable landing targets that can address specific questions about Venus' surface chemistry and mineralogy, as well as the interaction of the surface with the atmosphere. In addition to the list provided here, the VEXAG Exploration Targets Workshop (Sharpton et al., 2014) also assessed the scientific and technical rationale for multiple types of landing sites. They concluded that the highest priority targets were (1) tesserae, (2) volcanic plains, and (3) young volcanic terrain. The key to selecting an appropriate target for the Venera-D lander is to identify the key scientific questions of interest and then to select an appropriate target to address those questions.

References

- Basilevsky, A.T. et al. (2012) Geologic interpretation of the near-infrared images of the surface taken by the Venus Monitoring Camera, Venus Express, *Icarus*, 217, 434–450. doi: 10.1016/j.icarus.2011.11.003.
- Campbell, I. H., Taylor, S. R. (1983) No water, no granites — No oceans, no continents, *J. Geophys. Res.*, 10, 1061–1064.
- Campbell, D. B. et al. (1992) Magellan observations of extended impact crater related features on the surface of Venus, *J. Geophys. Res.*, 97(E10) 16,249–16,277.
- Campbell, B. A. et al. (2015) Evidence for crater ejecta on Venus tessera terrain from Earth-based radar images, *Icarus*, 250(C), 123–130.
- Filberto, J., Treiman, A. H. (2017) Geochemistry of Venus basalts with constraints on magma genesis, *48th Lunar and Planetary Science Conf.*, Houston, TX, USA, 1148.
- Gilmore, M. S. (2016) Which tesserae are the most pristine?, *47th Lunar and Planetary Science Conf.*, Houston, TX, USA, 2621.
- Gilmore, M. S., Mueller, N., Helbert, J. (2015) VIRTIS emissivity of Alpha Regio, Venus, with implications for tessera composition, *Icarus*, 254(C), 350–361.
- Goals, Objectives, and Investigations for Venus Exploration* (2016) VEXAG, Venus Exploration Analysis Group, <https://www.lpi.usra.edu/vexag/reports/GOL-Space-Physics-Update-0816.pdf>.

- Guest, J.E. et al. (1992) Small volcanic edifices and volcanism in the plains of Venus, *J. Geophys. Res.*, 97(E10), 15,949–15,966.
- Herrick, R.R. (2014) Cleopatra Crater, a Circular Portal to the Soul of Venus, *Workshop on Venus Exploration Targets*, ed. V. Sharpton, Houston, TX, USA, 6025.
- Ivanov, M.A., Head, J.W. (1996) Tessera terrain on Venus: A survey of the global distribution, characteristics, and relation to surrounding units from Magellan data, *J. Geophys. Res.*, 101(E6), 14,861–14,908.
- Ivanov, M.A., Head, J.W. (2011) Global geological map of Venus, *Planetary and Space Science*, 59(13) 1559–1600.
- Marcq, E. et al. (2012) Variations of Sulphur dioxide at the cloud top of Venus's dynamic atmosphere, *Nature Geoscience*, 6, 25–28.
- McKinnon, W.B. et al. (1997) Cratering on Venus: Models and observations, In: Venus II, 1997, eds. Bougher S.W., Hunten D.M., Phillips R.J., Univ. Arizona Press. Tucson, AZ, USA, 969–1014.
- Mueller, N. et al. (2008) Venus surface thermal emission at 1 mm in VIRTIS imaging observations: Evidence for variation of crust and mantle differentiation conditions, *J. Geophys. Res.*, 113(E00B17), doi: 10.1029/2008JE003118.
- Pettengill, G. et al. (1992) Venus surface radiothermal emission as observed by Magellan, *J. Geophys. Res.*, 97(E8), 13,091–13,102.
- Shalygan, E.V. et al. (2015) Active volcanism on Venus in the Ganiki Chasma rift zone, *Geophys. Res. Lett.*, 42(12), 4762–4769, doi: 10.1002/2015GL064088.
- Sharpton, V., Esposito, L., Sotin, C. (2014) Final Report of the Venus Exploration Targets Workshop, *Venus Exploration Workshop*, May 19–21, 2014, Houston, TX, USA, <http://www.lpi.usra.edu/vex-ag/WorkshopTargets20160115.pdf>.
- Smrekar, S.E. et al. (2010) Recent hotspot volcanism on Venus from VIRTIS emissivity data, *Science*, 328(5978), 605–608.
- Treiman, A., Harrington, E., Sharpton, V. (2016) Venus' radar-bright highlands: Different signatures and materials on Onda Regio and on Maxwell Montes, *Icarus*, 280, 172–182.
- Visions and Voyages for the Decade 2013–2022* (2010) National Academies Press.
- Weitz, C.M., Basilevsky, A.T. (1993) Magellan observations of the Venera and Vega landing site regions, *J. Geophys. Res.*, 98, 17,069–17,097.

ESTIMATES OF THE FREQUENCY DISTRIBUTION OF SHORT-BASELINE (1–3 m) SLOPES FOR DIFFERENT TERRAINS ON VENUS USING TERRESTRIAL ANALOGS

M. Ivanov¹, N. Eismont², M. Gerasimov², N. Ignatiev², I. Khatuntsev², O. Korablev², M. Marov¹, L. Zasova², L. Zelenyj², O. Vaisberg²

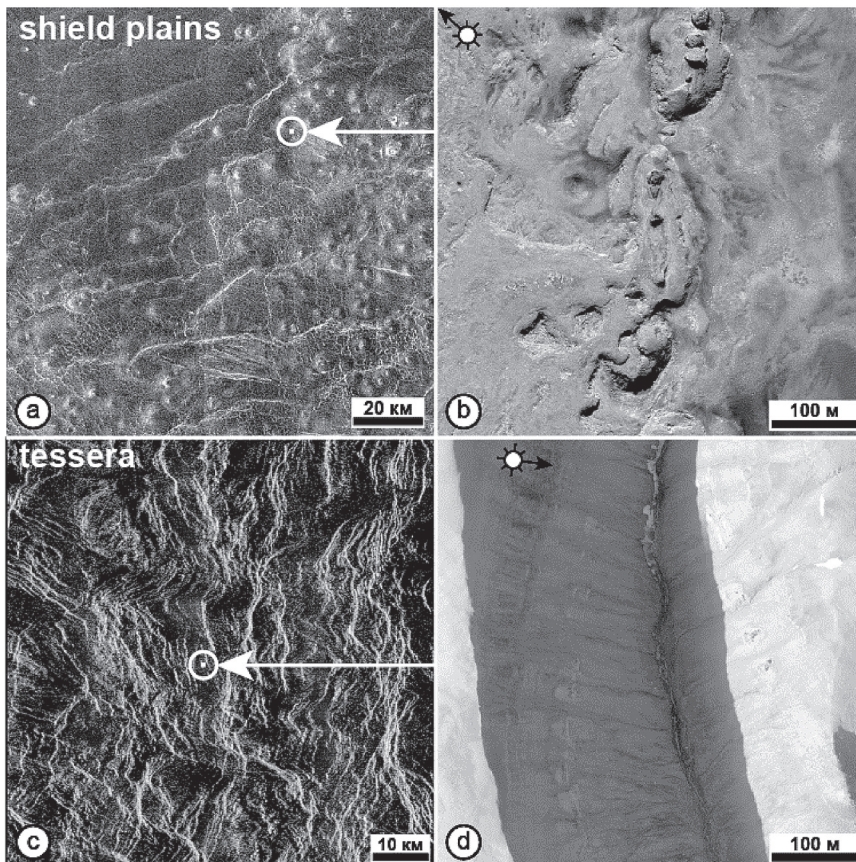
¹ Vernadsky Institute of Russian Academy of Sciences, mikhail_ivanov@brown.edu

² Space Research Institute of Russian Academy of Sciences

Keywords: Venus, Venera-D mission, short-baseline slopes

Introduction

The Venera-D mission includes a lander. The selection of a safe landing site requires estimations of the frequency distribution of slopes on baselines that are comparable to the horizontal dimensions of a lander, 1–3 m, which is impossible with the available altimetry data for Venus (Ford, Pettengill, 1992). In our study, we implemented an analogue approach and used digital terrain models (DTM) for several regions in Iceland (E. Hauber, DLR, personal communication). Spatial resolution of these DTMs is as high as 0.5 m and vertical resolution is 0.1 m. From a range of available DTMs, we have selected those for landscapes in Iceland that morphologically are similar to the terrains on Venus.



Venus.

Figure 1: Examples of terrains on Venus and their possible terrestrial analogs

Approach

Several areas in Iceland mimic landscapes that characterize surfaces on Venus. These areas have little vegetation and their topography reflects modern glacial, fluvial, and volcanic activity. The freshness of the relief is crucially important because of the low rate of erosion on Venus (e.g., Arvidson et al., 1992). The mode of formation of specific landforms in Iceland does not play a significant role in the assessment of the frequency distribution of slopes because processes of different nature may result in formation of morphologically similar landscapes on Venus and Earth. For example, smooth plains can represent a result of either volcanic (pahoehoe lava fields), or fluvial (outwash plains), or impact (fine-grained ejecta deposits) processes. Areas with numerous small volcanic constructs in Iceland represent a possible example of shield plains on Venus (Fig. 1a, b). The fractured glacier surfaces resemble the surface of densely lineated plains on Venus. The spurs of mountains in Iceland mimic both morphologic and topographic situations that likely characterize tessera regions on Venus (Fig. 1c, d).

Results and discussion

Tessera analogues: In order to model possible tessera landscapes, we used DTMs for mountain spurs and combined them together in order to model a wider range of morphologies that are expected to occur within tessera terrain. However, the surface of tessera shows very high morphological diversity (Fig. 1c) and, thus, our results of the topographic analysis of a possible terrestrial analogue can describe only the general characteristics of the model tessera surfaces. From the results of our study, we believe that tessera may have the following characteristics of the distribution of the short-baseline slopes (Fig. 2).

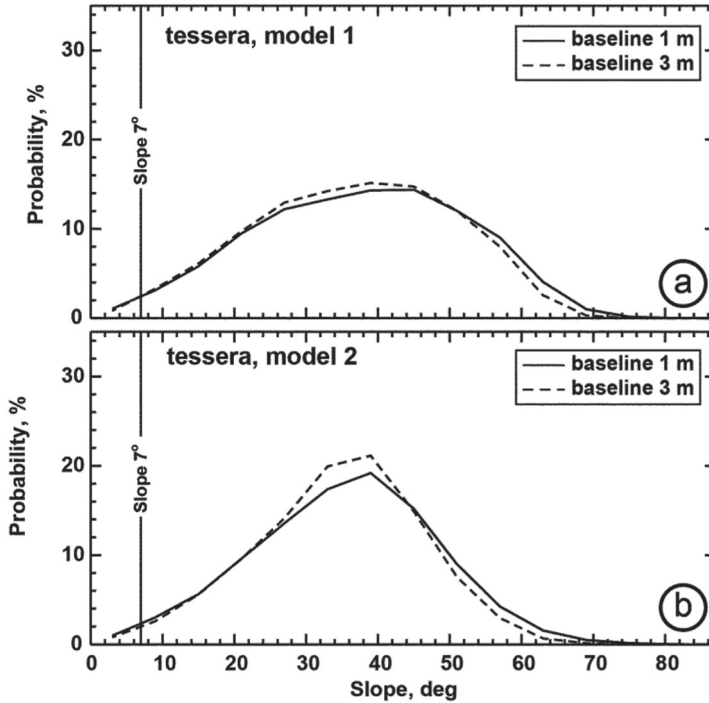


Figure 2: Estimates of the short-baseline slopes frequency distributions in possible terrestrial analogs of tessera

(1) The mode of the distribution should be right-shifted toward the steeper slopes. The mode position may easily exceed the broadly adopted the 7° safety limit (for slopes on 1–3 m baseline) (Arvidson et al., 1992). (2) The histogram of the slopes distribution can be broad with weakly pronounced mode, which indicates the higher probability of encounter of steep slopes upon landing on tessera. (3) The frequency distributions of slopes on 1 and 3 m baselines are close to each other and, thus, the probability of encountering the shallower slopes is not changed significantly for different short baselines. This suggests that the increase of the dimensions of a lander (in reasonable limits) will not noticeably increase the safety conditions of landing on tessera.

Plains analogues: Both the visual inspection of morphology and topographic profiles show that the volcanic plains on Venus have a longer-wavelength (hundreds of meters) topography with significantly smaller amplitude than either tessera or the other tectonized terrains. The smaller topographic variations within the plains units on Venus suggest that their terrestrial morphologic counterparts of different origin will better mimic both the qualitative and quantitative parameters of the slope frequency distribution within the Venusian plains.

The distribution of the short-baseline slopes on the surface in Iceland, which imitates shield plains on Venus, has the mode between 10-20°, and the entire histogram has a long tail toward the steeper slopes (Fig. 3a). The fraction of the steeper slopes is noticeably decreasing for the 3-m-baseline. However, the fraction of the slopes <7° is slightly over 20% (Fig. 3a). The distribution of the slopes on a surface that model regional plains on Venus is similar to that for shield plains model (Fig. 3b). For the morphological analogue of regional plains, the mode of the distribution is narrower and is between 8 and 15°. The decreasing of the fraction of the steeper slopes at a 3-m-baseline is more pronounced than that for the shield plains model (Fig. 3).

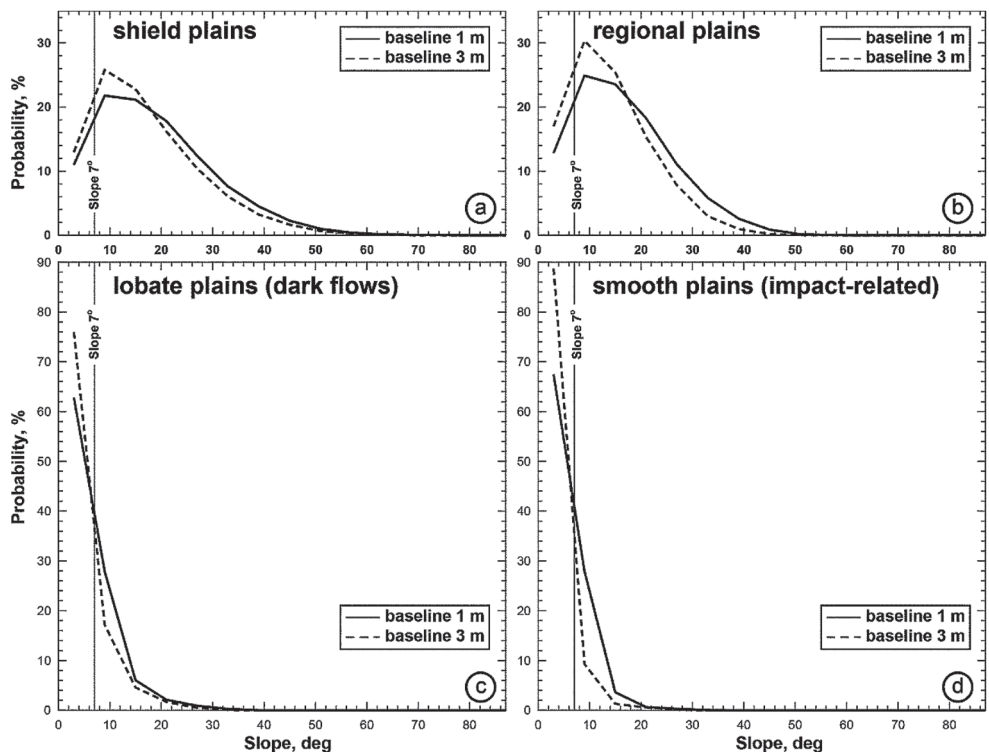


Figure 3: Estimates of the short-baseline slopes frequency distributions in possible terrestrial analogs of plains units on Venus

The distributions of the slopes on the surfaces that imitate the radar-dark flows of lobate plains and smooth plains of impact origin are similar to each other and strongly different from all other distributions (Fig. 3c, d). The main difference is that the histograms for the dark flows and smooth plains are very narrow and fraction of the steeper slopes decreases more significantly for a 3-m-baseline. For example, the fractions of the slopes <7° for a 1-m-baseline are 63 and 67% for the dark flows and smooth plains, respectively. For a 3-m-baseline, the fraction of the shallow slopes becomes 75 and 78% for the flows and the plains, respectively.

These results suggest that the dark flows of lobate plains and smooth impact plains (the surfaces within the dark parabolas) represent flatter, more horizontal and, thus, safer landing targets compared with the other modeled surfaces. The dark flows of lobate plains, however, are relatively small, a few tens of kilometers across, and always occur in a tight spatial association with the radar-bright flows. The enhanced radar signal from the bright flows suggests that the flows likely represent very rough aa-lavas (Fig. 4), the landing on which will cause failure of the mission.



Figure 4: Typical surface of aa-lavas (Moon National Park, USA; source: <http://waymarinc.com/images/blocky-lava-flow>)

Conclusions

Among the analyzed terrains, only smooth plains of the impact origin represent extensive areas where the probability of the encountering of the steeper slopes ($>7^\circ$ at 1–3 m baselines) is low. These plains, thus, are the most attractive regions for the selection of the Venera-D landing sites. The scientific value of the impact-generated plains is also high because the plains consist of highly homogenized, fine-grained materials that likely represent an integrated sample of the upper crust of Venus. In order to collect robust estimates of the frequency distribution of the short-baseline slopes in tessera additional measurements of topography of terrestrial mountain regions of different maturity are required.

References

- Arvidson, R.E., Greeley, R., Malin, M.C. et al. (1992) Surface modification of Venus as inferred from Magellan observation of plains, *J. Geophys. Res.*, 97(E8) 13,303–13,317.
- Beyer, R.A., McEwen, A.S., Kirk, R.L. (2003) Meter-scale slopes of candidate MER landing sites from point photogrammetry, *J. Geophys. Res.*, 108(E12) 8085.
- Ford, P.G., Pettengill, G.H. (1992) Venus topography at kilometer-scale slopes, *J. Geophys. Res.*, 97(E8), 13,103–13,114.

TECHNOLOGY

A PROTOTYPE OF SOIL SAMPLING SYSTEM FOR THE VENERA-D

M. V. Gerasimov, V. I. Mikhalsky, A. V. Nosov

Space Research Institute of Russian Academy of Sciences

Abstract

The information about the chemical composition of Venusian crust can help to answer many fundamental questions on the evolution of the Venus. The information on chemical composition of its crustal material can be received only from automated laboratories, delivered to Venusian surface, which permit direct analysis of soil samples by various methods. The delivery of a piece of crustal material inside a Lander is extraordinary difficult due to the extreme temperature and pressure at surface of the Venus. The sampling of the Venus surface soil and its analysis using XRF method was done for the first time during Venera-13, -14 and Vega-2 missions in 1982 and 1985 respectively. The Soil Sampling System (SSS), which was developed for these missions, provided quick and reliable sampling of Venusian soil in automatic mode. This SSS can be used as a prototype of the SSS for the Venera-D. The new set of instruments of the Lander must be able to make more detailed analysis of surface rocks both in elemental composition and in mineralogy. The use of different methods of analysis and a respective set of instruments inside the Lander of the planned Venera-D implies the need to have a certain upgrade of the former SSS to have a possibility to do multiple sampling, to distribute a sample between respective instruments, and to document the sampling procedure.

Introduction

Venus is usually considered as a “sister” planet of the Earth. Nevertheless, information about the chemical composition of Venusian crust is still an intriguing scientific goal which can help to answer many fundamental questions on differentiation of the Earth-like planets and their origin. The thickness of the atmosphere of Venus does not permit remote sensing of its surface.

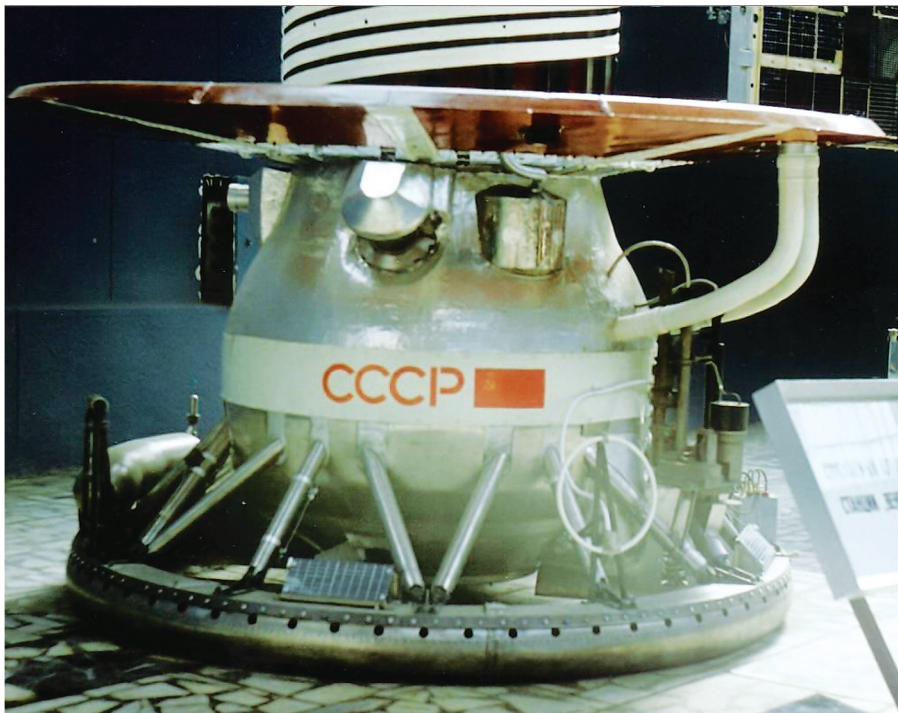


Figure 1: General view of the Venera-13, -14 and Vega-2 Landers. The Soil Sampling System is seen on the right side over the dampening torus. The vacuum tank of the Soil Sampling System is seen over the dampening torus on the left side

That is why the information on the chemical composition of its crustal material can be received only from scientific automated laboratories delivered directly to the planetary surface. At the surface of Venus there are two possibilities to investigate the composition of the soil: nearby remote sensing from the Lander (e.g. gamma spectroscopy or LIBS) and direct analysis of soil samples, which are delivered inside the Lander, by various methods of analysis. Both methods are complementary but a direct analysis of soil samples can be more informative and provide higher accuracy.

Delivery of the Lander to the surface of Venus is technically a very ambitious task but delivery of a sample of soil inside the Lander is also extraordinary difficult due to the extreme temperature and pressure at the surface of Venus. Both tasks were successfully fulfilled in the 1980's during Soviet missions to Venus. The sampling of the Venus surface soil and its analysis using XRF method was done for the first time during Venera-13, -14 and Vega-2 missions in 1982 and 1985 respectively. The Soil Sampling System (SSS), which was developed for these missions, provided quick and reliable sampling of Venusian soil. Thus, it is worth to use elements of the SSS as prototypes for the development of the new sampling system for the Venera-D mission given that the former Lander is considered as a prototype for the Venera-D Lander. Figure 1 shows the general view of Venera and Vega Landers.

Description of the Soil Sampling System VB-02

The Soil Sampling System of Venera-13, -14 and Vega-2 Landers was given an index name, "VB-02". The task of VB-02 was to take a sample of soil, transport it inside a vessel, and provide its readiness for analysis by the X-ray fluorescent spectrometer "Arakhis". The sampling was necessary to perform at around 500 °C temperature and 10 MPa pressure of CO₂ with the reduction of temperature and pressure during delivery down to 20–30 °C and 5–6 kPa. The operation had to be performed in automatic mode. The roughness and hardness of rocky material at the landing site was unknown.

The SSS VB-02 included the following functional parts (Barmin, Shevchenko, 1983) (Fig. 2):

- drilling mechanism;
- pyro cartridge assemblage with gas transfer tubes;
- sample transfer mechanism;
- intake chute of the XRF instrument;
- vacuum tank.

The drilling mechanism was located on a damping torus of the Lander without thermal insulation. The pyro-cartridge assemblage and the sample transfer mechanism were mounted outside of the vessel but under the outer thermal insulation.

The Drilling Mechanism (DM)

The DM was designated to come into contact with the planetary surface under the Lander, to drill surface rocks, take in a sample of fractionated rocks, and transfer it into the sabot of the sample transfer mechanism. The DM consisted of an electrical motor, gear assembly, a sampling device, and a transportation mechanism (Fig. 3). The sampling device had the drilling tool which could propagate down to 40 cm until it would come into contact with surface rocks. Subsequently, it was fixed by a ball lock and further forced propagation was performed by the block-and-tackle mechanism. Both rotation of the tool and propagation of the block-and-tackle mechanism was activated by the electrical motor. At the end of the drilling tool there was an anchoring plate with spikes to fix the positioning of the tool over the rocks. The drilling tool resembled a tube with a wing-like feature. The upper side of the drilling tube was connected with the transportation mechanism by a transfer tube which ended over the sabot of the sample transfer mechanism. The transportation mechanism had a sealed tank with a pressure of about 100 kPa which was connected to the sample transfer tube in the vicinity of the sabot. The end of this tube had a filter to prevent passage of the fractionated soil into the tank (Fig. 4).

Operation of the DM started with the activation of the motor. It unblocked the drilling tool and provided its propagation down to the planetary surface. Drilling of the surface material was performed under the pressure created by the block-and-tackle mechanism. The duration of the drilling was 2 min. The depth of the rilling was about 3 cm. When the drilling was finished, the pyro-cartridge opened the sealed tank and the outside pressure provided an intense flow of CO₂ into the tank. Fractionated soil was transported by the flow through the tubes down to the filter. The transported sample of soil at the end of the flow dropped by gravity into the sabot. The volume of the sample was varied from 1 to 6 cm³ (Barmin, Shevchenko, 1983).

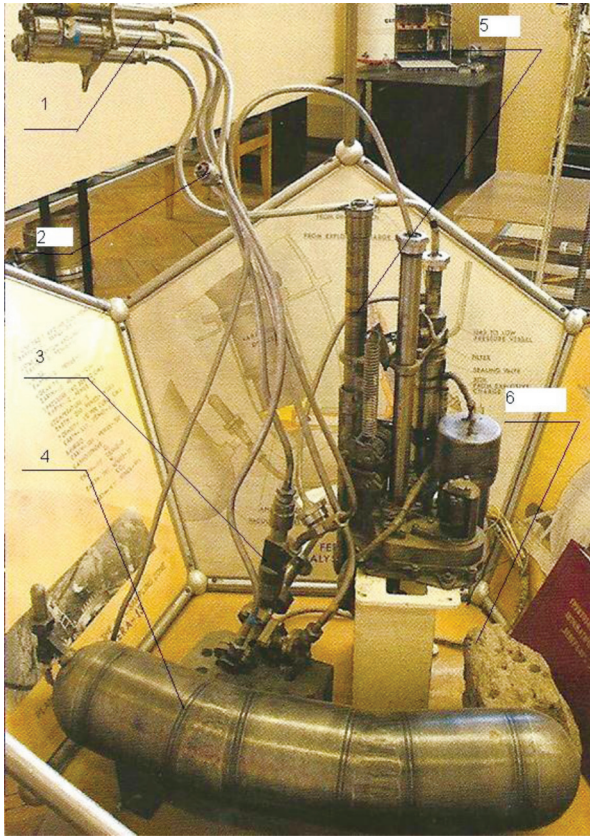


Figure 2: General view of the Soil Sampling System VB-02: 1 — pyro-cartridge assemblage; 2 — gas transfer tubes; 3 — sample transfer mechanism; 4 — vacuum tank; 5 — the drill; 6 — modeling stones

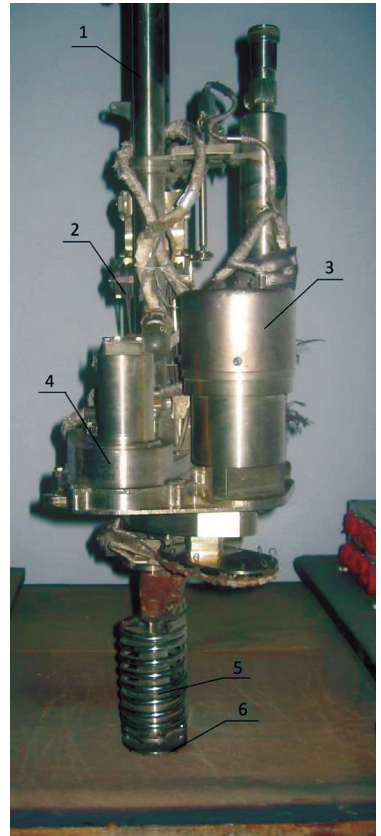


Figure 3: The Drilling Mechanism: 1 — advancing cylinder; 2 — block-and-tackle mechanism; 3 — electric motor; 4 — gear box; 5 — drilling tool (tube with a wing-like feature); 6 — anchoring plate

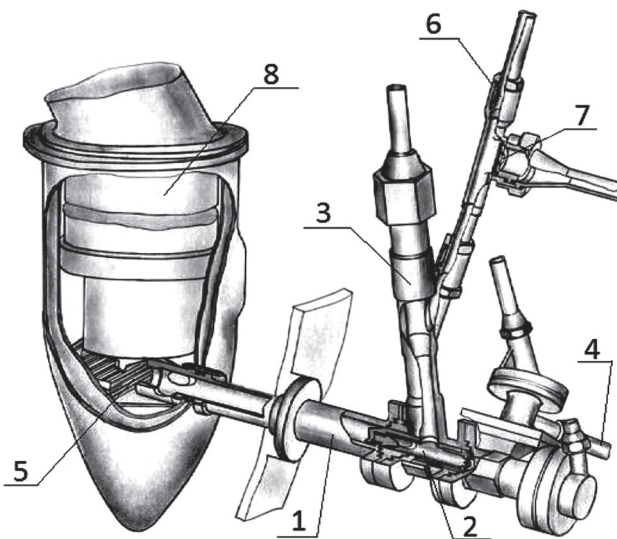


Figure 4: Design of the sample transfer mechanism: 1 — sample transfer mechanism; 2 — sabot; 3 — plug; 4 — tube to the vacuum tank; 5 — intake chute of the XRF instrument; 6 — sample transfer tube from the drill; 7 — filter and tube to the sealed tank; 8 — the XRF instrument "Arakhis"

The sample transfer mechanism

The sample transfer mechanism was mounted onto the flange by the side of the Lander under the outer thermal insulation. The goals of the sample transfer mechanism were the following: to take in the soil sample, to cut the volume with the sample from the external atmosphere, to drop the pressure of the residual gas to allow the XRF analysis, and to move the sample to the intake chute of the XRF instrument.

Activation of the sample transfer mechanism started after the completion of loading of the sabot. The plug driven by the pyro-cartridge encapsulated the internal part of the mechanism from the atmosphere. Next pyro-cartridge opened the tube to the vacuum tank. The vacuum tank had a 10 liter volume and was prevacuated down to less than 1 kPa. Expansion of residual gas into the vacuum tank dropped the pressure over the sample down to 5–6 kPa. Afterwards the new pyro-cartridge sent the sabot into the area of the XRF instrument. It stopped in front of the intake chute of the XRF instrument and the fine-grained sample by inertia propagated and covered the surface of the chute.

SSS for Venera-D

Successful and reliable operation of the SSS VB-02 provided the first measurements of elemental composition of Venusian surface material using the XRF instrument. The former measurements of Venera-13, -14 and Vega-2 Landers and the planned measurements of the Venera-D mission will be separated in time for more than 40 years and this implies correspondence to the up-to-date requirements of surface material analysis. The XRF instrument "Arakhis" had a mass of 8 kg (Surkov et al., 1983) and a volume of more than 7 liter. The up-to-date instruments are more portable and have sufficiently better performance. This allows to use several instruments for soil sample characterization.

While planning the new mission it is worth considering the possibility to make more detailed analysis of surface rocks both in elemental composition and in mineralogy. Characterization of the elemental composition should include the measurement of rock-forming and trace elements as well. The list of baseline instrumentation of the Venera-D Lander includes instruments with two methods of elemental analysis: laser induced mass-spectrometry (LIMS) of the Chemical Analysis Package (CAP) and alpha-particle-X-ray-spectrometry (APXS) mode of the Moesbauer Spectrometer. APXS provides integral characterization of mostly rock-forming elements while LIMS can provide in situ analysis of mineral grains and several trace elements. The characterization of mineralogy of surface rocks is planned to be performed using a Moesbauer Spectrometer and a Raman Spectrometer.

The use of different methods of analysis and a respective set of instruments inside the Lander implies the need to have a new distribution system which must provide each instrument with a soil sample. All the methods of analysis can deal with a fractionated rocky sample and it makes rather reasonable to incorporate the same method of sampling as on the prototype. Distribution of the sample between instruments is a novel engineering task since the sample must be separated and placed in specific carriers since different instruments have individual requirements for vacuum and sample refinement.

The Lander at surface of the Venus has a lifetime of around two hours. The sampling cycle takes several minutes. Methods such as LIMS have a short time of analysis and this opens the possibility to perform analysis of several samples. From the scientific point of view it is interesting to collect such objects as dust, weathered crust of rocks, and internal parts of rocks. The dust in case of Mars represents a globally mixed material which is different from surface rocks and provides information on surface-atmosphere interaction. Pictures of the Venus surface do not show the presence of valuable dust layers but an attempt to collect dust can be performed easily by a vacuum-cleaning effect at the surface without the activation of the DM. The weathered crust of rocks can be sampled by abrasion of the first few millimeters of rocks. Solid stone material can be sampled by a regular drilling of several centimeters inward. For this it is necessary to make a certain modification of the drilling tool and modify the cycle of the DM operation. It is also worth considering the possibility of using video cameras to document the sampling object on the surface.

In general, the SSS VB-02 can be used as a prototype of the SSS for the Venera-D due to its quick and reliable sampling during the previous Venus missions. A certain upgrade of mechanical and control units should be done:

- a) to consider the possibility of multiple sampling;
- b) to build a new soil preparation and distribution system inside the Lander for redistribution of samples between respective instruments;
- c) to consider alternative pumping methods at the respective instruments to gain the necessary vacuum for analysis;
- d) to consider the possibility of sample.

Acknowledgements

This work was supported by the FASO project “Venera-D”.

References

- Barmin, I.V., Shevchenko, A. A. (1983) The Soil Sampling System of “Venera-13” and “Venera-14” Spacecrafts, *Kosmicheskie Issledovaniya*, 21(2), 171–175.
- Surkov, Yu. A., Scheglov, O. P., Moskalyeva, L. P., Kirichenko, V. S., Dudin, A. D., Gimadov, V. L., Kurochkin, S. S., Rasputnuyi, V. N. (1983) The Method and Instrumentation for Analysis of Soil Which Was Used on “Venera-13” and “Venera-14” Spacecrafts, *Kosmicheskie Issledovaniya*, 21(2), 297–307.

LONG-LIVED IN-SITU SOLAR SYSTEM EXPLORER (LLISSE)

T. Kremic¹, G.W. Hunter¹, L. Nero²

¹ NASA Glenn Research Center, Cleveland, USA

² Alcyon Technical Services, Cleveland, USA

Abstract

Venus, while having similar size, mass, and location in the solar system to Earth, varies from Earth in many ways. The differences include its climate, atmosphere, and surface conditions. Surface conditions present formidable engineering challenges due to the high temperature and pressure. To date, landed missions have not been able to last more than about 2 hours on the surface (Hall et al., 2009). This has resulted in significant knowledge gaps about the surface conditions of this important body in the solar system. The science community has effectively no in-situ temporal data on Venus surface conditions (temperature, pressure, winds and chemistry). These data are critical for the development of a thorough understanding of Venus' weather and the processes by which chemical species interact with each other, and are transported throughout the atmospheric column. This will help understand aspects of the atmosphere/planet interactions such as momentum exchange. To date, no capability has been available to enable a long lived surface probe to make these kinds of measurements. However, recently developed Silicon Carbide based electronics, sensors, and other technologies have matured to a state where a simple, but powerful long-life scientific probe would be feasible for Venus. It is now possible to directly qualify the durability and functionality of these components in a simulated Venus surface environment and demonstrate the ability to return valuable scientific data.

Introduction

Development has begun on an integrated probe system to enable a long lived surface mission. This probe, the Long-Life In-situ Solar System Explorer (LLISSE), would provide key measurements to help make progress in our understanding of three key questions for Venus exploration. These are identified in the planetary science decadal survey and the Venus exploration Goals, Objectives, and Investigations document (GOI) as produced by the Venus Exploration Analysis Group (VEXAG). The key questions addressed by this probe include better knowledge of super-rotation of the atmosphere (Goal 1, Objective B), the climate and its evolution (Goal 1, Objective B), and surface — atmosphere interaction/weathering (Goal 3, Objective B).

Discussion

LLISSE Concept Overview

LLISSE is a small (~10 kg) and completely independent probe for Venus surface applications. The LLISSE project includes the design and development of the probe(s) and the demonstration of the probe(s) to function at the surface conditions of Venus and communicate periodic measurements of temperature, pressure, wind velocity and direction, and chemical composition (Kremic et al.,

2016a) (Fig. 1). These periodic measurements (every 8 hours or better) would occur over the duration of a Venus day-light period including the terminator at one or both ends of that period. The goal of LLISSE is to operate in Venus conditions for approximately 60 Earth days. If deployed on Venus, LLISSE would provide unique and significant science impact.



Figure 1: Notional wind powered version of the Long-Life In-situ Solar System Explorer Venus Probe Concept

The main product for the first three years of the project's development will be a primary battery powered version capable of surviving the approximately 60 Earth and transmit data at approximately 10 MHz. The fifth-year product is the demonstration of the wind-powered version and increasing transmit capability of the probe to between 50 and 150 MHz.

The capabilities that enable LLISSE include:

- High temperature Sensors, Electronics, Communications, and Power Generation.
- High fidelity test/validation capability, in particular the Glenn Extreme Environment Rig (GEER) Fig. 2 (Kremic et al., 2016b).
- Creative operations approach including the simple operation premise of periodic data transmission.



Figure 2: Testing in GEER at Venus surface conditions

High Temperature Electronics

Advancements in high temperature electronics are particularly enabling to multiple aspects of LLISSE. Standard electronics for planetary instrumentation/operations are often silicon (Si) based. However, Si-based electronics do not operate at Venus temperatures (Neudeck et al., 2002). This implies a need to use wide bandgap electronics, such as silicon carbide (SiC), or other high temperature electronic systems. The design choices available in a small package, the capability to withstand harsh environments including high pressure/temperature for potentially prolonged time periods, and the ability to form complex integrated circuits (IC’s) suggest SiC as the most viable technology for multiple high temperature applications.

Recent work has notably expanded capabilities and produced the world’s first microcircuits of moderate complexity (Medium Scale Integration) that have the potential for sustained operation at 500 °C (Hunter, 2016; Hunter et al., 2015; Spry et al., 2016a, b). These circuits contain 10’s of JFETs and two metal interconnect layers, an order of magnitude more complicated than previous long-term 500 °C demonstrations. This enables a wide range of on-board data processing, including signal amplification, local processing, and wireless transmission of data. Operational life at 500 °C for thousands of hours has been shown for several circuits. Table 1 shows a sample compilation of circuits fabricated that can enable other Venus and harsh environment applications. A direct extension of the processing provides other circuit types with prolonged 500 °C operational lifetimes.

Table 1: A sampling of high temperature circuits fabricated and in development

| Circuit | Standard inputs | Outputs | Comments |
|-----------------------|--|---------------------------------|---|
| Ring Oscillators | Capacitive sensors, Resonator Circuits | Frequency modulated signals | Can add on-chip large transistors for power amplification |
| Binary RF Transmitter | Low power binary signal | High-Power RF signal to antenna | Conditions the signal for wireless transmission and feeds antenna |
| Op Amp, 2-Stage | Differential inputs | Voltage gains to 50 | Crucial circuit building block for signal processing |
| 4-Bit D/A | 4 digital Inputs | 1 analog | A/D circuit also achievable given these components |
| Logic gates | Up to 8 inputs/outputs | Typically 1 digital | Types include: NOT, NOR, NAND, XNOR |
| 4x4 Bit Static RAM | Read, Write, Data Lines, Address Lines | 4 bit parallel digital latch | Memory element |

Key elements leveraged

A significant Venus relevant activity associated with moderately complex electronics occurred when [Hunter, 2015] high temperature electronics, including a high temperature ring oscillator, were demonstrated in GEER at Venus conditions. To very briefly summarize [Neudeck et al., 2016], a packaged SiC JFET ring oscillator chip was immersed in the simulated Venus atmosphere for over 21 days. Simulated conditions included temperature, pressure, and atmospheric species. The test was successful only before ending for scheduling reasons. The SiC ring oscillator integrated circuit fully functioned at 1.26 ± 0.06 MHz over the entire 521 hours it was exposed to Venus surface atmospheric conditions. This was the world's first demonstration of moderately complex electronics operating for an extended period in-situ in Venus surface atmospheric conditions and this represents a major advancement in technology, and notably expands potential for new Venus missions. It is upon this potential that not only missions such as LLISSE can be envisioned, but a new range of future planetary exploration.

Scientific Measurements with Low Data Volume

Presently the LLISSE probe will measure surface wind speed, wind direction (relative to surface), surface temperature and pressure, near-surface atmospheric chemical composition, and incident solar radiance. Surface wind speed sensor, surface temperature and pressure sensors, radiance and near-surface atmospheric chemical composition sensors have recently been tested at Venus conditions in the GEER for 60 days. These sensors have several things in common which contribute to the LLISSE science theme and help enable the extended life. First, the sensors target science is the enabled or significantly enhanced by temporal measurements. Second, the science return does not require large volumes of data, which contributes to power conservation and hence, longer life.

Battery Development

NASA has a dual-approach for battery development. Figure 3 highlights the first version of the LLISSE probe. The first approach is to develop a high-temperature tolerant battery (HTTB) technology to achieve safe, long-life, high specific energy operation, and powered only by the charged battery. The battery is operated only in the discharge mode. The non-rechargeable battery would have a life of 3000 hours of operation if data is sent for two minutes every eight hours. The main product for the first three years of LLISSE development will be a battery powered probe with capability to transmit data using a ~ 10 MHz carrier RF transmitter. The LLISSE probe would stay dormant during cruise and launch. It automatically powers on and begins operation at the surface of Venus. A high temperature battery development is in progress with backup approaches available if required.

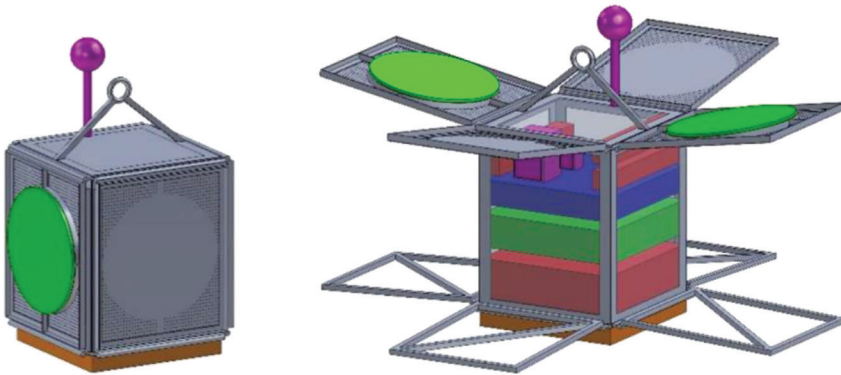


Figure 3: Schematic of LLISSE-B Battery Prototype

The second approach is a re-chargeable battery with a wind turbine. Surface winds on Venus would recharge the battery via a small wind turbine mounted on the top of the LLISSE prototype probe, perhaps appearing as depicted in Fig. 4. The wind version could theoretically have indefinite life (but the goal would be life expectancy of a Venus year or 224 Earth days or more). This approach however may result in variable data transmission frequency due to the uncertain wind conditions as no one has measured these over time. The fifth-year product of the LLISSE project is the demonstration of the rechargeable battery, wind powered version of the probe. GEER testing of wind turbine motor component materials is planned by end of 2021.

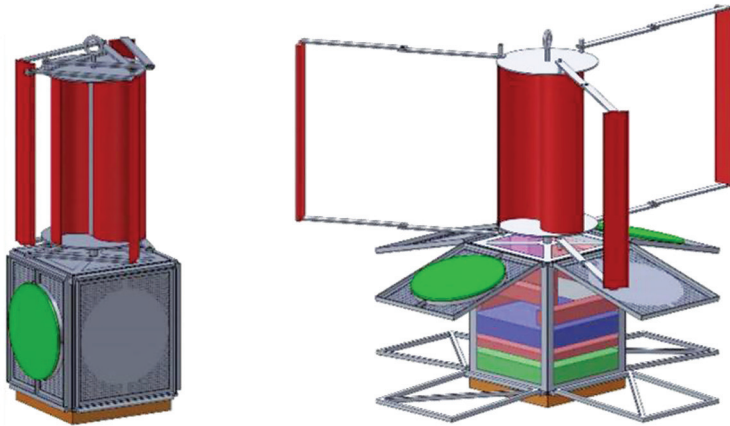


Figure 4: Schematic of LLISSE-W Wind Turbine/Rechargeable

LLISSE and Venera-D

An exciting potential application of LLISSE could be to serve as the “long-lived station” on the potential Venera-D mission. The Venera-D JSDT is currently recommending the inclusion of a long lived station to the mission to begin to take the temporal measurements that LLISSE is targeting. If employed on Venera-D, LLISSE could be deployed in several ways. One is to be attached and serve as an instrument on the main lander. LLISSE could also be deployed independently in its own entry shell separate from the lander, or it could be part of an aerial platform payload and dropped from the platform when desired. Finally, multiple copies of LLISSE could be deployed to several locations if packaged and released accordingly from an entry capsule. The Venera-D mission concept is in early formulation phase so how that potential application or contribution is yet to be defined and determined.

Conclusion

The component level hardware exists and performance has been demonstrated at Venus temperatures to enable a probe to survive for extended periods on the surface of Venus. Recent successes in high temperature electronics, multispecies chemical sensor array, and high temperature pressure and temperature sensors are paving the ways to successful LLISSE probe development effort where operation on Venus will be demonstrated. The non-rechargeable battery is targeting demonstration in late 2019 and the wind powered version in late 2021. Venera-D may be an opportunity to contribute LLISSE to a Venus mission. That contribution could enable temporal science that has not been possible to date.

References

- Hall, J. L., et al. (2009) Final Report of the Venus Science and Technology Definition Team, Venus Flagship Mission Study, NASA Jet Propulsion Laboratory, Pasadena, CA, <http://vfm.jpl.nasa.gov/files/Venus+Flagship+Mission+Study+090501-compressed.pdf>.
- Hunter G. (2015) High Temperature Electronics Task, *Planetary Instrument Concepts for the Advancement of Solar System Observations (PICASSO) Program*.
- Hunter, G. (2016) High Temperature Rad-Hard Electronics, Atmospheric Measurements, and Sensor Systems for Venus Exploration and Other Planetary Missions, *New Frontiers 4 Technology Workshop*, June 1, 2016, Washington, DC.
- Hunter, G.W., Ponchak, G. E., Beheim, G.M., Neudeck, P.G., Spry, D.J., Scardelletti, M. C., Meredith, R. D., Taylor, B., Beard, S., Kiefer, W. S. (2015) High Temperature Seismometer, Electronics, and Sensor Development for Venus Applications, *Venus Science Priorities for Laboratory Measurements and Instrument Definition Workshop*, 4016.
- Kremic, T., Zasova, L.V., Limaye, S., Hunter, G. (2016a) Long-Lived In-Situ Solar System Explorer (LLISSE), *14th Meeting of the Venus Exploration and Analysis Group (VEXAG)*, https://www.lpi.usra.edu/vexag/meetings/archive/vexag_14/presentations/27-Kremic-Long-Lived%20Venus%20Station.pdf.
- Kremic, T., Nakley, L. M., Vento, D., Balcerski, J., Kulis, M. J., Jacobson, N. S., Costa, G. C. C. (2016b), Glenn Extreme Environments Rig (GEER) for Planetary Science, *Lunar and Planetary Science Conference 47*, 2146.

- Neudeck, P.G., Okojie, R.S., Chen, L.-Y. (2002) High-temperature electronics - a role for wide bandgap semiconductors? *Proceedings of the IEEE*, 90(6), 1065–1076. doi: 10.1109/JPROC.2002.1021571.
- Neudeck, P.G., Meredith, R. D., Chen L., Spry, D. J., Nakley, L. M., Hunter, G.W. (2016) Prolonged silicon carbide integrated circuit operation in Venus surface atmospheric conditions, *AIP Advances*, <https://aip.scitation.org/doi/10.1063/1.4973429>.
- Spry, D. J., Neudeck, P. G., Chen, L.-Y. et al. (2016a) Processing and Characterization of Thousand-Hour 500 °C Durable 4H-SiC JFET Integrated Circuits, *High Temperature Electronics Conference (HiTEC)*, 249–256.
- Spry, D. J., Neudeck P.G., Chen L.Y., Lukco D., Chang C.W., Beheim, G. M. (2016b) Prolonged 500 °C Demonstration of Two-Level Interconnect 4H-SiC JFET ICs // *IEEE Electr. Device*, 37(5), 625–628, doi: 10.1109/LED.2016.2544700.

THE RADIOMETER FOR THERMAL SOUNDING OF LOW ATMOSPHERE AND SULFUR COMPOUND DETECTION

V. Gromov, A. Kosov

Space Research Institute of Russian Academy of Sciences

Abstract

The millimeter-wave radiometer is developed for the Venera-D orbiter. This instrument is devoted to remote sensing of Venus atmosphere by detection of thermal atmospheric radiation at wavelengths from 3 to 15 mm.

Introduction

Ground-based microwave radiometric observations of Venus (Kolodner et al., 1998; Butler et al., 2001; Jenkins et al., 2002) detected gaseous sulfuric acid and sulfur dioxide in a lower atmosphere. Their success was based on laboratory measurements of cm- and mm-wave absorption at simulated conditions of the Venus atmosphere (Ho et al., 1966; Fahd, Steffes 1992; Kolodner et al., 1998). Radiometric ground-based observations demonstrated a high efficiency, but have spatial and temporal restrictions. New laboratory data (Steffes et al., 2015; Bellotti et al., 2016; Akins et al., 2017) permits to improve accuracy of radiometric measurement interpretation. Continuous mapping of Venus, from an orbit around it, could provide a greater volume of information.

The following devices could be used as prototypes of the orbital instrument: the radiometer for Earth atmosphere sounding (Gromov et al., 1992), the high sensitive superheterodyne devices constructed for Relikt-2 project (Strukov et al., 1991), the radiometer of Relikt-1 mission for measurements of CMB anisotropy (Strukov et al., 1984).

The Radiometer Concept

A brightness temperature T_b of an atmospheric thermal radiation, registered by a radiometer, depends on altitude distribution of atmospheric temperature $T(h)$ and distributions of atmospheric constituents, represented here by volume mixing ratios $q_{con}(h)$. A dominating absorption of the Venus troposphere in cm- and mm-wave region is due to gaseous molecules CO_2 , H_2SO_4 and SO_2 .

In accordance with the radiation transfer equation: $T_b = \int_0^{\tau_m} T(h) e^{-\tau} d\tau$, where an optical depth $\tau(s) = \int_0^s \alpha(\sigma) d\sigma$; s and σ are coordinates along a line of sight; $\alpha(h)$ is an atmospheric absorption coefficient in layered atmospheric model. A value $s = 0$ at the point of sight, and $h = 0$ at the Venus surface.

In approximation of plane layers $h = \sigma/\cos\theta$, where θ is an angle between line of sight and nadir. For approximation of spherical layers, dependence between h and σ is slightly more complicated. An upper limit of integration $\tau_m = \tau(s_m)$, and a point s_m should be taken in depth of atmosphere, where $\tau_m \gg 1$, or outside of atmosphere (if absorption is low, and direction is close to limb, for example). If line of sight intersect the surface of Venus at some $\sigma = \sigma_o$ and corresponding $\tau_o \lesssim 1$, then a reflected radiation should be taken into account. Corresponding equations are well known and could be considered elsewhere.

Millimeter-wave absorptivity of the Venesian atmosphere

The absorptivity $\alpha(h) = \alpha_m + \alpha_s$ is defined by concentrations of main (m) and small (s) constituents, temperature and pressure at an altitude h . A main part of atmospheric absorption is generated by induced dipole moments of molecules CO_2 and N_2 . In accordance with (Ho et al., 1966; Butler et al., 2001):

$$\alpha_m = \left[q_{CO_2}^2 + 0.25(1 - q_{CO_2}) + 0.0054(1 - q_{CO_2})^2 \right] k_{CO_2},$$

where q is a volume mixing ratio; $q_{CO_2} = 0.965$; $(1 - q_{CO_2}) \approx q_{N_2}$; coefficient $k_{CO_2} = 1.15 \cdot 10^8 f^2 p^2 T^{-5} \text{ km}^{-1}$, f is a frequency in GHz; p is a pressure in bars.

Absorption by small constituents of the atmosphere could be expressed as: $\alpha_s(f, T, p) = \sum q_i k_i(f, T, p)$, where index $i = 1$ relates to H_2SO_4 and $i = 2$ relates to SO_2 .

Weight functions

A contribution of different atmospheric layers to a measured brightness temperature could be characterized by the weight function $W(h)$:

$$T_b = \int_0^{\infty} T(h)W(h) dh, \quad W(h) = \alpha_m(h) \cdot \cos\theta \cdot e^{-\tau(h)}.$$

For digital calculation, an upper limit of integration could be taken at some value h_u , which corresponds to negligible atmospheric absorption. Fig. 1 shows weight functions of 4-channels radiometer pointed in nadir direction or at some angle θ to nadir.

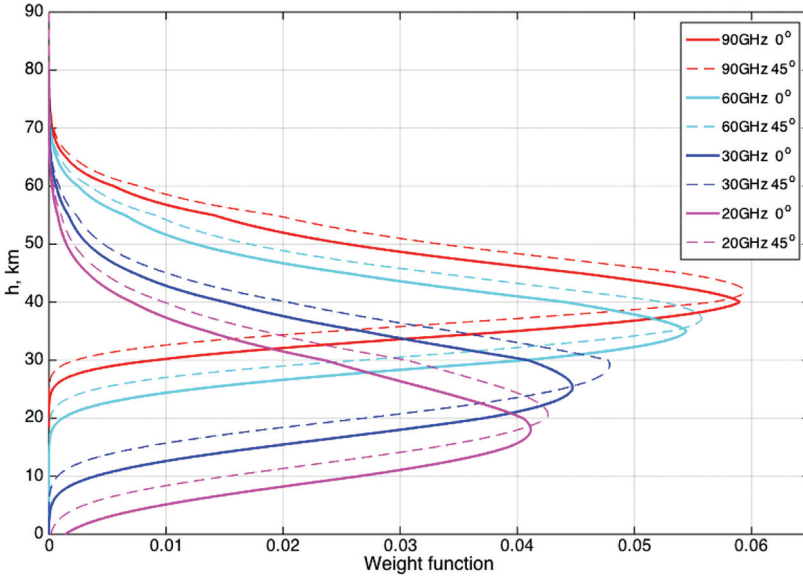


Figure 1: Weight functions for Venus atmosphere thermal emission. Frequencies and nadir angles θ are shown at right

Weight functions $W(h)$ use a linearity of the equation with respect to temperature profile $T(h)$. Linearisation of equations with respect to other profiles $q_1(h)$, $q_2(h)$ could be implemented, taking into account relatively small values of mixing ratios ($q_1 < 10^{-5}$, $q_2 < 2 \cdot 10^{-4}$) and of profile deviations $\Delta T(h) = T(h) - T_r(h)$, $\Delta p(h) = p(h) - p_r(h)$, where $T_r(h)$, $p_r(h)$ are initial approximation profiles (reference atmospheric profiles). A frequency dependence of $\Delta T_b(f) = T_{bm}(f) - T_{bc}(f)$, a difference between measured brightness temperature T_{bm} and T_{bc} calculated with $q_1 = q_2 = 0$, $T(h) = T_r(h)$ gives information on contents of these sulfur compounds.

In linear approximation:

$$\Delta T_b = \int_0^{\infty} \Delta T(h)W(h, \theta) dh + \sum_0^{\infty} \int_0^{\infty} q(h)W_i(h, \theta) dh,$$

where

$$W_i(h, \theta, f) = k_i(T_r, p_r) \cos\theta \left[e^{-\tau(h, \theta)} T_r(h) - \int_0^h T_r(\eta) W(\eta, \theta) d\eta \right].$$

Analysis of data of measurements

A result of one measurement consists of a set of $\Delta T_{bj} = \Delta T_b(f_j, \theta_j)$, $j = 1, 2, \dots, n$, where $n = 8$ for a case of Fig. 1. If profile deviations $\Delta T(h)$, $q_i(h)$ could be represented as

$$\Delta T(h) = \sum_{j=1}^{j_1} x_j f_j(h), \quad q_1(h) = \sum_{j=1}^{j_2} x_j f_j(h), \quad q_2(h) = \sum_{j=2}^n x_j f_j(h),$$

where x_j are unknown parameters, $f_j(h)$ are some defined probe-functions, for example, polynomials, then the initial linear system of integral equations could be solved by solution of a system of plain linear equations with respect to unknown x_j :

$$\Delta T_{b_j} = \sum a_{kj} x_k, \quad j, k = 1, \dots, n,$$

where

$$a_{kj} = \int_0^\infty f_k(h) F_j(h) dh, \quad \begin{cases} 1 \leq j \leq j_1: F_j = W(h, f_j, \theta_j), \\ j_1 < j \leq j_2: F_j = W_1(h, f_j, \theta_j), \\ j_2 < j \leq n: F_j = W_2(h, f_j, \theta_j). \end{cases}$$

Nonlinear effects could be corrected by iteration methods. An alternative to use of probe-functions is a use of more sophisticated mathematical methods (Troitsky et al., 1993).

The Instrument

The radiometer includes four independent radiometric channels with separate antennas. General parameter of the instrument are given in Table 1. Parameters of the channels are given in Table 2. Fluctuation threshold of sensitivity of the channels is better than 0.05 K. The prototypes of the radiometer are shown on Fig. 2 (in laboratory test of parameters) and on Fig. 3 (in field measurements of atmospheric emission).

Table 1: General parameters of the instrument

| | |
|--------------------|-----------------|
| Beam width | 7° |
| Mass | 2 kg |
| Power consumption | 6 W |
| Information output | 70–100 kB/orbit |

Table 2: Parameters of spectral channels

| | | | | |
|-------------------------------|------|-----|-----|-----|
| Center of frequency band, GHz | 90 | 60 | 30 | 20 |
| Band width, GHz | 10 | 6 | 3 | 2 |
| Noise temperature, K | 1000 | 600 | 200 | 200 |
| Sensitivity threshold*, mK | 28 | 27 | 27 | 36 |

* δT_b for integration time 1 s, taking into account brightness temperature of the Venus atmosphere.

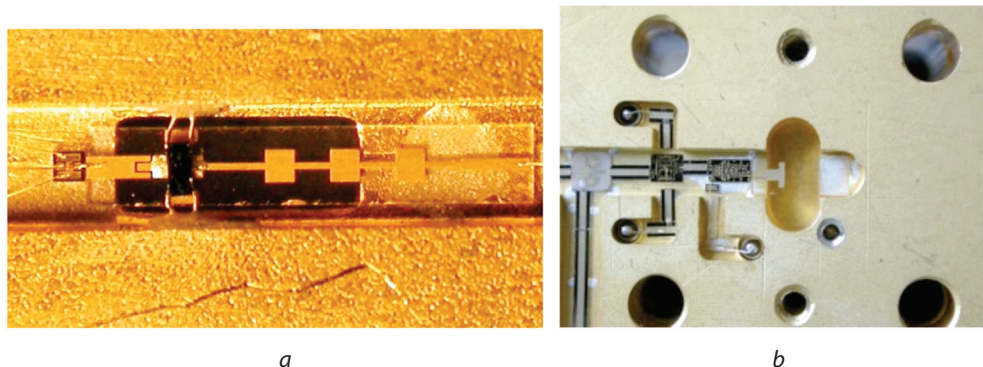


Figure 2: Elements of the radiometer prototype: *a* — the mixer of the 90 GHz channel with the $f/3$ local oscillator; *b* — a part of the microwave unit, containing the signal mixer and the Low Noise Amplifier

All channels are constructed with a similar superherodyne circuit diagram, using different elements and having different mixer design, with frequency multiplication for high frequency channels (double or triple, as for device on Fig. 2a). Microwave units are designed with use of unpackaged

chips of integrated circuits, as shown on Fig. 2. Microwave chip-circuits are integrated into hybrid microwave units with use of microelectronic technologies.

A high accuracy, which is necessary for manufacturing of microwave units and antennas, provided by workshop in IKI with use of machines under computer numerical control and with computer-aided design. High-frequency waveguides produced by electrical discharge machines.

High-frequency channels are supplied with horn antennas, low-frequency ones — with patch antennas. The horn antenna is shown on Fig. 4. Such horn use a specifically grooved internal surface to suppress side lobes of antenna beam-pattern, and therefore to improve an accuracy of brightness temperature measurements. For angle 90° to beam axis, such antenna has side-lobe level -80 dB, while a simple horn has this value between -20 dB and -30 dB.

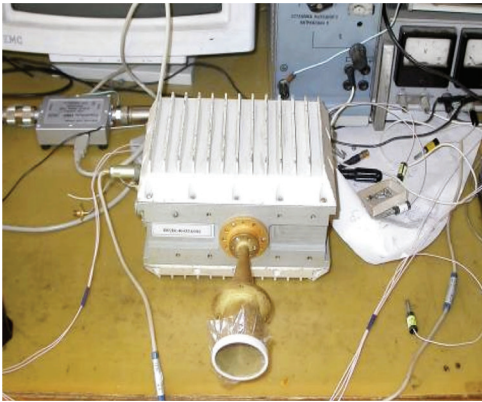


Figure 3: Single-channel prototype of the radiometer during laboratory tests of microwave characteristics

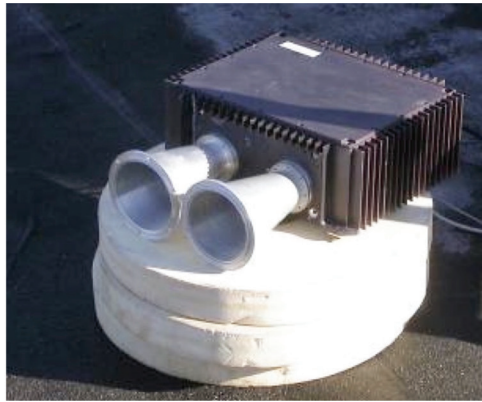


Figure 4: Two-channel prototype of the radiometer during field tests

Scientific Objectives

- Investigations under Venusian atmospheric cloud layer of sulfuric compounds (gaseous sulfuric acid, sulfur dioxide, and other), particularly their spatial variations on background of temperature profiles change, for better understanding of dynamical processes in Hadley cells.
- Measurements of temporal evolution of spatial distributions of H_2SO_4 and SO_2 , for exploration of tropospheric circulation and for understanding of thermo-chemical processes, restricting abundances of other trace gases (SO_3 , CO , OCS and H_2O).

Conclusions

The radiometer for the Venera-D orbiter is developed for sounding of a Venus atmosphere by detection of its thermal radiation. Multi-wavelength measurements of this radiation gives information about altitude profiles of atmospheric temperature and abundances of gaseous sulfuric acid H_2SO_4 and sulfur dioxide SO_2 at altitudes from 5 to 70 km above a surface. These data could contribute to one of main tasks of Venera-D project — investigation of a structure, composition, properties, and dynamics of Venusian atmosphere.

References

- Akins, A. B., Bellotti, A., Steffes, P.G. (2017) Simulation of the Atmospheric Microwave and Millimeter Wave Emission from Venus Using a Radiative Transfer Model Based on Laboratory Measurements, *Venus Modeling Workshop*, 9–11 May, 2017, Cleveland, Ohio, LPI Contribution No. 2022, ID 8009.
- Bellotti, A., Steffes, P.G. (2016) The millimeter-wavelength sulfur dioxide absorption spectra measured under simulated Venus conditions, *Icarus*, 254, 24–33, doi: 10.1016/j.icarus.2015.03.028.
- Butler, B. J., Steffes, P.G., Suleiman, S. H., Kolodner, M. A., Jenkins, J. M. (2001) Accurate and Consistent Microwave Observations of Venus and Their Implications, *Icarus*, 154, 226–238, doi: 10.1006/icar.2001.6710.
- Fahd, A. K., Steffes, P.G. (1992) Laboratory measurements of the microwave and millimeter-wave opacity of gaseous sulfur dioxide (SO_2) under simulated conditions for the Venus atmosphere, *Icarus*, 97, 200–210. doi: 10.1016/0019-1035(92)90128-T.

- Gromov, V.D., Kadygrov, E.N., Kosov, A.S. (1992) Remote sensing of atmospheric boundary layer at 5 mm wavelength, *Open symposium "Wave propagation and remote sensing"*, Ravenscar, UK, 8–12 June 1992, 3.4.1–3.4.5.
- Ho, W., Kaufman, I.A., Thaddeus, P. (1966) Laboratory Measurement of Microwave Absorption in Models of the Atmosphere of Venus, *J. Geophysical Research*, 71, 5091. doi: 10.1029/JZ071i021p05091.
- Jenkins, J.M., Kolodner, M.A., Butler, B.J., Suleiman, S.H., Steffes, P.G. (2002) Microwave Remote Sensing of the Temperature and Distribution of Sulfur Compounds in the Lower Atmosphere of Venus, *Icarus*, 158, 312–328. doi: 10.1006/icar.2002.6894.
- Kolodner, M., Steffes, P. (1998) The Microwave Absorption and Abundance of Sulfuric Acid Vapor in the Venus Atmosphere Based on New Laboratory Measurements, *Icarus*, 132, 151–169, doi: 10.1006/icar.1997.5887.
- Steffes, P.G., Shahan, P., Barisich, C.G., Bellotti, A. (2015) Laboratory measurements of the 3.7–20 cm wavelength opacity of sulfur dioxide and carbon dioxide under simulated conditions for the deep atmosphere of Venus, *Icarus*, 245, 153–161. doi: 10.1016/j.icarus.2014.09.012.
- Strukov, I.A., Skulachev, D.P. (1984) Deep-Space Measurements of the Microwave Background Anisotropy — First Results of the Relikt Experiment, *Soviet Astronomy Letters*, 10, 1–4.
- Strukov, I., Skulachev, D., Budilovich, N., Nemlikher, Yu., Korogod, V., Kosov, A., Rukavicin, A., Aniskovich, V., Borovski, R., Nechaev, V. (1991) RELICT 2 project: Scientific program and structure, *Acta Astronautica*, 24, 251–257, doi: 10.1016/0094-5765(91)90173-3.
- Troitsky, A.V., Gajkovich, K.P., Gromov, V.D., Kadygrov, E.N., Kosov, A.S. (1993) Thermal sounding of the atmospheric boundary layer in the oxygen absorption band center at 60 GHz, *IEEE Trans. Geoscience and Remote Sensing*, 31, 116–120, doi: 10.1109/36.210451.

“TO VENUS TOGETHER”: INTERNATIONAL PROJECT IMPLEMENTATION ON VENUS PLANET RESEARCH

S. Lemeshevskii, V. Vorontsov, O. Grafodatskiy, Kh. Karchaev, S. Teselkin

Lavochkin Science and Production Association, Russia, vorontsov@laspace.ru

Keywords: international cooperation, development, technology

Mission Venera-D developed by Lavochkin Association implies a long-term study of Venus with the scientific equipment of wide range. International pay-load will be installed on orbiter, lander and long-living station on Venus surface. The project can serve as a basis for further large-scale international missions to Venus to resume fundamental studies of “the morning star”, actively carried out in 1960–1980s and early 1990s by Soviet and American spacecraft. Over these years a large amount of data on structure and composition of soil, atmosphere, cloud layers, wind speed on the surface of the planet were accumulated.

Brilliant Soviet Venus research program was completed in 1986 by landing of stations of the project VEGA (Venus-Halley’s comet), one of the most successful projects in Lavochkin history. Since 1994 (the year of completion of Venus mapping program with the NASA Magellan mission) Venus was studied by two spacecraft: Venus-Express (ESA, 2005–2014) and Akatsuki (JAXA, launch in 2010, start of operation in 2015).

The first steps related to the mission Venera-D appeared in the early 2000s with the idea to provide operations for a landing station on the planet’s surface for several hours and possibly days. As a prototype for an automatic interplanetary station destined to Venus Lavochkin experts consider the mission VEGA taking into account the latest developments, unification of design solutions and new technical tools used in-house.

A great interest in participation in Venera-D programme is being shown by the scientists and technicians of space faring states: USA, EU and China. An activity of Russian – USA Venera-D Joint Scientific Group consisting of Roscosmos / Space Research Institute (IKI) / Lavochkin Association – NASA / U.S universities is focusing on analysis of the mission architecture as well as review of joint cooperation. Russian lander and orbiter assumed to be the main elements of the mission. As NASA possible contribution, the development of the Venus atmospheric maneuverable platform, VAMP (Venus Atmospheric Maneuverable Platform) is considered. As another option, several small drop-probes made on the basis of high-temperature electronics could operate on Venus surface for several hours. They could be dropped on different spots of the planet where they would study parameters of the atmosphere near the surface. The most prolonged operation of the station on the surface of the planet was up to 2 hours (VEGA project). The possibility of inclusion into the mission of freely drifting balloons or small sub-satellites is also foreseen. The next step of the study of Venus, as suggested by scientists of both countries, should be the investigation of atmospheric dynamics, problems of super rotation, giant greenhouse effect and evolution of the “morning star”.

The Russian Federation and the United States of America have long and rich experience in Venus studies and, for sure, it gives confidence in successful implementation of joint program on “the morning star” researches.

“TOWARDS VENUS TOGETHER”: THE PRELIMINARY ARCHITECTURE OF “VENERA-D” MISSION ON THE BASIS OF JOINT SCIENTIFIC PROGRAM PROPOSALS OF ROSCOSMOS – NASA JOINT STUDY GROUP ON VENUS RESEARCHES

O. Grafodatskiy, A. Martynov, S. Ustinov, A. Simonov, S. Teselkin, V. Vorontsov

Lavochkin Science and Production Association, Russia, vorontsov@laspace.ru

Keywords: mission architecture, technology, baseline

Mission Venera-D, developed by Lavochkin Association together with Space Research Institute of Russian Academy of Science (IKI RAN) and Russian-USA Joint Study Definition Team (JSDT) constituted by Roscosmos and NASA is preparing a long-term study of Venus. The scientific equipment, the product of international cooperation, will be installed on spacecraft comprised of orbiter, lander and long-living station on Venus surface. The project is based on Soviet experience of Venus researches in 1960-80s and early 1990s, American Magellan Mission in 1994–1996, European Venus-Express (2005–2014) and Japanese Akatsuki (from 2015).

Since JSDT is working on a mission scientific plan the Lavochkin Association is carrying out the mission architecture on its basis. Among the priorities of scientific goals are data concerning the structure and composition of the atmosphere, cloud layers, wind speed, soil composition on the surface of the planet. The study of atmospheric dynamics, problems of super rotation, giant greenhouse effect and evolution will be of interest.

The general principals of spacecraft Venera-D design are discussed in this paper. The mission VEGA (up to 2 hours operation on the surface) was taken as a prototype for the development of automatic interplanetary station destination to “the morning star”. The latest developments, unification of the design solutions and new technical tools used in-house has been taken into account. Particular attention is given to ballistics issues, i.e. orbits options, landing site discussion review, communication parameters including radio-lines “lander-orbiter” and “orbiter-Earth” are presented. The most challenging issues for the mission are discussed in heating scenarios. The general approaches and recommendations for the mission’s, sub-mission’s and separate devices’ life time are analyzed. Several hours or even days of surviving for the landing station are on agenda. As NASA possible contribution, the development of the Venus atmospheric maneuverable platform VAMP (Venus Atmospheric Maneuverable Platform) and small drop-probes made on the basis of high-temperature electronics are considered. Freely drifting balloons or small sub satellites is also foreseen.

VENERA-D: THE LANDER-ORBITER RADIOLINK

A. S. Kosov on behalf of radio-science team IKI RAN

Space Research Institute of Russian Academy of Sciences, akosov@iki.rssi.ru

Keywords: radio link, communication, Venus, transmitter, UHF band, scientific information

Introduction

The Venera-D project needs to transmit 1.6 Gbit scientific information from lander to orbiter per 1 hour.

Radio link basic concept

Figure 1 shows basic concept of lander — orbiter radio link.

Signal to noise ratio on receiver input per 1 Hz noise bandwidth:

$$S/N = \frac{P_T G_T G_R \lambda^2}{16\pi^2 R^2 L k T_N}$$

Energy per 1 bit to noise spectral density

$$E_b/N_0 = S/N/(\text{Bit rate})$$

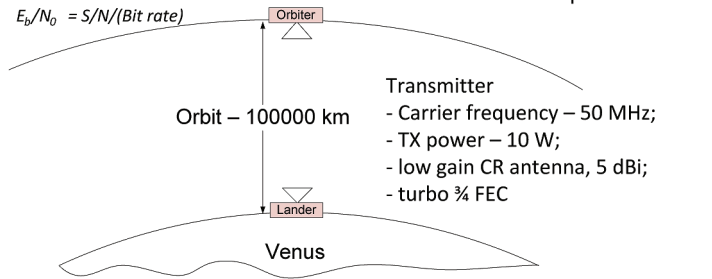


Figure 1

Venera-D radio link implementation

| Lander's transmitter | Orbiter's receiver |
|--------------------------|---------------------------------|
| Carrier frequency 50 MHz | Orbit 100 000 km |
| TX power 10 W | Low gain CR antenna 5 dB |
| Low gain CR antenna 3 dB | Antenna noise temperature 100 K |
| Turbo 3/4 FEC | |

Maximum bit rate estimation

Parameters:

- $E_b/N_0 = 3$ dB, threshold, BER = 10^{-3} ;
- $L = 1$ dB, atmosphere attenuation.

Threshold information rate

- $S/N = 58$ dB;
- Bit rate 630 kbit/s;
- Information rate **470 kbit/s**;
- Transmitted information for 1 hour — **1.692 Gbit**.

Summary

Venera-D lander-orbiter radio link can be implemented at 50 MHz carrier frequency for orbit 100 000 km using low gain antennas and Turbo 3/4 FEC, TX power 10 W, TX efficiency more 50 %, 1.6 Gbit information can be transmitted for 1 hour.

VENERA-D PROJECT: SCENARIO AND TRAJECTORY DESIGN PROBLEMS

N. A. Eismont¹, L. V. Zasova¹, R. R. Nazirov¹, A. V. Simonov²

¹ *Space Research Institute of the Russian Academy of sciences, neismont@iki.rssi.ru*

² *Lavochkin Science and Production Association, Russia, alex.simonov@laspace.ru*

Keywords: orbital dynamics, mission scenarios, orbital planning

The Venera-D project is currently in an early development phase of design, planning to launch the spacecraft onto transfer trajectory to Venus in 2026. Studies are being performed by Roscosmos and the Russian Academy of Sciences in cooperation with NASA. It is planned to resolve objectives of Venus exploration with the use of contemporary instruments with enhanced characteristics which were not reachable during previous missions decades ago. For this several probes are to be delivered to the vicinity of Venus which include: comparatively big principal Lander; Orbiter for atmospheric studies and for communication between the Lander and ground stations; Subsatellite of the Orbiter; Atmospheric platform for in situ measurements. Besides, several small landers are to be dropped onto Venus surface in order to receive some measurements from different regions. It is assumed that they will have the components which allow to withstand hostile Venus environment during long enough time (for months) transmitting the scientific data to the Orbiter. The principal Lander equips much more sophisticated instruments and has a rather constrained time of operations on the surface (about two hours). Two versions of flyers are under consideration: one is based on the use of inflatable airplane with solar arrays, another is supposed to use balloons. All these system elements, such as the main Lander, are to communicate with ground stations through the Orbiter.

The main goal of the trajectory and scenario design is to reach optimal balance between different tasks of the mission. In the presentation methods to resolve this problem are described. Peculiarities of the mission are generated by requirements to put different elements to the different destinations. The highest priority is given to the Orbiter and to the main Lander because failure from any of these two means the failure of the mission at large. Other tasks are considered, to some extent, as complementary.

Thus, the first phase of the solution procedure is the optimization of transfer trajectory taking into account the demands to minimize the sum of delta-V necessary for putting all constituents of the mission onto this orbit during the start from low near-Earth orbit and to deliver the Orbiter onto Venus satellite orbit. Together with the Orbiter, the Subsatellite is planned to be put onto the same orbit by applying a delta-V impulse. To reach the surface of Venus the main Lander and the small stations are planned to be installed inside a joint reentry module. Also mounted inside this module will be the folded atmospheric balloons. Unlike the Orbiter, the reentry module enters the atmosphere directly without applying a deceleration impulse.

The following sequence of separation after arrival was considered. The first operation is the final correction maneuver applied to the composite spacecraft in order to put it onto the reentry trajectory. After this, the reentry module is separated and its further motion is going without any orbital control until reaching the atmosphere. The remaining part of the composite spacecraft performs the maneuver by engine burn in order to avoid its entry in the atmosphere and to transfer it onto a high elliptical orbit planned for the atmospheric platform. Next, the platform is separated and after inflation begins its autonomous flight. Finally, the Orbiter is to be put on its operational near polar orbit with one day period that is preceding by inclination change maneuver. The presentation describes the scenario of mentioned maneuver determined by the optimal choice of their parameters taking into account requirements to settle the Lander in the selected point on the surface and to guarantee the duration of data transmission from the Lander to the Orbiter.

The presentation demonstrates how by comparatively small delta-V maneuvers it is possible to reach most favorable relative position of the arriving orbital planes for the Orbiter and the Lander, simultaneously keeping reentry overload in acceptable level, and satisfying demands on the telemetry data rate from the Lander. Described technology allows to select most interesting areas

of the Venus surface for the Lander keeping the constraints on trajectory of the Orbiter, including those which influence the evolution of its parameters.

It is shown that the basic parameters of the mission can be reached by the use of Angara-5 launch vehicle.

ACTIVE GAMMA RAY SPECTROMETER PROPOSED FOR FUTURE VENUS SURFACE MISSIONS

M. L. Litvak, A. B. Sanin, D. V. Golovin, I. G. Mitrofanov, A. A. Vostrukhin

Space Research Institute of Russian Academy of Sciences, litvak@mx.iki.rssi.ru

Keywords: gamma-ray spectroscopy, Venus, elemental composition

Introduction

Nuclear instrumentation based on neutron and gamma-ray spectroscopy methods were often used by different planetary missions to derive the bulk elemental abundances of surface materials. Usually these nuclear instruments were implemented on orbital missions to produce global elemental maps [Boynton et al., 2004, 2006; Prettyman et al., 2006, 2011]. For surface operations, active gamma-ray spectrometers could be accommodated onboard landing missions. For such instrumentation, a pulsed neutron generator that can generate short and very intense pulses of high energy neutrons (14 MeV) is used to irradiate subsurface under the lander and produce secondary gamma emission. The use of active gamma and neutron spectrometers commonly occurs in various Earth applications related to geology, security applications, transportation, medicine, etc. Active gamma ray and neutron spectrometers have been proposed for space missions to the planets and satellites of the solar system, including Moon, Mars and Venus.

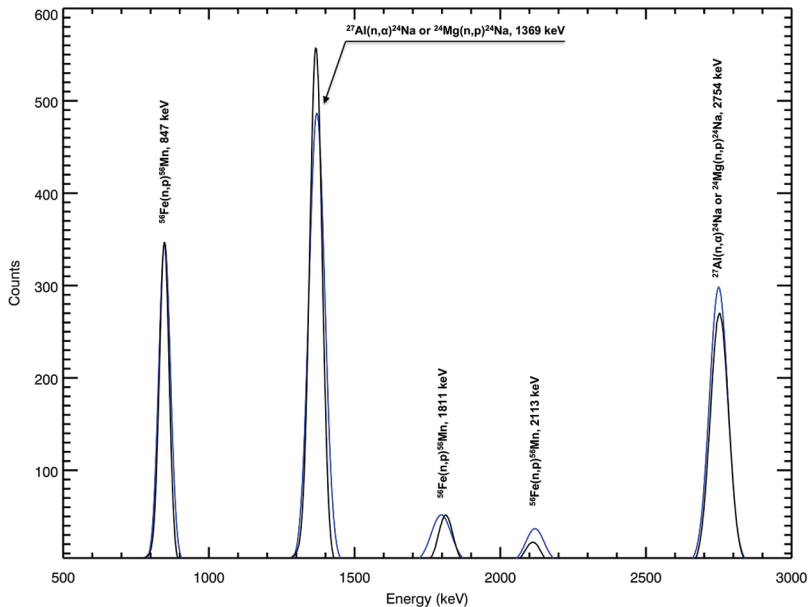


Figure 1: The example of comparison between measured by gamma spectrometer (blue color) and numerically modeled (black color) gamma ray lines for radioisotopes produced in the reactions with Al, Mg, Fe with fast neutrons

In our study, we presented the results of a series of ground tests with a prototype of an active gamma-ray spectrometer based on a new generation of scintillation crystal (CeBr₃). These tests have been conducted with a consideration to its applicability to future Venus landing missions. We evaluated the instrument's capability to distinguish the subsurface elemental composition of primary rock forming elements such as O, Na, Mg, Al, Si, K and Fe. We have estimated that the expected accuracies achieved in this approach could be as high as 1–10 % for the particular chemical element being studied.

References

Boynton, W.V., Feldman, W.C., Mitrofanov, I.G. et al. (2004) The Mars Odyssey Gamma-Ray Spectrometer Instrument Suite, *Space Sci., Rev.*, 110, 37–83.

- Boynton, W.V., Taylor, G.J., Evans, L.G. et al. (2006) Concentration of H, Si, Cl, K, Fe, and Th in the low- and mid-latitude regions of Mars, *J. Geophysical Research*, 112(E12S99), doi: 10.1029/2007JE002887.
- Prettyman, T.H., Hagerty, J.J., Elphic, R.C. et al. (2006) Elemental composition of the lunar surface: Analysis of gamma ray spectroscopy data from Lunar Prospector, *J. Geophysical Research*, 111, CiteID E12007.
- Prettyman, T.H., Feldman, W.C., McSween Jr., H.Y. et al. (2011) Dawn's Gamma Ray and Neutron Detector, *Space Sci. Rev.*, 163(1–4), 371–459.
- Bruckner, J., Waenke, H., Reedy, R.C. et al. (1987) Neutron-induced gamma ray spectroscopy — Simulations for chemical mapping of planetary surfaces, *J. Geophysical Research*, 92, E603–E616.
- Jun, I., Kim, W., Smith, M., Mitrofanov, I., Litvak, M. (2011) A study of Venus surface elemental composition from 14 MeV neutron induced gamma ray spectroscopy: Activation analysis, *Nucl. Instr. and Meth. Phys. Res. A*, 629, 140–144.
- Litvak, M.L., Mitrofanov, I.G., Barmakov, Yu.N. et al. (2008) The Dynamic Albedo of Neutrons (DAN) experiment for NASA's 2009 Mars Science Laboratory, *Astrobiology*, 8(3), 605–612.
- Litvak, M.L., Golovin, D.V., Jun, I. et al. (2016) Implementation of gamma-ray instrumentation for solid solar system bodies using neutron activation method, *Nucl. Instr. and Meth. Phys. Res. A*, 822, 112–124.
- Litvak, M.L., Sanin, A.B., Golovin, D.V. et al. (2017) Ground tests with prototype of CeBr3 active gamma ray spectrometer proposed for future Venus surface missions, *Nucl. Instr. and Meth. Phys. Res. A*, 848, 9–18.
- Mitrofanov, I.G., Junm I. (2011) Neutron-activated gamma ray spectrometer (NAGRS) for the venus surface and atmosphere geochemical explorer (SAGE) mission, In: *European Planetary Science Congress 2010*, held 20–24 September 2011, Rome, Italy, 264
- Parsons, A., Bodnarik, J., Evans, L. et al. (2011), Active Neutron and Gamma-Ray Instrumentation for In-Situ Planetary Science Applications, *Nuclear Instruments and Methods in Physics Research A*, 652, 674–679.